Advancements and optimization in ancient DNA protocols

Dissertation

To Fulfil the

Requirements for the Degree of

„Doctor of Philosophy“ (PhD)

Submitted to the Council of the Faculty

of Biological Sciences

of the Friedrich Schiller University Jena

by Cody Parker, MSc Biology, BSc (Honours) Biology

born on 18/12/1981 in Fort Smith, Arkansas, United States of America

Gutachter:
1. Prof. Dr. rer. nat. Johannes Krause
   The Max Planck Institute For Evolutionary Anthropology, Leipzig, Germany
2. Prof. Dr. rer. nat. Manuela Nowotny
   Friedreich Schiller University, Jena, Germany
3. Prof. Dr. Laura Weyrich
   Pennsylvania State University, Pennsylvania, USA

Beginn der Promotion: 01 February 2016
Dissertation eingereicht am: 22 January 2022
Tag der öffentlichen Verteidigung: 30 June 2022

Table of Contents

1. Introduction

Since the early 1980's the analyses of DNA obtained from archaeological remains has proved to be a valuable tool for the investigation of human history (Higuchi et al. 1984, Pääbo 1985, Pääbo et al. 1988, Rollo et al. 1988, Pääbo et al. 2004; Rizzi et al. 2012; Pickrell and Reich 2014; Hagelberg, Hofreiter, and Keyser 2015). The introduction of next-generation sequencing techniques and associated protocols has further reinforced this value, and consequently the popularity of ancient DNA (aDNA) analyses, by providing the means to produce an unprecedented depth of data from which to work (Schuster 2008; Knapp and Hofreiter 2010; Loreille et al. 2011; Overballe-Petersen, Orlando, and Willerslev 2012; Der Sarkissian et al. 2015). The data obtained from archaeological remains can shed light on a myriad of topics including human evolution (Itan et al. 2009; Sankararaman et al. 2014; Ermini et al. 2015), population genetics (Orlando et al. 2002; Haak et al. 2005; Malmström et al. 2009; Haak et al. 2010; Brandt et al. 2013) , the genetic history of domestication and subsequent evolution of domesticated species (Jaenicke-Després et al. 2003; Larson et al. 2007; Scheu et al. 2008; Kimura et al. 2011; MacHugh, Larson, and Orlando 2017), host-pathogen co-evolution (Hunter 2014; Donoghue et al. 2015; Harkins and Stone 2015), and the evolution of the microbiome (Weyrich, Dobney, and Cooper 2015; Schnorr et al. 2016; Groussin et al. 2017; Lugli et al. 2017). The sampling of remains for aDNA analyses, however, is an inherently destructive process where irreplaceable parts of the anthropological record are damaged or outright destroyed to in order to gain access to the DNA preserved within them. This raises considerable ethical dilemmas, particularly as these remains are a not only finite resource important for the investigation of innumerable aspects of history but can also be of great cultural significance and educational value (Cooper and Poinar 2000; Kaestle and Horsburgh 2002; Prendergast and Sawchuk 2018; Palsdottir et al. 2019).

In response, aDNA researchers have invested significant resources into investigating potential methodological and analytical optimizations aimed to ensure the balance between data production and anthropological preservation (Ubelaker 2010; Sholts, Bell, and Rick 2016; Sirak et al. 2017; Sirak and Sedig 2019). Here I present a body of work designed to further this goal by systematically exploring aDNA preservation across human skeletal elements and further elucidating the need for routine, broad screening of aDNA datasets for information regarding other historically and culturally important phenomena that may be hidden within, such as endogenous microbial content (both pathogenic and commensal), even in the absence of visual, historical, or contextual evidence of their presence. In this context, I will detail current theory as to how DNA is preserved in ancient tissue, laboratory protocols for the sampling of ancient remains, and the effect of current sampling strategies on the archaeological record as an introduction to the relevance of methodological development and optimization in aDNA analyses.

1.1 Characteristics of ancient DNA

The DNA available for analyses in archaeological remains differs significantly from that extracted from modern remains, not only in its source, but also its basic characteristics. In modern genetic analyses, material from DNA rich soft tissue is often the primary source of the genetic information used in downstream applications. In archaeological terms, however, this soft tissue is rarely recovered excepting in instances of extraordinary preservation, such as in the case of mummification or remains preserved within the permafrost (Lassen, Hummel, and Herrmann 1994; Nerlich et al. 1997; Lewis et al. 2008; Bellemain et al. 2013). Most aDNA studies, however, rely on the recovery of DNA preserved within the dense hydroxyapatite matrix of tissues such as cortical bone, cementum, and dentin.

The formation and subsequent remodeling of these tissues are variable processes but are generally driven by the secretion of hydroxyapatite from osteoblasts (Boskey 1992) or odontoblasts (dentin and cementum). In cortical bone, where hydroxyapatite mineralization replaces a pre-existing collagen scaffold (endochondral ossification), these osteoblasts become trapped within this crystalline matrix where they then differentiate into osteoclasts. These living cells continuously refresh the hydroxyapatite matrix throughout the lifespan of an individual. In teeth odontoblasts secret hydroxyapatite along a collagen membrane (intramembranous ossification; (Nanci 2017). Rather than becoming trapped within this matrix, the odontoblasts elongate and form subsequent channels (Tomes fibers) throughout the dentin as the nuclear portion of the cells migrates inward along the collagen membrane. Upon cell death, it is theorized that the preservation of endogenous DNA is a product of the molecule's binding affinity to both the hydroxyapatite matrix (Kawasaki, Takahashi, and Ikeda 1985) of bone and to type 1 collagen (Collins et al. 2002), which traps the bound DNA molecules in a dense, protective matrix where it remains relatively protected from the environment and decay processes. The binding of DNA to the hydroxyapatite matrix is not, however, restricted to DNA endogenous to the host, as microbial DNA shares this affinity and often binds to the hydroxyapatite matrix as well, both during the lifetime of the host and during post-mortem exposure to the environment and subsequent decomposition processes

In vivo, DNA spontaneously degrades through processes such as hydrolysis, oxidation, and methylation and subsequently triggers specific DNA repair processes (Lindahl 1993). However, although the cell-free DNA bound in the hydroxyapatite matrix of bones is relatively protected from the degradation processes associated with decomposition, it cannot be repaired in this manner. The result is a continuous build-up of spontaneous damage such as the weakening of the sugar-phosphate backbone, subsequent fragmentation of DNA molecules, and the deamination of the amino acid cytosine into uracil over time (Lindahl 1993, Höss et al.

1996; Briggs et al. 2007; Dabney, Meyer, and Pääbo 2013). In ancient double-stranded DNA fragments, it has been observed that the deamination process is somewhat limited to the ends of fragments, as it is thought that the cytosines present near the central portion of ancient DNA fragments are somewhat protected by the structure of DNA (Briggs et al. 2007). As a result, analysis of the frequencies of cytosine deamination and its location along isolated DNA fragments can be used to authenticate recovered DNA as ancient (Krause et al. 2010, Meyer et al. 2014, Renaud et al. 2019). However, environmental conditions (temperature, soil/sediment composition, time interred, etc) have been shown to greatly influence the demineralization of ancient bone, resulting in the desorption of bound DNA molecules and their subsequent chemical decay. Additionally, microbial activity may have a similar effect, as it has been shown that the microbial digestion of bone increases its overall porosity, exposing trapped DNA to increasing rates of chemical decomposition (Pinhasi and Mays 2008). Consequently, while DNA damage analysis remains a central method for authenticating that recovered DNA is ancient in origin, it has been shown that it cannot be used as a reliable predictor of age (Sawyer et al. 2012).

This inherent damage to ancient DNA, although important for authentication, can also hinder downstream sequence recovery and analyses. DNA that has been degraded over time is often significantly fragmented, with most fragments comprised of < 50 base pairs (Handt et al. 1994, Dabney et al, 2013), is affected by strand lesions which inhibit or prevent reading of the molecule by polymerases (Hansen et al, 2001), and/or has single-strand breaks resulting in the omission of these endogenous fragments from standard sequencing libraries (Höss et al. 1996, Hofreiter et al. 2001, Gansauge et al. 2017). Additionally, ancient samples often contain considerably more contaminant (both modern human and environmental) DNA than authentic endogenous, effectively drowning out the recovery of host DNA during sequencing (Kolman and Tuross 2000, Gilbert et al 2005, Willerslav and Cooper 2005).

Novel DNA extraction protocols optimized for short fragment recovery (Dabney et al 2019), targeted-enrichment techniques which isolate and selectively amplify either specific areas of interest within host genomes or the entirety of the host genome itself (Briggs et al. 2009, Mathieson et al. 2015) , as well as single-stranded library preparation methods which first denature extracted DNA and then ligate sequencing primers to each resulting fragment of single-stranded DNA independently (Meyer et al. 2012, Gansauge and Meyer 2013) have been shown to substantially mitigate many of the issues surrounding the effective recovery of authentic ancient endogenous DNA sequence recovery. These techniques drastically increase the chances that significantly damaged DNA fragments are recovered and successfully sequenced (Gansauge et al. 2017). This means that, although there is an inherent difficulty involved in computationally determining if observed differences between modern and ancient genomes are authentic or merely sequencing artefacts or the result of damaged DNA templates (Lindahl 1993, Höss et al. 1996, Hofreiter et al. 2001, Prüfer et al. 2010), it is now possible to remove undamaged contaminant reads. This, combined with the greater depth of host genomic coverage (and subsequent advances in ancient DNA mapping strategies, e.g., the EAGER pipeline, Peltzer et al. 2016, Fellows Yates et al. 2021, and similar techniques) generated by the recovery of higher proportions of authentic endogenous DNA, makes it possible to detect traces of evolution and change in populations over deep time more confidently (Rizzi et al. 2012, Dehasque et al. 2020).

1.2 Extraction of DNA from ancient bone

The first successful extraction of DNA from ancient remains, from a museum specimen of the extinct Quagga, was done via the cloning of short DNA fragments in the bacterium *Escherichia coli* (Higuchi et al. 1984), soon followed by the isolation of DNA from an ancient Egyptian mummy (Pääbo 1985). With the introduction of polymerase chain reaction (PCR) techniques (Mullis 1990), DNA isolation protocols were further refined and the use of aDNA analyses began to be recognized as a viable tool for archaeological studies (Malainey 2011). The field was further bolstered after next-generation sequencing methods were adapted, (Schuster 2008; Knapp and Hofreiter 2010; Overballe-Petersen, Orlando, and Willerslev 2012) resulting in drastically increased demand for DNA analyses from ancient remains (Kaestle and Horsburgh 2002; Slatkin and Racimo 2016).

Typically, the extraction of DNA from bone samples for use in high-throughput sequencing involves the generation of bone powder from excavated remains accomplished via either the removal and subsequent milling of small portions of said remains, or through the collection of powder produced via drilling into the bone (Lassen, Hummel, and Herrmann 1994; Damgaard et al. 2015; Pinhasi et al. 2015; Campos et al. 2012; Dabney and Meyer 2019). The bone powder is then demineralized to release bound DNA, which is then isolated and purified (Rohland et al. 2018; Dabney and Meyer 2019). This process results not only in the depletion/destruction of the bone powder but can also lead to considerable damage to the remains from which it is generated.

Early aDNA analyses indicated that DNA extraction from ancient bone material harvested from areas of dense cortical bone of long bones provided optimal DNA recovery in comparison to those extractions utilizing cancellous, e.g., trabecular bone, tissue (Leney 2006; Campos et al. 2012). However, though relatively few comparative studies of aDNA preservation across ancient skeletal elements have been attempted to date (eg. Hansen et al. 2017;

Gamba et al. 2012; Sirak et al. 2020), it has since been shown that DNA can be more reliably extracted from ancient tissues such as the dentin and cementum of teeth (Adler et al. 2011; Damgaard et al. 2015; Hansen et al. 2017; Margaryan et al. 2018) and, more particularly from the densest portion of the petrous pyramid, the part of the temporal bone housing the cochlea (Gamba et al. 2012; Pinhasi et al. 2015; Hansen et al. 2017; Gaudio et al. 2019). As such, the petrous pyramid has emerged as the most sought-after skeletal element for ancient DNA analyses based on numerous highly successful studies (Llorente et al. 2015; Lazaridis et al. 2017; Harney et al. 2018; Feldman et al. 2019). Additionally, the petrous pyramid, has repeatedly been shown to be an excellent source of aDNA in cases where environmental conditions have been shown to be highly unfavourable to DNA preservation (Llorente et al. 2015; Harney et al. 2018; León et al. 2018; Feldman et al. 2019).

However, this increased demand for the petrous portion has raised ethical questions as to the benefit of its use when the potential damage to the anthropological record is taken into account (Sirak and Sedig 2019; Charlton, Booth, and Barnes 2020). Sampling of the petrous pyramid has historically involved the sectioning or sandblasting of the isolated temporal bone (Pinhasi et al. 2019) in order to access the dense region of bone surrounding the cochlear region (Pinhasi et al. 2015), though recent advancements in minimally invasive sampling have mitigated this issue considerably (Sirak et al. 2017). This is especially relevant as the petrous portion of the temporal bone is also heavily utilized in context of morphological assessments (Norén et al. 2005; Bar-Oz and Dayan 2007; Nagaoka and Kawakubo 2015) and damage to intact crania can lessen their value in terms of exhibition. These factors have subsequently induced hesitancy on the part of the curators of archaeological collections to provide these coveted samples for aDNA analyses. In addition, as techniques to amplify ancient DNA selectively (Harakalova et al. 2011; Schuenemann et al. 2011; Mathieson et al. 2015; Cruz-Dávalos et al.

2017) are becoming more readily accessible, the ability of researchers to target entire genomes of interest from more poorly preserved remains has greatly increased. As such, the systematic search for alternative sampling locations has become increasingly imperative. This has been hampered, however, by the distinct lack of published protocols detailing the successful generation of bone powder from sampling locations other than for a handful of skeletal elements (e.g., dentin, femora, and the petrous pyramid).

In Manuscript 1 of this thesis, I systematically investigate endogenous DNA preservation across twenty-three sampling locations stemming from eleven medieval individuals. I identify seven anatomical sampling locations across four skeletal elements which, while not performing as well as sampling from the *pars petrosa,* are all viable alternatives to the destructive sampling of the petrous pyramid. Furthermore, in Manuscript 2, I detail the sampling (bone powder generation) protocols that I created, optimized, utilized, and subsequently published for each of the eight, best performing anatomical sampling locations identified in Manuscript 1. The combined goal of these manuscripts is to make the efficient DNA sampling from a wider variety of ancient remains more accessible to the entirety of the aDNA community.

1.3 Analyses of ancient DNA datasets

As previously mentioned, as the methods for the generation of ancient DNA datasets have evolved, so to have the techniques for their subsequent analyses. Early aDNA studies relied on the selective isolation and analyses of relatively small portions of the genome such as diagnostic regions of mitochondrial or nuclear genomes using a targeted polymerase chain reaction. Today, however, high-throughput, next generation sequencing can generate truly massive datasets, potentially covering not only all of the host's nuclear and mitochondrial genomes, but also the genomes of the host's corresponding microbial flora, both in terms of the

microbiome (Schnorr et al. 2016; Warinner 2016; Groussin et al. 2017; Mann et al. 2018; Lugli et al. 2017) and pathogens (Drancourt et al. 1998; Bos et al. 2011; Harkins and Stone 2015; Margaryan et al. 2018; Hübler et al. 2019). The reliability of these analyses depends heavily on the authenticity and quality of the DNA recovered through the destructive sampling of ancient remains (see Section 1.1). As such, the thorough screening of those datasets for all potential informative uses, such as screening for pathogens even in the absence of historical, contextual, or osteological evidence of infection is imperative to ensure the balance between maximizing data production with the need to preserve the anthropological record.

1.3.1 Detection of ancient pathogens

Detection of ancient pathogens, from the genetic perspective, has typically involved the screening of teeth from individuals excavated from areas where there exists either direct historical evidence for plague infection such as written accounts and/or contextual evidence such as mass burial or osteological evidence of infection (Bos et al. 2016; Feldman et al. 2016). Often these targeted pathogen studies do not include substantial (if any) population genetic analyses, resulting in an incomplete picture of host-pathogen co-evolution through time. Similarly, wide ranging ancient pathogen data produced in population genetic studies of archaeological sites lacking any indicators of potential infectious disease often goes unanalysed, further hindering our understanding of host-pathogen co-evolution through deep time. This has remained the most common practice until relatively recently with the publication of ancient *Yersinia pestis* genome recovered from Bronze and Iron Age samples exhibiting no *a priori* indication of infection (Rasmussen et al. 2015), as well as studies such as that of Kocher et al. 2021.

1.3.2 The genetic history of *Yersina pestis*

Yersina pestis, the bacterium first postulated to be the causative agent of plague in 1894 by both Alexandre Yelsin and Kitsano Shibasaburo (independently during the Third Pandemic) and later genetically confirmed to also be the causative agent of the Black Death and subsequent Second Pandemic (Perry and Fetherston 1997; Drancourt et al. 1998; Raoult et al. 2000; Haensch et al. 2010; Bos et al. 2011), is one example of a pathogen species which has been identified through the screening remains without *a priori* evidence of infection (Bronze and Iron age remains: Rasmussen et al. 2015; Spyrou et al. 2018; Keller et al. 2019). *Y. pestis* primarily infects rodent populations and can be zoonotically transferred to humans via infected fleas (Vadyvaloo et al. 2010; Sun et al. 2014). This cycle of zoonotic reinfection had led to at least three major pandemic outbreaks throughout human history, such as the First Pandemic (ca. 541AD – 750AD) (Wagner et al. 2014; Feldman et al. 2016; Keller et al. 2019); Second Pandemic (ca. 1346AD – mid 18th century AD) (Benedictow 2006); and the ongoing global Third Pandemic (ca. 1772AD – Present) (Bramanti et al. 2019). Beyond these well documented pandemics, recent genetic evidence suggests that *Y. pestis* has continually infected human populations for at least the last 5,000 years (Rasmussen et al. 2015; Spyrou et al. 2018), though the severity and impact of these infections prior to the First Pandemic is still unclear.

Though the most well-known outbreak of the Second Pandemic is undoubtedly that of the Black Death, it only accounts for ca. 6 years of the ca. 400 which this pandemic spanned. The Black Death itself was introduced into Europe via trade from the Black Sea region ca. 1347. The infection then rapidly spread throughout the continent and is thought to have resulted in the death of up to half the population of Europe (Clouse 2002; Wood, Ferrell, and Dewitte-Aviña 2003; DeWitte 2014). The Black Death epidemic itself lasted for approximately

10 years (ending ca. 1356), however, subsequent outbreaks of *Y. pestis* resulted in a near continuous pandemic affecting local European populations for the better part of the next four centuries (Benedictow 2006; Bos et al. 2016). The origin of these secondary strains remains a topic of much historical debate. Two competing theories based on the same historical evidence have subsequently emerged: A). These resurgences are the result of repeated introductions of *Y. pestis* evolved from the original Black Death reservoir and travelling along trade routes (Namouchi et al. 2018). B). The original Black Death strain retreated into various local rodent refugia where new strains independently evolved and consequently spread back to human hosts periodically as these rodent populations fluctuated (Carmichael 2015, Seifert et al. 2016). In either case, all of these resurgent strains appear to be closely derived from the original Black Death Strain, with most emerging to decimate the local populations before fading into eventual extinction (e.g., the "post-Black Death lineages"; Spyrou 2019).

The proposed first re-emergence of plague post-Black Death, *Pestis secunda* (MacArthur 1949; Gottfried 2010; Namouchi et al. 2018), however, has been genetically linked to the *Y. pestis* strain thought to be the causative agent of the Third Pandemic (Spyrou et al. 2016). *Pestis secunda* was first identified in samples from a mass burial excavated in Bergen Op Zoom, Netherlands (Haensch et al. 2010, Curtis and Roosen 2017). Subsequent examples of *Pestis secunda* have also been identified a dedicated portion of the Saint Mary Graces cemetery in London (Bos et al. 2011) as well as in samples from Bolgar City Russia (Spyrou et al. 2016). While each of these examples varies slightly on a genetic level (each with its own set of private alleles), there are two distinct SNPs present in all populations and thus diagnostic for *Pestis secunda.*

In Manuscript 3 I further explore the benefits of comprehensive, combined analyses of aDNA datasets by detailing two new *Pestis secunda* genomes discovered during the screening of the dataset generated from Manuscripts A and B. One of the genomes presented in this

manuscript, a direct genetic intermediate between the Black Death and previously observed examples of *Pestis secunda*, was first identified through an untargeted, wide-ranging pathogen screening of the sequence data used in Manuscript 1. Subsequent targeted *Y. pestis* screening (including the targeted screening of ca. 50 additional individuals from the same site) and enrichment resulted in not only a > 30x coverage genome of this strain, but also a second, ca. 18x coverage, genome clustering within the previously defined clade of *Pestis secunda*. Within this manuscript, I argue that maximizing the use of datasets obtained through the destructive sampling of ancient remains is an important step towards minimizing the damage these techniques cause to the archaeological record.

1.3.3 The evolution of the human oral microbiome

Similar to investigations of potential pathogens, the study of the ancient human microbiome has become increasingly popular as large ancient metagenomic datasets are more available. This is particularly true for the oral microbiome, as ancient dental calculus has been found to be incredibly rich in microbial DNA endogenous to the biofilms present in the oral cavity (Preus et al. 2011; Warinner, Speller, and Collins 2015; Mann et al. 2018). However, as metagenomic analyses of the modern, let alone ancient, oral microbiome is a relatively new area of study, there exists significant gaps in our genetic knowledge of this microbial community. Currently, approximately 475 species of ca. 700 prokaryote species thought to make up the oral microbiome have been officially described, with reference genomes for ca. 400 taxa available (Escapa et al. 2018). Generating reference genomes of culturable genomes generally involves the deep sequencing and subsequent *de novo* assembly of DNA extracted from pure colonies. However, this same technique is not suitable for the genomes of undescribed or unculturable species, as *de novo* assembly must be attempted in a metagenomic context. As a result, the detection of, let alone the detailing of, entire genomes of many potential human oral

microbiome species and their evolution in ancient material is not effectively possible. This greatly hinders the investigation of the evolution of the oral microbiome over time by limiting the available data to only those patterns observable in the more easily isolated, already described species. Manuscript 4 outlines a method for the extraction of high molecular weight DNA stemming from known constituents of the oral microbiome from modern dental calculus samples for use in long-read sequencing (e.g., Oxford nanopore technology), which, when used in conjunction with short-read sequencing (e.g., the Illumina platform) has been shown to increase the ease and accuracy of whole genome assembly using metagenomic sequencing data (Sanders et al. 2019). This manuscript is a working proof-of-concept where I conclusively show that not only does dental calculus harbour significant amounts of recoverable high molecular weight DNA, but also that this DNA does, in fact, stem from bacterial species which have been identified as members of the human oral microbiome. Though long-read sequencing and mixed read, metagenomic assembly were not done in this initial study, it paves the way for future work in the metagenomic assembly of genomes from currently undescribed and/or unculturable constituents of the human oral microbiome.

2. Aim of the thesis

The overarching aim of this thesis is to investigate, develop, and implement methods for the more efficient use of destructive aDNA sampling from archaeological remains. The manuscripts presented here use emerging laboratory and analytical methods in aDNA to (A) help identify and characterize those sampling locations most likely to successfully yield usable quantities of aDNA; (B) make aDNA research more accessible by publishing a detailed account of the sampling methods used; (C) demonstrate the utility and necessity of more rigorous systematic screening of aDNA datasets by presenting pathogen genomes discovered through the comprehensive screening of an aDNA dataset where infection was not archaeologically apparent; and (D) develop new methods for the potential expansion of existing reference databases to make this screening more effective. The methods described within this thesis all seek to mitigate the ethical issues surrounding the use of ancient remains for DNA analyses by optimizing the generation and use of aDNA datasets in an effort to minimize potential damage to the anthropological record. More specifically, the questions studied in this thesis are as follows:

Manuscript 1:

- How much aDNA can be recovered from potential alternative sampling locations compared to that recovered from the petrous pyramid?
- What is the quality and general characteristics of aDNA extracted from these alternative sampling locations?
- Under normal laboratory and analytical constraints, how well do the datasets generated from this DNA perform in standard population genetic analyses?
- What does the performance of alternate sampling locations mean in terms of the development of sampling strategies for aDNA research?

Manuscript 2:

- Given the knowledge obtained in Manuscript 1, how can we make the generation of aDNA datasets from destructive sampling more available to the field as a whole?

Manuscript 3:

- How does the systematic screening of aDNA datasets for potential pathogens aid in the elucidation of host-pathogen co-evolution?
- Can historical *Y. pestis* infection be confidently identified in post-cranial remains?
- What is the evolutionary history of *Y. pestis* during the Second Pandemic?
- Where did the post-Black death emergence of *Pestis secunda* potentially originate?

Manuscript 4:

- Is it possible to extract high-molecular weight microbial DNA from modern dental calculus samples?
- Are known constituents of the human oral microbiome identifiable in these metagenomic high-molecular weight DNA datasets?
- How can this then translate into expanding the reference pool of the human oral microbiome?

3. Manuscript 1

"A systematic investigation of human DNA preservation in medieval skeletons"

Cody Parker, Adam B. Rohrlach, Susanne Friederich, Sarah Nagel, Matthias Meyer, Johannes Krause, Kirsten I. Bos, Wolfgang Haak

Published: Scientific Reports, 26/10/2020

Parker, C. E., Bos, K. I., Haak, W., & Krause, J. (2021). Optimized Bone Sampling Protocols for the Retrieval of Ancient DNA from Archaeological Remains. *JoVE (Journal of Visualized Experiments)*, *177*, e63250. https://doi.org/10.3791/63250

The field of ancient human DNA analyses is tasked with maintaining a strong ethical balance between the generation of data elucidating the genetic history of our species via the destructive sampling of archaeological remains and the need to preserve the anthropological record whenever possible by maximizing data output and sampling efficiency. In Manuscript 1 we sampled multiple locations across ten skeletal elements from each of eleven individuals excavated from the abandoned medieval cemetery associated with Krakauer Berg, near Peißen, Saxony-Anhalt, Germany to systematically evaluate ancient DNA recovery across the human skeleton (a total of 246 sampling efforts). We analysed multiple metrics of DNA quantity and quality including percentage of human DNA recovered in respect to total DNA, library complexity, the ratio of nuclear DNA recovered in respect to mitochondrial DNA, deamination patterns, and suitability for downstream processes (e.g., bait-capture efficacy and Y-haplotype resolution). Additionally, using mixed effect modelling we were able to simulate 55,000 separate sampling efforts to create a predictive model of how often each sampling location was likely to return the highest yields of human DNA. We found that, as expected, material stemming from the dense cochlear region of the petrous pyramid performed best in terms of raw

human DNA recovery. However, we also observed that seven other sampling locations across four alternative skeletal elements (material from the cementum, dentin, and pulp chamber of *in situ* molars; cortical bone from the vertebral body and superior vertebral arch, cortical bone from the distal phalanx, and dense tissue harvested from the exterior of the talus), which while yielding less human DNA overall than the petrous pyramid, perform similarly in all other contexts, including downstream applications commonly used in ancient population genetics studies.

Note: The referenced "Supplementary File 1," is comprised of a single, large data table in excel format, and as such can be accessed online as part of the accepted manuscript.

Author contributions

CP is the primary author (75%) and was responsible for the majority of laboratory work, including the gathering, processing, sampling from, and DNA extraction from all samples (80%), as well as their subsequent analyses (40%). Additionally, CP aided in the experimental design of the project (20%). ABR performed all statistical analyses and coding, as well as authoring the corresponding methods sections and the editing of the overall manuscript. SF of the State Office for Heritage Management and Archaeology, Saxony-Anhalt (State Museum of Prehistory, Halle (Saale)) contributed archaeological remains sampled in this study and the archaeological context. SN produced single-stranded libraries for all samples at the Max Planck Institute for Evolutionary Anthropology, Leipzig, Germany. MM oversaw single-stranded library preparation at the Max Planck Institute for Evolutionary Anthropology, Leipzig, Germany, aided in the editing of the manuscript. KB acted as co-

supervisor to the primary author, provided funding, aided in the experimental design of this study, and contributed to the writing and editing of this manuscript. WH acted as co-supervisor to the primary author, provided funding, aided in the experimental design of this study, coordinated sample selection, and contributing to the writing and editing manuscript. JK acted as co-supervisor to the primary author, aided in experimental design, and provided funding for the study.

Author	Conception	Data analyses	Experimentation	Writing	Sample procurement
C.P.	20%	40%	80%	75%	0%
A.B.R.	N/A	60%	N/A	5%	N/A
S.F.	5%	N/A	N/A	N/A	90%
S.N.	N/A	N/A	15%	N/A	N/A
M.M.	N/A	N/A	5%	N/A	N/A
J.K.	25%	N/A	N/A	N/A	N/A
K.B.	25%	N/A	N/A	10%	N/A
W.H.	25%	N/A	N/A	10%	10%

scientific reports

OPEN

A systematic investigation of human DNA preservation in medieval skeletons

Cody Parker[1]✉, Adam B. Rohrlach[1,2], Susanne Friederich[3], Sarah Nagel[4], Matthias Meyer[4], Johannes Krause[1]✉, Kirsten I. Bos[1] & Wolfgang Haak[1]✉

Ancient DNA (aDNA) analyses necessitate the destructive sampling of archaeological material. Currently, the cochlea, part of the osseous inner ear located inside the petrous pyramid, is the most sought after skeletal element for molecular analyses of ancient humans as it has been shown to yield high amounts of endogenous DNA. However, destructive sampling of the petrous pyramid may not always be possible, particularly in cases where preservation of skeletal morphology is of top priority. To investigate alternatives, we present a survey of human aDNA preservation for each of ten skeletal elements in a skeletal collection from Medieval Germany. Through comparison of human DNA content and quality we confirm best performance of the petrous pyramid and identify seven additional sampling locations across four skeletal elements that yield adequate aDNA for most applications in human palaeogenetics. Our study provides a better perspective on DNA preservation across the human skeleton and takes a further step toward the more responsible use of ancient materials in human aDNA studies.

The study of ancient DNA (aDNA) has progressed rapidly over the past decade following the introduction of next generation sequencing[1–3], where genome-level analyses of archaeological specimens are now standard[4–12]. The increased analytical resolution offered by large scale datasets, coupled with the establishment of laboratory techniques that permit parallel processing of large sample sizes, has resulted in an increasing demand for ancient skeletal samples for assessment of human population genetics, microbiome ecology, and investigations of pathogen evolution. Laboratory processing of ancient remains is intrinsically a destructive process[13–16], which poses ethical challenges related to the use of irreplaceable resources. Coupled with the high processing costs of aDNA work (from the perspective of both financial and time investments), there is benefit in optimizing approaches for material sampling. Multiple investigations have demonstrated superior human aDNA preservation in the dense inner petrous pyramid, the portion of the temporal bone that houses the inner ear. This observation is based on a collection of comparative PCR[15,17–20] and whole genome aDNA surveys[16–18,21,22] that were often limited in either the number of individuals and/or skeletal elements tested. Despite the paucity of a systematic comparative analysis of preservation across the skeleton, aDNA obtained from the petrous portions of human remains has been utilized to great success in the contexts of both ancient human population genetics (e.g.[23–27]) and forensic investigations[17,28].

Historically, sampling of the isolated petrous pyramid has typically involved sectioning or sand-blasting of the temporal bone to isolate the cochlea[16], making this a highly destructive process[13]. Recent advances in minimally invasive sampling techniques[29] have led to a better balance between preservation of the anthropological record and the need for the production of reliable genetic data[30,31]; however, the threat of damage to internal microstructures that form an important basis of morphological assessments[32–34] can still introduce hesitancy on the part of curators and physical anthropologists in making the petrous pyramid available for aDNA applications. These factors, in conjunction with the chance of incomplete recovery of crania at excavation[35] or restricted sampling of highly valued skeletal samples, make the identification of alternative sampling locations based on quantitative evaluations of DNA preservation across the skeleton of clear benefit. Teeth have been widely used for the study of aDNA[36,37], though the 30-fold covered genome of an archaic hominin from Denisova Cave from a distal phalanx demonstrates molecular preservation in elements that are not typically considered for paleogenetics work[4]. Despite these successes, a systematic and extensive study of differential DNA preservation across multiple

[1]Max Planck Institute for the Science of Human History, Jena, Germany. [2]ARC Centre of Excellence for Mathematical and Statistical Frontiers, The University of Adelaide, Adelaide, SA, Australia. [3]Landesamt für Denkmalpflege und Archäologie, Sachsen-Anhalt, Halle (Saale), Germany. [4]Max Planck Institute for Evolutionary Anthropology, Leipzig, Germany. ✉email: parker@shh.mpg.de; krause@shh.mpg.de; haak@shh.mpg.de

Skeletal element	Rationale	Sampling location	Rationale
Molar (n = 11)	Widely used in aDNA studies and easily available, in situ molars preferentially selected for best preservation	Cementum	Previously shown to be an excellent source of ancient human aDNA[21]
		Dentin	Frequently used in aDNA studies[14,15,36,55]
		Pulp	Preferred option in pathogen (i.e. *Yersinia pestis*) studies[34,67,70]
Petrous pyramid (n = 11)	Currently most sought-after skeletal element for aDNA research	Dense cochlear portion	Currently considered the best source of endogenous ancient human DNA[21,22]
Clavicle (n = 10)	Highly vascularized tissue, not studied in terms of aDNA retention	Cortical bone from shaft	Cortical bone previously shown to harbour the most endogenous human aDNA[36,48]
		Cancellous bone from facet	Richly vascularized[a]
Rib (n = 11)	Readily available	Cortical bone from shaft	Cortical bone previously shown to harbour the most endogenous human aDNA[36,48]
		Cancellous bone from facet	Richly vascularized[a]
Thoracic vertebrae (n = 11)	Readily available	Cortical bone from spinous process	Cortical bone previously shown to harbour the most endogenous human aDNA[36,48]
		Cortical bone from vertebral body	Cortical bone previously shown to harbour the most endogenous human aDNA[36,48]
		Cancellous bone from vertebral body	Richly vascularized[a]
		Cortical bone from neural foramen	Cortical bone previously shown to harbour the most endogenous human aDNA[36,48]
		Cortical bone from superior vertebral arch	Cortical bone previously shown to harbour the most endogenous human aDNA[36,48]
Metacarpal (n = 11)	Readily available	Cortical bone from shaft	Cortical bone previously shown to harbour the most endogenous human aDNA[36,48]
		Cancellous bone from head	Richly vascularized[a]
Distal phalanx (n = 10)	Shown previously to be a good source of ancient human DNA[4]	Cortical bone from pad	Cortical bone previously shown to harbour the most endogenous human aDNA[36,48]
		Cancellous bone from head	Richly vascularized[a]
Ischial tuberosity (n = 9)	Dense, weight bearing bone not studied previously for aDNA retention	Cortical bone from exterior surface	Cortical bone previously shown to harbour the most endogenous human aDNA[36,48]
		Cancellous bone from interior	Richly vascularized[a]
Femur (n = 11)	Long-bone commonly used in the early aDNA studies[46]	Cortical bone from shaft	Cortical bone previously shown to harbour the most endogenous human aDNA[36,48]
		Cancellous bone from head	Richly vascularized[a]
Talus (n = 10)	Dense, weight bearing bone, not studied previously for aDNA retention	Cortical bone and compacted cancellous bone from exterior surface	Consists primarily of densely compacted trabecula with a very thin coating of cortical bone
		Cancellous bone from interior	Richly vascularized[a]

Table 1. Sampling locations across all skeletal elements and the rationale behind each. [a]Vascularization has been theorized to effect the recovery of pathogen DNA from ancient remains[37,69], and as such was used as a selection criteria in order to assess if there is a similar effect on host DNA preservation.

human skeletal elements, such as those done in the context of modern forensics[38,39], has yet to be attempted on archaeological remains. Our limited understanding of DNA preservation across the human skeleton is a significant hurdle for the efficient, practical, and ethical study of aDNA, which has particular relevance to the field of ancient population genetics where large sample sizes are needed for robust analytical resolution.

DNA preservation can be influenced by many factors. Chronological age shows some relationship with the deamination of terminal bases, though this has been demonstrated to play a secondary role to other factors such as environmental and climatic conditions contributing to the overall thermal age of a sample[40,41]. Additionally, burial practises, post-mortem treatment of the deceased, and geology may also influence DNA survival[42]. Beyond these historical factors affecting DNA preservation, laboratory processing methods, such as bleach pre-treatments to remove contamination (e.g.[43–45]), may also affect DNA recovery from a sample. To serve as a baseline for future investigations seeking to incorporate and extrapolate the effects of these sources of variation, e.g. across other species, time series, or geographic regions we present a broad survey of aDNA preservation across a range of skeletal elements. Our source material, consequently, has been deliberately restricted to one archaeological site and time period to control for these factors that can influence molecular recovery as much as possible. The range of elements chosen for this survey consist of petrous bones (chosen for their demonstrated value in aDNA recovery[21,22]), in situ molars, clavicles, the first ribs, thoracic vertebrae, metacarpals, distal phalanges, ischial tuberosities, femora (once widely used in ancient DNA studies[46]), and tali. Multiple locations on each element were sampled from and evaluated for DNA content. A detailed list of skeletal elements, sampling locations and the rationale for why each element was selected for study is provided in Table 1 (see also Supplementary Material: Section 1.2; additionally, for discussion of the sampling of epiphyseal plates, which were not present in sufficient numbers for statistical analyses, see Supplementary Material: Section 2.5). Differential DNA preservation across these elements was investigated in individuals excavated from the church cemetery associated with the

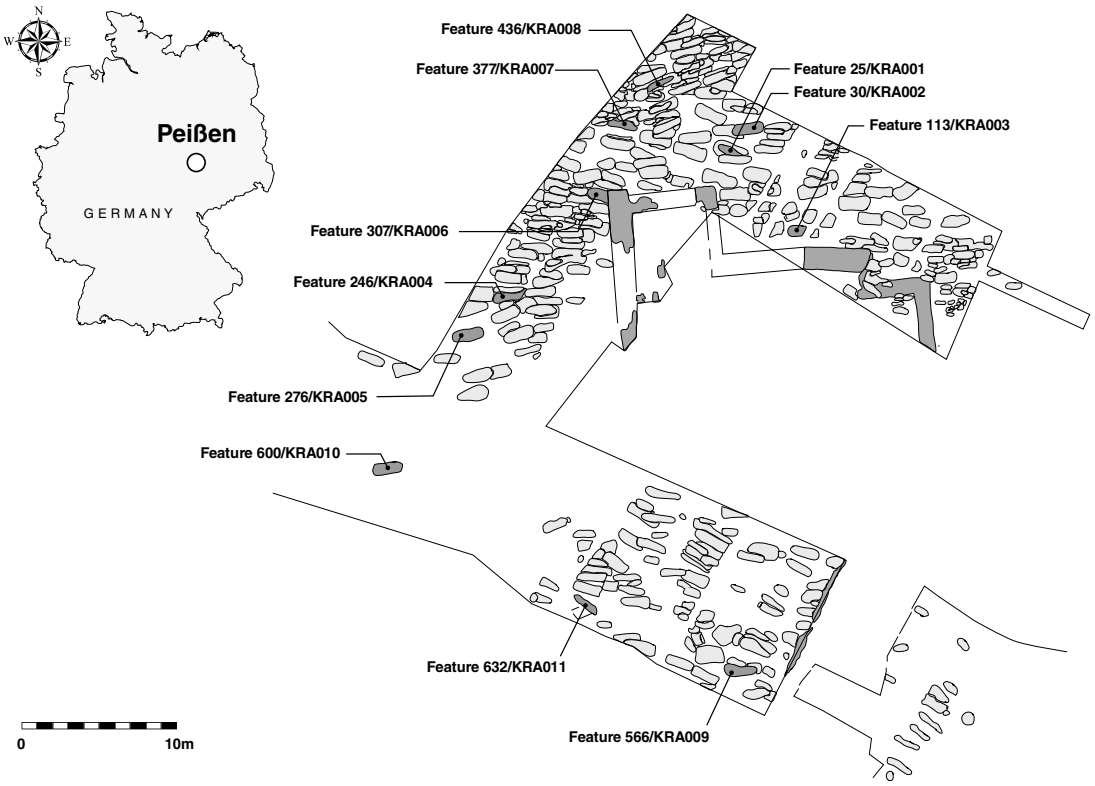

Figure 1. Map of the Krakauer Berg excavation. Graves corresponding to individuals sampled are denoted with both the archaeological ID and assigned sample name.

abandoned medieval settlement of Krakauer Berg, near Peißen, Saxony-Anhalt, Germany (Fig. 1). Overall, the site exhibited excellent morphological preservation, as expected from a medieval burial in a temperate region. Though preservation of this scale is often not observed in older material or that obtained from climatic regions less suited to molecular preservation, the sampling from complete (or nearly complete) skeletons was a prerequisite for this study in order to maximize the comparability of the elements selected for analyses while also maximizing the chances of successful DNA extraction from each sampling location. It should be noted that the findings of this study are presented as a first systematic exploration of human DNA preservation within a single temporal and geographic context. Whether the trends we report will scale globally can only be determined via similar undertakings of material that derives from different preservation contexts.

To our knowledge, this study presents the most comprehensive systematic evaluation of aDNA preservation across the human skeleton in the published literature. While we further confirm the superior performance of cortical bone stemming from the cochlear portion of the petrous pyramid to yield the highest amounts of recoverable human DNA[21,22,47], several alternative sampling locations are identified as suitable for downstream population genetic analyses such as the tali, distal phalanges, vertebrae, and teeth.

Results

Our analytical matrix consists of shotgun sequencing data from single-stranded DNA libraries stemming from 23 separate sampling locations paired end sequenced (2 × 75 cycles) to approximately 5,000,000,000 reads each (Table 1; Supplementary File 1: Source; Raw reads sequenced). These were obtained from ten skeletal elements from each of eleven individuals who were all buried, excavated, documented, stored, sampled from, and ultimately processed and sequenced under the same conditions, in order to eliminate as many confounding variables as possible. All individuals selected for study had at least nine elements available, and all elements were present in at least nine individuals. In total, this resulted in 246 single-stranded aDNA libraries for comparison. In addition, as the use of hybridization capture technology in aDNA studies has become a popular alternative to shotgun sequencing[27], an additional 87 libraries were subsequently enriched by hybridization capture for 1,240,000 informative variant SNPs across the human genome using the 1240k[27] human SNP array and paired end sequenced (2 × 75 cycles) to a depth of approximately 40 million reads each. Our goals in evaluating this dataset are to ascertain which of the chosen sampling locations are most efficient in terms of authentic host DNA recovery, processing cost, and limiting damage to the anthropological record. To achieve a balance between aDNA

recovery and drilling damage, as well as to more accurately compare the expected yields from a single instance of sampling, each sampling location was screened only one time. Additionally, all skeletal remains were sampled from approximately the same location on each bone by the same worker (CP) in order to minimize differences in DNA yield and quality stemming from the natural variations in DNA preservation within each individual skeletal element and the effect of inter-observer variations in sampling procedures (i.e. potential variations from one area of a bone to the next[48]). Analyses normalized in terms of input material available from each sampling location can be found in the provided Supplementary text in Section 2.4. The results for each metric examined in this study are presented in the chronological order in which they are typically assessed, in the experience of the research team, and are not prioritized in any subjective order of importance.

One of the most frequently used metrics for the evaluation of successful DNA recovery in human archaeological material is the proportion of human DNA recovered relative to DNA from other sources. This is often the first criterion considered to determine if a sample is suitable (both economically and analytically) for further testing. In this context we examined the average proportion of total (prior to duplicate removal) human DNA recovered post paired-end read merging, accommodating filters for sequence length and mapping quality (see "Methods": Eq. 1). Among the 23 sampling locations we find the highest average proportion of human DNA in the petrous pyramid (34.70% human DNA on average), followed by dense tissue obtained from the neck and articular surfaces of the talus (21.25%), the cementum (18.97%), cortical bone from the distal phalanx (18.89%), material from the dental pulp chamber (15.09%), cortical bone from the vertebral body (15.04%), the dentin (14.27%), and cortical bone from the superior vertebral arch (8.32%). All other sampling locations evaluated contained an average human DNA proportion lower than the overall average of 8.16% (Fig. 2a, Supplementary File 1: % mapping q37) across all elements tested.

To provide a realistic approximation of the cost efficiency of human DNA retrieval from each sampling location and to estimate complexity within each single-stranded library, we further compared the average number of unique human reads per million reads of sequencing effort across all samples (see "Methods": Eq. 2). Here we again find the highest average in the petrous pyramid (1.14×10^5 unique reads mapping per million), followed by the talus (6.43×10^4 unique reads mapping per million), the dental pulp chamber (5.26×10^4 unique reads mapping per million), the distal phalanx (5.23×10^4 unique reads mapping per million), cementum (4.89×10^4 unique reads mapping per million), the vertebral body (4.81×10^4 unique reads mapping per million), the dentin (4.76×10^4 unique reads mapping per million), and the superior vertebral arch (2.79×10^4 unique reads mapping per million). All other sampling locations fall below the overall average of 2.43×10^4 (Fig. 2b, Supplementary File 1: Unique reads/million reads). Furthermore, an average unique reads/million lower than that found in the highest of our extraction blanks (2.96×10^3 unique reads per million) was observed in all sampling locations on the ribs and clavicula, as well as cancellous material from the ischial tuberosities. When normalized to reflect the amount of input material from each sampling effort, we find those sampling locations with the lowest available input material to yield the highest average number of unique mapping reads per million per mg of input material, followed by the petrous pyramid (cementum: 3751 unique reads mapping/million reads/mg, material from the pulp chamber: 2736 unique reads mapping/million reads/mg, and petrous pyramid 2087 unique reads mapping/million reads/mg) (Supplementary Figure S14, Supplementary File 1: Unique reads/mg/million), suggesting that material from the cementum and dental pulp chamber may be especially rich in human DNA.

While human DNA content in the negative controls was relatively high on average (10.77%), this metric is not directly informative for the evaluation of potential contamination as there are comparatively few DNA molecules in negative controls and as a result high numbers of amplification rounds are typically required, yielding an abundance of clonal PCR duplicates (see Supplementary File 1: Reads raw sequencing effort, Reads after merging, and Unique reads/million reads). The number of unique mapping reads per million is, therefore, a more informative metric.

Here the average among our controls is an order of magnitude lower than what we report for our samples (an average of 1.67×10^3 unique reads mapping per million in extraction blanks vs an average of 2.43×10^4 unique reads mapping per million reads overall; see Supplementary File 1: Unique reads/million reads). Using this approach, we considered all individual sampling efforts that yielded a lower number of unique reads/million than what was observed in the highest of the negative controls (2.96×10^3 unique reads mapping/million reads) to be unsuccessful, regardless of potential authenticity as determined by characteristic patterns of DNA decay typically indicating ancient origin. (see Supplementary File 1: Damage signals). With this in mind, however, all "failing" samples were retained for all downstream comparative analyses so as to more accurately represent the expected outcomes of sampling efforts across a given sampling location. We additionally observed that all cancellous samples, as well as cortical bone samples stemming from ribs, claviculae, metacarpals, ischial tuberosities, femora, neural foramen and spinous process of the thoracic vertebrae (15 sampling locations, $n = 158$) exhibited average human DNA contents lower than the overall averages (> 8.16% for human DNA proportion, and 2.43×10^4 for unique human reads/million reads) making them unlikely to be among the most efficient sampling locations in any metric. Accordingly, we removed these sampling locations from further analyses to allow for the deeper investigation of the remaining eight sampling locations consisting of the dentin, cementum, and dental pulp chambers as well as cortical bone from the cochlear portion of the petrous pyramid, vertebral body, superior vertebral arch, distal phalanx, and talus (eight sampling locations, $n = 87$).

Restriction of our dataset to these eight sampling locations also permitted generation of a predictive model of expected human DNA yields via mixed effects beta regression (Fig. 2c). Using this approach, we were able to account for unavoidable sources of variation such as those stemming from individual preservation at particular skeletal locations (i.e. the natural variability among sampling locations across individuals). Due to the high variability of the proportion of human DNA recovered across both sampling locations and individuals, 55,000 iterations of this simulation were run to evaluate overall consistency of the expected proportion of human DNA recovered from each sampling location (Supplemental Material: Table S1). Here, the petrous pyramid

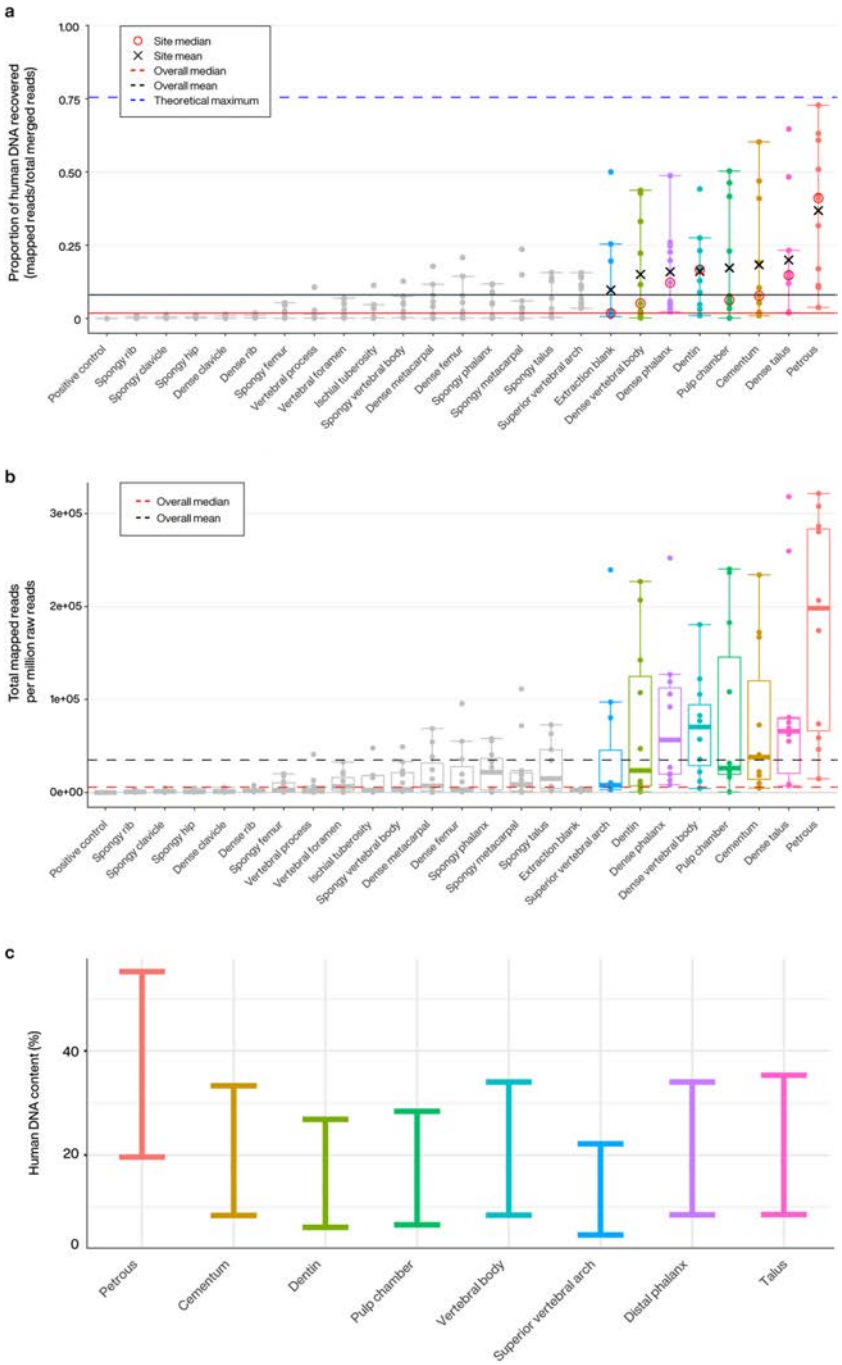

Figure 2. (**a**–**c**) Human DNA content for all screened samples. Black lines represent the overall mean, red the median (solid: human DNA proportion, dashed: mapped human reads per million reads generated). Individual sampling locations with an average human DNA proportion higher than the overall mean (8.16%) are colourized in all analyses. (**a**) Proportion of reads mapping to the hg19 reference genome. The blue dashed line represents the theoretical maximum given the pipeline's mapping parameters (generated using Gargammel[94] to simulate a random distribution of 5,000,000 reads from the hg19 reference genome with simulated damage). Individual means (black X) and medians (red circle) are reported for those samples sites with a higher average human DNA proportion than the overall mean. (**b**) Number of unique reads mapping to the hg19 reference genome per million reads of sequencing effort (75 bp paired end Illumina). (**c**) Predicted range of expected human DNA recovery (in proportion of total reads) for each top scoring sampling site. Predictions were generated using a beta-fitted mixed effects model to simulate 55,000 sampling iterations.

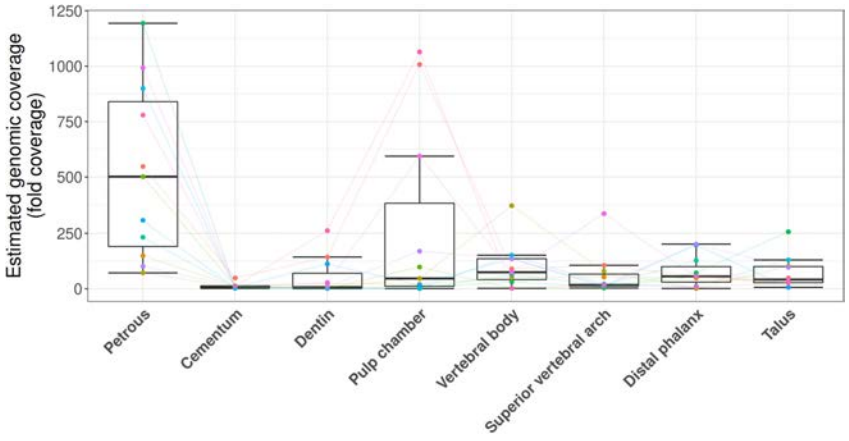

Figure 3. Estimated fold coverage of the hg19 reference genome contained within each single-stranded library. Coloured points and lines denote sampling across individuals.

significantly outperformed all other tested elements in terms of the expected range of proportions of recovered human DNA (all p-values < 0.0279), and yielded the highest predicted proportion of human DNA in the greatest number of simulations (41.87% of 55,000 simulations). The seven remaining alternative sampling locations on four other elements, although second to the petrous pyramid, also exhibited excellent human DNA recovery with yields statistically indistinguishable from each other (p-values > 0.1) (Fig. 2c). The distal phalanx, vertebral body, cementum and talus yielded the highest proportion of human DNA in 9.93–10.61% of simulations, followed by the pulp chamber, dentin, and superior vertebral arch, which yielded the highest proportions in 4.28–7.22% of the simulations.

Although the proportion of human DNA is vitally important for the identification of suitable sampling locations, both the quantity and quality of that DNA are also important for the success of downstream analyses. With that in mind, we examined several additional aspects of DNA preservation. As many studies require the confident assignment of genetic variants at individual loci, it is important that aDNA libraries are of sufficient complexity and show low signals of contamination with present-day human DNA. The aDNA libraries produced in this study were not sequenced to exhaustion, and as a consequence duplication rates were too low to be informative in terms of estimating library complexity in both the pre-enrichment libraries (average duplication factor 1.21) and the post-capture libraries (average duplication factor 1.22) (see Supplementary File 1: Duplication factor). Instead, we used the number of unique molecules in each library as determined by quantitative PCR and the proportion of mapped sequences to estimate the total genomic coverage within each library[49] as a predictor of library complexity (see "Methods": Eq. 3). The range of estimated genomic coverages within each sampling location was asymmetrically distributed and the data were subsequently transformed by a factor of $X^{0.1}$ in order to fit a linear model, as suggested by Box–Cox transformation, to evaluate significance (untransformed data is shown in Fig. 3 and Supplementary file 1: Est. genomic coverage; for transformed analyses see Supplementary Figure S11). Here, the petrous pyramid has the greatest potential to provide higher genomic coverage from an individual library (untransformed median estimated genomic coverage 501.55×, p-values < 0.0056), where all other sampling locations aside from the cementum were statistically indistinguishable (untransformed median estimated genomic coverages for each sampling location: 74.54× for the vertebral body, 55.94× for the phalanx, 46.51× for the pulp chamber, 41.44× for the talus, 17.38× for the superior vertebral arch, and 7.14× for dentin). DNA libraries derived from cementum yielded significantly lower estimates of genomic coverage within each library compared to all other sampling locations (untransformed median of 10.42×, p-values < 0.047) except for those libraries from dentin and the superior vertebral arch (Fig. 3). Normalized for input material, cementum yielded slightly higher median genomic coverage than that observed in the dentin and superior vertebral arch (0.46×, 0.16×, and 0.31× per mg input respectively) while the petrous pyramid yielded the highest (7.96× per mg input), followed by material from the pulp chamber (2.14× per mg input) (see Supplementary Figure S15, Supplementary File 1: Est. genomic coverage/mg).

Additionally, we find significant variation in both the frequency of C → T damage caused by nucleotide misincorporations at the ends of the reads and how far into the reads this signal can be detected (Fig. 4, Supplementary File 1: Damage signals). Within sampling locations, variations in the frequency of C → T damage patterns were very low (Supplementary Figure: S13, Supplementary File 1: Damage signals), suggesting that the observed variations across sampling locations are unlikely to result from modern human contamination. Reads generated from the petrous pyramid have the highest damage signal, a 5′ terminal C → T frequency of approximately 21% on average (all pairwise comparison p-values < 0.001). By comparison, cementum shows significantly lower signals than all other sampling locations (all pairwise comparison p-values < 0.001), with approximately half this frequency of damage at the terminal 5′ position. The distal phalanx, talus, and vertebral body form a statistically indistinguishable group with deamination frequencies slightly higher on average compared to the

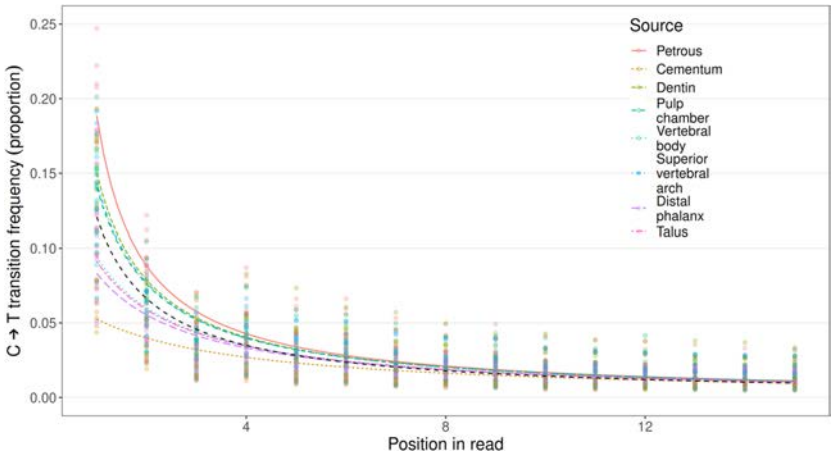

Figure 4. Average proportion of C → T transitions as observed in the first 15 reads of the 5′ end of reads. The black line represents the mean damage observed across all elements and individuals. Coloured lines indicate the average proportion of transitions within sampling locations, while points represent the corresponding range of individual data within each sampling location.

Sampling location	Average cluster factor (#all mapping reads/#unique reads) pre-enrichment (post-enrichment)	Average fragment length (median) in bp	Contamination estimates (X chromosome; average proportion of human DNA)	Average number of SNPs covered on X at ≥ 3× (per million reads)
Petrous pyramid	1.188 (1.159)	65.40 (60.09)	0	73.83
Cementum	1.197 (1.288)	67.28 (61.36)	0.011	94.78
Dentin	1.188 (1.283)	60.22 (55.54)	0.002	57.33
Pulp	1.179 (1.206)	55.14 (50.55)	0.013	44.88
Distal phalanx	1.191 (1.257)	65.95 (59.36)	0.013	127.75
Vertebral body	1.194 (1.247)	66.14 (60.54)	0.008	119.71
Superior vertebral arch	1.190 (1.208)	63.02 (57.91)	0.021[a]	51.13
Talus	1.198 (1.206)	68.20 (62.40)	0.011	92.50

Table 2. Duplication levels, average fragment length, and X chromosome contamination estimates for top performing sampling locations. [a]The sample from KRA005 was removed as an outlier with a very high (0.195) contamination estimate.

cementum, followed by the dentin, the dental pulp chamber, and the superior vertebral notch, with deamination frequencies lower than the petrous pyramid but higher than the aforementioned group (all pairwise comparison p-values between groupings < 0.001).

Contamination estimates based on X chromosome mapping coverage were calculated for all enriched libraries originating from individuals genetically assigned as male (n = 7, 8 samples per individual, 56 total samples) using the ANGSD pipeline[50] to scan known informative SNPs on the X chromosome for polymorphisms. All but one of the 56 samples exhibited low contamination with values statistically indistinguishable across sampling locations (< 4% X chromosome contamination for all enriched libraries from all sampling locations other than the superior vertebral arch of individual five (KRA005), which exhibited contamination levels of 19.52%; p-value = 0.48; see Table 2; also see Supplementary Materials Section 2.6: Additional measures of contamination and discussion of mitochondrial contamination estimates[51,52]).

Average read lengths and the ratio of nuclear genome read recovery to those mapping to the mitochondrial genome (NUC/MT) were also evaluated across the eight sampling locations with the highest average human DNA proportions. After filtering to remove all reads < 30 bp, the dental pulp chamber housed significantly shorter reads in comparison to all other sampling locations except for dentin (averages of approximately 55 bp and 60 bp respectively, pair-wise p-values < 0.019) (Table 2, Supplementary File 1: Average length), with no significant variation observed between any other sampling locations. An asymmetrical distribution of the NUC/MT ratio was observed within sampling locations and as such was transformed by a factor of $X^{0.5}$ to fit our model (for visual analyses of transformed data see Supplementary Figure S12). We find that nuclear reads were lowest in dentin (untransformed median 1:2769, p-values < 0.011), followed by the pulp chamber (untransformed median 1:539 and not significant when compared to cementum, p-value > 0.45), with all other sampling locations statistically indistinguishable (individual untransformed medians 1:64 in the vertebral body, 1:94 for the distal phalanx,

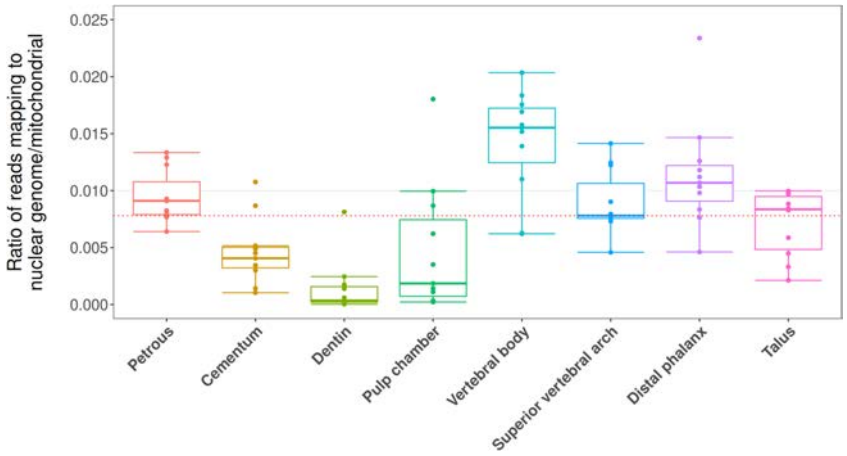

Figure 5. Ratio of reads originating from the nuclear genome to those of the mitochondrial genome. The black line denotes the overall average, the red the overall median.

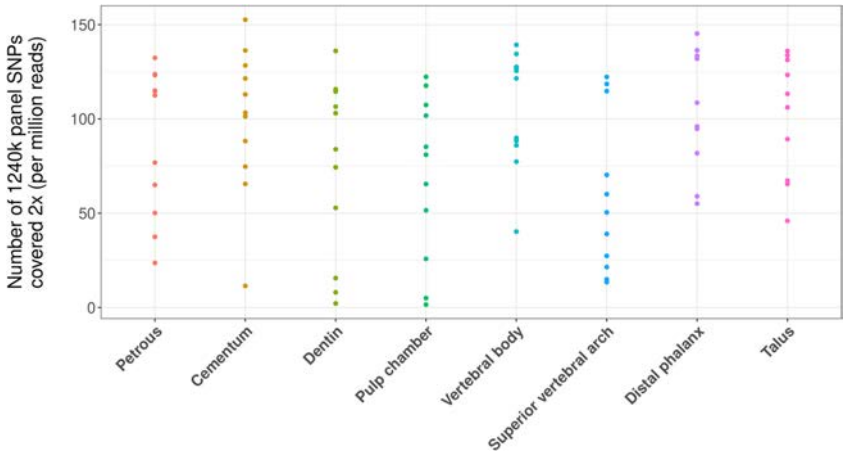

Figure 6. Comparison of 1240k SNP positions covered at least 2× post-capture across skeletal elements normalized by sequencing effort (number of raw reads generated) shown in SNPs per million reads generated.

1:109.86 in the petrous pyramid, 1:128 in the superior vertebral arch, and 1:246 in the cementum) (Fig. 5, Supplementary File 1: NUC/MT). Average GC content was calculated for all libraries from the eight sampling locations with average human DNA proportions higher than the mean (8.16%) and ranged between 37.14% and 39.87% (see Supplementary File 1; GC content).

Since many aDNA analyses, especially those used in population genetics, require a relatively high coverage of informative loci across the genome, libraries are often enriched for these loci by targeted capture. In our case, this was done for the eight sampling locations that yielded human DNA in proportions higher than the calculated mean for our dataset. To determine the practical usability of the data generated, we compared the relative number of SNPs covered by at least two reads (per million reads sequencing depth) post-1240k capture-enrichment across these eight sampling locations. Here we find that SNP coverage per million reads sequencing effort is statistically indistinguishable between sampling locations. Given that these libraries were not sequenced to exhaustion, this strongly suggests all of these sampling locations are equally suited for SNP analyses at our current sequencing depths (Fig. 6). When normalized for available input material the cementum provided significantly higher SNP coverage than all other sampling locations (p-values < 0.02) (see Supplementary Figure S16). As an alternative example of practical usability, we also investigated the phylogenetic resolution for Y-haplotype assignment among all seven male individuals using the ISOGG list of diagnostic SNPs (current as of 26 November 2019) to determine how confidently Y-haplogroups could be called at the approximately 40 million read sequencing depth considered here. The resolution of Y-haplotype assignment was high across most elements and individuals (Table 3). In two individuals (KRA003 and KRA004), the dentin and pulp chamber had a much lower resolution

Individual	Y-haplogroup resolution (ISOGG SNP positions covered)							
	Petrous	Cementum	Dentin	Pulp	Superior vertebral arch	Vertebral Body	Distal phalanx	Talus
KRA001	R1a1a1b1a1a1c (24,624)	R1a1a1b1a1a1c1 (22,102)	R1a1a1b1a1a1c (20,192)	R1a1a1b1a1a1c (16,052)	R1a1a1b1a1a1c (23,345)	R1a1a1b1a1a1c1 (17,492)	R1a1a1b1a1a1c (8383)	R1a1a1b1a1a1c (11,475)
KRA003	R1a1a (6540)	R1a1a1b1a1a (20,569)	R (1060)	R (2919)	R1a1a1b1a1a1c (22,012)	R1a1a1b1a1a1c1 (28,747)	R1a1 (9689)	R1a1a1 (16,716)
KRA004	I1a2a1a1d (26,477)	I1a2a1a1d (26,305)	N/A[a] (271)	I1 (7186)	I1 (2682)	I1a2a1a1d (16,032)	I1a2a1a1d (28,127)	I1a2a1a1d (24,327)
KRA005	E1b1b1a1b1a (29,675)	E1b1b1a1b1a (27,699)	E1b1b1a1b1a (14,366)	E1b1b1a1b1a (15,098)	E1b1b1a1b1 (5470)	E1b1b1a1b1a (27,296)	E1b1b1a1b1a (30,390)	E1b1b1a1b1a (33,106)
KRA008	I2a1a2b1a1a (9606)	I2a1a2b1a1 (28,209)	I2a1a2b1a1 (26,795)	I2a1a2b1a1 (17,317)	I2a1a2b1a1 (10,267)	I2a1a2b1a1a (26,993)	I2a1a2b1a1a (28,079)	I2a1a2b1a1 (10,683)
KRA009	R1a1 (4616)	R1a1a1b1a1a (11,042)	R1a1a1b1a1a1c (16,815)	R1a1a1b1a1a1c (16,942)	R1a1a1b1a1a1c1 (12,172)	R1a1a1b1a1a1c1 (23,230)	R1a1a1b1a1a1c (30,160)	R1a1a1b1a1a1c1 (30,787)
KRA010	J2b2a1a1a1a1a (22,337)	J2b2a1a1a1a1a1a (23,201)	J2b2a1a1a1a1a1a (21,564)	J2b2a1a1a1a1a1a (28,040)	J2b2a1a1a1a1a1 (27,044)	J2b2a1a1a1a1a1a (26,140)	J2b2a1a1a1a1a (24,591)	J2b2a1a1a1a1a1a (24,697)

Table 3. Y-haplotyping resolution post-1240k enrichment across all males and associated sampling locations. [a]Zero resolution in Y-haplotyping.

compared to other elements; however, this is most likely an artefact of the low human DNA proportions observed in these samples both before and after SNP capture (Supplementary File 1: % mapping q37, Sheets 1 and 2 respectively), rather than any biological trend.

Discussion

Based on previous successes in DNA recovery, the petrous pyramid is currently the most sought-after skeletal element for aDNA analyses[21–27]. Our investigation of multiple skeletal elements further confirms the value of the petrous pyramid in the recovery of ancient human DNA (Fig. 2a–c). We also find that single-stranded aDNA libraries constructed from material retrieved from the cochlear region of the petrous pyramid are higher in complexity (in terms of the estimated genomic coverage within each library) than those stemming from all other tested sampling locations (Fig. 3) in line with previous studies[21,28,29]. Importantly, however, libraries stemming from the petrous pyramid performed comparably to those from all other sampling locations in terms of fragment length, number of reads mapping to the nuclear genome (Table 2, Fig. 5, Supplementary File 1: Avg. length and NUC/MT), X chromosome contamination estimates (the lowest of all sampling locations with an average of 0, though not statistically significant, Table 2), and SNP coverage post-1240k enrichment (Fig. 6). Human DNA fragments recovered from the petrous pyramid show a much higher frequency of cytosine deamination than any other element[21] (Fig. 4, Supplementary Figure S13, Supplementary File 1: Damage signals), which helps to support their authenticity as ancient[40,53–57]. It should be noted however, that a higher frequency of deamination may necessitate either the production of libraries treated with repair enzymes such as uracil-DNA glycosylase[58] or the removal of damaged bases by read trimming to improve mapping. These treatments, however, can result in an overall reduction in read length which can translate to a lower coverage of the reference genome as some reads may no longer reach minimum read length thresholds. While the comparatively lower deamination signal identified in the other sampling locations here may result from modern DNA contamination, our data shows no overall correlation between the proportion of human DNA recovered and the proportion of terminal cytosine deamination. Additionally, we do not observe higher amounts of contamination in other sampling sites based on our X chromosome contamination analysis (Table 2), nor do we see significant variation in deamination patterns within sampling locations across individuals (Supplementary Figure S14). However, a high overall fragment length in conjunction with low deamination frequencies (as observed in cementum) may be indicative of contamination with modern human DNA[59]. A previous comparison of deamination patterns in cementum and petrous pyramid yielded a similar differential to what we report here[21], where cementum exhibited approximately half the frequency of deamination at the 5′ terminus with no indication of modern contamination. Despite its excellent potential for human aDNA recovery, sampling from the petrous pyramid may not always be possible for a variety of reasons including hesitancy on the part of curators in regards to potential damage to the anthropological record, despite the fact that in cases where skulls are fully preserved and sampling of the temporal bone would otherwise be particularly damaging, cranial base drilling techniques have recently been investigated and recommended[29].

In the remaining skeletal elements where higher than average proportions of human DNA were recovered (>8.16%), we find that in situ molars are inferred to have a high probability of endogenous DNA recovery across all three separate sampling locations (Fig. 2a–c). Library complexity was high in both the dentin and material from the pulp chamber (Fig. 3), and contamination estimates low (Table 3). Cementum stands out as having both the highest average fragment length (Table 3) and the lowest deamination frequency (Fig. 4) which, as previously noted, may indicate elevated levels of contamination with modern human DNA, despite a low contamination signal observed in X chromosome analyses (Table 2). The dentin and pulp chamber, conversely, returned the shortest average read lengths and were second only to the petrous pyramid in terms of having the highest proportion of detectable deamination damage.

In terms of the ratio reads mapping to the nuclear genome/reads mapping to the mitochondrial genome, we find the dentin to harbour far less nuclear material than any other sampling location (Fig. 5, Supplementary File 1 NUC/MT). In particular, we observe a substantial differential in nuclear to mitochondrial mapping reads between the dentin and material from the dental pulp chamber (average ratios of 1:2769 and 1:539 respectively). It should be noted that these two sampling locations are not actually separate tissue types and instead are only differentiated by their physical location within the same substrate. To explain this observation, it is important to look at the process by which dentin is formed. Starting in from the outer surface (mantle) of the tooth, odontoblasts first secrete a type-1 collagen matrix, which is then mineralized in a process similar to the endochondral ossification of bone. However, odontoblasts, unlike their cognates in skeletal tissue, do not become trapped in the resulting hydroxyapatite matrix. Instead, thin extensions of the cell called odontoblast processes (alternatively Tome's fibres) remain within the calcified matrix, forming permanent channels throughout the dentin (dentinal tubules) while the rest of the cell, including the nuclear portion, migrates inwards towards the pulp chamber[60]. The bulk of the dentin itself is essentially void of nuclear DNA during life, though organelles such as mitochondria can persist within the odontoblast processes. When the odontoblasts die, however, nuclear DNA can bind to the hydroxyapatite matrix along the wall of the pulp chamber[61–63]. The result is an extreme disparity between the number of nuclear reads recovered from the superficial layer of dentin sampled as part of the pulp chamber and the dentin sampled from deeper within the tooth. As a consequence, pulp chamber sampling is generally more suitable for nuclear studies, whereas the deeper layers of dentin are better suited for mitochondrial investigations.

However, the fact that dental samples harbour three sampling locations that performed well in terms of human DNA content and two in terms of post-1240k-capture-coverage is an indication of their value. Our observation that dentin exhibited the lowest post-enrichment coverage out of the top sampling locations could be due to its lower nuclear read to mitochondrial read ratio and thus has fewer nuclear reads in the library available for capture. Of note, despite drilling from multiple locations, the enamel, which is frequently examined in isotope[64,65], histological[66] and morphological[67,68] studies, often remains entirely undamaged throughout the sampling process, as minimally invasive sampling methods for teeth focused on the avoidance of alterations to enamel structures have long been established[67]. Finally, the two sampling locations most limited in available material (in the context of sampling efforts from a single element) are the cementum and the dental pulp chamber. Both of these sampling locations performed well when directly compared to all other sampling locations (with up to 10× more material available for DNA extraction in some cases, Supplementary File 1) regardless of the amount of material used in extraction. When weight of the sample used for extraction is factored in, however, material from the dental pulp chamber and cementum outperforms all sampling locations other than the petrous pyramid with respect to average number of unique reads mapped per mg of input material (Supplementary Section 2.4). This suggests both sampling materials are particularly rich in DNA content though the complexity of this content in the cementum may not be as high as that found in material from the dental pulp chamber. These factors, combined with the known potential for teeth to harbour oral bacterial and pathogen DNA[37,69–72], make sampling from molars valuable as an alternative to the petrous pyramid.

Two sampling locations on the thoracic vertebrae, namely the cortical bone collected from the vertebral body and the junction of the lamellae and spinous process (the superior vertebral arch) were found to yield high average proportions of human DNA (Fig. 2a–c, Supplementary File 1: % mapping q37 and Unique reads/million). Additionally, library complexity (Fig. 3, Supplementary File 1: Est. genomic coverage), average fragment length (Table 2, Supplementary File 1: Avg. length), post-capture SNP coverage (Fig. 6), nuclear to mitochondrial read ratio (Fig. 5, Supplementary File 1: NUC/MT), and deamination frequencies (Fig. 4, Supplementary File 1: Damage signals) fell well within the ranges of the other top performing sampling locations (aside from the petrous pyramid). As with teeth, thoracic vertebrae have multiple high-yield sampling sites, are often well preserved, have been shown to harbour traces of ancient pathogens such as tuberculosis[73,74], and in the absence of pathological changes, are of less value in morphological studies given that they are numerous.

Both the talus and distal phalanx exhibited high human DNA recovery rates (Fig. 2a–c, Supplementary File 1: % mapping q37 and Unique reads/million) and showed high average fragment length (Table 2, Supplementary File 1: Avg. length) and complexity (Fig. 3, Supplementary File 1: Est. genomic coverage), as well as low contamination estimates (Table 2), nuclear-mitochondrial read ratios (Fig. 5, Supplementary File 1: NUC/MT), and deamination frequency at the 5′ terminus (Fig. 4, Supplementary File 1: Damage signals). While both elements have been under-utilised in aDNA investigations to date, the distal phalanx has previously been shown to yield sufficient aDNA to reconstruct a 30-fold genome from a Denisovan specimen[4].

Among the other sampling locations considered in this survey, those yielding human DNA proportions that are, on average, lower than the overall mean (8.16%) were not considered for further analyses, as our goal was to ascertain the most efficient and cost-effective sampling locations from which to retrieve human DNA. As such, we determined that samples from the femur, metacarpal, ischial tuberosity, metacarpal, ribs, and *clavicula,* as well as any samples derived from cancellous (spongy) material (in order of decreasing yield) are all unlikely to yield high amounts of endogenous human DNA. In light of this, we feel sampling from these elements, or from cancellous tissue in general, for aDNA analysis should be avoided if possible to circumvent the needless destruction of archaeological samples for minimal gains.

Conclusions

As intensifying ethical scrutiny surrounds the field of aDNA with regards to the destruction of irreplaceable archaeological human remains[30,42,75–77], it is imperative for those conducting such research to maximize the chances of successful data generation from minimally invasive sampling. It is of similar importance to both maximize the potential amount of information obtained from and to simultaneously minimize laboratory processing times for each sampling effort to balance the high cost of aDNA research with the aforementioned ethical

Individual (laboratory ID)	Archaeological ID (burial Nr.-individual Nr.)	Sex	Age at death	^{14}C dates (AD, Cal 2-sigma)
KRA001	25-1a	Male	25–35	1058–1219
KRA002	20-2a	Female	20–22	1227–1283
KRA003	113-6a	Male	25	1059–1223
KRA004	246-1a	Male	15	1284–1392
KRA005	276-2a	Male	10–12	1170–1258
KRA006	307-4a	Female	30–40	1218–1266
KRA007	377-6a	Female	25–30	1167–1251
KRA008	436-6a	Male	20	1301–1402
KRA009	566-3a	Male	Unknown adult	1158–1254
KRA010	600-7a	Male	25	1276–1383
KRA011	632-2a	Female	30–45	1040–1159

Table 4. Biological sex (genetically determined), age at death (archaeologically determined), and calibrated ^{14}C dates (in calendar years AD) of individuals selected for aDNA sampling.

considerations. As such, our large cross-sectional evaluation of aDNA recovery across the skeleton helps to facilitate this balance by increasing perspectives on molecular preservation not only in previously studied sampling locations, but also in a set of new ones. Our results demonstrate that, from the locations we consider here, the dense cochlear portion of the petrous pyramid remains the best sampling location for high-quality ancient DNA while sampling from cancellous tissue from any tested skeletal element should be avoided if possible. However, we also report on seven additional sampling locations on four other skeletal elements, all of which performed equally well in relation to each other in our evaluations. Though lesser in respect to proportion of human DNA recovered and library complexity than that observed in the petrous pyramid, these seven sampling locations show promise as suitable alternatives. While our sample set is limited both temporally and geographically, our results are likely informative for other climatic regions, time periods and perhaps even in anatomically comparable species as has already been demonstrated for the petrous portions itself[78–81]. It should also be noted that, as this study has focused on identifying the most efficient sampling locations from which host (in this case human) DNA can be recovered, the sampling strategies and suggestions put forth here may not be applicable in studies seeking to retrieve DNA from pathogens, the microbiome, or other co-cohabitating organisms within the host.

By providing researchers with more varied options for the successful recovery of endogenous ancient human DNA, we hope to provide a framework in which successful collaborations between archaeologists and geneticists can continue to enrich our knowledge of history and heritage. At the same time, continuing efforts to fully optimize our sampling strategies will allow the above collaborations to go forward in a more ethical fashion by minimizing damage to the finite archaeological record.

Methods

Sample selection, pre-treatment, and bone powder generation. Individuals from the Krakauer Berg collection housed at the State Office for Heritage Management and Archaeology, Saxony-Anhalt [State Museum of Prehistory, Halle (Saale)] (Fig. 1) were sampled for DNA extraction. This collection consists of approximately 800 individuals and represents a typical medieval burial, with age and sex distribution consistent with an attritional context. Ten skeletal elements were selected as targets for aDNA sampling (Table 1, Supplementary Material: Section 1.2). For each individual, morphological preservation of these pre-selected elements was assessed, and individuals were included in the study if a minimum of eight elements were present and were sufficiently well preserved. This resulted in a study set of eleven individuals, seven males and four females (genetically assigned, see below), who ranged in age at death from approximately 10–45 years, with two juveniles and nine adults. Radiocarbon dating of ribs from each individual (performed at the Curt Engelhorn Centre for Archaeometry in Mannheim, Germany) placed the skeletal series in a time interval of approximately 1040–1402 cal AD (Table 4).

To reduce external contamination as much as possible, all elements were processed in a dedicated ancient DNA laboratory under controlled conditions. Similarly, variation in both skeletal sampling[48] and DNA extraction was eliminated as much as feasibly possible by allocating these tasks to a single individual (CP). At least two sampling locations (Table 1, Supplementary Material: Section 1.2) were selected for each element other than the petrous pyramid, one of which was comprised of cortical bone and the other of cancellous bone. Sampling of the petrous pyramid followed previously established sampling procedures[47] and involved the sectioning of the petrous pyramid to allow access to the dense bone surrounding the cochlea for drilling. Sampling of teeth was performed in a three-step process and involved removal of the cementum followed by sectioning and drilling of the pulp chamber and dentin portions. Prior to sampling, all relevant locations on each element were cleaned with bleach (0.01% v/v) via 5-min incubation, followed by rinsing with distilled water and exposure to UV light for 30 min to cross-link any residual surface contamination from modern DNA. Where applicable the outermost surface of bone was removed by abrasion with a standard dental drill (KaVo K-POWERgrip EWL 4941) and size 016 round bit (NTI Kahla). Approximately 100 mg of bone powder was drilled from each sampling location with exception of the cementum and dental pulp chambers where an average of approximately 19 mg

(standard deviation of 10.8 mg) and approximately 24 mg (standard deviation of 15.03 mg), respectively, of bone powder was recovered, the entirety of which was used for DNA extraction. An average of approximately 54 mg (standard deviation of 11 mg) of bone powder was used in downstream DNA extractions for all other sampling locations (Supplementary File 1: mg input). For molars, cementum was removed by abrasion using a diamond coated rotary cutting disc (NTI Kahla). The tooth was then sectioned at the cemento-enamel junction using a jeweller's saw (Präzisions-Sägebogen Antilope, with 75 mm blade). Powder from a first pass drilling of the pulp chamber was collected before further sampling of the underlying dentin (Supplementary Material: Section 1.2).

DNA extraction, library preparation, and sequencing. All DNA extractions were conducted in the clean room facility of the Department of Archaeogenetic of the Max Planck Institute for the Science of Human History (MPI-SHH) located in Jena, Germany, using a modified filter column protocol[14] (Supplementary Section 1.3.1). Single-stranded DNA libraries[82] were prepared from all extracts by automation[83] using the Agilent Bravo Liquid Handling System at the Max Planck Institute for Evolutionary Anthropology in Leipzig, Germany. Subsequent to initial analysis, libraries from all sampling locations found to have average human DNA content of 8.16% or greater were enriched by bait capture[84] for regions in the human 1240k[27] reference dataset. Sequencing was done via a 75 bp paired-end kit on an Illumina HiSeq 4000 platform to a depth of approximately 5 million reads for initial screening and approximately 40 million reads following 1240k capture enrichment.

Evaluation criteria. One of the most common metrics for the evaluation of molecular preservation in archaeological remains percentage of endogenous (i.e. human) aDNA recovered after sequencing. However, a high percentage of endogenous DNA on its own provides limited information on the utility of a given DNA library for downstream analysis. For example, it is important that both the proportion of human DNA relative to that of potential contaminants as well as the quantity (e.g. the number of sequences mapping to the reference as well as the as the proportion of the reference actually covered) of human DNA are high for whole genome sequencing, whereas the quantity alone is the most important criterion when using target enrichment approaches[85]. Beyond this, the integrity of the DNA molecules themselves plays an important role in the downstream mapping of sequencing data[86–88] as well as in the authentication of ancient DNA[40,53–57]. For this reason, we integrated additional measures of data quality into our initial evaluation[89], including the quantity of recovered human DNA, estimated DNA library complexity (in terms of both sequence duplication levels and total estimated genomic coverage), estimates of modern human DNA contamination, the ratio of nuclear to mitochondrial read recovery, average DNA fragment length, and patterns of deamination observed in reads mapping to the human reference genome. All resulting data was normalized to reflect outcomes expected from equal sequencing efforts (raw number of sequences generated prior to merging, duplicate removal, as well as length and quality filtering) across all samples where appropriate. The aim of our study was to develop a predictive model of DNA recovery based on the relative performance of each sampling location in terms of quality and quantity of recovered human DNA. We, therefore, opted not to normalize our analyses against the amount of sampling input material, despite the restricted amounts available in some locations (see Supplementary Section 2.4 for normalized analyses).

Contamination estimates. Contamination estimates for each individual sampling location were calculated using the ANGSD[50] software package to examine the probability of foreign X chromosome contamination in samples from male individuals using the post-capture enrichment data sets generated for eight sampling locations with human DNA recovery above 8.16%. Mitochondrial contamination estimates were generated at an individual level for all individuals using the Schmutzi[52] software package. Multi-dimensional scaling analyses of all enriched samples was performed with the *R Statistical Software Package*[90] using the *ggplot2* package[91].

Mapping. Human DNA content and sequence quality were determined by mapping reads to the hg19 human reference genome (accession number: GCF_000001405.13) using the EAGER[92] pipeline: BWA[93] settings: -n set at 0.1 and a mapping quality filter of q37. To assess resolution of the above pipeline in detecting ancient human DNA sequences, we created a simulated dataset based on the hg19 human reference for mapping evaluation and to act as a best-case scenario for comparative purposes. We first cut the reference sequence into fragments of average length and size distribution modelled after a representative sample (KRA001.B0102, petrous pyramid single-stranded library; see Supplementary File 1: Average and Median length). We then used the software Gargammel[94] to artificially add a deamination pattern to the data that simulated an ancient DNA damage signal consistent with the same sample (see Supplementary File 1: Damage signals). The resulting simulated aDNA dataset was then mapped as above.

Calculations. Percentage of human reads recovered from each sampling effort was calculated as:

$$\frac{\text{Total number of reads mapping to reference prior to duplicate removal and post quality filtering}}{\text{Total reads after merging and filtering for quality and length}} \quad (1)$$

The number of unique reads mapping to the human genome per million reads sequencing effort was calculated as:

$$\frac{\text{Number of reads mapping to reference after duplicate removal and quality filtering}}{\text{Number of reads generated pior to merging or filtering}} \times 1,000,000 \quad (2)$$

Total genomic coverage within a library[44] was estimated by calculating:

$$\frac{\text{Number of DNA molecules in library} \times \text{Proportion of human DNA recovered} \times \text{Avg. length of mapping reads}}{\text{Length of reference genome}} \quad (3)$$

Mixed effects modelling. All statistical analyses involving generalized linear models and mixed effects models described here were performed using the *R Statistical Software Package*[90], where a p-value of 0.05 was considered significant. When multiple hypotheses were performed, p-values were adjusted to control for a family-wise error rate of 0.05 using the *p.adjust* function.

In all mixed effects models we considered the skeletal element to be a fixed effect with the individual as a random effect. Backward model selection was performed using ANOVA, including for testing whether random effects in the final analyses were deemed significant.

When modelling response variables with an obvious upper bound (i.e. endogenous DNA content of 100%), we implemented beta mixed effects regression as implemented in the *glmmTMB* package[95]. Optimal power transformations for theoretically unbounded response variables were performed using a Box–Cox transformation as implemented in the *MASS* package[96].

We compared the effects of skeletal elements on response variable by inspecting the estimated marginal means in our optimal mixed effects and fixed effects models using the *emmeans* package[97].

All visualizations of analyses included in this manuscript were produced in the R environment using the ggplot2 package[91].

Data availability

Sequence data is available through the European Nucleotide Archive under accession number PRJ-EB36983.

Code availability

All programs and R libraries used in this manuscript are freely and publicly available from their respective authors. All custom written R code is available by request.

Received: 23 May 2020; Accepted: 7 October 2020
Published online: 26 October 2020

References

1. Mardis, E. R. Next-generation DNA sequencing methods. *Annu. Rev. Genomics Hum. Genet.* **9**, 387–402 (2008).
2. Schuster, S. C. Next-generation sequencing transforms today's biology. *Nat. Methods* **5**, 16–18 (2008).
3. Knapp, M. & Hofreiter, M. Next generation sequencing of ancient DNA: requirements, strategies and perspectives. *Genes (Basel)* **1**, 227–243 (2010).
4. Meyer, M. *et al.* A high-coverage genome sequence from an archaic Denisovan individual. *Science* **338**, 222–226 (2012).
5. Burrell, A. S., Disotell, T. R. & Bergey, C. M. The use of museum specimens with high-throughput DNA sequencers. *J. Hum. Evol.* **79**, 35–44 (2015).
6. Broushaki, F. *et al.* Early Neolithic genomes from the eastern Fertile Crescent. *Science* **353**, 499 (2016).
7. Rivollat, M. *et al.* When the waves of European Neolithization Met: first paleogenetic evidence from early farmers in the Southern Paris Basin. *PLoS ONE* **10**, e0125521 (2015).
8. Slatkin, M. & Racimo, F. Ancient DNA and human history. *PNAS* **113**, 6380–6387 (2016).
9. Marciniak, S. & Perry, G. H. Harnessing ancient genomes to study the history of human adaptation. *Nat. Rev. Genet.* **18**, 659–674 (2017).
10. Skoglund, P. & Mathieson, I. Ancient genomics of modern humans: the first decade. *Annu. Rev. Genomics Hum. Genet.* **19**, 381–404 (2018).
11. Der Sarkissian, C. *et al.* Ancient genomics. *Philos. Trans. R. Soc. B Biol. Sci.* **370**, 20130387 (2015).
12. Pickrell, J. K. & Reich, D. Toward a new history and geography of human genes informed by ancient DNA. *Trends Genet.* **30**, 377–389 (2014).
13. Palsdottir, A. H., Bläuer, A., Rannamäe, E., Boessenkool, S. & Hallsson, J. Not a limitless resource: ethics and guidelines for destructive sampling of archaeofaunal remains. *R. Soc. Open Sci.* https://doi.org/10.1098/rsos.191059 (2019).
14. Dabney, J. & Meyer, M. Extraction of highly degraded DNA from ancient bones and teeth. In *Ancient DNA: Methods and Protocols* (eds Shapiro, B. *et al.*) (Springer, New York, 2019). https://doi.org/10.1007/978-1-4939-9176-1_4.
15. Adler, C. J., Haak, W., Donlon, D. & Cooper, A. Survival and recovery of DNA from ancient teeth and bones. *J. Archaeol. Sci.* **38**, 956–964 (2011).
16. Pinhasi, R., Fernandes, D. M., Sirak, K. & Cheronet, O. Isolating the human cochlea to generate bone powder for ancient DNA analysis. *Nat. Protoc.* **14**, 1194–1205 (2019).
17. Pilli, E. *et al.* Neither femur nor tooth: petrous bone for identifying archaeological bone samples via forensic approach. *Forensic Sci. Int.* **283**, 144–149 (2018).
18. Coulson-Thomas, Y. M. *et al.* DNA and bone structure preservation in medieval human skeletons. *Forensic Sci. Int.* **251**, 186–194 (2015).
19. Rohland, N. & Hofreiter, M. Ancient DNA extraction from bones and teeth. *Nat. Protoc.* **2**, 1756–1762 (2007).
20. Höss, M., Jaruga, P., Zastawny, T. H., Dizdaroglu, M. & Paabo, S. DNA damage and DNA sequence retrieval from ancient tissues. *Nucleic Acids Res.* **24**, 1304–1307 (1996).
21. Hansen, H. B. *et al.* Comparing ancient DNA preservation in petrous bone and tooth cementum. *PLoS ONE* **12**, e0170940 (2017).
22. Gamba, C. *et al.* Genome flux and stasis in a five millennium transect of European prehistory. *Nat. Commun.* **5**, 1–9 (2014).
23. Feldman, M. *et al.* Ancient DNA sheds light on the genetic origins of early Iron Age Philistines. *Sci. Adv.* **5**, eaax0061 (2019).
24. Harney, É. *et al.* Ancient DNA from Chalcolithic Israel reveals the role of population mixture in cultural transformation. *Nat. Commun.* **9**, 1–11 (2018).
25. Lazaridis, I. *et al.* Genetic origins of the Minoans and Mycenaeans. *Nature* **548**, 214–218 (2017).
26. Llorente, M. G. *et al.* Ancient Ethiopian genome reveals extensive Eurasian admixture in Eastern Africa. *Science* **350**, 820–822 (2015).

27. Mathieson, I. *et al.* Genome-wide patterns of selection in 230 ancient Eurasians. *Nature* **528**, 499–503 (2015).
28. Gaudio, D. *et al.* Genome-wide DNA from degraded petrous bones and the assessment of sex and probable geographic origins of forensic cases. *Sci. Rep.* **9**, 1–11 (2019).
29. Sirak, K. A. *et al.* A minimally-invasive method for sampling human petrous bones from the cranial base for ancient DNA analysis. *Biotechniques* **62**, 283–289 (2017).
30. Sirak, K. A. & Sedig, J. W. Balancing analytical goals and anthropological stewardship in the midst of the paleogenomics revolution. *World Archaeol.* **51**, 1–14 (2019).
31. Prendergast, M. E. & Sawchuk, E. Boots on the ground in Africa's ancient DNA 'revolution': archaeological perspectives on ethics and best practices. *Antiquity* **92**, 803–815 (2018).
32. Ponce de León, M. S. *et al.* Human bony labyrinth is an indicator of population history and dispersal from Africa. *Proc. Natl. Acad. Sci. U.S.A.* **115**, 4128–4133 (2018).
33. Nagaoka, T. & Kawakubo, Y. Using the petrous part of the temporal bone to estimate fetal age at death. *Forensic Sci. Int.* **248**(188), e1-7 (2015).
34. Norén, A., Lynnerup, N., Czarnetzki, A. & Graw, M. Lateral angle: a method for sexing using the petrous bone. *Am. J. Phys. Anthropol.* **128**, 318–323 (2005).
35. Bar-Oz, G. & Dayan, T. FOCUS: on the use of the petrous bone for estimating cranial abundance in fossil assemblages. *J. Archaeol. Sci.* **34**, 1356–1360 (2007).
36. Campos, P. F. *et al.* DNA in ancient bone—where is it located and how should we extract it?. *Ann. Anat.* **194**, 7–16 (2012).
37. Margaryan, A. *et al.* Ancient pathogen DNA in human teeth and petrous bones. *Ecol. Evol.* **8**, 3534–3542 (2018).
38. Latham, K. E. & Miller, J. J. DNA recovery and analysis from skeletal material in modern forensic contexts. *Forensic Sci. Res.* **4**, 51–59 (2019).
39. Mundorff, A. Z., Bartelink, E. J. & Mar-Cash, E. DNA preservation in skeletal elements from the world trade center disaster: recommendations for mass fatality management. *J. Forensic Sci.* **54**, 739–745 (2009).
40. Sawyer, S., Krause, J., Guschanski, K., Savolainen, V. & Pääbo, S. Temporal patterns of nucleotide misincorporations and DNA fragmentation in ancient DNA. *PLoS ONE* https://doi.org/10.1371/journal.pone.0034131 (2012).
41. Smith, C. I., Chamberlain, A. T., Riley, M. S., Stringer, C. & Collins, M. J. The thermal history of human fossils and the likelihood of successful DNA amplification. *J. Hum. Evol.* **45**, 203–217 (2003).
42. Trinkaus, E. The labyrinth of human variation. *Proc. Natl. Acad. Sci. U.S.A.* **115**, 3992–3994 (2018).
43. Boessenkool, S. *et al.* Combining bleach and mild predigestion improves ancient DNA recovery from bones. *Mol. Ecol. Resour.* **17**, 742–751 (2017).
44. Malmström, H. *et al.* More on contamination: the use of asymmetric molecular behavior to identify authentic ancient human DNA. *Mol. Biol. Evol.* **24**, 998–1004 (2007).
45. Gilbert, M. T. P., Hansen, A. J., Willerslev, E., Turner-Walker, G. & Collins, M. Insights into the processes behind the contamination of degraded human teeth and bone samples with exogenous sources of DNA. *Int. J. Osteoarchaeol.* **16**, 156–164 (2006).
46. Hagelberg, E. *et al.* Analysis of ancient bone DNA: techniques and applications [and discussion]. *Philos. Trans. Biol. Sci.* **333**, 399–407 (1991).
47. Pinhasi, R. *et al.* Optimal ancient DNA yields from the inner ear part of the human petrous bone. *PLoS ONE* **10**, e0129102 (2015).
48. Alberti, F. *et al.* Optimized DNA sampling of ancient bones using computed tomography scans. *Mol. Ecol. Resour.* **18**, 1196–1208 (2018).
49. Gansauge, M.-T. *et al.* Single-stranded DNA library preparation from highly degraded DNA using T4 DNA ligase. *Nucleic Acids Res.* **45**, e79 (2017).
50. Korneliussen, T. S., Albrechtsen, A. & Nielsen, R. ANGSD: analysis of next generation sequencing data. *BMC Bioinform.* **15**, 356 (2014).
51. Furtwängler, A. *et al.* Ratio of mitochondrial to nuclear DNA affects contamination estimates in ancient DNA analysis. *Sci. Rep.* **8**, 1–8 (2018).
52. Renaud, G., Slon, V., Duggan, A. T. & Kelso, J. Schmutzi: estimation of contamination and endogenous mitochondrial consensus calling for ancient DNA. *Genome Biol.* **16**, 224 (2015).
53. Skoglund, P. *et al.* Separating endogenous ancient DNA from modern day contamination in a Siberian Neandertal. *PNAS* **111**, 2229–2234 (2014).
54. Dabney, J., Meyer, M. & Pääbo, S. Ancient DNA damage. *Cold Spring Harb. Perspect. Biol.* **5**, a012567 (2013).
55. García-Garcerà, M. *et al.* Fragmentation of contaminant and endogenous DNA in ancient samples determined by shotgun sequencing; prospects for human palaeogenomics. *PLoS ONE* **6**, e24161 (2011).
56. Brotherton, P. *et al.* Novel high-resolution characterization of ancient DNA reveals C > U-type base modification events as the sole cause of post mortem miscoding lesions. *Nucleic Acids Res.* **35**, 5717–5728 (2007).
57. Briggs, A. W. *et al.* Patterns of damage in genomic DNA sequences from a Neandertal. *PNAS* **104**, 14616–14621 (2007).
58. Briggs, A. W. *et al.* Removal of deaminated cytosines and detection of in vivo methylation in ancient DNA. *Nucleic Acids Res.* **38**, e87 (2010).
59. Lindahl, T. Recovery of antediluvian DNA. *Nature* **365**, 700 (1993).
60. Nanci, A. *Ten Cate's Oral Histology* 9th edn. (Elsevier, Amsterdam, 2017).
61. Cafiero, C. *et al.* Optimization of DNA extraction from dental remains. *Electrophoresis* **40**, 1820–1823 (2019).
62. Higgins, D., Rohrlach, A. B., Kaidonis, J., Townsend, G. & Austin, J. J. Differential nuclear and mitochondrial DNA preservation in post-mortem teeth with implications for forensic and ancient DNA studies. *PLoS ONE* **10**, e0126935 (2015).
63. Higgins, D. & Austin, J. J. Teeth as a source of DNA for forensic identification of human remains: a review. *Sci. Justice* **53**, 433–441 (2013).
64. Pellegrini, M., Pouncett, J., Jay, M., Pearson, M. P. & Richards, M. P. Tooth enamel oxygen "isoscapes" show a high degree of human mobility in prehistoric Britain. *Sci. Rep.* **6**, 34986 (2016).
65. Clementz, M. T. New insight from old bones: stable isotope analysis of fossil mammals. *J. Mammal.* **93**, 368–380 (2012).
66. Falin, L. I. Histological and histochemical studies of human teeth of the Bronze and Stone Ages. *Arch. Oral Biol.* **5**, 5–13 (1961).
67. Beniash, E. *et al.* The hidden structure of human enamel. *Nat. Commun.* **10**, 4383 (2019).
68. Smith, T. M. *et al.* Variation in enamel thickness within the genus Homo. *J. Hum. Evol.* **62**, 395–411 (2012).
69. Schuenemann, V. J. *et al.* Targeted enrichment of ancient pathogens yielding the pPCP1 plasmid of *Yersiniapestis* from victims of the Black Death. *Proc. Natl. Acad. Sci.* **108**, E746–E752 (2011).
70. Schuenemann, V. J. *et al.* Genome-wide comparison of medieval and modern *Mycobacteriumleprae*. *Science* **341**, 179–183 (2013).
71. Keller, M. *et al.* Ancient Yersinia pestis genomes provide no evidence for the origins or spread of the Justinianic Plague. Preprint at https://www.biorxiv.org/content/10.1101/819698v2 (2019).
72. Bos, K. I. *et al.* A draft genome of *Yersiniapestis* from victims of the Black Death. *Nature* **478**, 506–510 (2011).
73. Bos, K. I. *et al.* Pre-Columbian mycobacterial genomes reveal seals as a source of New World human tuberculosis. *Nature* **514**, 494–497 (2014).
74. Taylor, G. M., Goyal, M., Legge, A. J., Shaw, R. J. & Young, D. Genotypic analysis of *Mycobacteriumtuberculosis* from medieval human remains. *Microbiology* **145**, 899–904 (1999).
75. Lewis-Kraus, G. Is ancient DNA research revealing new truths—or falling into old traps? *The New York Times* (2019).

76. Charlton, S., Booth, T. & Barnes, I. The problem with petrous? A consideration of the potential biases in the utilization of pars petrosa for ancient DNA analysis. *World Archaeol.* **51**, 574–585 (2020).
77. Booth, T. J. A stranger in a strange land: a perspective on archaeological responses to the palaeogenetic revolution from an archaeologist working amongst palaeogeneticists. *World Archaeol.* https://doi.org/10.1080/00438243.2019.1627240 (2019).
78. Prendergast, M. E. *et al.* Ancient DNA reveals a multistep spread of the first herders into sub-Saharan Africa. *Science* **365**, eaaw275 (2019).
79. Fages, A. *et al.* Tracking five millennia of horse management with extensive ancient genome time series. *Cell* **177**, 1419-1435.e31 (2019).
80. Posth, C. *et al.* Language continuity despite population replacement in Remote Oceania. *Nat. Ecol. Evol.* **2**, 731–740 (2018).
81. Soubrier, J. *et al.* Early cave art and ancient DNA record the origin of European bison. *Nat. Commun.* **7**, 1–7 (2016).
82. Gansauge, M.-T. & Meyer, M. A method for single-stranded ancient DNA library preparation. In *Ancient DNA: Methods and Protocols* (eds Shapiro, B. *et al.*) 75–83 (Springer, New York, 2019). https://doi.org/10.1007/978-1-4939-9176-1_9.
83. Slon, V. *et al.* Neandertal and Denisovan DNA from Pleistocene sediments. *Science* **356**, 605–608 (2017).
84. Harakalova, M. *et al.* Multiplexed array-based and in-solution genomic enrichment for flexible and cost-effective targeted next-generation sequencing. *Nat. Protoc.* **6**, 1870–1886 (2011).
85. Cruz-Dávalos, D. I. *et al.* Experimental conditions improving in-solution target enrichment for ancient DNA. *Mol. Ecol. Resour.* **17**, 508–522 (2017).
86. Günther, T. & Nettelblad, C. The presence and impact of reference bias on population genomic studies of prehistoric human populations. *PLoS Genet.* **15**, e1008302 (2019).
87. Schubert, M. *et al.* Improving ancient DNA read mapping against modern reference genomes. *BMC Genomics* **13**, 178 (2012).
88. Prüfer, K. *et al.* Computational challenges in the analysis of ancient DNA. *Genome Biol.* **11**, R47 (2010).
89. Key, F. M., Posth, C., Krause, J., Herbig, A. & Bos, K. I. Mining metagenomic data sets for ancient DNA: recommended protocols for authentication. *Trends Genet.* **33**, 508–520 (2017).
90. R Core Team. *R: A language and environment for statistical computing* (R Foundation For Statistical Computing, 2016).
91. Wickham, H. *ggplot2: Elegant Graphics for Data Analysis* (Springer International Publishing, Cham, 2016). https://doi.org/10.1007/978-3-319-24277-4.
92. Peltzer, A. *et al.* EAGER: efficient ancient genome reconstruction. *Genome Biol.* **17**, 60 (2016).
93. Li, H. & Durbin, R. Fast and accurate short read alignment with Burrows-Wheeler transform. *Bioinformatics* **25**, 1754–1760 (2009).
94. Renaud, G., Hanghøj, K., Willerslev, E. & Orlando, L. gargammel: a sequence simulator for ancient DNA. *Bioinformatics* **33**, 577–579 (2017).
95. Brooks, M. E. *et al.* glmmTMB balances speed and flexibility among packages for zero-inflated generalized linear mixed modeling. *R J.* **9**, 378–400 (2017).
96. Venables, W. N. & Ripley, B. D. *Modern Applied Statistics with S* (Springer, New York, 2002). https://doi.org/10.1007/978-0-387-21706-2.
97. Lenth, R., Singmann, H., Love, J., Buerkner, P. & Herve, M. *emmeans: Estimated Marginal Means, aka Least-Squares Means* (2019).

Acknowledgements

The authors would like to thank the laboratory staff at the Max Planck Institute for Evolutionary Anthropology, Leipzig, Germany as well as all the technicians, students, and scientific colleagues at the Max Planck Institute for the Science of Human History, Jena, Germany, with particular thanks to technicians Antje Wissgott and Franziska Aron for aiding in the laboratory work behind this publication as well as Elizabeth Nelson for her help in identifying osteological features. In addition, the authors would also like to thank the State Office for Heritage Management and Archaeology, Saxony-Anhalt [State Museum of Prehistory, Halle (Saale)] for opening up their collection and providing all samples used in this study and Xandra Dalidowski for leading the excavation. This study was funded by the Max Planck Society, the European Research Council (ERC) under the European Union's Horizon 2020 research and innovation program under grant agreements No 771234—PALEoRIDER (WH, ABR) and No. 805268—CoDisEASe (KIB).

Author contributions

C.P. is the primary author and was responsible for the gathering, processing, sampling from, and DNA extraction from all samples, as well as their subsequent analyses. A.B.R. performed all statistical analyses and coding, as well as authoring the corresponding methods sections and the editing of the overall manuscript. S.F. of the State Office for Heritage Management and Archaeology, Saxony-Anhalt [State Museum of Prehistory, Halle (Saale)] contributed archaeological remains sampled in this study and the archaeological context. S.N. produced single-stranded libraries for all samples at the Max Planck Institute for Evolutionary Anthropology, Leipzig, Germany. M.M. oversaw single-stranded library preparation at the Max Planck Institute for Evolutionary Anthropology, Leipzig, Germany, and aided in the editing of the manuscript. K.I.B. acted as co-supervisor to the primary author, provided funding, aided in the experimental design of this study, and contributed to the writing and editing of this manuscript. W.H. acted as co-supervisor to the primary author, provided funding, aided in the experimental design of this study, coordinated sample selection, and contributed to the writing and editing of this manuscript. J.K. acted as co-supervisor to the primary author, aided in experimental design, and provided funding for the study.

Funding

Open Access funding enabled and organized by Projekt DEAL.

Competing interests

The authors declare no competing interests.

Additional information

Supplementary information is available for this paper at https://doi.org/10.1038/s41598-020-75163-w.

Correspondence and requests for materials should be addressed to C.P., J.K. or W.H.

Reprints and permissions information is available at www.nature.com/reprints.

Additional Files

Additional File 1

Format: Word Document (*.docx)

Title: Supplementary Material

Description: Detailed supplements to the Results and Methods sections including supplementary figures, tables, and analyses.

A systematic investigation of human DNA preservation in medieval skeletons: Supplementary material

Cody Parker[1*], Adam B. Rohrlach[1,2], Susanne Friederich[3], Sarah Nagel[4], Matthias Meyer[4], Johannes Krause[1*], Kirsten I. Bos[1], Wolfgang Haak[1*]

Affiliations:
[1]Max Planck Institute for the Science of Human History, Jena, Germany
[2]ARC Centre of Excellence for Mathematical and Statistical Frontiers, The University of Adelaide, Adelaide, South Australia, Australia
[3]Landesamt für Denkmalpflege und Archäologie, Sachsen-Anhalt, Halle a. d. Saale, Germany
[4]Max Planck Institute for Evolutionary Anthropology, Leipzig, Germany

Corresponding Authors:
Cody Parker: parker@shh.mpg.de*
Wolfgang Haak: haak@shh.mpg.de*
Johannes Krause: krause@shh.mpg.de*

Adam B. Rohrlach: rohrlach@shh.mpg.de
Susanne Friederich: sfriederich@lda.stk.sachsen-anhalt.de
Sarah Nagel: sarah_nagel@eva.mpg.de
Matthias Meyer: mmeyer@eva.mpg.de
Kirsten I. Bos: bos@shh.mpg.de

1. Laboratory Processing

1.1 Pre-treatment

All samples were initially cleaned with 0.01% v/v bleach to remove dirt, then rinsed with distilled water before being exposed to ultraviolet light for 30 minutes.

1.2 Bone powder generation

All bone powder was generated by drilling using a standard dental drill with standard drill bit on a low-speed, high-torque setting unless otherwise noted.

1.2.1 *Pars Petrosa*

The petrous pyramid was first cut in half along the lateral line using a jeweller's saw (Figure S1b). The interior portion was then visibly examined, and bone powder generated from the densest area (Figure S1a).

a

b

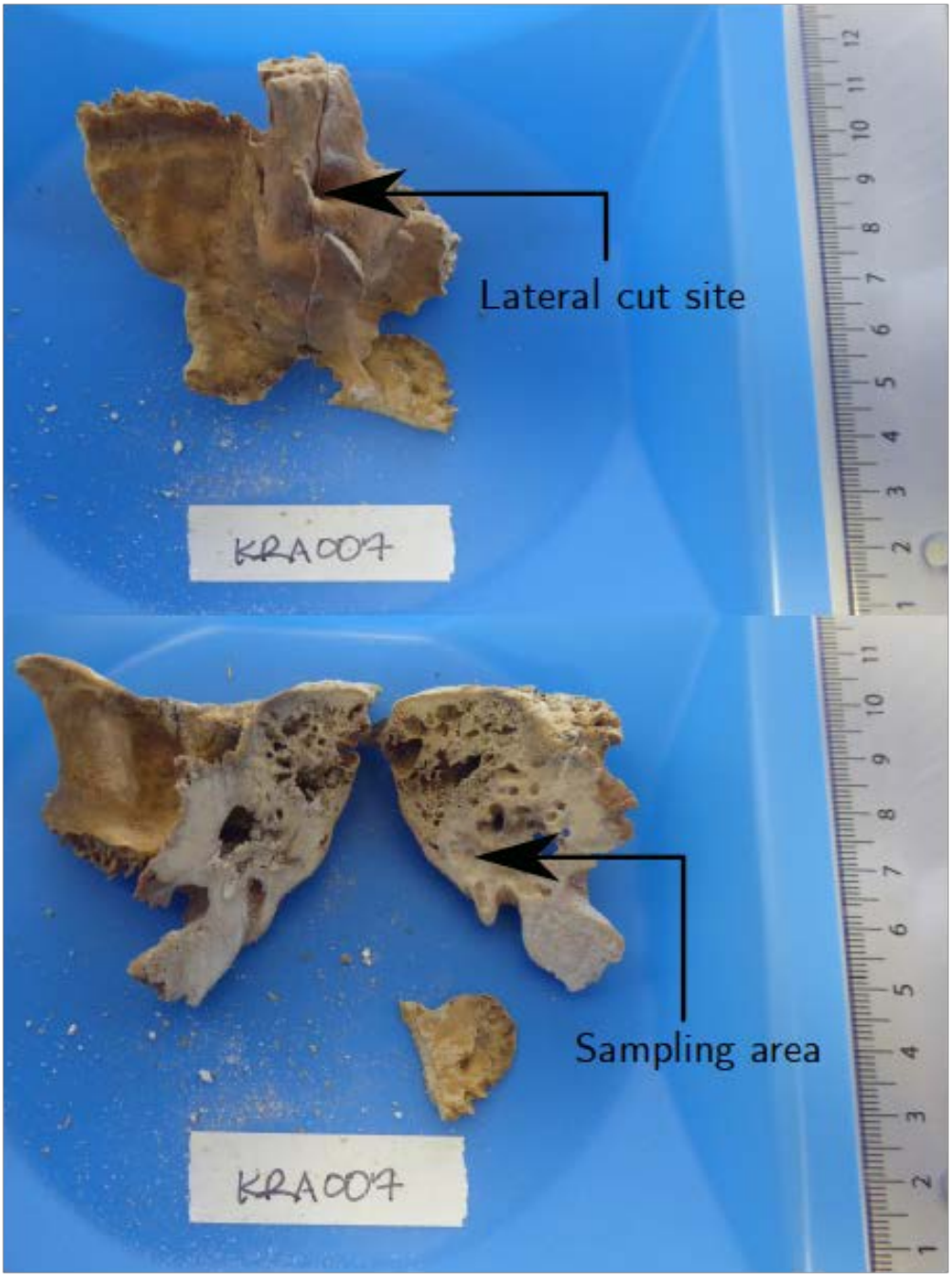

Figure S1a-b: Posterior view of *Pars petrosa* pre-sectioning (a) and post, showing the sectioning and subsequent drilling sites (b).

1.2.2 Teeth

Cementum was removed from the root portion of the tooth using a standard dental drill fitted with a circular cutting attachment. The blade of the cutting wheel was placed lightly against the root at a 20° angle (relative to the bottom of the root) on a low-speed, high-torque setting and the cementum scraped off downward (Figure S2a-b). The tooth was then bisected along the cementum-enamel junction. Powder from pulp chamber was generated using a standard dental drill bit from the first pass of the interior of the crown. Subsequent passes were used to generate bone powder from dentin (Figure S2c).

a.

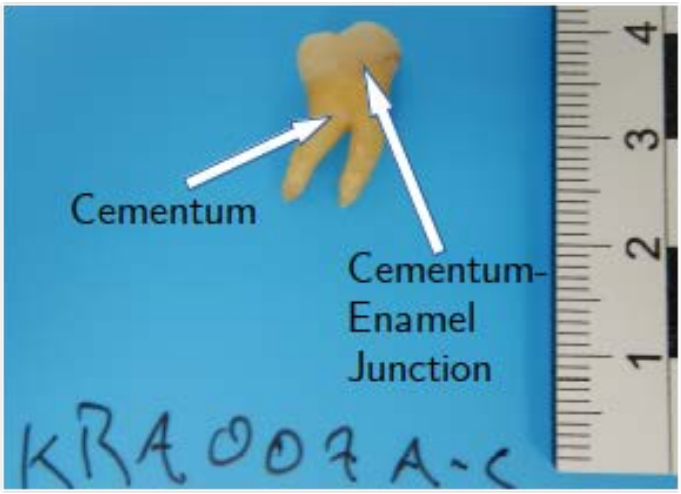

b.

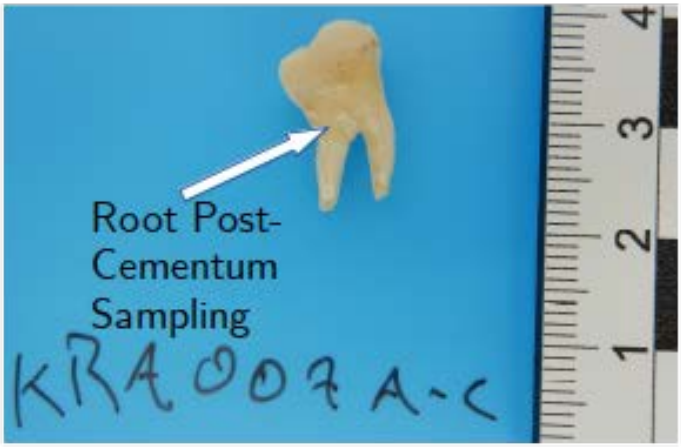

c.

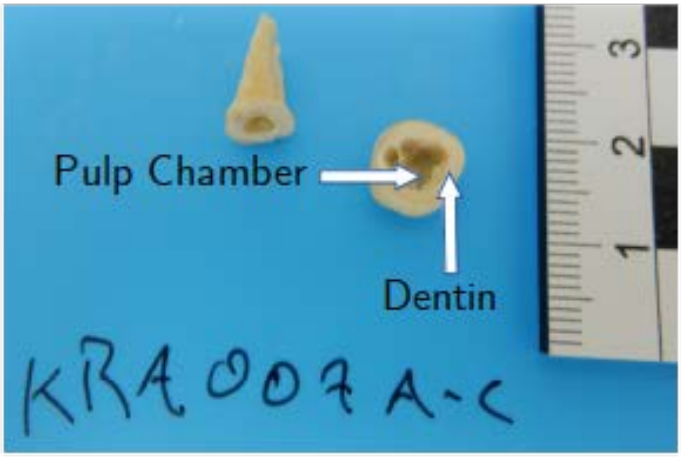

Figure S2a-c: *In situ* molar pre (a) and post (removal of cementum, as well as pre (b) and post (c) sectioning and drilling of the pulp chamber and underlying dentin.

1.2.3 Clavicles

Cortical bone powder was collected from the exterior apex of anterior sternal curve of the shaft of the clavicle, and cancellous bone powder from the interior of the acromial facet (Figure S3).

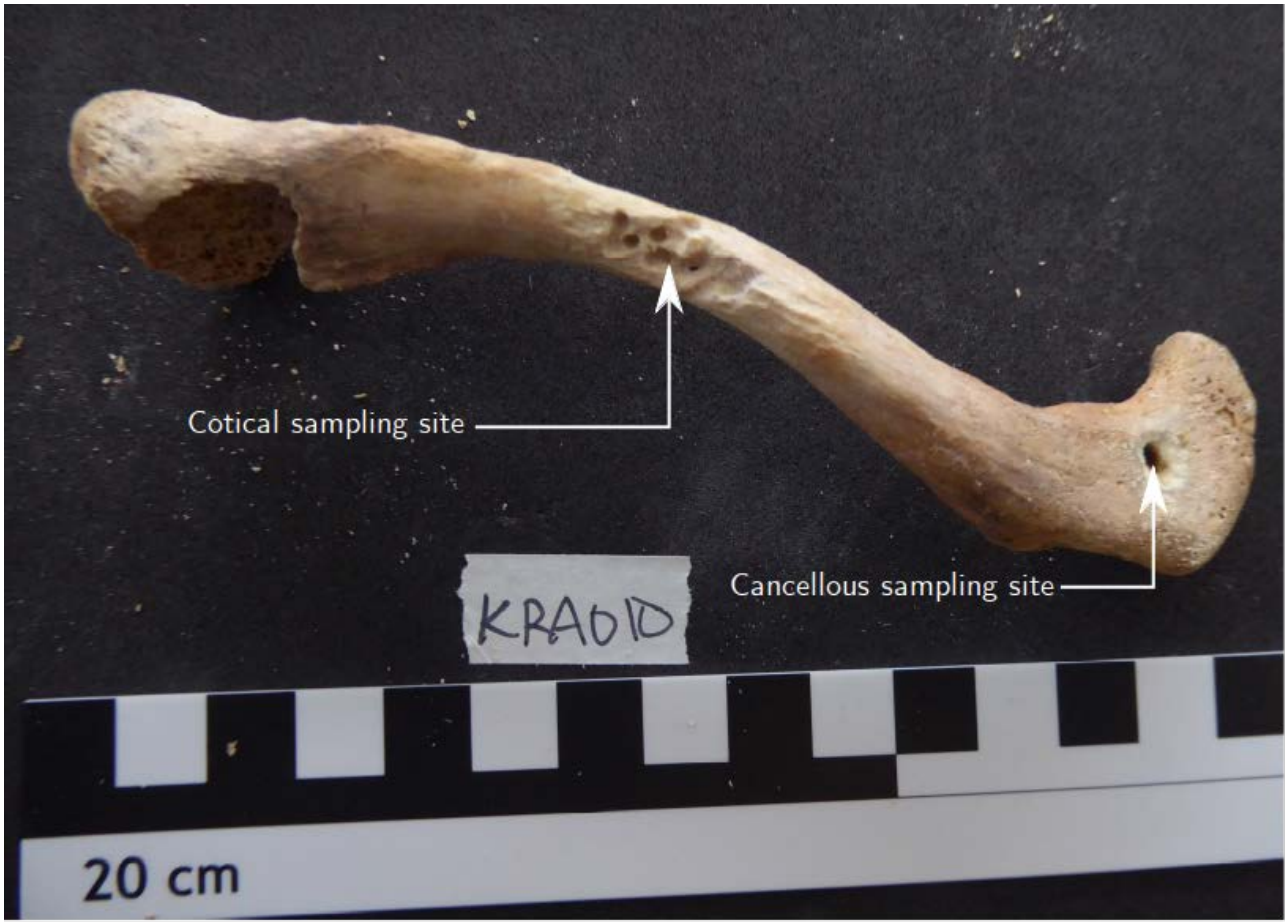

Figure S3: Sampling sites of the clavicle (anterior view) showing drilling locations for both cortical and cancellous tissue.

1.2.4 Vertebrae

Cortical bone powder was generated from the spine of the spinous process, the exterior of the vertebral body, the interior surface of the neural foramen, and the superior apex of junction of the lamellae and spinous process (superior vertebral arch). Cancellous bone powder was collected from the interior of the vertebral body (Figure S4).

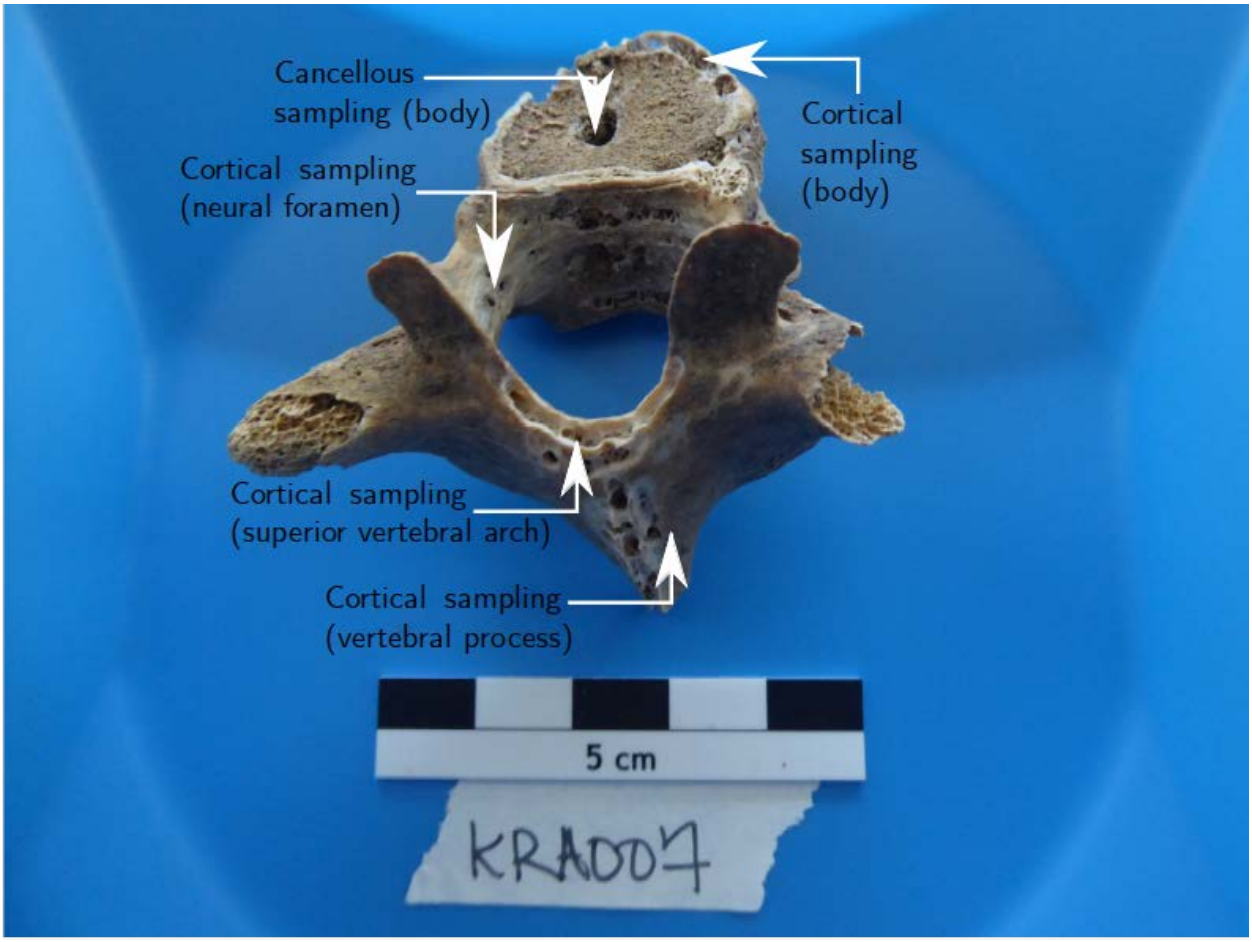

Figure S4: All sampling locations (post-drilling) of the thoracic vertebrae (superior view)**.**

1.2.5 Ribs (1st)

Cortical bone powder was sampled from the outer surface of the serratus anterior, cancellous powder from the interior of the costoclavicular ligament attachment site (Figure S5).

Figure S5: Cortical and Cancellous sampling locations on the first rib (superior surface).

1.2.6 Metacarpals

Cortical bone was collected from the exterior surface of the shaft, cancellous from the interior of the head (Figure S6).

Figure S6: Metacarpal (palmar aspect) showing drilling locations for the collection of both cortical and cancellous tissue

1.2.7 Distal Phalanx

Cortical bone powder was collected from the pad and shaft of the distal phalanx, cancellous bone from the interior of the base (Figure S7).

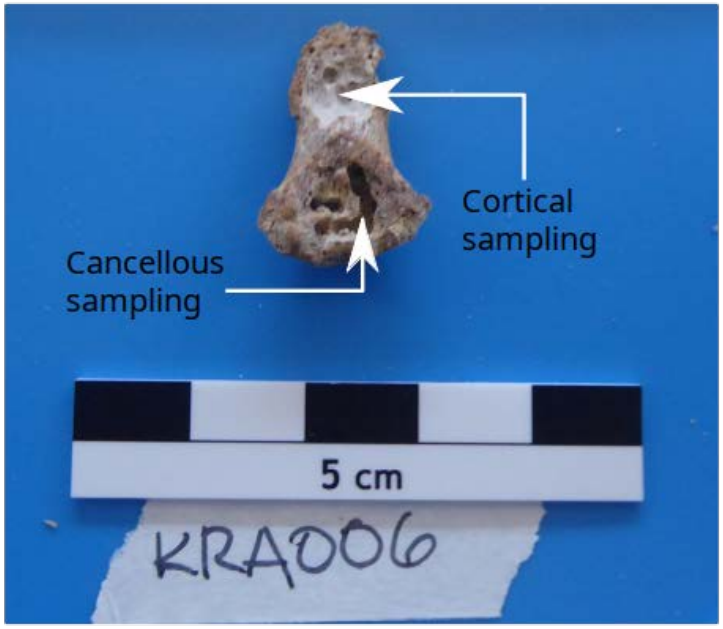

Figure S7: Distal phalanx (palmar aspect) showing drilling locations for the collection of both cortical and cancellous tissue.

1.2.8 Ischial Tuberosity

Cortical bone was collected from the exterior surface of the tuberosity, cancellous from the interior (Figure S8).

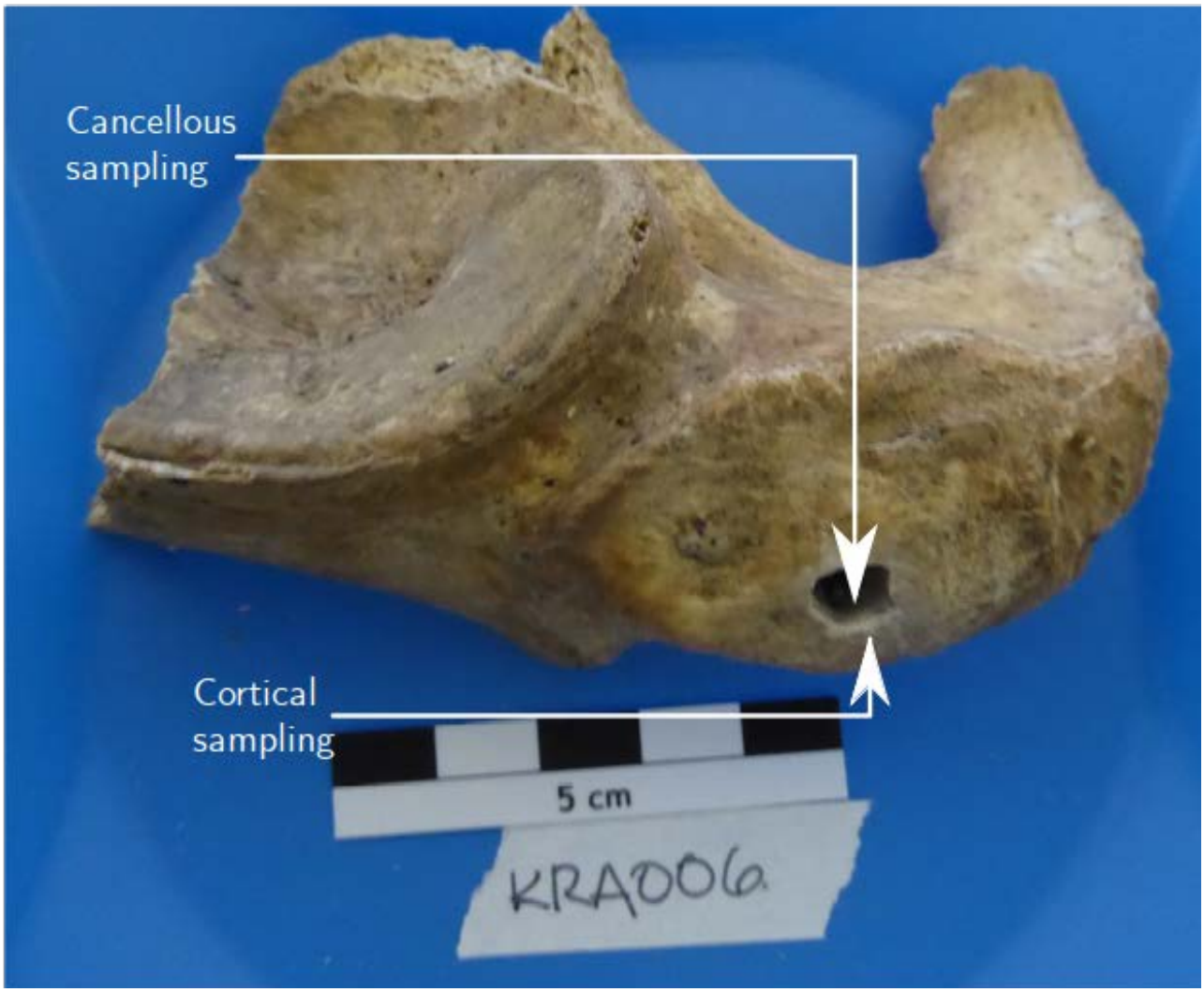

Figure S8: Ischial tuberosity (lateral view) showing drilling sites for the collection of both cortical and cancellous material.

1.2.9 Femora

Cortical bone material was collected from the shaft, just below the lesser trochanter and cancellous from the interior of the head (Figure S9).

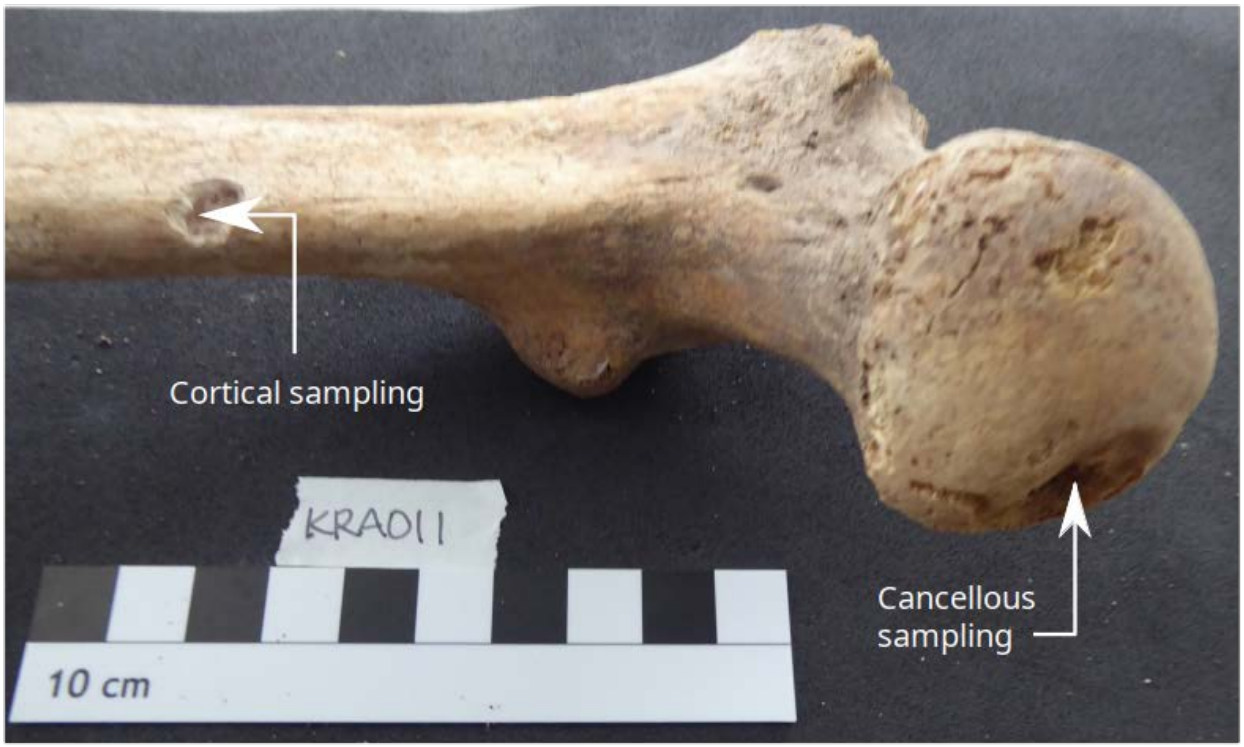

Figure S9: Femur (anterior view) showing drilling sites for the collection of both cortical and cancellous material.

1.2.10 Tali

Dense tissue was collected from the “neck” and articular surface, less compact cancellous from the interior of the medial facet (Figure S10).

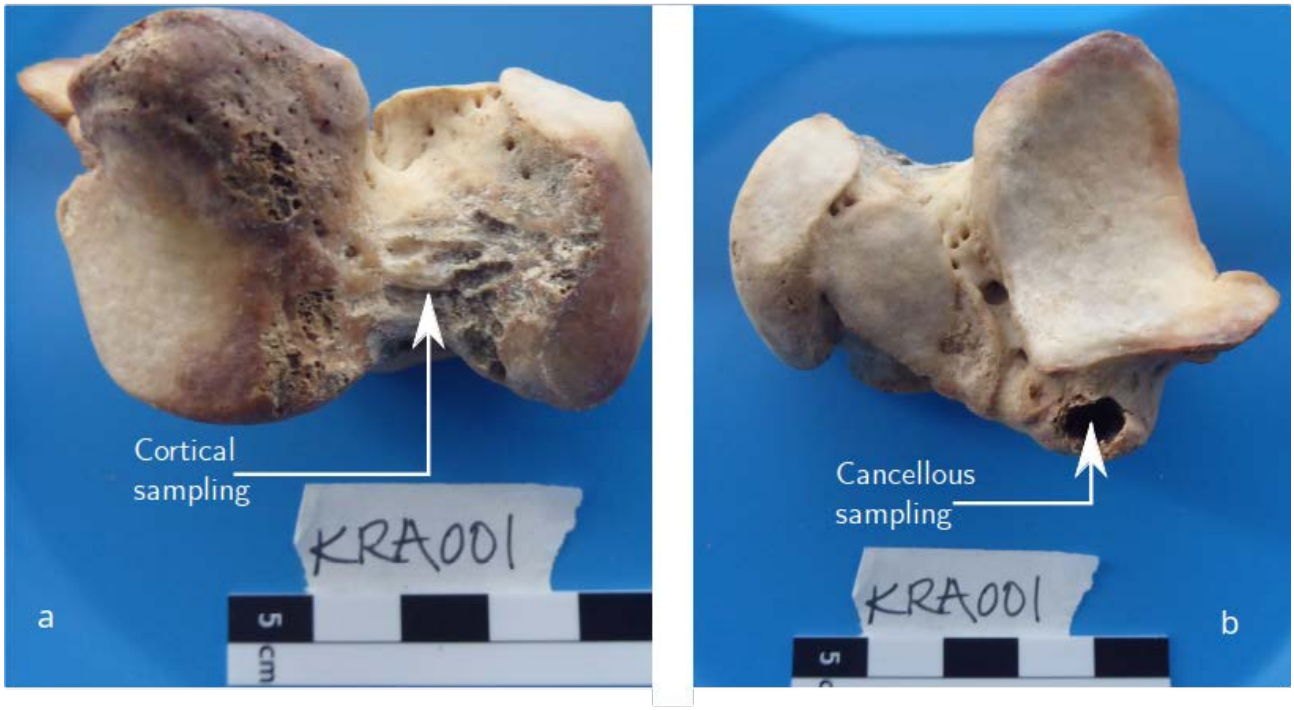

Figure S10: Talus showing drilling sites for the collection of both cortical (a; lateral surface and loosely packed cancellous tissue (b; inferior surface).

1.3 DNA extraction

One millilitre of UV-purified extraction buffer (900µl 0.5M EDTA; 75µl UV-treated, HPLC grade water; and 25µl 10mg/ml Proteinase K) was added to approximately 50mg of bone powder (where available) in a 2ml Eppendorf Biopur microcentrifuge tube and incubated (with rotation) overnight at 37°C. The mixture was then centrifuged for 2 minutes at 14000rpm and the supernatant collected and transferred to 50ml Falcon tube containing 10ml of UV-treated binding buffer (6ml 5M GuHCl, 4ml isopropanol) and 400µl 3M sodium acetate (pH: 5.2) and the contents mixed by inversion. This was then transferred into the funnel of a High Pure Viral Extract Extender Assembly and centrifuged for 8 minutes at 1500rpm. The column was then removed from the funnel and transferred to a fresh collection tube before being dry-centrifuged for 2 minutes at 14000rpm. 450µl of wash buffer (provided in the High Pure Viral Nucleic Acid Extraction Kit) was then added and the column spun at 14000rpm for 1 minute. The collection tube was then emptied and the wash repeated. The column was then dry-spun at 14000rpm for 1 minute before being transferred to a 1.5ml siliconized microcentrifuge tube for elution. Elution was done in two cycles of adding 50µl of Tris-EDTA-Tween buffer (Applichem low EDTA 1x Tris-EDTA buffer, 0.05% Tween 20), incubating at room temperature for 3 minutes, and centrifuged at 14000rpm for 1 minute, resulting in 100µl of purified aDNA extract.

2. Supplemental Analysis

2.1 Expected proportion of human DNA recovered simulations

Table S1. Frequency of observed rankings of skeletal elements in terms of human DNA-richness after 55,000 simulated samplings.

Skeletal Element	Frequency of observed rankings in endogenous DNA-richness (%)							
	1st	2nd	3rd	4th	5th	6th	7th	8th
Pars petrosa	41.87	22.08	14.03	9.68	6.40	4.20	2.07	0.81
Cementum	10.23	13.30	14.08	14.30	14.07	13.59	12.38	9.20
Dentin	6.34	9.03	10.74	12.50	13.80	15.16	16.94	16.62
Pulp	7.23	10.10	11.73	12.85	13.99	14.96	15.78	14.52
Vertebral Body	10.61	13.58	14.34	14.45	14.19	13.22	11.88	8.88
Superior Vertebral Arch	4.28	6.44	8.59	10.12	12.00	14.77	19.51	25.44
Distal Phalanx	10.65	13.91	14.43	14.30	14.02	13.48	11.92	8.42
Talus	9.93	12.72	13.21	12.94	12.67	11.76	10.67	8.06

2.2 Transformed graphs for both estimated genomic coverage and nuclear to mitochondrial read ratio.

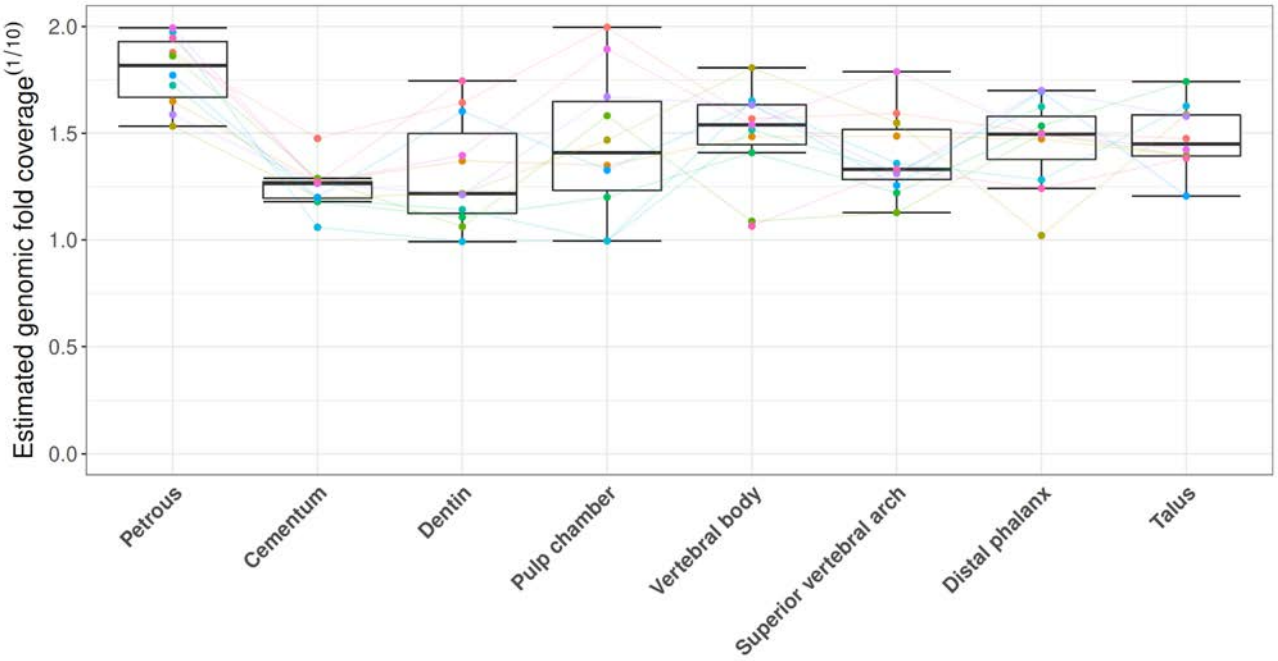

Figure S11. Transformed ($X^{0.1}$) estimated genomic coverage across the eight sampling locations with average proportion of human DNA content higher than the overall mean (>8.16%). Coloured points and lines represent the genomic coverage across sampling locations within an individual.

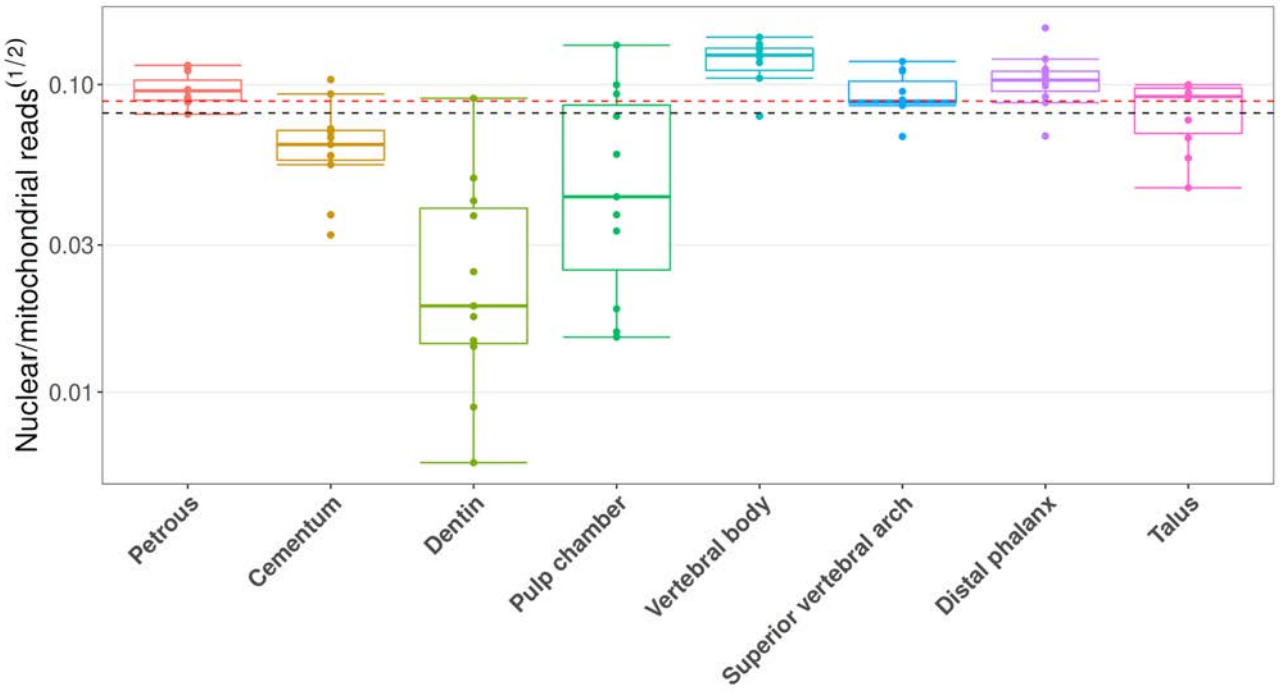

Figure S12. Transformed ($X^{0.5}$) nuclear to mitochondrial read ratio across the eight sampling locations with average proportion of human DNA content higher than the overall mean (>8.16%). The red line represents the overall median, the black line the overall mean.

2.3 Consistency of deamination patterns across both sampling location and individual.

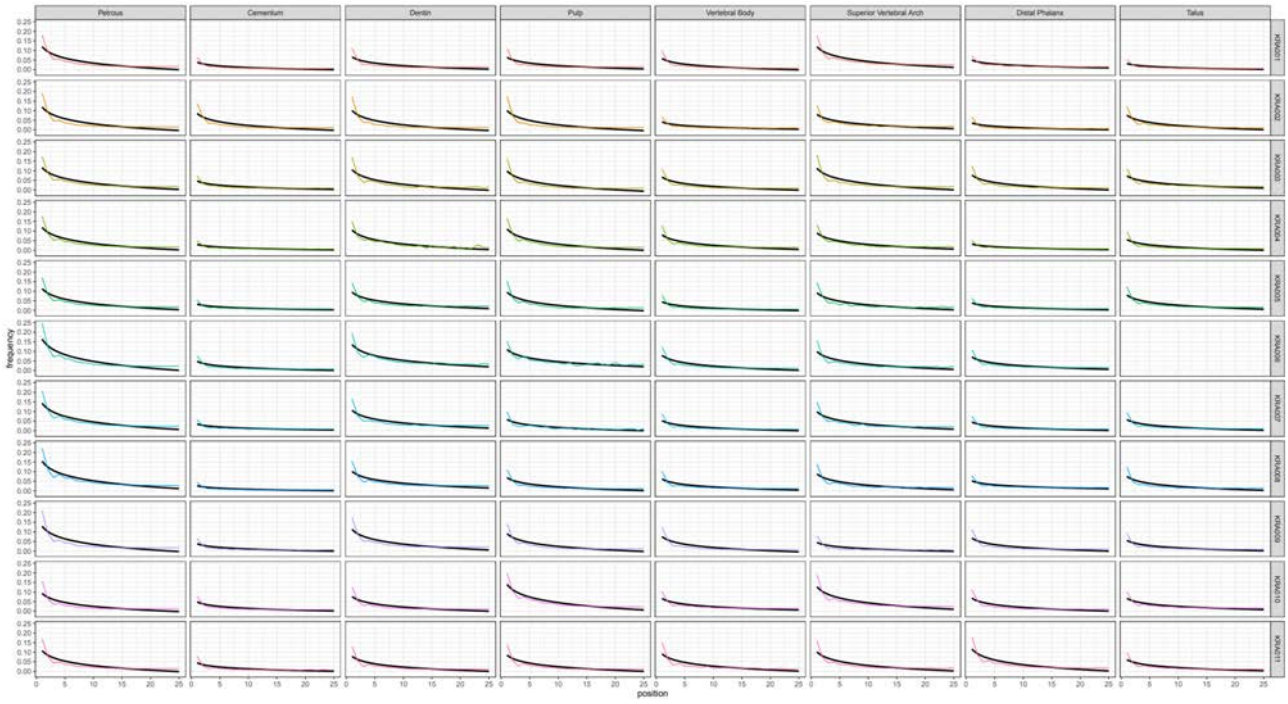

Figure S13. Deamination patterns for all eight sampling locations with higher average human DNA content than the overall mean (>8.16%) showing the consistency within each sampling location. Black lines represent lines of best fit.

2.4 Richness per milligram input material

The per mg richness of each individual sampling location is beyond the scope of this investigation. However, it was still noted that the cementum and the dental pulp chambers, despite yielding less starting material, were still comparable to all other sampling locations. As such, all relevant analyses were also performed after normalization of milligrams of material used in each DNA extraction.

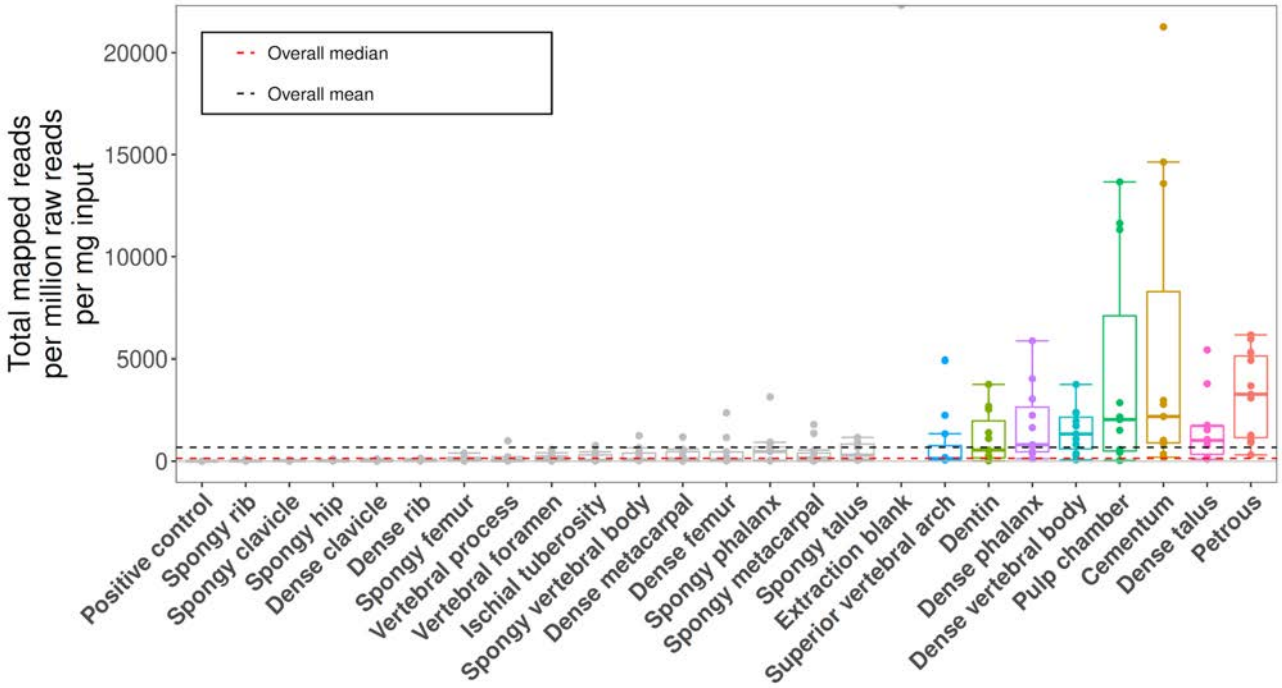

Figure S14. Total unique reads mapped to the hg19 human reference after normalization for starting input material and sequencing effort, showing the dental pulp chambers and cementum to be especially rich in DNA per mg. The extraction blank is included here for consistency only.

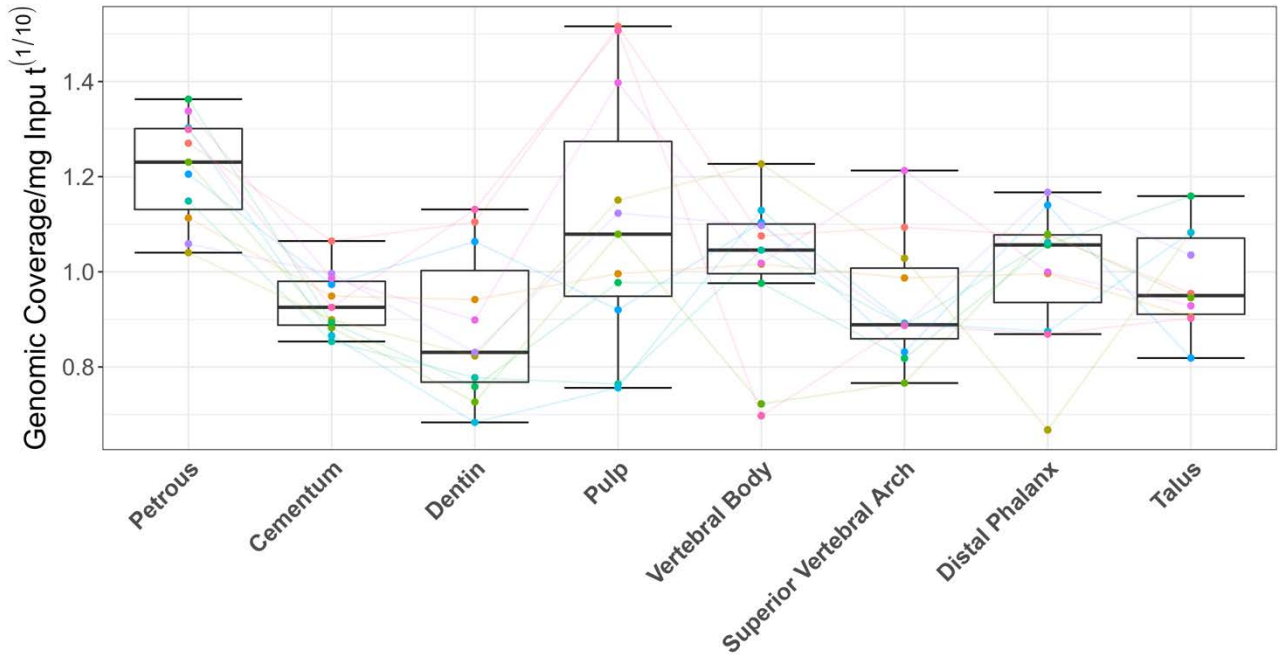

Figure S15. Estimated genomic coverage/mg contained within DNA libraries from each sampling location, showing the richness of the dental pulp chamber and increased richness in the cementum (to a level comparable with all other sampling locations) when input material is factored in. Coloured points and lines represent values within individuals.

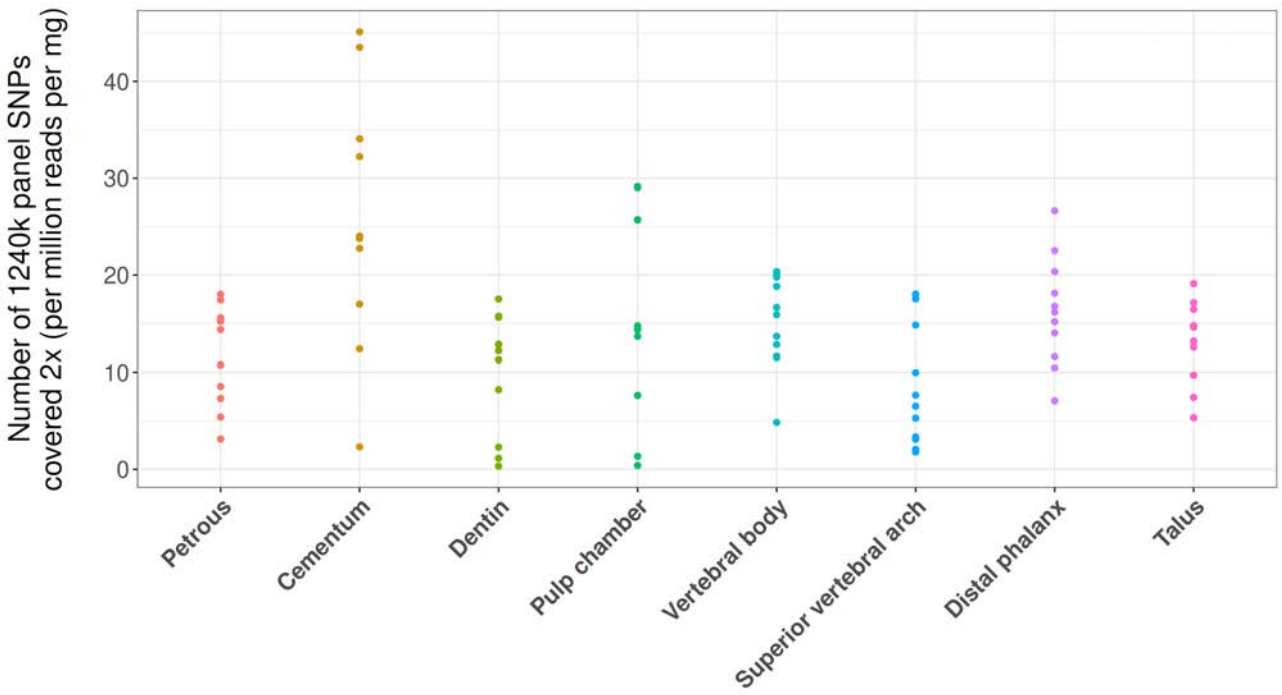

Figure S16. Number of 1240k panel SNPs covered at least 2x per read sequenced per mg of input material for all sampling locations, showing the increased richness of both the cementum and dental pulp chamber.

2.5 Evaluation of epiphyseal plates found in the two juvenile individuals included in the eleven individuals used for sampling.

Sampling was also conducted on the epiphyseal plates identified among the skeletal elements/individuals used for the main body of this study (from two individuals: in the femur, hip, and metacarpal of KRA004, in the femur and metacarpal of KRA005). As there were not enough instances of these features, they were excluded from the comparative analyses presented in the main body of this study. However, it should be noted that libraries stemming from epiphyseal plates performed well in terms of proportion of human DNA recovered, reads mapping to the human genome per million reads, and estimated genomic coverage with respect to libraries from other sampling locations from the same element in that individual (as evidenced in the corresponding Supplementary File 1). As such, further study into aDNA preservation in skeletal features such as epiphyseal plates in subadult individuals may be worthy of future consideration.

2.6 Additional measures of contamination

While contamination estimates derived from mitochondrial data can be useful for the evaluation of the four female individuals included in this study, they have been found to only offer similar accuracy to X chromosome contamination estimates for samples where the nuclear to mitochondrial read ratio exceeds 1:200[1], and a such are not appropriate for all sampling locations. Additionally, as the samples in this study were not sequenced deeply enough, nor target-enriched for mitochondrial reads, the majority of sampling locations did not yield sufficient numbers of mitochondrial reads to allow the accurate calculation of mitochondrial contamination estimates. However, it was possible to combine all enriched libraries for each individual and estimate mitochondrial contamination on the individual level using the Schmutzi pipeline[2]. Here we find no detectable mitochondrial contamination (0% reported, with upper and lower bounds of 0-0.5%) in ten of the eleven individuals regardless of genetic sex. In individual KRA011 (a genetic female), we observe 12.5% potential mitochondrial contamination (upper and lower bounds of 5.5%-19.5%), but are unable to ascertain if this is a systemic issue or limited to only certain sampling locations. Of note, after visual and manual inspection of all MT reads assemblies per individual (Geneious Prime 2020.1.2; http://www.geneious.com/), we find no indication of any contaminating sources, including in the assembly of KRA011. In our experience, contamination of 12.5% should result in a clearly visible background in the read assembly. However, in the case of KRA011 deviations from the variant calls could only be observed at an average of 2.85% at C>T or G>A positions, more parsimoniously explained by residual aDNA damage. All eleven individuals produced unambiguous haplotype calls (Table S2) when applying Haplogrep2 on the consensus sequences, further adding to the fidelity of the ancient sequence data[3].

Additionally, multi-dimensional scaling analysis was performed for all enriched libraries as a qualitative means to reinforce the ANGSD contamination estimates (Supplementary Material

Figure S17), here all sampling locations from each individual clustered together, apart from the libraries corresponding to the dentin of individuals KRA003 and KRA004). It should be noted that all three of these samples are of low coverage (2,979 and 220 1240k panel SNPs covered 2x respectively, see Supplementary File 1: 1240k_SNP_Capture; covered2x_1240kpanel), making any inference of contamination based on this analysis for these samples challenging.

Supplementary Table S2. Individual level mitochondrial haplotype assignments

Individual (Laboratory ID)	**Archaeological ID (Burial Nr.-Individual Nr.)**	**Mitochondrial haplotype**
KRA001	25-1a	X2x1b
KRA002	20-2a	HV0a
KRA003	113-6a	H73a
KRA004	246-1a	U3a
KRA005	276-2a	H23
KRA006	307-4a	H5a1a
KRA007	377-6a	U5b1e1
KRA008	436-6a	T1a10
KRA009	566-3a	H13a1a1e
KRA010	600-7a	H26a1
KRA011	632-2a	J1c4

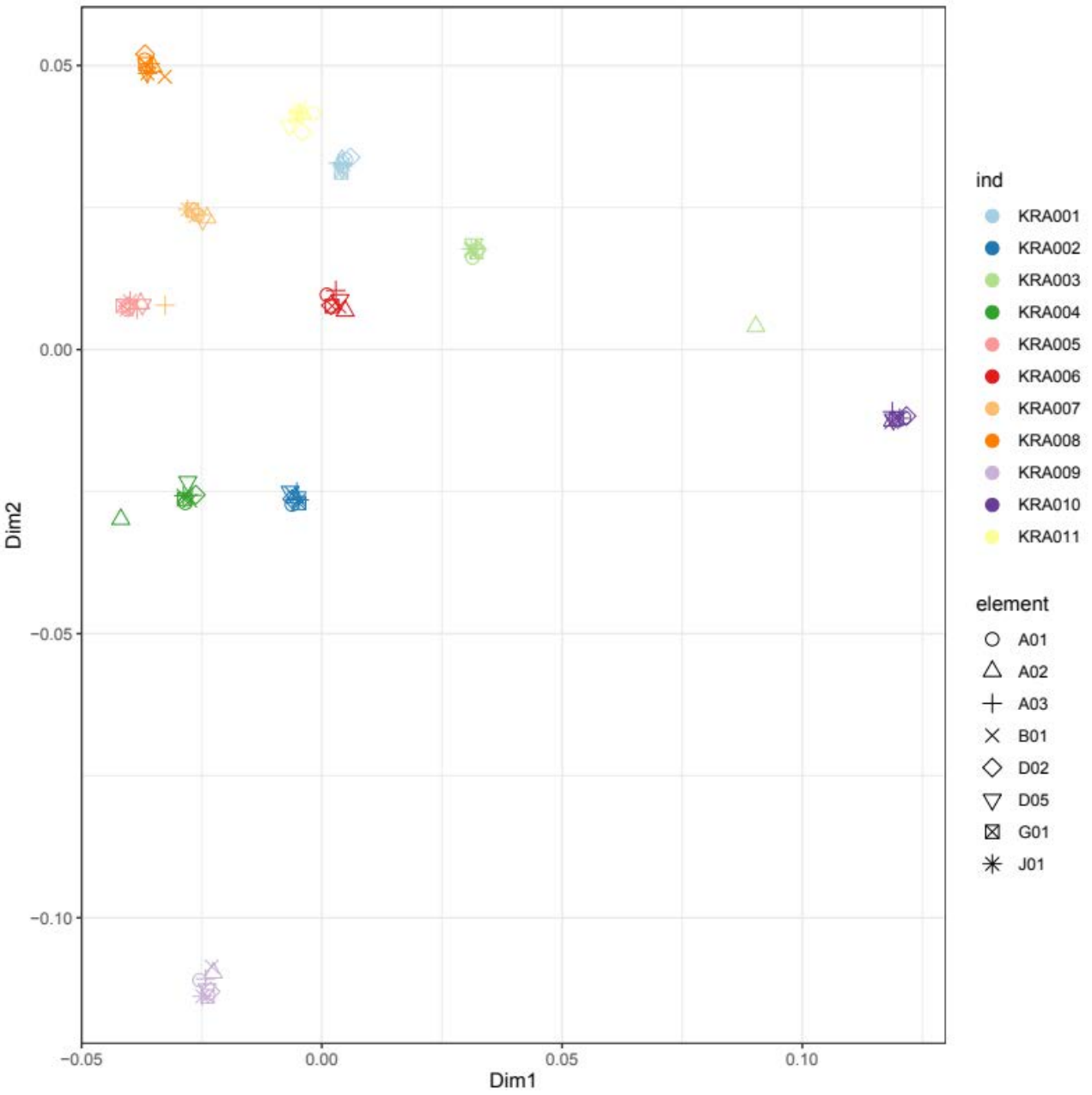

Figure S17. Multi-dimensional scaling plot of all 1240k enriched samples showing the consistent clustering of samples within each individual. Element codes A01, 02 and 03 refer to the cementum, dentin, and pulp chamber sampling locations (respectively); B01 to the petrous pyramid, D02 and 05 to the vertebral body and superior vertebral arch (respectively), G01 to the distal phalanx, and J01 to the talus. Samples KRA003.A02, KRA004.A02, and KRA005.A03 are low coverage samples (2,979 and 220 1240k panel SNPs covered 2x respectively).

References

*1. Furtwängler, A. et al. Ratio of mitochondrial to nuclear DNA affects contamination estimates in ancient DNA analysis. Scientific Reports **8**, 1–8 (2018).*

*2. Renaud, G., Slon, V., Duggan, A. T. & Kelso, J. Schmutzi: estimation of contamination and endogenous mitochondrial consensus calling for ancient DNA. Genome Biology **16**, 224 (2015).*

*3. Weissensteiner, H. et al. HaploGrep 2: mitochondrial haplogroup classification in the era of high-throughput sequencing. Nucleic Acids Res. **44**, W58-63 (2016).*

Additional File 2

Format: Excel spreadsheet (*.xlsx)

Title: Supplementary File 1

Description: Complete data table showing full descriptions of sampling and DNA extraction yields from all samples processed, including all positive and negative controls. Additionally, this file contains all raw data used in all downstream analyses.

3. Manuscript 2

"Optimized Bone Sampling Protocols for the Retrieval of Ancient DNA from Archaeological Remains"

Cody E Parker, Kirsten I. Bos, Wolfgang Haak, Johannes Krause
Published: JoVE, 30/11/2021

Parker, C.E., Bos, K.I., Haak, W., Krause, J. Optimized Bone Sampling Protocols for the Retrieval of Ancient DNA from Archaeological Remains. J. Vis. Exp. (177), e63250, doi:10.3791/63250 (2021).

Throughout the production of Manuscript 1, we observed a distinct lack of easily accessible sampling techniques across the majority of the twenty-three separate sampling locations analyzed. As such, in Manuscript 2 we present the full, video annotated, sampling techniques for the production of bone powder from the sampling locations found to be the most efficient for downstream aDNA extraction in analyses in Manuscript 1 (material from the dense cochlear region of the petrous pyramid, material from the cementum, dentin, and pulp chamber of *in situ* molars; cortical bone from the vertebral body and superior vertebral arch, cortical bone from the distal phalanx, and dense tissue harvested from the exterior of the talus), in order to make these techniques more openly available across the scientific community.

Author contributions

CP is the primary author (95%) and was responsible for all laboratory procedures including the gathering, processing, method development, sampling from, and DNA extraction from all samples (90%), and their subsequent analyses (60%). KB acted as co-supervisor, provided funding, aided in the experimental design of this study, and contributed to the writing and editing of this manuscript. WH acted as co-supervisor, provided funding, aided in the experimental design of this study, coordinated sample selection, and contributed to the

writing and editing manuscript. JK acted as co-supervisor, aided in experimental design, and provided funding for the study.

Author	Conception	Data analyses	Experimentation	Writing	Sample procurement
C.P.	30%	N/A	100%	90%	N/A
J.K.	30%	N/A	N/A	N/A	N/A
K.B.	20%	N/A	N/A	5%	N/A
W.H.	20%	N/A	N/A	5%	N/A

jove

Optimized Bone Sampling Protocols for the Retrieval of Ancient DNA from Archaeological Remains

Cody E. Parker[1,2], **Kirsten I. Bos**[1,3], **Wolfgang Haak**[1,3], **Johannes Krause**[1,3]

[1] Department of Archaeogenetics, Max Planck Institute for the Science of Human History [2] School of Human Evolution and Social Change, Arizona State University [3] Department of Archaeogenetics, Max Planck Institute for Evolutionary Anthropology

Corresponding Author

Cody E. Parker
cody.parker@asu.edu

Citation

Parker, C.E., Bos, K.I., Haak, W., Krause, J. Optimized Bone Sampling Protocols for the Retrieval of Ancient DNA from Archaeological Remains. *J. Vis. Exp.* (177), e63250, doi:10.3791/63250 (2021).

Date Published

November 30, 2021

DOI

10.3791/63250

URL

jove.com/video/63250

Abstract

The methods presented here seek to maximize the chances for the recovery of human DNA from ancient archaeological remains while limiting input sample material. This was done by targeting anatomical sampling locations previously determined to yield the highest amounts of ancient DNA (aDNA) in a comparative analysis of DNA recovery across the skeleton. Prior research has suggested that these protocols maximize the chances for the successful recovery of ancient human and pathogen DNA from archaeological remains. DNA yields were previously assessed by Parker et al. 2020 in a broad survey of aDNA preservation across multiple skeletal elements from 11 individuals recovered from the medieval (radiocarbon dated to a period of circa (ca.) 1040-1400 CE, calibrated 2-sigma range) graveyard at Krakauer Berg, an abandoned medieval settlement near Peißen Germany. These eight sampling spots, which span five skeletal elements (*pars petrosa*, permanent molars, thoracic vertebra, distal phalanx, and talus) successfully yielded high-quality ancient human DNA, where yields were significantly greater than the overall average across all elements and individuals. Yields were adequate for use in most common downstream population genetic analyses. Our results support the preferential use of these anatomical sampling locations for most studies involving the analyses of ancient human DNA from archaeological remains. Implementation of these methods will help to minimize the destruction of precious archaeological specimens.

Introduction

The sampling of ancient human remains for the purposes of DNA recovery and analysis is inherently destructive[1,2,3,4]. The samples themselves are precious specimens and morphological preservation should be preserved wherever possible. As such, it is imperative that sampling practices be optimized to both avoid unnecessary destruction of irreplaceable material and to maximize the probability of success. Current best practice techniques are based on a

small cohort of studies limited to either forensic surveys[5,6], studies of ancient specimens where the development of optimal sampling is not the direct aim of the study[7], or dedicated studies utilizing either non-human remains[8] or targeting a very small selection of anatomical sampling locations (used here to denote a specific area of a skeletal element from which bone powder, for use in downstream DNA analyses, was generated)[9,10]. The sampling protocols presented here were optimized in the first large-scale systematic study of DNA preservation across multiple skeletal elements from multiple individuals[11]. All samples stemmed from skeletal elements recovered from 11 individuals excavated from the church graveyard of the abandoned medieval settlement of Krakauer Berg near Peißen, Saxony-Anhalt, Germany (see **Table 1** for detailed sample demographics) and, as such, may need modification for use with samples outside of this geographical/temporal range.

Individual	Sex	Estimated age at death	^{14}C dates (CE, Cal 2-sigma)
KRA001	Male	25-35	1058-1219
KRA002	Female	20-22	1227-1283
KRA003	Male	25	1059-1223
KRA004	Male	15	1284-1392
KRA005	Male	10-12	1170-1258
KRA006	Female	30-40	1218-1266
KRA007	Female	25-30	1167-1251
KRA008	Male	20	1301-1402
KRA009	Male	Unknown	1158-1254
KRA010	Male	25	1276-1383
KRA011	Female	30-45	1040-1159

Table 1: Genetically determined sex, archaeologically determined estimated age at death, and radiocarbon dating (^{14}C Cal 2-sigma) for all the 11 individuals sampled. This table has been adapted from Parker, C. et al. 2020[11].

These protocols allow for a relatively straightforward and efficient generation of bone powder from eight anatomical sampling locations across five skeletal elements (including the *pars petrosa*) with limited laboratory-induced DNA contamination. Of these five skeletal elements, seven anatomical sampling locations found on four skeletal elements have been determined to be viable alternatives to the destructive sampling of the petrous pyramid[11,12]. These include the cementum, dentin, and pulp chamber of permanent molars; cortical bone gathered from the superior vertebral notch as well as from the body of thoracic vertebrae; cortical bone stemming from the inferior surface of the

apical tuft and shaft of the distal phalanges; and the dense cortical bone along the exterior portion of the tali. While there are several widely applied methods for the sampling of the *pars petrosa*[4,12,13,14], dentin, and the dental pulp chamber[1,2,15], published methods describing the successful generation of bone powder from the cementum[16], vertebral body, inferior vertebral notch, and talus can be difficult to obtain. As such, here we demonstrate optimized sampling protocols for the petrous pyramid (step 3.1); cementum (step 3.2.1), dentin (step 3.2.2), and dental pulp (step 3.2.3) of adult molars; cortical bone of the vertebral body (step 3.3.1) and superior vertebral arch (step 3.3.2); the distal phalanx (step 3.4); and the talus (step 3.5) in order to make the effective use of these skeletal elements for both aDNA and forensic research more widely accessible.

Protocol

All research presented herein was performed in compliance with the guidelines set forth by the Max Planck Institute for the Science of Human History, Jena, Germany for working with ancient human remains. Before performing any steps of this protocol ensure to adhere to all local/state/federal ethical requirements pertaining to both obtaining permission for the scientific study and use of human remains for destructive sampling in your area. All procedures/chemical storage should be performed according to individual institutional safety guidelines.

1. Considerations before sample processing

1. Treat samples with care as ancient remains are an irreplicable and finite resource (e.g., sampling should be as minimally wasteful as possible, and all remains returned to their respective and lawful providers if possible).
2. Perform all steps in a clean-room environment, preferably at a dedicated ancient DNA facility[17,18,19]. Use personal protective equipment (PPE) consisting of sterile microporous coveralls with hood, sterile gloves (two pairs), surgical mask, protective eyewear, and sterile boots or non-slip shoes with sterile covers (see **Table of Materials**). Change gloves frequently, especially between samples.
3. Clean and disinfect all equipment and surfaces thoroughly with bleach/DNA decontamination solution/ ethanol and UV irradiation (wavelength: 254 nm) where possible (e.g., drill bits, drills, vises/clamps, etc.). Finally, it is highly recommended to take regular ergonomic breaks (every 2-3 h if possible) to avoid over-exhaustion due to the clean-room environment.

   NOTE: All skeletal remains should be appropriately documented (e.g., photographed, weighed, and if possible micro-CT scanned, 3D imaged, etc.) before sampling (protocols for appropriate documentation are not covered in this manuscript). All sampling protocols may be paused between sampling iterations and the samples can be stored indefinitely in a dry, temperature controlled (25 °C), sterile environment.

2. Pretreatment

1. Decontaminate all anatomical sampling locations prior to bone powder generation to minimize the risk of contamination[18].

   NOTE: The efficacy of bleach and/or surface removal (see NOTE in step 3.3.2 for surface removal steps) for sample decontamination is still a matter of debate among

aDNA researchers[8,19,20,21,22,23,24,25] as both may influence overall DNA yields, especially in highly degraded samples. As such, the following steps are considered optional and are included here as they were used in all samples to generate the representative results presented in this paper. It is recommended that the use of these pre-treatment protocols be determined on a case-by-case basis based on the molecular application, age, rarity, and level of morphological degradation of each sample set.

1. Perform all sampling in a dedicated clean room under a UV light equipped polymerase chain reaction (PCR) hood or biosafety cabinet with airflow turned off. Spread sterile aluminum foil across the benchtop to catch any stray bone powder/fragments.
2. Ensure all bone fragments are recovered (for repatriation) before disposing of the foil. Change the foil between the treatment of each skeletal element. Dispose of used foil in an autoclavable biohazard bag/receptacle.
3. Remove as much loose dirt/detritus as possible from anatomical sampling locations by gently wiping the area with a lint-free dry sterile wipe (see **Table of Materials**). Dispose of the wipes in autoclavable biohazard bags or receptacles.
4. Decontaminate the cleaned surface by wiping with a sterile wipe moistened with diluted commercial bleach (~0.01% v/v, diluted with ultrapure DNase/RNase free water) and allow to incubate for 5 min. Dispose of the wipes in autoclavable biohazard bags or receptacles.

   CAUTION: Bleach is a highly corrosive and reactive chemical; hence appropriate safety precautions should be in place before its use.
5. Remove as much residual bleach as possible from the anatomical sampling location with a sterile wipe moistened with ultrapure DNase/RNase-free water. Dispose of the wipes in autoclavable biohazard bags or receptacles.
6. Expose all cleaned anatomical sampling locations to UV radiation for 30 min (wavelength: 254 nm), and then allow to dry fully at room temperature. Ensure that the anatomical sampling locations are completely dry before proceeding with sampling or returning to storage to not only make bone powder generation easier but also to prevent further degradation of the sample (e.g., mold).

   CAUTION: Exposure to UV radiation can be harmful to the eyes.
7. Move immediately to sampling or store skeletal elements in a dry, temperature controlled (25 °C) sterile environment.

3. Bone powder generation

NOTE: The following protocols are intended for use in DNA extraction following the Dabney et al. 2019 protocol[26].

1. Sampling of *pars petrosa*

   NOTE: This protocol is adapted from procedures described in Pinhasi et al. 2019[4] and is presented here for ease of use. This protocol does not represent the current, least destructive method for the sampling of *pars petrosa*. As such, it is recommended to use the protocol described by Sirak et al. 2017[13] or Orfanou et al.

2020[14] for samples where morphological preservation is of maximum importance.

1. Perform all sampling in a dedicated clean room under a UV light equipped PCR hood or biosafety cabinet (wavelength: 254 nm) with airflow turned off. Spread sterile aluminum foil across the benchtop to catch any stray bone powder/fragments.
2. Ensure all bone fragments and as much powder as possible is recovered (for repatriation) before disposing of foil. Change the foil between each sampling. Dispose of the used foil in an autoclavable biohazard bag/receptacle.
3. Secure the dry, decontaminated element using a sterilized clamp or vise.
4. Cut the *pars petrosa* in half along the superior *sulcus petrosus* (see **Figure 1**) using a standard jeweler's saw equipped with a 0.6 mm blade (see **Table of Materials**) at medium speed to avoid overheating (see NOTE below step 3.1.6).
   CAUTION: The *pars petrosa* is very dense, and as such may be difficult to cut. Take care to keep the element securely clamped to avoid injury. Dispose of any broken saw blades in the appropriate sharps' receptacle.
5. Remove the petrous portions from the clamp. Recover and save any loose/excess material.
6. Place weigh paper in a sterile weighing boat
7. Hold the petrous portion over the weigh paper, cut side tilted toward the weighing tray. Drill into the dense cortical bone between the facial canal and mastoid antrum (appears shinier than the surrounding material, see **Figure 1**) using dental drill equipped with a small gauge bit (see **Table of Materials**) and set to medium speed, medium torque to produce bone powder.
   NOTE: Drilling/Cutting should be done in short bursts at low to medium speeds to avoid overheating the bone and potentially destroying/damaging DNA. Anecdotally, when the dense portion of the petrous begins to overheat a smell described as cooking bacon may be observed. Cease drilling/sawing immediately and allow the bone to rest until sufficiently cool before resuming.
8. Repeat drilling until approximately 50-100 mg of powder is collected in the weigh paper, as measured using an enclosed balance accurate to at least 0.01 mg (see **Table of Materials**).
   NOTE: Where possible it is suggested to gather 100 mg of bone powder to allow for two replicate DNA extraction of 50 mg each. However, this may not always be possible based on either limitation of the anatomical sampling locations themselves (e.g., the distal phalanx, dental pulp chamber) or the need for morphological preservation. For other locations, such as the cementum, considerably less than 50 mg of the material may be available. However, the cementum, dental pulp chamber, and distal phalanx have all been shown to yield significant endogenous DNA[11,27,28], despite lower initial input of bone powder from the extraction process.
9. Transfer powder from the weigh paper to a 2 mL labeled low-bind, safe-lock tube for extraction or storage. Store samples at -20 °C, indefinitely.
10. Store remaining bone/excess powder in a dry, temperature controlled (25 °C) sterile environment until return/repatriation can be completed.

11. Dispose of all waste in autoclavable biohazard bags or receptacles. Sterilize/decontaminate all reusable equipment (e.g., clamps, drill bits, drills, saws, etc.) using bleach/DNA decontamination solution/ethanol and UV (wavelength: 254 nm) exposure, as applicable, between each sampling.

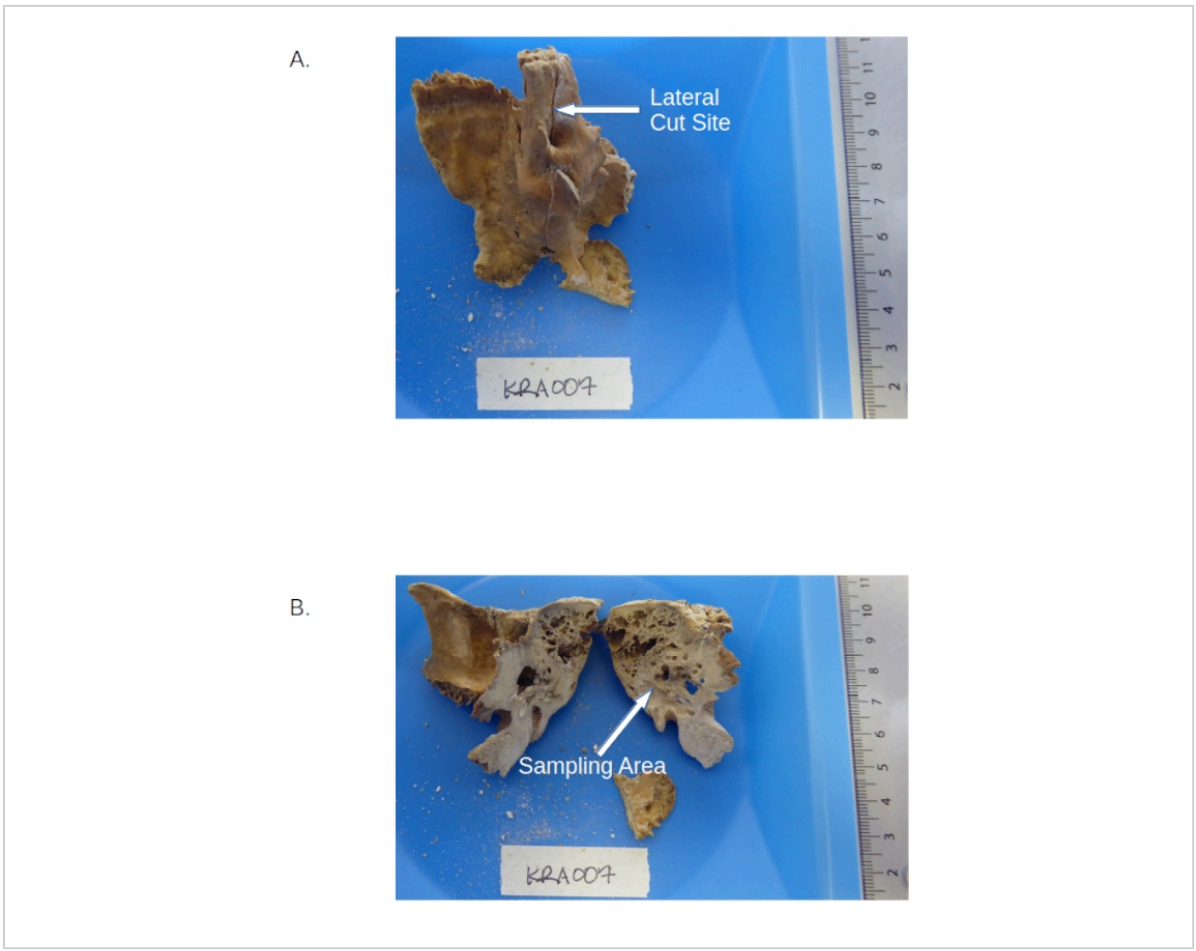

Figure 1: Temporal bone including the *pars petrosa*. (**A**) Sample pre-cutting showing the locations of the petrous pyramid and the *sulcus petrosa*. (**B**) Petrous portion post-cutting highlighting the dense areas to be drilled. Please click here to view a larger version of this figure.

2. Sampling of permanent molars

   NOTE: For the sampling of permanent molars, pre-select *in situ* molars with fused roots and ideally void of caries, cracks in the enamel, or excessive wear for best results. Remove any dental calculus sampling and store at -20 °C for possible future analyses of the oral microbiome (procedure not covered here).

1. Sampling of the cementum
    1. Perform all sampling in a dedicated clean room under a UV light equipped PCR hood or biosafety cabinet (wavelength: 254 nm) with airflow turned off. Spread sterile aluminum foil across the benchtop to catch any stray bone powder/fragments.
    2. Ensure all bone fragments and as much powder as possible are recovered (for repatriation) before disposing of foil. Change the foil between each sampling. Dispose of used foil in an autoclavable biohazard bag/receptacle.
    3. Place a sheet of weigh paper into a sterile weighing tray.
    4. Hold/secure the decontaminated molar by the enamel, root down, over a weighing tray using a hand-held clamp such as an adjustable wrench (see **Table of Materials**).
    5. Equip a dental drill with a diamond-edged circular cutting wheel. With the drill set to a medium speed/torque setting, lightly touch the edge of the bit to the root at an angle of approximately -20°.
    6. Scrape downward into the tray to remove/collect the yellow, outermost material from the root (cementum). Stop collection when the lighter (white) material of the dentin becomes visible.
    NOTE: It is important to match the direction of rotation of the cutting bit in relation to the collection tray to avoid the powder becoming aerosolized and potentially wasting the sample by missing the tray entirely. The cementum is particularly rich in DNA; however, typical yields of material are much smaller than other anatomical sampling locations (~7-20 mg)[11,27,28].
    7. Record mass of powder collected in weigh paper using an enclosed balance accurate to at least 0.01 mg (see **Table of Materials**).
    8. Transfer powder from the weigh paper to a 2 mL low-bind, safe lock tube for extraction. Store at -20 °C, indefinitely.
2. Sampling of the pulp chamber
    1. After the cementum has been collected (if desired), section the molar along the cemento-enamel junction using a jeweler's saw to remove the crown (see **Figure 2**).
    2. Place a new sheet of weigh paper in a new weighing tray.
    3. Secure the crown section in a handheld clamp or vise, over the weighing tray. Hold cut side tilted downward and drill/scrape material as the first pass with a dental drill equipped with a small gauge drilling bit (see **Table of Materials**) along the edges of the pulp chamber within the crown portion (see **Figure 2**).
    NOTE: Only the first pass of the interior of the pulp chamber is to be collected and labeled as pulp material (5-15 mg typical yield), anything deeper into the tooth is considered dentin.
    4. Turn the tooth with the inferior portion facing down, tap the clamp with a hammer, and collect the liberated powder on the weigh paper.
    5. Record the weight of the powder collected in the weigh paper using an enclosed balance

accurate to at least 0.01 mg (see **Table of Materials**).

6. Transfer powder from the weigh paper to a 2 mL low-bind, safe-lock tube for extraction. Store at -20 °C, indefinitely.

3. Sampling of the dentin

1. Place a new sheet of weigh paper in a new weighing tray.

2. Hold the crown section over the weighing tray (as per step 3.2.2.3), drill out and collect further 50-100 mg of dentin as measured using an enclosed balance accurate to 0.01 mg (see **Table of Materials**) from the interior of the pulp chamber in the same manner for further dentin sampling (see **Figure 2**).

3. Transfer bone powder from the weigh paper to a 2 mL low-bind, safe-lock tube for extraction. Store at -20 °C, indefinitely.

4. Store the remaining tooth pieces/excess powder in a dry, temperature controlled (25 °C) sterile environment until return/repatriation can be completed.

5. Dispose of all waste in autoclavable biohazard bags or receptacles. Sterilize/decontaminate all reusable equipment (e.g., clamps, drill bits, drills, saws, etc.) using bleach/DNA decontamination solution/ethanol and UV (wavelength: 254 nm) exposures as applicable, between each sampling.

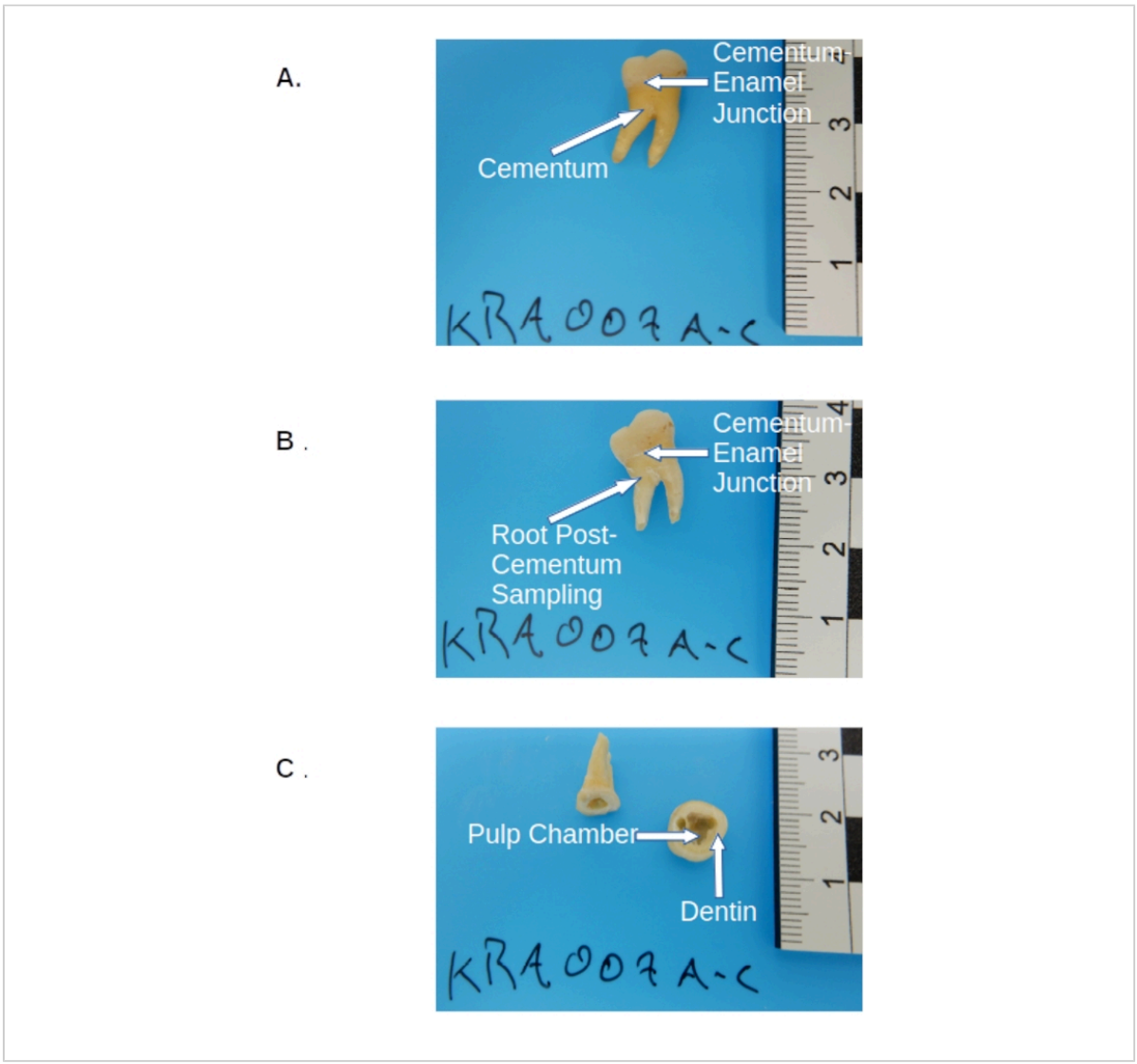

Figure 2: Permanent molar pre-sampling. (**A**) Pre-treated molar prior to sampling, showing crown, cementum (yellowish layer of the root), and the cutting site at the cemento-enamel junction. (**B**) The same molar post-cementum collection, showing the cut site at the cemento-enamel junction. (**C**) Molar post-cutting and sampling showing anatomical sampling locations for the dental pulp chamber and dentin within the crown. Please click here to view a larger version of this figure.

3. Sampling of the thoracic vertebrae

1. Sampling of the vertebral body

1. Perform all sampling in a dedicated clean room under a UV light equipped PCR hood or biosafety cabinet (wavelength: 254 nm) with airflow turned off. Spread sterile aluminum foil across the benchtop to catch any stray bone powder/fragments.
2. Ensure all bone fragments and as much powder as possible are recovered (for repatriation) before disposing of foil. Change the foil between each sampling. Dispose of used foil in an autoclavable biohazard bag/receptacle.
3. Place a small sheet of weigh paper into a standard weighing tray.
4. Secure the vertebrae with a clamp or hand vise, with the vertebral body outward.
5. Hold the vertebrae over the weighing tray with the vertebral body tilted downward. Using a dental drill equipped with a small gauge drilling bit (see **Table of Materials**) set to low-speed high torque, drill along the outermost rim (inferior and superior) of the cortical bone surrounding the cancellous inner tissue of the vertebral body (see **Figure 3**).
6. Scrape the bit against the cortical layer over a standard weighting tray until 50-100 mg of material is collected, as measured using an enclosed balance accurate to 0.01 mg (see **Table of Materials**).
7. Transfer bone powder from the weigh paper to a 2 mL low-bind, safe lock tube for extraction. Store at -20 °C, indefinitely.

2. Sampling of the superior vertebral arch

NOTE: This step is optional. Remove and discard the outermost layer of the cortical bone of the superior vertebral arch using a dental drill equipped with a small gauge drilling bit (see **Table of Materials**) by scraping it along the surface[19]. This is not suggested for sampling from the vertebral body, as the layer of cortical bone is generally very thin and likely to be entirely depleted by this process (see NOTE in section 2).

1. Place a small sheet of weigh paper into a standard weighing tray.
2. Secure the vertebrae in a hand clamp/vise with the vertebral process outward, superior aspect down.
3. While holding the vertebrae, superior aspect down, over a weighing tray, drill upwards into the center of the V shaped notch formed by the fusion of the spinous process with the lamellae (see **Figure 3**) using a dental drill with a small gauge bit (see **Table of Materials**) set to low speed and high torque.
4. Cease drilling when there is a noticeable drop in resistance. Change the drilling position slightly and repeat until 50-100 mg of bone powder is collected, as measured using an enclosed balance accurate to 0.01 mg (see **Table of Materials**).
5. Transfer bone powder from the weigh paper to a 2 mL low-bind tube for extraction. Store at -20 °C, indefinitely.
6. Store remaining bone/excess powder in a dry, temperature controlled (25 °C) sterile environment until return/repatriation.

7. Dispose of all waste in autoclavable biohazard bags or receptacles. Sterilize/decontaminate all reusable equipment (e.g., clamps, drill bits, drills, saws, etc.) using bleach/DNA decontamination solution/ethanol and UV (wavelength: 254 nm) exposure, as applicable, between each sampling.

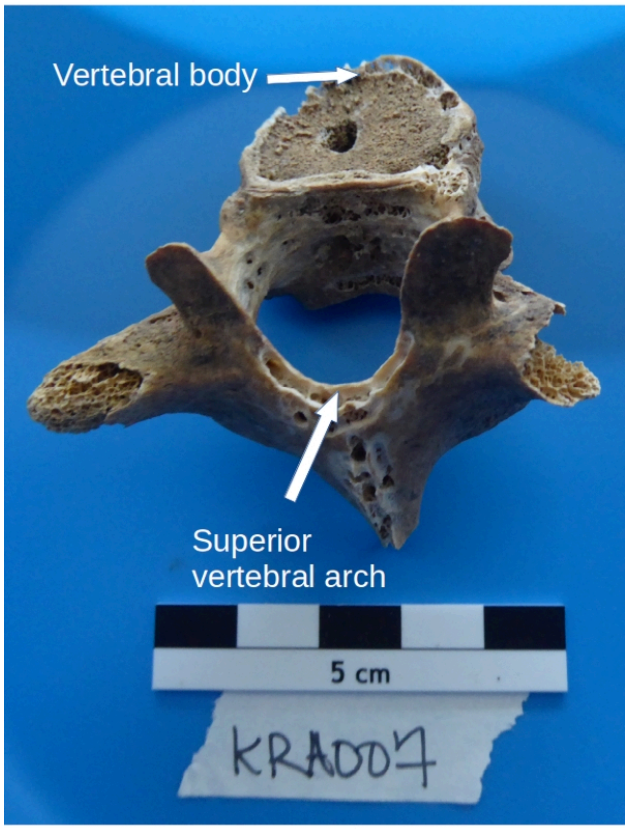

Figure 3: Vertebral body and superior vertebral arch cortical bone anatomical sampling locations of the thoracic vertebra. Please click here to view a larger version of this figure.

4. Sampling of the distal phalanx

   NOTE: This step is optional. Remove and discard the outermost layer of the cortical bone of the shaft and/or apical tuft using a dental drill equipped with a small gauge drilling bit by scraping it along the surface[19]. This may not be possible for samples with excessively thin cortical bone or juvenile remains (see NOTE in section 2).

   1. Perform all sampling in a dedicated clean room, under a UV light equipped PCR hood or biosafety cabinet (UV wavelength: 254 nm) with airflow turned

off. Spread sterile aluminum foil across the benchtop to catch any stray bone powder/fragments.

2. Ensure all bone fragments and as much powder as possible are recovered (for repatriation) before disposing of foil. Change the foil between each sampling. Dispose of used foil in an autoclavable biohazard bag/receptacle.

3. Place a small sheet of weigh paper into a standard weighing tray.

4. Secure the sample in handheld clamp/vise, superior side upwards.

5. Hold the sample over the weighing tray, collect bone powder from the cortical bone from the inferior side of the apical tuft and shaft by drilling through the outermost dense layers (see **Figure 4**) using a dental drill equipped with a small gauge drilling bit (see **Table of Materials**).

6. Cease drilling when there is a marked decrease in resistance, as this signifies lighter, cancellous material. Repeat this process, radiating outward from the initial drilling until at least 50-100 mg of bone powder is collected, as measured using an enclosed balance accurate to 0.01 mg (see **Table of Materials**).

7. Transfer bone powder from the weigh paper to a 2 mL low-bind, safe-lock tube for extraction. Store at -20 °C, indefinitely.

8. Store the remaining bone/excess powder in a dry, temperature controlled (25 °C) sterile environment until return/repatriation.

9. Dispose of all waste in autoclavable biohazard bags or receptacles. Sterilize/decontaminate all reusable equipment (e.g., clamps, drill bits, drills, saws, etc.) using bleach/DNA decontamination solution/ethanol and UV exposure, as applicable, between each sampling.

   NOTE: For smaller samples (e.g., juvenile samples) there may be considerably less than the suggested 50-100 mg of cortical bone available to sample. However, even in low quantities, this anatomical sampling location has been shown to be particularly rich in DNA[11].

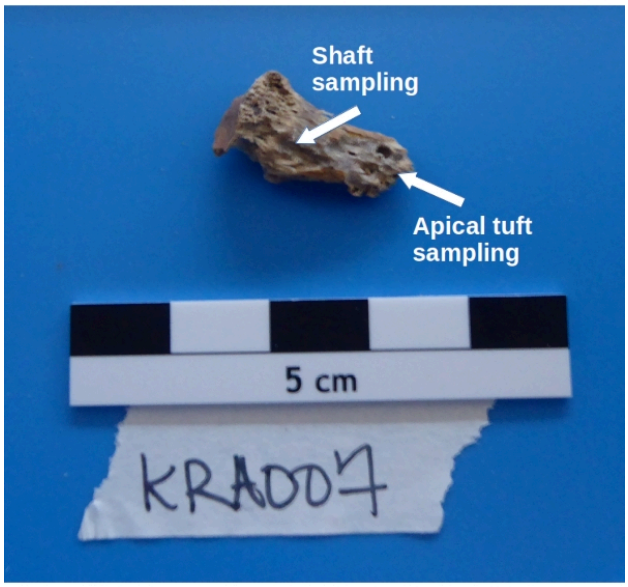

Figure 4: Distal phalanx showing the locations of dense cortical bone along the shaft and inferior side of the apical tuft. Please click here to view a larger version of this figure.

5. Sampling of the Talus

    1. Perform all sampling in a dedicated clean room under a UV light equipped PCR hood or biosafety cabinet (wavelength: 254 nm) with airflow turned off. Spread sterile aluminum foil across the benchtop to catch any stray bone powder/fragments.
    2. Ensure all bone fragments and as much powder as possible are recovered (for repatriation) before disposing of foil. Change the foil between each sampling. Dispose of used foil in an autoclavable biohazard bag/receptacle.
    3. Place a small sheet of weigh paper into a standard weighing tray.
    4. Secure the sample in handheld clamp/vise, dome upwards.
    5. Hold the talus, dome upward, and medial surface toward the collector, over the weighing tray. Scrape cortical bone from the neck of the talus to a depth of ~1 mm (see **Figure 5**) using a dental drill with a low gauge bit (see **Table of Materials**) set to low speed and high torque.
    6. Change the drilling position slightly and repeat until approximately 50-100 mg of bone powder is collected, as measured using an enclosed balance accurate to 0.01 mg (see **Table of Materials**).

7. Transfer bone powder from the weigh paper to a 2 mL low-bind tube for extraction. Store at -20 °C, indefinitely.
8. Store the remaining bone/excess powder in a dry, temperature controlled (25 °C) sterile environment until return/repatriation can be completed.
9. Dispose of all waste in autoclavable biohazard bags or receptacles. Sterilize/decontaminate all reusable equipment (e.g., clamps, drill bits, drills, saws, etc.) using bleach/DNA decontamination solution/ ethanol and UV (wavelength: 254 nm) exposure, as applicable, between each sampling.

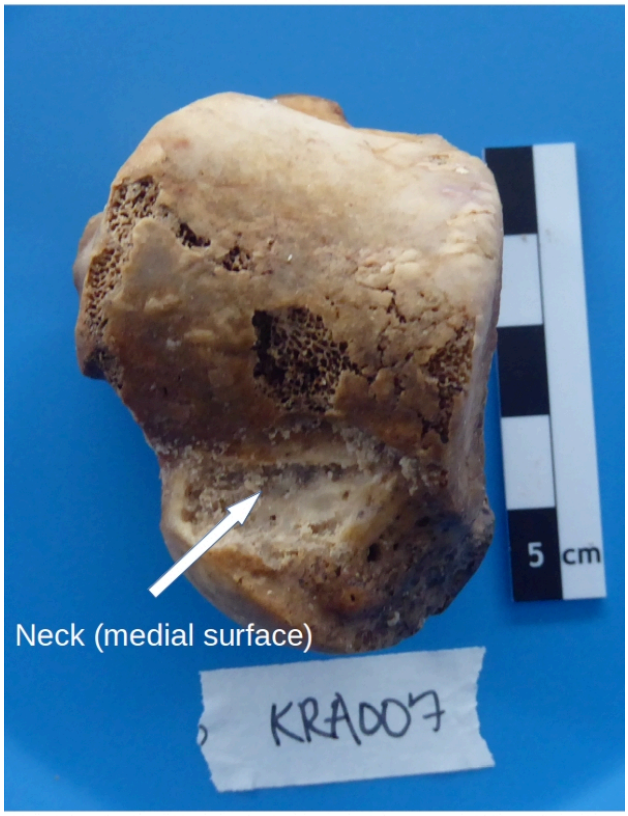

Figure 5: Sampling area of the talus for cortical bone recovery. Please click here to view a larger version of this figure.

NOTE: The talus has very little cortical bone (a thin outer layer). The material should not only be collected from the surface but also the underlying dense layer of cancellous bone.

Representative Results

In a separate study[11], DNA was extracted from bone powder generated from each anatomical sampling location in 11 individuals, using a standard DNA extraction protocol optimized for short fragments from calcified tissue[2]. Single-stranded libraries were then produced[28] and sequenced on a HiSeq 4000 (75 bp paired-end) to a depth of ~20,000,000 reads per sample. The resulting sequence data was then evaluated for endogenous human DNA content using the EAGER pipeline[29] (BWA settings: Seed length of 32, 0.1 mismatch penalty, mapping quality filter of 37). All representative results are reported using the same metrics as Parker et al. 2020[11] for consistency. Libraries from the powdered portions of the *pars petrosa* yielded, on average, higher endogenous DNA than any of the other 23 anatomical sampling locations surveyed (**Figure 6A-B**). The seven additional anatomical sampling locations presented in this protocol (the cementum, first pass of the dental pulp chamber, and dentin of permanent molars; cortical bone from the vertebral body and superior vertebral arch of the thoracic vertebra; cortical bone from the apical tuft of the distal phalanx; and cortical bone from the neck of the talus) produced the next highest yields (with no statistical significance between these anatomical sampling locations; **Figure 6A-B; Supplemental File 1:** EndogenousDNAPreCap). These alternative locations all consistently produced DNA yields adequate for standard population genetics analyses such as mitochondrial analyses and single nucleotide polymorphism (SNP) analyses. Duplication rates in libraries stemming from all anatomical sampling locations were low (cluster factors < 1.2 on average, calculated as the ratio of all mapping reads to unique mapping reads, **Table 2; Supplemental File 1**: ClusterFactor), indicating that all libraries screened were of very high complexity. Similarly, average exogenous human DNA contamination estimates were low, averaging < 2% (X chromosome contamination in males, n = 7, as reported by the ANGSD[30] pipeline) in all anatomical sampling locations except for the superior vertebral arch (average estimated contamination: 2.11%, with one sample removed as an outlier; KRA005: 19.52%, see **Table 2; Supplemental File 1**: Xcontamination). Average fragment length (after filtering to remove all reads < 30 bp) was lowest in the material collected from the dental pulp chamber and dentin, with no significant variation among other anatomical sampling locations (55.14 bp and 60.22 bp, respectively in comparison to an average median of 62.87, pair-wise p-values < 0.019, **Table 2; Supplemental File 1**: AvgFragLength). Additionally, the teeth and thoracic vertebrae each contain multiple anatomical sampling locations where high endogenous DNA recovery was observed, making them particularly suitable as alternatives to the *pars petrosa*.

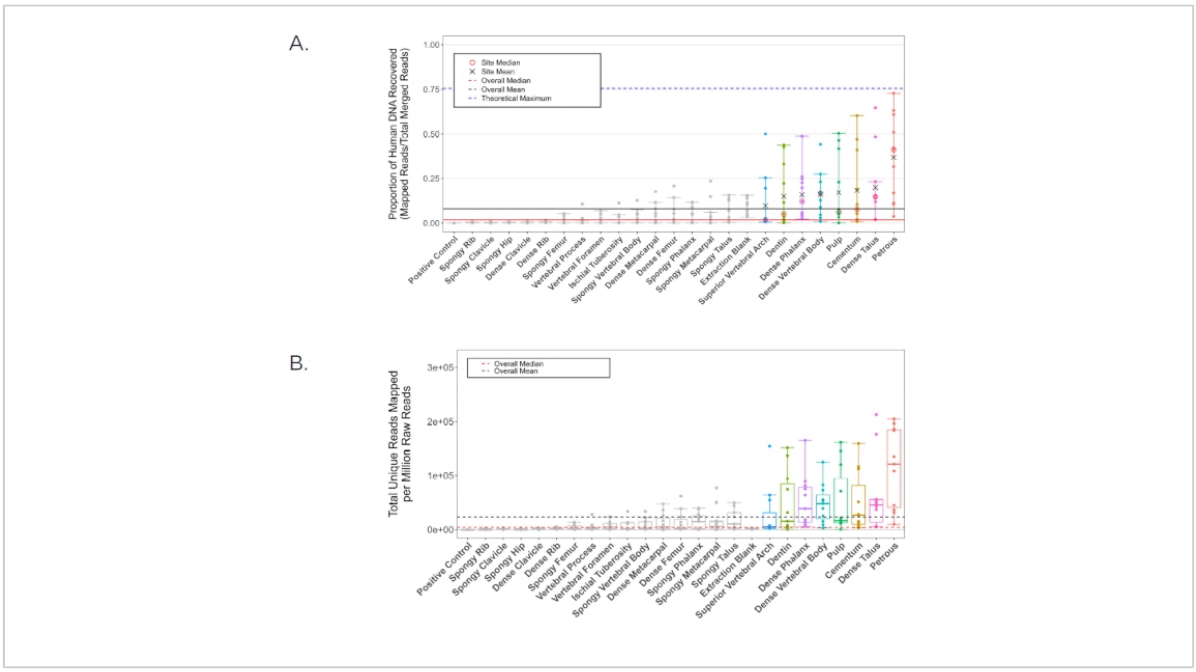

Figure 6: Human DNA content for all screened samples. Black lines represent the overall mean, while red lines represent the median (solid: human DNA proportion, dashed: mapped human reads per million reads generated). Individual anatomical sampling locations with an average human DNA proportion higher than the overall mean (8.16%) are colorized in all analyses. (**A**) The proportion of reads mapping to the hg19 reference genome. The blue dashed line represents the theoretical maximum given the pipeline's mapping parameters (generated using Gargammel[31] to simulate a random distribution of 5,000,000 reads from the hg19 reference genome with simulated damage). Individual means (black X) and medians (red circle) are reported for those samples with a higher average human DNA proportion than the overall mean. Confidence intervals indicate upper and lower bounds excluding statistical outliers. (**B**) The number of unique reads mapping to the hg19 reference genome per million reads of sequencing effort (75 bp paired end). Confidence intervals indicate upper and lower bounds excluding statistical outliers. This figure has been adapted from Parker, C. et al. 2020[11]. Please click here to view a larger version of this figure.

Table 2: Average duplication levels (mapping reads/ unique reads), average and median fragment lengths, and X chromosome contamination estimates for all anatomical sampling locations. Error reported as the standard error of the mean. This table has been adapted from Parker, C. et al. 2020[11].

Sampling location	Average duplication factor (# mapped reads / # unique mapped reads)	Average fragment length in bp	Average estimated proportion of X chromosome contamination
Petrous pyramid	1.188 ± 0.006	65.40 ± 1.36	0.000 ± 0.003
Cementum	1.197 ± 0.028	67.28 ± 1.76	0.011 ± 0.003
Dentin	1.188 ± 0.061	60.22 ± 2.37	0.002 ± 0.007
Pulp	1.179 ± 0.024	55.14 ± 2.90	0.013 ± 0.006
Distal phalanx	1.191 ± 0.049	65.95 ± 1.08	0.013 ± 0.005
Vertebral body	1.194 ± 0.037	66.14 ± 1.03	0.008 ± 0.003
Superior vertebral arch	1.19 ± 0.017	63.02 ± 1.23	0.021 ± 0.009*
Talus	1.198 ± 0.010	68.20 ± 1.24	0.011 ± 0.003
*Sample KRA005 removed as an outlier at 0.1952			

Code availability

All analyses programs and R modules used in the analyses of this manuscript are freely available from their respective authors. All custom R code is available by request.

Data availability

All raw data used in the calculation of representative results is freely available in the European Nucleotide Archive ENA data repository (accession number PRJ-EB36983) or supplemental materials of Parker, C. et al.[11].

Supplemental File 1. Please click here to download this File.

Discussion

Current practice in ancient human population genetics is to preferentially sample from the *pars petrosa* (step 2.1) whenever possible. However, the *pars petrosa* can be a difficult sample to obtain, as it is highly valued for a myriad of skeletal assessments (e.g., population history[32], the estimation of fetal age at death[33], and sex determination[34]), and, historically, sampling of the *pars petrosa* for DNA analysis can be highly destructive[3,4] (including the protocol presented here, although new, minimally invasive protocols[13,14] have now been widely adopted to alleviate this concern). This is compounded by the fact that, until very recently, a large-scale, systematic study of human DNA recovery across the skeleton had not been attempted[11], making finding an appropriate sampling strategy when the petrous pyramid is unavailable challenging.

The protocols presented here help to alleviate that challenge by providing a set of optimized procedures for DNA sampling

from archaeological/forensic skeletal remains including the *pars petrosa* as well as seven alternate anatomical sampling locations across four additional skeletal elements. The critical steps included are all intended to minimize the possibility of DNA loss/damage due to either inefficient sampling (steps 2.1.6 and 3.2.1.3) or overheating of samples during drilling/cutting (step 3.1.6). Additionally, it has been noted throughout the protocol that it may be necessary to modify/omit the pre-treatment steps to ensure the best performance in highly degraded samples. It should also be noted that even among the selected elements presented here, there remain several possible alternative sampling techniques (particularly for the *pars petrosa*[13,14]), as well as ample room for further optimization of the underexploited anatomical sampling locations presented here (i.e., the talus: step 2.5 and the vertebrae: step 2.3).

It is also important to keep in mind that these protocols have been designed and tested using ancient juvenile-adult remains of high quality (good morphological preservation) for the purposes of endogenous human DNA analyses. The results presented may not extend to more highly degraded materials, other preservation contexts, infant remains, non-human remains, or studies of pathogens or the microbiome, as a greater exploration into the use of these protocols in additional contexts is still needed. Additionally, the alternative skeletal elements presented here (the teeth, vertebrae, distal phalanx, and tali) may be challenging to assign to a single individual among commingled remains, necessitating sampling from multiple elements to ensure a single origin. Despite these limitations, making these protocols widely available can help alleviate some of the heterogeneity surrounding sample selection and processing by providing a generalized and quantitatively optimized framework for use in a wide range of future aDNA/forensic studies on human remains.

Disclosures

The authors have no conflicts of interest to report.

Acknowledgments

The authors would like to thank the laboratory staff of the Max Planck Institute for the Science of Human History for their help in the development and implementation of these protocols. This work would not have been possible without the input and hard work of Dr. Guido Brandt, Dr. Elizabeth Nelson, Antje Wissegot, and Franziska Aron. This study was funded by the Max Planck Society, the European Research Council (ERC) under the European Union's Horizon 2020 research and innovation program under grant agreements No 771234 - PALEoRIDER (WH, ABR) and Starting Grant No. 805268 CoDisEASe (to KIB).

References

1. Adler, C. J., Haak, W., Donlon, D., Cooper, A. Survival and recovery of DNA from ancient teeth and bones. *Journal of Archaeological Science*. **38** (5), 956-964 (2011).
2. Dabney, J., Meyer, M. Extraction of highly degraded DNA from ancient bones and teeth. *Ancient DNA: Methods and Protocols*. 25-29 (2019).
3. Palsdottir, A. H., Bläuer, A., Rannamäe, E., Boessenkool, S., Hallsson, J. Not a limitless resource: ethics and guidelines for destructive sampling of archaeofaunal remains. *Royal Society Open Science*. **6** (10), 191059 (2019).

4. Pinhasi, R., Fernandes, D. M., Sirak, K., Cheronet, O. Isolating the human cochlea to generate bone powder for ancient DNA analysis. *Nature Protocols.* **14** (4), 1194-1205 (2019).
5. Latham, K. E., Miller, J. J. DNA recovery and analysis from skeletal material in modern forensic contexts. *Forensic Sciences Research.* **4** (1), 51-59 (2019).
6. Mundorff, A. Z., Bartelink, E. J., Mar-Cash, E. DNA preservation in skeletal elements from the World Trade Center disaster: Recommendations for mass fatality management. *Journal of Forensic Sciences.* **54** (4), 739-745 (2009).
7. Gamba, C. et al. Genome flux and stasis in a five millennium transect of European prehistory. *Nature Communications.* **5** (1), 1-9 (2014).
8. Alberti, F. et al. Optimized DNA sampling of ancient bones using Computed Tomography scans. *Molecular Ecology Resources.* **18** (6), 1196-1208 (2018).
9. Hansen, H. B. et al. Comparing ancient DNA preservation in petrous bone and tooth cementum. *PLoS ONE.* **12** (1), e0170940 (2017).
10. Sirak, K. et al. Human auditory ossicles as an alternative optimal source of ancient DNA. *Genome Research.* **30** (3), 427-436 (2020).
11. Parker, C. et al. A systematic investigation of human DNA preservation in medieval skeletons. *Scientific Reports.* **10** (1), 18225 (2020).
12. Pinhasi, R. et al. Optimal ancient DNA yields from the inner ear part of the human petrous bone. *PLoS ONE.* **10** (6), e0129102 (2015).
13. Sirak, K. A. et al. A minimally-invasive method for sampling human petrous bones from the cranial base for ancient DNA analysis. *BioTechniques.* **62** (6), 283-289 (2017).
14. Orfanou, E., Himmel, M., Aron, F., Haak, W. *Minimally-invasive sampling of pars petrosa (os temporale) for ancient DNA extraction.* protocols.io. at <https://www.protocols.io/view/minimally-invasive-sampling-of-pars-petrosa-os-tem-bqd8ms9w> (2020).
15. Damgaard, P. B. et al. Improving access to endogenous DNA in ancient bones and teeth. *Scientific Reports.* **5** (1), 1-12 (2015).
16. Harney, É. et al. A minimally destructive protocol for DNA extraction from ancient teeth. *Genome Research.* **31** (3), 472-483 (2021).
17. Cooper, A., Poinar, H. N. Ancient DNA: Do it right or not at all. *Science.* **289** (5482), 1139 (2000).
18. Llamas, B. et al. From the field to the laboratory: Controlling DNA contamination in human ancient DNA research in the high-throughput sequencing era. *STAR: Science & Technology of Archaeological Research.* **3** (1), 1-14 (2017).
19. Llamas, B. et al. From the field to the laboratory: Controlling DNA contamination in human ancient DNA research in the high-throughput sequencing era. *STAR: Science & Technology of Archaeological Research.* **3** (1), 1-14 (2017).
20. Boessenkool, S. et al. Combining bleach and mild predigestion improves ancient DNA recovery from bones. *Molecular Ecology Resources.* **17** (4), 742-751 (2017).
21. García-Garcerà, M. et al. Fragmentation of contaminant and endogenous DNA in ancient samples determined

by shotgun sequencing; Prospects for human palaeogenomics. *PLoS ONE.* **6** (8), e24161 (2011).

22. Malmström, H. et al. More on contamination: The use of asymmetric molecular behavior to identify authentic ancient human DNA. *Molecular Biology and Evolution.* **24** (4), 998-1004 (2007).
23. Basler, N. et al. Reduction of the contaminant fraction of DNA obtained from an ancient giant panda bone. *BMC Research Notes.* **10**, 754 (2017).
24. Kemp, B. M., Smith, D. G. Use of bleach to eliminate contaminating DNA from the surface of bones and teeth. *Forensic Science International.* **154** (1), 53-61 (2005).
25. Korlević, P. et al. Reducing microbial and human contamination in DNA extractions from ancient bones and teeth. *BioTechniques.* **59** (2), 87-93 (2015).
26. Dabney, J., Meyer, M. Extraction of highly degraded DNA from ancient bones and teeth. *Methods in Molecular Biology.* **1963**, 25-29 (2019).
27. Hansen, H. B. et al. Comparing ancient DNA preservation in petrous bone and tooth cementum. *PLoS ONE.* **12** (1), e0170940 (2017).
28. Gansauge, M.-T. et al. Single-stranded DNA library preparation from highly degraded DNA using T4 DNA ligase. *Nucleic Acids Research.* **45** (10), e79 (2017).
29. Peltzer, A. et al. EAGER: efficient ancient genome reconstruction. *Genome Biology.* **17** (1), 60 (2016).
30. Korneliussen, T. S., Albrechtsen, A., Nielsen, R. ANGSD: analysis of next generation sequencing data. *BMC Bioinformatics.* **15**, 356 (2014).
31. Renaud, G., Hanghøj, K., Willerslev, E., Orlando, L. Gargammel: A sequence simulator for ancient DNA. *Bioinformatics.* **33** (4), 577-579 (2017).
32. Ponce de León, M. S. et al. Human bony labyrinth is an indicator of population history and dispersal from Africa. *Proceedings of the National Academy of Sciences of the United States of America.* **115** (16), 4128-4133 (2018).
33. Nagaoka, T., Kawakubo, Y. Using the petrous part of the temporal bone to estimate fetal age at death. *Forensic Science International.* **248**, 188.e1-188.e1887 (2015).
34. Norén, A., Lynnerup, N., Czarnetzki, A., Graw, M. Lateral angle: A method for sexing using the petrous bone. *American Journal of Physical Anthropology.* **128** (2), 318-323 (2005).

Additional File 1

Format: PDF

Materials List
Description: Complete materials list for all protocols presented in the manuscript

jove

Materials List for

Optimized Bone Sampling Protocols for the Retrieval of Ancient DNA from Archaeological Remains

Cody E. Parker[1,2], **Kirsten I. Bos**[1,3], **Wolfgang Haak**[1,3], **Johannes Krause**[1,3]

[1]Department of Archaeogenetics, Max Planck Institute for the Science of Human History [2]School of Human Evolution and Social Change, Arizona State University [3]Department of Archaeogenetics, Max Planck Institute for Evolutionary Anthropology

Corresponding Author

Cody E. Parker
cody.parker@asu.edu

Citation

Parker, C.E., Bos, K.I., Haak, W., Krause, J. Optimized Bone Sampling Protocols for the Retrieval of Ancient DNA from Archaeological Remains. *J. Vis. Exp.* (), e63250, doi:10.3791/63250 (2021).

Date Published

November 30, 2021

DOI

10.3791/63250

URL

jove.com/video/63250

Materials

Name	Company	Catalog Number	Comments
#16 Dental Drill Bit	NTI	H1-016-HP	example drilling bit
0.6 mm scroll saw blade	Fisher Scientific	50-949-097	blade for Jewellers Saw
22mm diamond cutting wheel	Kahla	SKU 806 104 358 514 220	Dremel cutting attachment
Commercial Bleach	Fisher Scientific	NC1818018	
Control Company Ultra-Clean Supreme Aluminum Foil	Fisher Scientific	15-078-29X	
DNA LoBind Tubes (2 mL)	Eppendorf	22431048	
Dremel 225-01 Flex Shaft Attachment	Dremel	225-01	Dremel flexible extension
Dremel 4300 Rotary Tool	Dremel	4300	Example drill
Dremel collet and nut kit	Dremel	4485	Adapters for various Dremel tool attachments/bits
Eagle 33 Gallon Red Biohazard Waste Bag	Fisher Scientific	17-988-501	
Eppendorf DNA LoBind 2 mL microcentrifuge tube	Fisher Scientific	13-698-792	
Ethanol (Molecular Biology Grade)	Millipore Sigma	1.08543	
FDA approved level 2 Surgical Mask	Fisher Scientific	50-206-0397	PPE
Fisherbrand Comfort Nitrile Gloves	Fisher Scientific	19-041-171X	PPE
Fisherbrand Safety Glasses	Fisher Scientific	19-130-208X	PPE
Granger Stationary Vise	Fisher Scientific	NC1336173	benchtop vise
Invitrogen UltraPure DNase/Rnase free distilled water	Fisher Scientific	10-977-023	
Jewellers Saw	Fisher Scientific	50-949-231	
Kimwipes	Sigma-Aldritch	Z188956	
Labconco Purifier Logic Biosafety cabinet	Fisher Scientific	30-368-1101	
LookOut DNA Erase	Millipore Sigma	L9042-1L	
Medium weighing boat	Heathrow Scientific	HS120223	

MSC 10pc plier/clamp set	Fisher Scientific	50-129-5352	Miscellaneous clamps/vise grips for securely holding samples while drilling/cutting
Sartorius Quintix Semi-Micro Balance	Fisher Scientific	14-560-019	enclosed balance
Tyvek coveralls with hood	Fisher Scientific	01-361-7X	PPE
Weigh paper	Heathrow Scientific	HS120116	

Additional File 2

Format: Excel spreadsheet (*.xlsx)

Title: Supplementary File 1

Description: Complete data table showing full descriptions of sampling and DNA extraction yields from all samples processed, including all positive and negative controls. Additionally, this file contains all raw data used in all representative analyses.

4. Manuscript 3

“

“14th century *Yersinia pestis* genomes support emergence of *Pestis secunda* within Europe”

Cody Parker and Alina N. Hiss, Maria Spyrou, Philip Slavin, Elizabeth Nelson, Gunnar Neumann Susanne Freiderich, Sarah Nagel, Alexander Herbig, Johannes Krause, Wolfgang Haak, Kirsten I Bos

In preparation

A method by which to maximize data production from irreplaceable archaeological remains is to broaden the scope of the analyses performed on each dataset resulting from their destructive sampling. In Manuscript 3 we present a novel, high coverage (ca. 30x), *Yersinia pestis* genome from the Second Pandemic, phylogenetically placed directly between the Black Death strain of *Y. pestis* and *Pestis secunda* (the Second Pandemic strain currently thought to be a precursor to the strain causing the Third, still ongoing, Pandemic) recovered through routine pathogen screening of the remains examined in Manuscripts A and B. There was no previous archaeological context pointing towards the possible presence of *Y. pestis* at this site, as the burials are not documented in historical texts, the individuals were interred in an attritional context (i.e., generally individual burials rather than multiple and lacking any physical evidence of suspected infectious disease such as the addition of lime to the gravesite), and early archaeological dating indicated the site dated to the 11th century (approximately a century after the First Pandemic and before the Second). In addition, we also find the first genetic evidence of verifiable historical *Y. pestis* infection in post-cranial skeletal elements, further reinforcing the utility of standardized screening of finds, after requesting appropriate permissions.

Author contributions

CP is the shared primary author (65%) with ANH, was responsible for the gathering, processing, method development, sampling from, and DNA extraction from all samples from the first round of screening (45% of total laboratory work) and aided in their subsequent analyses (10%). ANH was the shared primary author with CP, performed all laboratory work pertaining to the second set of screened individuals, and aided in their subsequent analyses. MS and GN were responsible for phylogenetic analyses and SNP verification. PS provided archaeological evidence linking our genome to documented plague outbreaks in the area. EN was responsible for the production of the 11x coverage double stranded library used for SNP verification. XD of the State Office for Heritage Management and Archaeology, Saxony-Anhalt (State Museum of Prehistory, Halle (Saale)) contributed the archaeological remains sampled in this study and initially excavated the site. AH aided in the analyses of recovered *Y. pestis* genomes KB acted as co-supervisor, provided funding, aided in the experimental design of this study, and contributed to the writing and editing of this manuscript. WH acted as co-supervisor, provided funding, and contributed to the writing and editing manuscript. JK acted as co-supervisor and provided funding for the study.

Author	Conception	Data analyses	Experimentation	Writing	Sample procurement
C.P.	25%	10%	45%	65%	0%
A.N.H.	10%	40%	45%	20%	30%
M.S.	N/A	10%	N/A	N/A	N/A
G.N.	N/A	10%	N/A	N/A	N/A
P.S.	N/A	5%	N/A	5%	N/A
E.N.	N/A	5%	5%	N/A	N/A
X.D.	N/A	N/A	N/A	N/A	60%
S.N.	N/A	N/A	5%	N/A	N/A
A.H.	20%	10%	N/A	N/A	N/A
J.K.	5%	N/A	N/A	N/A	N/A
W.H.	10%	N/A	N/A	N/A	10%
K.B.	30%	10%	N/A	10%	N/A

14th century *Yersinia pestis* genomes support emergence of *Pestis secunda* within Europe

Cody Parker[1,†], Alina N. Hiss[1,2,†], Maria Spyrou[1,3], Gunnar Neumann[1,2], Philip Slavin[4], Elizabeth Nelson[1], Sarah Nagel[2], Xandra Dalidowski[5], Susanne Friederich[5], Johannes Krause[1,2], Alexander Herbig[1,2], Wolfgang Haak[1,2], Kirsten I Bos[1,2,*]

[1]Max Planck Institute for the Science of Human History, Kahlaische Strasse 10, 07745 Jena, Germany
[2]Max Planck Institute for Evolutionary Anthropology, Deutscher Platz 6, 04103 Leipzig, Germany
[3]Tübingen Interfaculty Centre for Archaeology, University of Tübingen
[4]University of Stirling, Division of History and Politics, Stirling, FK9 4LA, Scotland UK
[5]Landesamt für Denkmalpflege und Archäologie, Sachsen-Anhalt, Halle (Saale), Germany

[†]These authors contributed equally to this manuscript

[*] Corresponding author:

Kirsten I. Bos: kirsten_bos@eva.mpg.de

Abstract

Pestis secunda is the earliest of a series of plague outbreaks in medieval Europe (1356-1366 CE) immediately following the Black Death (1346-1353 CE). The first genetic evidence of *Pestis secunda* was recovered from Bergen-op-Zoom in the Netherlands (ca 1358-1360 CE), with further examples subsequently recovered from St. Mary's Graces, London, United Kingdom (1361 CE) and Bolgar City, Russia (ca 1363-1364 CE). Unlike the majority of other post-Black Death strains of *Yersinia pestis* , which display diversity that accumulated over a period of centuries within a terminal sub-branch of the *Y. pestis* phylogeny, plague lineages descended from the *Pestis secunda* are thought to have persisted in non-human reservoirs in Eurasia and are genetically linked to the Third Pandemic (1772 CE – ongoing). It has been debated whether these post-Black Death strains are the result of local evolution of *Y. pestis* within Europe or if the disease was repeatedly reintroduced from a source external to Europe. Resolution of these competing hypotheses has been hindered by the low representation of *Y. pestis* genomes from this period in the skeletal collections investigated thus far. Here, we report on five individuals from Germany that were infected with lineages of plague associated with *Pestis secunda*, two of whom yielded genomes of high coverage. While one high coverage genome falls within the known diversity of the *Pestis secunda*, the second carries ancestral traits that place it early in the *Pestis secunda* pandemic. Through consideration of historical sources that explore first documentation of the pandemic in Central Germany, we argue that these data support a post-Black Death evolution of the pathogen within Europe rather than an introduction from abroad. Additionally, we demonstrate retrievability of *Y. pestis* DNA in post-cranial remains and highlight the importance of hypothesis-free pathogen screening approaches in evaluations of archaeological samples.

Author Summary

We present two high-coverage and three low-coverage *Y. pestis* genomes that represent previously described diversity within the *Pestis secunda*, as well as a newly identified precursor strain. Viewed in context with novel historical revelations, we further refine the time-span between the end of the Black Death and the emergence of the *Pestis secunda* to a three-year interval, offering support to the theory that this outbreak, similar to other post-Black Death outbreaks, had its source in *Y. pestis* diversification that evolved locally, rather than resulting from pathogen reintroduction from a distant plague focus.

Introduction

Yersinia pestis, the bacterium responsible for plague [1–4], is primarily spread from rodent populations to humans and other mammals via infected fleas [5–8]. There are three primary modes of potential progression after infection: bubonic, where lymph nodes are infected leading to painful swellings called buboes; pneumonic, where the lungs are infected and the disease is transmissible through expectorated droplets; and septicaemic, where systemic infection leads very rapidly to death [9]. At least three historically documented plague pandemics are known, and involvement of *Y. pestis* in each has been confirmed through DNA analysis: The First Pandemic, which began with the Justinianic plague/Plague of Justinian (541 CE - ca. 750CE) [10–13], the Second Great Pandemic, which started with the Black Death (1346 CE–ca. 18th century CE) [14,15], and the modern Third Pandemic (ca 1772 CE – currently ongoing) [16]. Recent evidence has shown that *Y. pestis* infection occurred as far back as the Neolithic [17–19], although the health impact of these cases on prehistoric societies remains a subject of scholarly debate.

The most widely studied of these three historical *Y. pestis* scourges is the Second Pandemic, which includes the Black Death 15] and the subsequent waves of resurgent infections that followed for several hundred years. The Black Death is thought to have started with the introduction of a single, clonal strain of *Y. pestis* [20] that was first historically reported in the Black Sea region and was carried via trade [15,21] through Constantinople before spreading into Europe via the Italian city of Messina [22,23]. After this initial introduction the Black Death spread rapidly throughout the entirety of Europe before abating in 1353 CE. Shortly thereafter, waves of infection periodically resurfaced in Europe until the 18th century CE, each resulting in episodes of various mortality [24–26].

Chronologically, the first known resurgence of plague in Europe after the Black Death, referred to as the *Pestis secunda* [25–28], has been genetically observed in remains excavated from plague-associated burials in Bergen Op Zoom, Netherlands (archaeologically dated to post-1358CE, and to 1359-60CE through historic context) [2,27,29], from the London St. Mary's Graces plague cemetery (historically dated to 1361CE) [14] and from a cemetery in Bolgar City, Russia (c.1363-4 CE) [28,30]. The strains detected in these *Pestis secunda* burials all differ from that responsible for the Black Death by only two diagnostic chromosomal polymorphisms: one at nucleotide position 699,494 (according to the CO92 AL590842 reference genome), "p3", that is a synonymous G to A transition in the *rpoD* gene) and another at 2,262,577 "p4", that is a non-synonymous G to T transversion affecting a hypothetical protein whose function remains unclear) [2,30]. Additionally, the *Pestis secunda* strains thus far identified do not group phylogenetically within the greater genomic diversity reported in other post-Black Death mortality events throughout Europe, which are argued to have evolved locally [20]. Instead, genetic evidence indicates that the known lineages common to this cluster, collectively referred to as 1B, extended eastward beyond Europe into Asia and subsequently Africa, and later gave rise to the prolific *Y. pestis* branch 1, which is highly diverse and is associated with the globally distributed and ongoing Third Pandemic [30–32].

The locations of plague foci that could have seeded the various post-Black Death *Y. pestis* resurgences are debated. Recent genetic studies of historical *Y. pestis* strains recovered from across Europe in the medieval and post-medieval periods have revealed a treelike structure with the Black Death at the root. This strongly supports the 14th century pandemic event as the ultimate source of all Second Pandemic outbreaks, with accumulated diversity resulting from continued local evolution within Europe [20]. From an ecological perspective, the waves of post-Black Death infection appear to be correlated with factors associated with the rise and

decline of regional sylvatic rodent populations [33,34]: As rodent populations expand and reach urban centres, susceptible domestic rodents such as *Rattus rattus* can also become infected. Once rodent populations collapse, disease infected fleas seek out new hosts such as humans. Infection rates then drop dramatically with declines in both human and local commensal rodent populations [33–36]. In the context of the Second Pandemic, the periodic outbreaks imply that *Y. pestis* persisted among local rodents where the bacteria periodically receded, evolved, and re-emerged as these populations fluctuated [28,33].

This model of evolution and expansion of Second Pandemic *Y. pestis* strains is consistent with the pattern of genetic diversity observed during the radiation of post-Black Death strains in Europe. South-Central Germany, for example, has been proposed as a plausible candidate location where plague may have become endemic in a local rodent population in the course of the Black Death, and thereafter a spillover event gave rise to the *Pestis secunda*[28]. However, as historical records first document waves of infection around major population centres and along corresponding trade routes, an alternative hypothesis posits that subsequent waves of infection are better explained by a series of continuous re-introductions of plague from either the original, as yet undefined, source of the Black Death or elsewhere in Asia [27,37–39]. It should be noted, however, that the vast majority of all late medieval plague data is recovered from urbanized/commercialized areas rather than from more sparsely populated rural areas: Hypotheses regarding the locations of epidemic emergences could thus be reflective of inherent biases in the availability of historic records rather than actual epidemiological phenomena. Additionally, direct genetic evidence of *Y. pestis* infection in medieval rodent populations has only recently [40] been documented. From a genetic standpoint, observational bias results from a dominant focus on skeletal collections for which a plague outbreak is either historically documented or is suspected based on burial context, which are often from areas

more easily accessed in terms of both travel and procurement of sample permits. Together these phenomena have the potential to limit the resolution of both an outbreak's origin and the context for its re-emergence.

A more systematic survey of plague DNA recovery from a wide range of spatio-temporal contexts both within and outside Europe has the potential to clarify the geographic origins of these recurrences [37]. Genetic data representative of the *Pestis secunda*, for example, is limited to only three sites. Here, through a hypothesis-free approach to pathogen screening of human remains from burials in Medieval Germany lacking the typical contexts associated with epidemic events (in terms of both demography and historical context), we present five historical *Y. pestis* genomes that further explore the genetic links between the Black Death and the *Pestis secunda.* These data parsimoniously support precipitation of the *Pestis secunda* as a local phenomenon rather than a disease reintroduction from afar.

Figure 1. Map of the cemetery excavation site at Krakauer Berg, near Peißen, Saxony-Anhalt, Germany. Graves highlighted in yellow mark those initially screened, while the green highlighted features represent those utilized for the second, targeted *Y. pestis* screening effort.

Table 1. SNP table showing seven diagnostic Second Pandemic *Y. pestis* SNPs (p1-p7) comparing profiles the Black Death strains, all Krakauer Berg samples (KRA0XX; high coverage denoted in blue, low coverage in orange), known examples of *Pestis secunda* (Bergen op Zoom, London St. Mary's Graces, Bolgar City), and the modern CO92 reference (accession number: AL590842). Amongst the two high-coverage genomes, a minimum of 3 reads covering each position were required for SNP identification, while SNPs in the low-coverage genomes were evaluated at 1x coverage. Sites where this coverage was not achieved (for both high or low-coverage genomes) are denoted with Ns. SNPs diagnostic of *Pestis secunda*/Branch 1 strains shown in bold.

	SNP (Position in reference to the CO92 reference genome)						
Individual/Site	**p1 (189,227)**	**p2 (1,871,476)**	**p3 (699,494)**	**p4 (2,262,577)**	**p5 (4,301,295)**	**p6 (3,806,677)**	**p7 (3,643,387)**
Black Death	C	G	G	G	G	T	G
KRA004	C	G	**A**	G	G	T	G
KRA008	N	N	**A**	G	N	N	G
KRA018	C	G	**A**	**T**	G	T	G
KRA028	C	G	**A**	G	G	T	G
KRA032	N	N	**A**	N	G	N	N
Bergen-op-Zoom	C	G	**A**	**T**	G	T	G
London, St. Mary's Graces	C	G	**A**	**T**	T	T	G
Bolgar City	C	G	**A**	**T**	G	**C**	T
CO92	C	G	**A**	**T**	G	**C**	G

Results

In a separate study, 247 single-stranded DNA libraries stemming from eleven individuals excavated from the 14th century Krakauer Berg cemetery in Halle, Germany were investigated for comparative ancient human DNA recovery based on bulk DNA (shotgun) content across various skeletal elements [41]. A non-targeted screening of these extensive data for ancient pathogen DNA using the HOPS pipeline [42,43] resulted in the discovery of two individuals (KRA004 and KRA008) who showed convincing evidence of *Y. pestis* infection. Eight libraries

stemming from separate sampling locations within each individual yielded traces of *Y. pestis* DNA after mapping to the CO92 reference genome (accession number: AL590842). Based on an evaluation of the number of unique mapping reads expressed per one million total sequenced reads, these included cementum from individuals KRA004 and KRA008 (4.79 and 1.41 unique reads, respectively), dentin (8.76 and 1.45 unique reads, respectively), and pulp chamber (217.02 and 4.78 unique reads, respectively) from both individuals, as well as the superior vertebral arch (3.00 unique reads) and femur (3.02 unique reads) from KRA004 (see Supplementary File 1: Pre-Capture Sequencing Data: MappedReadsperMillion). These results lend credence to previous assumptions that sampling from the teeth, specifically in the region of the dental pulp chamber, is an optimal strategy for recovery of blood-borne pathogens such as *Y. pestis* [4]. Given the demonstrated success of the dental sampling locations, 50 teeth from an additional 43 individuals excavated from the site were obtained to further explore plague's impact on the mortality of the population buried in the Krakauer Berg cemetery. Pulverised material from the dental pulp chambers were screened for the presence of *Y. pestis* DNA using a targeted PCR assay for the *pla* region of the pPCP1 plasmid [44]. Amplification products were observed in three of these individuals (KRA018, KRA028, and KRA032). Double-stranded DNA libraries treated with a uracil-DNA glycosylase (UDG) -half treatment were then generated from each candidate extract [45]. Together this yielded twelve libraries from the five putative plague victims (eight single-stranded and three double-stranded) for further analyses. An additional double-stranded library with UDG-full treatment was generated from the dental pulp chamber extract of KRA004 to verify single nucleotide polymorphism (SNP) authenticity against the single-stranded data, which retains a greater proportion of damaged template molecules.

Candidate libraries from the five individuals were enriched for *Y. pestis* DNA using in-solution bait capture [46] and were further sequenced (75x2bp on the Illumina platform) to a depth of ca. 10 million reads each. As initial analyses of individuals KRA028 and KRA032 resulted in genomes of low coverage (< 1X), a second double-stranded UDG-half library, as well as a further non-UDG treated single-stranded DNA library, were generated from the corresponding extracts, which were later enriched and sequenced as above. Reads mapping to the *Y. pestis* reference genome were authenticated as ancient based on the accord between patterns of deamination observed for both *Y. pestis* and HG19 human reference mapping (accession number: GCF_000001405.13, see Supplementary Figure S5).

Of these twelve libraries, *Y. pestis* genomes in excess of 10-fold coverage were reconstructed from both the single- and double-stranded libraries from the dental pulp chamber of KRA004 (ca. 40-fold and 11-fold coverage, respectively) as well as the double-stranded library from this sampling location of KRA018 (ca. 20-fold). SNPs were called at a minimum of 3-fold coverage and 90% identity. To assess the placement of the recovered *Y. pestis* strains within the greater diversity of historical *Y. pestis*, a bootstrapped maximum likelihood tree was constructed using RAXML [47] (98% partial deletion, 1000 bootstraps) for the combined enriched libraries from all sampling locations (cementum, dentin, dental pulp, superior vertebral arch, and femur sampling) from individual KRA004 and the enriched dental pulp library from individual KRA018 (Figure 2A).

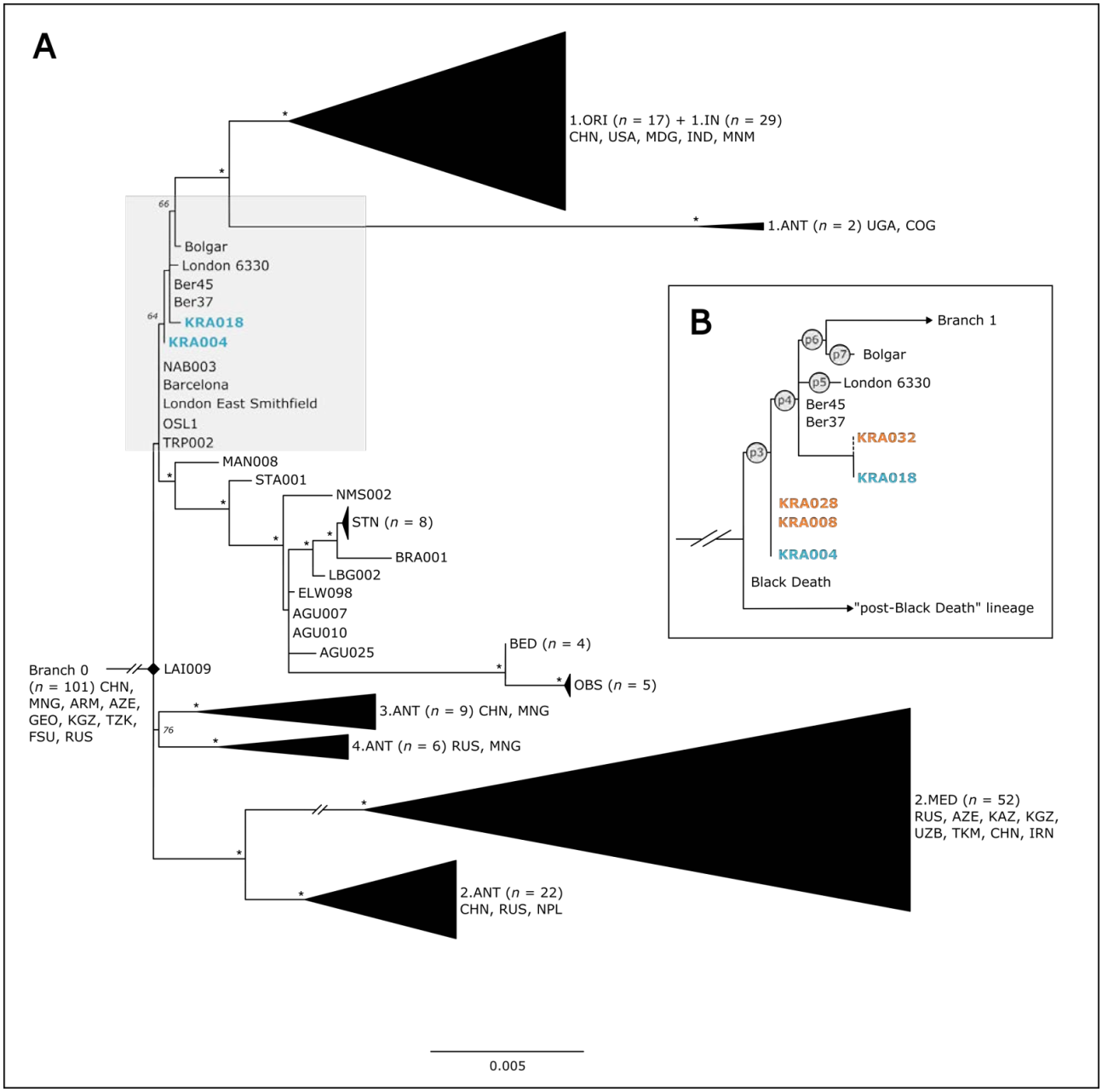

Figure 2. (A.) Overall historical *Y. pestis* diversity including the Justinianic, Second, and Third Pandemics. New, high-coverage genomes from Krakauer Berg are denoted in blue. **(B.)** Zoom in on the *Y. pestis* diversity within *Pestis secunda*, (grey area in A), high coverage genomes are denoted in blue, whereas the tentative, manual placements of low-coverage genomes are denoted in orange. Lineage-characteristic SNPs are indicated in circles at their respective nodes.

All genomes were investigated with regard to their SNP profiles, with special attention given to status at positions p3 and p4 that have previously defined the *Pestis secunda* lineages [30]. Our manual evaluation of the partial SNP profiles for the lower coverage genomes (KRA008, KRA028, and KRA032) were also used to infer/extrapolate their placement in the phylogenetic tree (Figure 2B). All genomes presented here show/carry the derived state at position p3, thus confirming their phylogenetic grouping within *Pestis secunda* as inferred through the maximum likelihood approximation. Importantly, position p4 did not yield consistent allele calls across the dataset: While present in the derived state for KRA018, the KRA004 genome carries the ancestral state (i.e., the nucleotide call is identical to the Black Death isolate). The ancestral state was also detected by visual inspection of the SNP profile for KRA028 and KRA0008. The low coverage of KRA032 precluded further assessment at this position. In addition, two derived alleles unique to KRA018 were detected (positions 1,009,185 and 1,526,22 with respect to the CO92 reference genome, 26-fold and 4-fold coverage respectively), indicating further divergence of this genome from the others presented here. Given that one of the above SNPs was also found in KRA032 (position 1,009,185, 1-fold coverage), we can infer that KRA0032 likely clusters together with KRA018, although this cannot be confirmed as the p4 position was, as previously noted, not recovered in this individual (Figure 2B). A presence/absence analysis of both high coverage genomes targeting genes known to be involved in *Y. pestis* virulence indicates that, aside from a filamentous prophage gene generally found in a few modern genomes (e.g., CO92), all expected virulence genes were present with no additional gene loss detected (Supplementary Figure S6). Radiocarbon dates were available for KRA004 (1284-1392 CE, Cal 2-sigma), and KRA008 (1301-1402 CE, Cal 2-sigma) from a previous publication [41], and additional dating was performed for KRA018 (1283-1389 CE, Cal 2-sigma) by the Curt-Engelhorn-Zentrum Archaeometrie GmbH in Mannheim.

Discussion

Although *Y. pestis* is the most densely studied ancient pathogen to date, many questions regarding its evolutionary history and past distribution persist. Here, through the application of a non-targeted screening approach, we demonstrate the unexpected presence of *Y. pestis* in skeletal material interred in the absence of typical epidemic-related contexts, as has been the case with nearly all previous examples of prehistoric *Y. pestis* findings. Two of the genomes presented here, namely those from individuals KRA018 and KRA032 (TBC), group within the diversity previously documented for plague burials linked to the *Pestis secunda.* Three additional genomes (KRA004 and KRA008, KRA028), however, are clearly basal to the diversity that previously defined the *Pestis secunda* cluster *.* Initial estimates for onset of the *Pestis secunda* suggest it occurred sometime between 1353 CE (the end of the Black Death in Europe) and ca 1359-1360 CE, the inferred historical date of the Bergen op Zoom burials, the earliest *Y. pestis* genomes confirmed to represent this widespread mortality event [27]. The outbreak reached England only a few short years later (commencing in London in Spring 1361 CE) and necessitated the consecration of the London St. Mary's Graces cemetery in the same year for victims of the pandemic. Details of the pandemic's temporal and geographic origins can be further refined using recently uncovered historical data, including chronicles, probated wills and local authority records, that together suggest that the *Pestis secunda* wave commenced in the summer of 1356 CE in South-Central Germany, possibly in the area around Frankfurt am Main. Consolidation of these sources allow us to build a provocative narrative detailing the course of plague's spread in the Germanic lands and beyond. In the following year (1357 CE) the plague spread out of Hesse: in the west, it reached Westphalia and east Rhineland-Palatinate; in the east, it appeared in Thuringia; in the north, it was circulating in the western parts of North Rhine and southern parts of Lower Saxony, while in the south, it

proliferated in the eastern part of Baden-Württemberg, Bavaria eventually reaching Lake Constance. In 1358 CE, the pandemic extended into north-west Germany, the eastern part of the bishopric of Constance (including the north-eastern tip of Switzerland), and the hinterland of Strasbourg, while a year later (1359 CE), it spread to Pomerania in the north-east, Austria in the south-east, and the Zurich hinterland and Alsace in the south-west [28]. Unfortunately, there are no surviving textual records about the *Pestis secunda* outbreak in Halle or its immediate hinterland. However, in 1357 plague was reported in both Meiningen (20km south-west of Halle) and Magdeburg (90km north of Halle), implying that Halle, situated between the two cities, experienced its outbreak most likely, in the same year [48,49]. Using a synthesis of these historical data and the new genomic data presented here we propose a temporal placement of the burials within a narrow time interval of 1353-1359 CE. While consistent with calibrated radiocarbon dates (KRA004: 1284-1392 CE, Cal 2-sigma [41], KRA008: 1301-1402 CE, Cal 2-sigma [41], and KRA018: 1283-1389 CE, Cal 2-sigma), our synthesis offers a far better resolution.

Recovery of the most basal lineage in the *Pestis secunda* cluster identified thus far from the Krakauer Berg cemetery is compatible with the earliest human mortality recorded in Germany and could be viewed as supporting hypotheses of the pandemic's emergence in South-Central Germany. This in turn supports historical interpretation of its endemic status in Europe in the 1350s, with the first human cases occurring in 1356 CE, just three years after the conclusion of the Black Death (in Central Russia) . Our data also support fixation of the derived p3 and p4 SNPs in Europe within a year or two of the pandemic onset (i.e., by 1357-8 CE).

The fact that the five genomes are clustered within two different phylogenetic clusters (KRA004, KRA008 and KRA028 on p3 and KRA018 and KRA032 on p4) may be explained by

two possible scenarios: one option is that genomes with a derived p3 and ancestral p4 reflect earlier stages of plague outbreak, while those with the derived state in both p3 and p4 are associated with later stages of the pandemic in the Halle region. This would imply that the mutation was either acquired through the course of the outbreak in Halle itself, or the disease was reintroduced to the region after accumulating diversity during the course of the pandemic. Historical evidence suggests that *Pestis secunda* outbreaks lasted , on average, half-a-year in different European cities, which is likely too short a time interval for fixation of two polymorphisms when viewed in the context of genomic data from other single spatio-temporal Second Pandemic events such as Stans (c.1485-1635 CE) and Marseille (1720-1722 CE), which show near clonality in their strain clusters [20]. The possibility that the p4 cluster reflects a reintroduction of the disease a few years later, possibly by the way of trade, is more in line with our knowledge of the genetics of plague outbreaks. Halle was an important salt producing and trading centre, with commercial ties to other parts of the German Empire and beyond [50–52]. Presence of the p4 SNP in the Netherlands and London indicates that the genotype achieved a wide geographic presence.

The basal position of the p3 genomes (KRA004, KRA008 and KRA028) and later phylogenetic positions of *Pestis secundas*-associated genomes (Bergen-op-Zoom and London in the West, and later in Bolgar City (on the Volga-Kama confluence in Tatarstan in the East), before the post-*Pestis secundas* migration of Branch 1B out of Europe and its eventual seeding of diverse lineages associated with the prolific Third, or modern, Pandemic [53,54], pair well with historical evidence of *Pestis secundas* spread in West Eurasia. From its inferred beginnings in Germany, the *Pestis secundas* undoubtedly ravaged the Netherlands in 1359-60, arrived in London in March 1361 (from Gascony or from the Low Countries) and circulated in the Volga

region in 1363-4, having arrived there, most likely, from the Azov Sea littoral, where it is documented in 1362. From there, the plague would continue westwards into Russian principalities (1364-5) and Lithuania (1366), where it finally abated [28]. In the east, the plague broke out in Armenia and Georgia in 1364-6 [55,56], but its subsequent global proliferation leading to the onset of the Third Plague Pandemic in 1772 in Western Yunnan cannot, at this point, be reconstructed. Additionally, our level of resolution suggests that all three strains (Black Death, and both *Pestis secundas* variants - p3 (associated with KRA004, KRA008 and KRA028) , and p4 (associated with KRA018 and KRA032) - were of similar genetic virulence potential.

While teeth have traditionally been the most targeted sampling location with respect to aDNA recovery of *Y. pestis* [43,54,57], our data, even if only based on results obtained from two individuals, further reinforces the idea that teeth (specifically the dental pulp chamber) should be the preferred location for sampling for investigation of bacteria present in the bloodstream. However, we show that the regular screening of postcranial elements can be potentially useful, as *Y. pestis* infection was detected in both a vertebra and the femur of individual KRA004, albeit with rather low recovery of pathogen DNA when compared to the tooth of the same individual. This is especially important in cases where it may be possible to request teeth from an individual where *Y. pestis* infection is detected via molecular analysis of postcranial remains.

In many cases, human remains acquired for molecular detection of infectious diseases are screened with a narrow focus on a target pathogen. Similarly, studies undertaken with a focus on population genetics have, in the past, neglected to screen the recovered molecules for potential pathogens, especially in the absence of historical documentation, burial context, or pathological evaluation suggestive of possible infection. While this can be resolved by the ret-

roactive screening of datasets from past projects in combination with new sampling endeavours, as done in the studies demonstrating the presence of *Y. pestis* DNA in Bronze and Iron Age samples [17,18], it may not always be possible to request additional material for subsequent analyses should pathogens be detected. Our findings here reinforce that the routine screening of all samples for both host and pathogen DNA (when authorized to do so by the relevant cultural authority) is not only of great use in terms of generating a more complete genetic picture of the past, but also allows researchers to maximize the amount of information that can be produced from destructive analyses of archaeological remains. Additionally, these findings also highlight how the screening of burials that lack features regarded as typical of epidemic contexts can identify early diversity in pathogens and potentially help pinpoint the epicentres of their associated epidemics. Continued examination of both human and associated faunal remains [40] from Medieval and post-Medieval periods, paired with relevant historical data, will be necessary to fully untangle the web of plague dissemination throughout Europe and its neighbouring continents.

Conclusion

This study provides genetic support for the notion that the *Pestis secundas,* as previously defined by *Y. pestis* genomes from Bergen Op Zoom [2,27,29], London St. Mary's Graces [14], and Bolgar City [31], likely originated within Europe These findings also further demonstrate the need to continue to expand screening approaches to include both geographical sites and skeletal elements not typically analyzed in these contexts due to a lack of physical or historical evidence indicating the potential presence of infectious agents.

Material and Methods

Sampling and initial screening:

Multiple skeletal elements from 11 individuals excavated from the abandoned medieval cemetery at Krakauer Berg, near Peißen, Saxony-Anhalt, Germany were provided by the State Museum of Prehistory, Halle [Saale], Germany. These elements consisted of *pars petrosae,* molars, clavicles, ribs, vertebrae, metacarpals, distal phalanx, ischia, femora, and tali from each individual [41]. As the subsequent screening for the presence of potential pathogens in these original 247 samples indicated the presence of *Y. pestis* in two of eleven individuals, an additional 50 teeth from 43 more individuals excavated were sampled to investigate the prevalence of plague at the site. Radiocarbon dating of ribs from each of the original 11 individuals and molar roots from the additional 43 individuals screen was (performed at the Curt Engelhorn Centre for Archaeometry in Mannheim, Germany).

For all samples, bone powder was generated from multiple sampling locations on each element in a dedicated ancient DNA (aDNA) clean room setting at the Max Planck Institute for the Science of Human History in Jena. For the initial screening, DNA was extracted from ~50-75mg of bone powder from the 23 sampling locations across ten skeletal elements gathered from eleven individuals each using a modified Dabney protocol [41,58]. The resulting DNA from those extractions was then used to generate single-stranded, non-UDG treated shotgun DNA libraries via automation [59], which were then sequenced on the Illumina platform (75bp X2, ca. 5,000,000 reads) and screened for the presence of *Y. pestis* using both the EAGER [60] and HOPS [42,43] pipelines. Reads mapping to the CO92 reference genome were authenticated as ancient through comparison of the observed deamination patterns post-mapping of shotgun libraries to the bacterial reference with those observed post-mapping to the

human reference genome hg19 using the Burrows-Wheeler Alignment (BWA) mapping [61] and MapDamage [62] tools contained within the EAGER pipeline. Those libraries determined to contain verifiable traces of historical *Y. pestis*, were then enriched for the pathogen using in-solution bait capture [46,63] based on the CO92 reference genome and sequenced using the Illumina platform (75bp X2, ca. 10,000,000 reads). An additional enriched, double-stranded, UDG treated library was generated from the same extraction of pulp-chamber sample of individual KRA004 [64] for use in downstream SNP verification, as the most reads mapping to the *Y. pestis* reference genomes were observed in this sample Supplementary File 1, Pre-Capture Sequencing Data, MappedReads).

After the presence of historical *Y. pestis* was confirmed for the site, an additional 50 teeth were collected from an additional 43 individuals, sampled as indicated in previously published methods [65], and DNA extracted from the pulp chamber portion using the same modified Dabney protocol. Extractions stemming from these additional samples were then screened for the presence of the bacterium using a qPCR assay targeting the *pla* gene located on the pPCP1 *Y. pestis* plasmid [66]. Double-stranded, shotgun and enriched UDG-half libraries were then generated from each positively screened extraction [64] and further sequenced using the Illumina platform (75bp 1X, ca, 10,000,000 reads). As low coverage was found in two of these libraries, the extracts from KRA028 and KRA032 were used to generate an additional double-stranded (UDG-half) and single-stranded (non-UDG) enriched libraries for each individual which were then further sequenced as previously described.

Analysis:

Analysis of the captured libraries was done by first concatenating all libraries stemming from a single individual and then using a combination of the EAGER pipeline to generate alignments to the CO92 reference genome using BWA (seed length 19, 0.01 mismatch penalty, mapping quality filter 37) as well as verify that the reads showed a damage pattern consistent with aDNA. Post-enrichment, all reads from non-UDG libraries were trimmed to remove any residual damage (5bp for single-stranded libraries, 1bp for UDG half, double stranded libraries) and remapped with more stringent BWA mapping parameters (seed length 32, 0.1 mapping stringency, mapping quality filter of 37).

SNP calling was performed using GATK [66]. MultiVCFAnalyzer [67] was applied to generate SNP tables for each library with a mean coverage above 3x in comparison with 233 published modern and 52 published ancient genomes, with *Y. pseudotuberculosis* (IP23953) included as an outgroup. SNP analysis and verification were performed using IGV [68] and SNPEvaluation [10]. After filtering of the SNPs, only polymorphic positions covered in at least 98% of the genomes were kept for generating a maximum likelihood tree with RaxML [47] based on the General Time Reversible (GTR) substitution model with 1000 bootstrap replicates. Phylogenetic placements of low-coverage genomes were done manually based on the aforementioned SNP analysis of the libraries stemming from individuals KRA008, KRA028, and KRA032. Additionally, SnpEff [69] was applied to classify possible effects of SNPs on any associated genes and/or gene products.

The two high coverage *Y. pestis* genomes retrieved from KRA004 and KRA018 were investigated for presence or absence of virulence factors [70] alongside other published ancient (Bolgar 2370, London 6330, Ber45, NAB003, London ES 8124/8291/11972, Barcelona 3031, OBS137, STN014, Altenerding, RISE509) and modern (CO92, *Y. pseudotuberculosis* IP32953)

genomes. The genomes were mapped against the *Y. pestis* CO92 chromosome and plasmids without quality filter (-q 0, Samtools [64]). The resulting bam files were taken as input for Bedtools [71] to produce bed files to check for the presence of previously defined genes, known to be involved in virulence. Based on these bed files a heat-map was generated showing their presence/absence (1 if the entire gene is present; 0 if absent) across all genomes investigated using R Studio (v1.2.5033) [72].

Acknowledgments:

The authors would like to thank the laboratory staff at the Max Planck Institute for Evolutionary Anthropology, Leipzig, Germany as well as all the technicians, students, and scientific colleagues at the Max Planck Institute for the Science of Human History, Jena, Germany. In addition, the authors would also like to thank the State Office for Heritage Management and Archaeology, Saxony-Anhalt (State Museum of Prehistory, Halle (Saale)) for opening up their collection and providing all samples used in this study. This study was funded by the Max Planck Society, the European Research Council (ERC) under the European Union's Horizon 2020 research and innovation program under grant agreements No. 771234 – PALEoRIDER (to WH) and No. 805268 CoDisEASe (to KIB).

Author contributions:

CP and ANH are the primary co-authors and contributed equally to the writing of this manuscript. In addition, CP was responsible for gathering, processing, sampling, DNA extraction, and subsequent analyses of the 247 samples from the initial 11 individuals. ANH was responsible for the collection, processing, sampling, DNA extraction and library construction, qPCR assay, and subsequent analyses of the extended screening samples (50 teeth from 43 individuals). MS and GN aided heavily in the phylogenetic analyses of all samples. PS wrote sections

on the historical contexts within the manuscript. SN oversaw production of the single-stranded libraries generated from the initial screening at the Max Planck Institute for Evolutionary Anthropology, Leipzig, Germany. EN produced the UDG-treated double-stranded libraries used for SNP verification. XD is the primary archaeologist responsible for excavating the site. SF provided all archaeological remains used in this study on behalf of the State Office for Heritage Management and Archaeology, Saxony-Anhalt (State Museum of Prehistory, Halle (Saale)). JK acted as co-supervisor to CP, aided in experimental design, and provided funding for the study. AH acted as co-supervisor to ANH and contributed to the writing and editing of this manuscript. WH acted as co-supervisor to both CP and ANH, provided funding, coordinated sample selection, and contributed to the writing and editing of this manuscript. KB acted as co-supervisor to CP, provided funding, aided in the experimental design, and contributed to the writing and editing of this manuscript.

Code Availability

All code used in the analyses of samples for this manuscript is available freely via GitHub.

Data Availability:

Statement of Conflicts of Interests

The authors have no conflicts of interest to report.

References:

1. Bos KI, Stevens P, Nieselt K, Poinar HN, DeWitte SN, Krause J. Yersinia pestis: New Evidence for an Old Infection. PLOS ONE. 2012;7: e49803. doi:10.1371/journal.pone.0049803

2. Haensch S, Bianucci R, Signoli M, Rajerison M, Schultz M, Kacki S, et al. Distinct Clones of Yersinia pestis Caused the Black Death. PLoS Pathog. 2010;6. doi:10.1371/journal.ppat.1001134

3. Parkhill J, Wren BW, Thomson NR, Titball RW, Holden MT, Prentice MB, et al. Genome sequence of Yersinia pestis, the causative agent of plague. Nature. 2001;413: 523–527. doi:10.1038/35097083

4. Raoult D, Aboudharam G, Crubézy E, Larrouy G, Ludes B, Drancourt M. Molecular identification by "suicide PCR" of Yersinia pestis as the agent of Medieval Black Death. PNAS. 2000;97: 12800–12803. doi:10.1073/pnas.220225197

5. Sun Y-C, Jarrett CO, Bosio CF, Hinnebusch BJ. Retracing the Evolutionary Path that Led to Flea-Borne Transmission of Yersinia pestis. Cell Host & Microbe. 2014;15: 578–586. doi:10.1016/j.chom.2014.04.003

6. Green MH. Pandemic disease in the medieval world: rethinking the Black Death. 2014.

7. Vadyvaloo V, Jarrett C, Sturdevant DE, Sebbane F, Hinnebusch BJ. Transit through the Flea Vector Induces a Pretransmission Innate Immunity Resistance Phenotype in Yersinia pestis. PLOS Pathogens. 2010;6: e1000783. doi:10.1371/journal.ppat.1000783

8. Perry RD, Fetherston JD. Yersinia pestis--etiologic agent of plague. Clin Microbiol Rev. 1997;10: 35–66.

9. Titball RW, Williamson ED. Vaccination against bubonic and pneumonic plague. Vaccine. 2001;19: 4175–4184. doi:10.1016/S0264-410X(01)00163-3

10. Keller M, Spyrou MA, Scheib CL, Neumann GU, Kröpelin A, Haas-Gebhard B, et al. Ancient Yersinia pestis genomes from across Western Europe reveal early diversification during the First Pandemic (541–750). PNAS. 2019;116: 12363–12372. doi:10.1073/pnas.1820447116

11. Feldman M, Harbeck M, Keller M, Spyrou MA, Rott A, Trautmann B, et al. A High-Coverage Yersinia pestis Genome from a Sixth-Century Justinianic Plague Victim. Mol Biol Evol. 2016;33: 2911–2923. doi:10.1093/molbev/msw170

12. Wagner DM, Klunk J, Harbeck M, Devault A, Waglechner N, Sahl JW, et al. Yersinia pestis and the Plague of Justinian 541–543 AD: a genomic analysis. The Lancet Infectious Diseases. 2014;14: 319–326. doi:10.1016/S1473-3099(13)70323-2

13. Eppinger M, Worsham PL, Nikolich MP, Riley DR, Sebastian Y, Mou S, et al. Genome Sequence of the Deep-Rooted Yersinia pestis Strain Angola Reveals New Insights into the Evolution and Pangenome of the Plague Bacterium. Journal of Bacteriology. 2010;192: 1685–1699. doi:10.1128/JB.01518-09

14. Bos KI, Schuenemann VJ, Golding GB, Burbano HA, Waglechner N, Coombes BK, et al. A draft genome of Yersinia pestis from victims of the Black Death. Nature. 2011;478: 506–510. doi:10.1038/nature10549

15. Ole J. Benedictow. The Black Death 1346-1353: The Complete History. 1 edition. Woodbridge: Boydell Press; 2006.

16. Bramanti B, Dean KR, Walløe L, Chr. Stenseth N. The Third Plague Pandemic in Europe. Proc Biol Sci. 2019;286. doi:10.1098/rspb.2018.2429

17. Rasmussen S, Allentoft ME, Nielsen K, Orlando L, Sikora M, Sjögren K-G, et al. Early Divergent Strains of Yersinia pestis in Eurasia 5,000 Years Ago. Cell. 2015;163: 571–582. doi:10.1016/j.cell.2015.10.009

18. Spyrou MA, Tukhbatova RI, Wang C-C, Valtueña AA, Lankapalli AK, Kondrashin VV, et al. Analysis of 3800-year-old Yersinia pestis genomes suggests Bronze Age origin for bubonic plague. Nature Communications. 2018;9: 1–10. doi:10.1038/s41467-018-04550-9

19. Rascovan N, Sjögren K-G, Kristiansen K, Nielsen R, Willerslev E, Desnues C, et al. Emergence and Spread of Basal Lineages of Yersinia pestis during the Neolithic Decline. Cell. 2019;176: 295-305.e10. doi:10.1016/j.cell.2018.11.005

20. Spyrou MA, Keller M, Tukhbatova RI, Scheib CL, Nelson EA, Andrades Valtueña A, et al. Phylogeography of the second plague pandemic revealed through analysis of historical Yersinia pestis genomes. Nature Communications. 2019;10: 1–13. doi:10.1038/s41467-019-12154-0

21. Barker H. Laying the Corpses to Rest: Grain, Embargoes, and *Yersinia pestis* in the Black Sea, 1346–48. Speculum. 2021;96: 97–126. doi:10.1086/711596

22. Aberth J. Introduction: The Black Death in History. In: Aberth J, editor. The Black Death: The Great Mortality of 1348–1350: A Brief History with Documents. New York: Palgrave Macmillan US; 2005. pp. 1–7. doi:10.1007/978-1-137-10349-9_1

23. Cesana D, Benedictow OJ, Bianucci R. The origin and early spread of the Black Death in Italy: first evidence of plague victims from 14th-century Liguria (northern Italy). Anthropological Science. 2017;125: 15–24. doi:10.1537/ase.161011

24. DeWitte SN. Mortality Risk and Survival in the Aftermath of the Medieval Black Death. PLoS One. 2014;9. doi:10.1371/journal.pone.0096513

25. Wood JW, Ferrell RJ, Dewitte-Aviña SN. The temporal dynamics of the fourteenth-century Black Death: new evidence from English ecclesiastical records. Hum Biol. 2003;75: 427–448. doi:10.1353/hub.2003.0067

26. Clouse M. The Black Death Transformed: Disease and Culture in Early Renaissance Europe.Samuel K Cohn Jr. London and New York: Arnold and Oxford University Press, 2002, pp. 318, US$65.00 (HB) ISBN: 0-340-70646-5. Int J Epidemiol. 2002;31: 1280–1281. doi:10.1093/ije/31.6.1280

27. Namouchi A, Guellil M, Kersten O, Hänsch S, Ottoni C, Schmid BV, et al. Integrative approach using *Yersinia pestis* genomes to revisit the historical landscape of plague during the Medieval Period. Proc Natl Acad Sci USA. 2018;115: E11790–E11797. doi:10.1073/pnas.1812865115

28. Slavin P. Out of the West: Formation of a Permanent Plague Reservoir in South-Central Germany (1349–1356) and its Implications∗. Past & Present. 2021;252: 3–51. doi:10.1093/pastj/gtaa028

29. Curtis DR, Roosen J. The sex-selective impact of the Black Death and recurring plagues in the Southern Netherlands, 1349–1450. American Journal of Physical Anthropology. 2017;164: 246–259. doi:10.1002/ajpa.23266

30. Spyrou MA, Tukhbatova RI, Feldman M, Drath J, Kacki S, Beltrán de Heredia J, et al. Historical Y. pestis Genomes Reveal the European Black Death as the Source of Ancient and Modern Plague Pandemics. Cell Host & Microbe. 2016;19: 874–881. doi:10.1016/j.chom.2016.05.012

31. Bos KI, Herbig A, Sahl J, Waglechner N, Fourment M, Forrest SA, et al. Eighteenth century Yersinia pestis genomes reveal the long-term persistence of an historical plague focus. Neher RA, editor. eLife. 2016;5: e12994. doi:10.7554/eLife.12994

32. Green MH. Putting Africa on the Black Death map: Narratives from genetics and history. Afriques Débats, méthodes et terrains d'histoire. 2018. doi:10.4000/afriques.2125

33. Stenseth NC, Samia NI, Viljugrein H, Kausrud KL, Begon M, Davis S, et al. Plague dynamics are driven by climate variation. PNAS. 2006;103: 13110–13115. doi:10.1073/pnas.0602447103

34. McCormick M. Rats, Communications, and Plague: Toward an Ecological History. Journal of Interdisciplinary History. 2003;34: 1–25. doi:10.1162/002219503322645439

35. Samia NI, Kausrud KL, Heesterbeek H, Ageyev V, Begon M, Chan K-S, et al. Dynamics of the plague–wildlife–human system in Central Asia are controlled by two epidemiological thresholds. PNAS. 2011;108: 14527–14532. doi:10.1073/pnas.1015946108

36. Linné Kausrud K, Viljugrein H, Frigessi A, Begon M, Davis S, Leirs H, et al. Climatically driven synchrony of gerbil populations allows large-scale plague outbreaks. Proc Biol Sci. 2007;274: 1963–1969. doi:10.1098/rspb.2007.0568

37. Guellil M, Kersten O, Namouchi A, Luciani S, Marota I, Arcini CA, et al. A genomic and historical synthesis of plague in 18th century Eurasia. PNAS. 2020;117: 28328–28335. doi:10.1073/pnas.2009677117

38. Yue RPH, Lee HF, Wu CYH. Trade routes and plague transmission in pre-industrial Europe. Sci Rep. 2017;7. doi:10.1038/s41598-017-13481-2

39. Schmid BV, Büntgen U, Easterday WR, Ginzler C, Walløe L, Bramanti B, et al. Climate-driven introduction of the Black Death and successive plague reintroductions into Europe. PNAS. 2015;112: 3020–3025. doi:10.1073/pnas.1412887112

40. Morozova I, Kasianov A, Bruskin S, Neukamm J, Molak M, Batieva E, et al. New ancient Eastern European Yersinia pestis genomes illuminate the dispersal of plague in Europe. Philosophical

Transactions of the Royal Society B: Biological Sciences. 2020;375: 20190569. doi:10.1098/rstb.2019.0569

41. Parker C, Rohrlach AB, Friederich S, Nagel S, Meyer M, Krause J, et al. A systematic investigation of human DNA preservation in medieval skeletons. Scientific Reports. 2020;10: 18225. doi:10.1038/s41598-020-75163-w

42. Hübler R, Key FM, Warinner C, Bos KI, Krause J, Herbig A. HOPS: automated detection and authentication of pathogen DNA in archaeological remains. Genome Biology. 2019;20: 280. doi:10.1186/s13059-019-1903-0

43. Herbig A, Maixner F, Bos KI, Zink A, Krause J, Huson DH. MALT: Fast alignment and analysis of metagenomic DNA sequence data applied to the Tyrolean Iceman. 2016. doi:10.1101/050559

44. Schuenemann VJ, Bos K, DeWitte S, Schmedes S, Jamieson J, Mittnik A, et al. Targeted enrichment of ancient pathogens yielding the pPCP1 plasmid of Yersinia pestis from victims of the Black Death. Proceedings of the National Academy of Sciences. 2011;108: E746–E752. doi:10.1073/pnas.1105107108

45. Briggs AW, Stenzel U, Meyer M, Krause J, Kircher M, Pääbo S. Removal of deaminated cytosines and detection of in vivo methylation in ancient DNA. Nucleic Acids Res. 2010;38: e87. doi:10.1093/nar/gkp1163

46. Harakalova M, Mokry M, Hrdlickova B, Renkens I, Duran K, van Roekel H, et al. Multiplexed array-based and in-solution genomic enrichment for flexible and cost-effective targeted next-generation sequencing. Nature Protocols. 2011;6: 1870–1886. doi:10.1038/nprot.2011.396

47. Stamatakis A. RAxML-VI-HPC: maximum likelihood-based phylogenetic analyses with thousands of taxa and mixed models | Bioinformatics | Oxford Academic. 2006 [cited 17 Apr 2020]. Available: https://academic.oup.com/bioinformatics/article/22/21/2688/251208

48. Hegel K. Die Chroniken der niedersächsischen städte. S. Hirzel; 1869.

49. Keyser, Erich. Deutsches Städtebuch, Band II - Mitteldeutschland. Stuttgart: W. Kohlhammer; 1941.

50. Ulshöfer K. Der hällische Salzhandelund in Hall und das Salz. Beiträge zur hällischen Stadt- und Salinengeschichte ed by Kuno Ulshöfer and Herta Beutter. Jan Thorbecke; 1983. pp. 95–112.

51. Hermmann V. Die ehemalige Marktkirsche St. Marien in Halle (Saale). Bau- und Grabbefunde der Ausgrabungen von 2004 bis 2006. Der Markt der Staft Halle im Mittelalter Ausgrabungen zu Marktkirche, Kirchhof und erzbischOflichem Kaufhaus. Halle: Harald Meller; 2018. pp. 15–140.

52. Bruns F, Weczerka H. Hansische Handelsstrassen. Textband. Weimar: Böhlau Verlag; 1967.

53. Gottfried RS. Black Death. Simon and Schuster; 2010.

54. MacArthur WP. The Identification of Some Pestilences Recorded in the Irish Annals. Irish Historical Studies. 1949;6: 169–188.

55. Dadoyan SB. Samuēl Anetsʻi ew sharunakoghner - Zhamanakagrutʻiwn Adamitsʻ minchʻew 1776. Christian-Muslim Relations 1500 - 1900. Brill; Available: https://referenceworks.brill-lonline.com/entries/christian-muslim-relations-ii/samuel-anetsi-ew-sharunakoghner-zha-manakagrutiwn-adamits-minchew-1776-COM_31368

56. Brosset M-F. Histoire de la Géorgie Depuis l'Antiquité Jusqu'au Xixe Siècle, Vol. 1: Histoire Ancienne, Jusqu'en 1469 de J.-C. Forgotten Books; 2018.

57. Drancourt M, Aboudharam G, Signoli M, Dutour O, Raoult D. Detection of 400-year-old Yersinia pestis DNA in human dental pulp: An approach to the diagnosis of ancient septicemia. PNAS. 1998;95: 12637–12640. doi:10.1073/pnas.95.21.12637

58. Dabney J, Meyer M. Extraction of Highly Degraded DNA from Ancient Bones and Teeth. In: Shapiro B, Barlow A, Heintzman PD, Hofreiter M, Paijmans JLA, Soares AER, editors. Ancient DNA: Methods and Protocols. New York, NY: Springer; 2019. pp. 25–29. doi:10.1007/978-1-4939-9176-1_4

59. Gansauge M-T, Meyer M. A Method for Single-Stranded Ancient DNA Library Preparation. In: Shapiro B, Barlow A, Heintzman PD, Hofreiter M, Paijmans JLA, Soares AER, editors. Ancient DNA: Methods and Protocols. New York, NY: Springer; 2019. pp. 75–83. doi:10.1007/978-1-4939-9176-1_9

60. Peltzer A, Jäger G, Herbig A, Seitz A, Kniep C, Krause J, et al. EAGER: efficient ancient genome reconstruction. Genome Biology. 2016;17: 60. doi:10.1186/s13059-016-0918-z

61. Li H, Durbin R. Fast and accurate short read alignment with Burrows-Wheeler transform. Bioinformatics. 2009;25: 1754–1760. doi:10.1093/bioinformatics/btp324

62. Ginolhac A, Rasmussen M, Gilbert MTP, Willerslev E, Orlando L. mapDamage: testing for damage patterns in ancient DNA sequences. Bioinformatics. 2011;27: 2153–2155. doi:10.1093/bioinformatics/btr347

63. Andrades Valtueña A, Mittnik A, Key FM, Haak W, Allmäe R, Belinskij A, et al. The Stone Age Plague: 1000 years of Persistence in Eurasia. 17 May 2017 [cited 8 Feb 2021]. doi:10.1101/094243

64. Meyer M, Kircher M. Illumina Sequencing Library Preparation for Highly Multiplexed Target Capture and Sequencing. Cold Spring Harb Protoc. 2010;2010: pdb.prot5448. doi:10.1101/pdb.prot5448

65. Neumann GU. Tooth Sampling from the inner pulp chamber for ancient DNA Extraction. 2020 [cited 8 Feb 2021]. doi:10.17504/protocols.io.bqebmtan

66. Matero P, Pasanen T, Laukkanen R, Tissari P, Tarkka E, Vaara M, et al. Real-time multiplex PCR assay for detection of Yersinia pestis and Yersinia pseudotuberculosis. APMIS. 2009;117: 34–44. doi:https://doi.org/10.1111/j.1600-0463.2008.00013.x

67. Bos KI, Harkins KM, Herbig A, Coscolla M, Weber N, Comas I, et al. Pre-Columbian mycobacterial genomes reveal seals as a source of New World human tuberculosis. Nature. 2014;514: 494–497. doi:10.1038/nature13591

68. Thorvaldsdóttir H, Robinson JT, Mesirov JP. Integrative Genomics Viewer (IGV): high-performance genomics data visualization and exploration. Brief Bioinform. 2013;14: 178–192. doi:10.1093/bib/bbs017

69. Cingolani P, Platts A, Wang LL, Coon M, Nguyen T, Wang L, et al. A program for annotating and predicting the effects of single nucleotide polymorphisms, SnpEff. Fly (Austin). 2012;6: 80–92. doi:10.4161/fly.19695

70. Zhou H, Yu Z, Hu Y, Tu J, Zou W, Peng Y, et al. The Special Neuraminidase Stalk-Motif Responsible for Increased Virulence and Pathogenesis of H5N1 Influenza A Virus. PLOS ONE. 2009;4: e6277. doi:10.1371/journal.pone.0006277

71. Quinlan AR, Hall IM. BEDTools: a flexible suite of utilities for comparing genomic features. Bioinformatics. 2010;26: 841–842. doi:10.1093/bioinformatics/btq033

72. RACINE JS. RSTUDIO: A PLATFORM-INDEPENDENT IDE FOR R AND SWEAVE. Journal of Applied Econometrics. 2012;27: 167–172.

Additional Files

Additional File 1

Format: Word Document (*.docx)

Title: Supplementary Material

Description: Supplementary methods and subsequent analyses of the *Y. pestis* genomes presented in the manuscript.

Supplementary Material

1.1 Detailed Sampling Methods:

The following steps were performed in a dedicated clean room facility associated with the Max Planck Institute for the Science of Human history in accordance with all local, federal, and international handling of human remains and safety regulations therein.

1.1.1 Untargeted Screening (Reprinted from the Supplementary Materials of Parker et al. 2020[1]).

1.1.1.1 Teeth

Cementum was removed from the root portion of the tooth using a standard dental drill fitted with a circular cutting attachment. The blade of the cutting wheel was placed lightly against the root at a 20° angle (relative to the bottom of the root) on a low-speed, high-torque setting and the cementum scraped off downward (**Figure S1a-b)**. The tooth was then bisected along the cementum-enamel junction. Powder from the pulp chamber was generated using a standard dental drill bit from the first pass of the interior of the crown. Subsequent passes were used to generate bone powder from dentin (**Figure S1c**).

a.

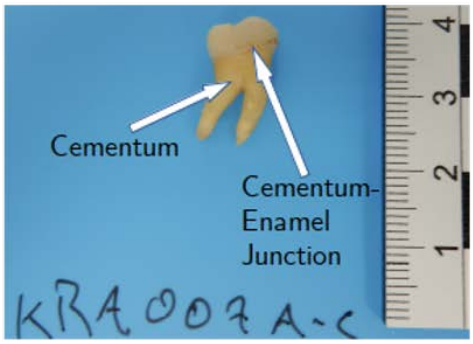

b.

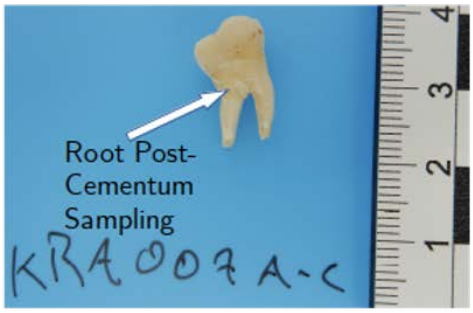

c.

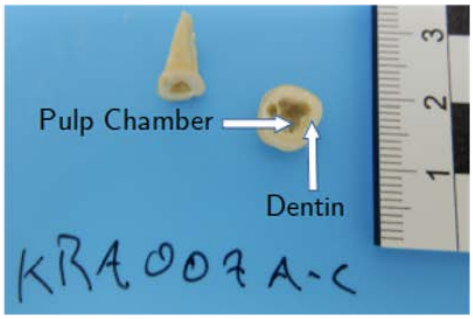

Figure S1a-c: *In situ* molar pre (a) and post (b) removal of cementum, as well as pre (b) and post (c) sectioning and drilling of the pulp chamber and underlying dentin.

1.1.1.2 Superior Vertebral Arch Sampling

Cortical bone powder was collected from the superior apex of the junction of the lamellae and spinous process (superior vertebral arch; Figure S2).

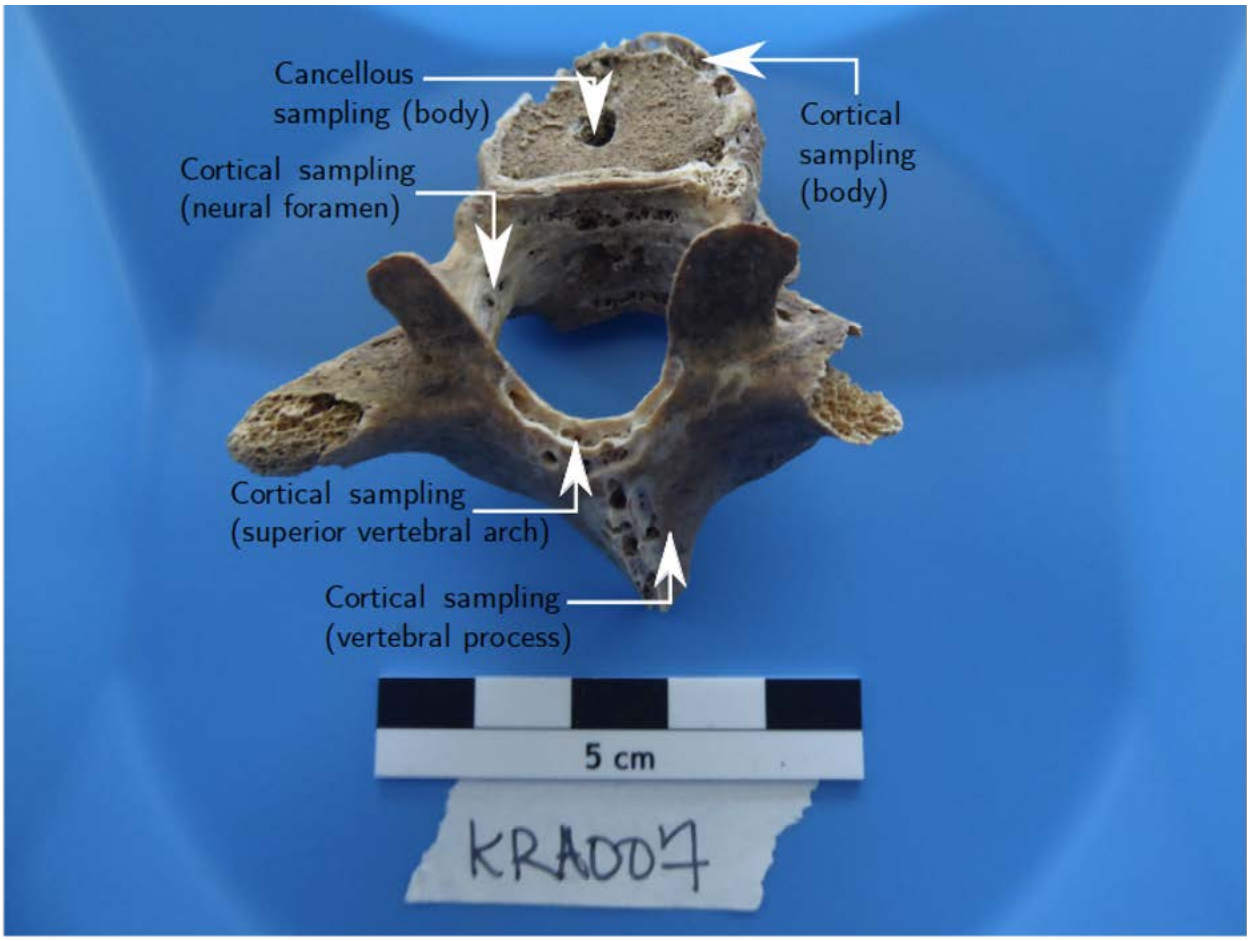

Figure S2: All sampling locations (post-drilling) of the thoracic vertebrae (superior view)**.**

1.1.1.3 Femur Sampling

Cortical bone material was collected from the shaft, just below the lesser trochanter (**Figure S3**).

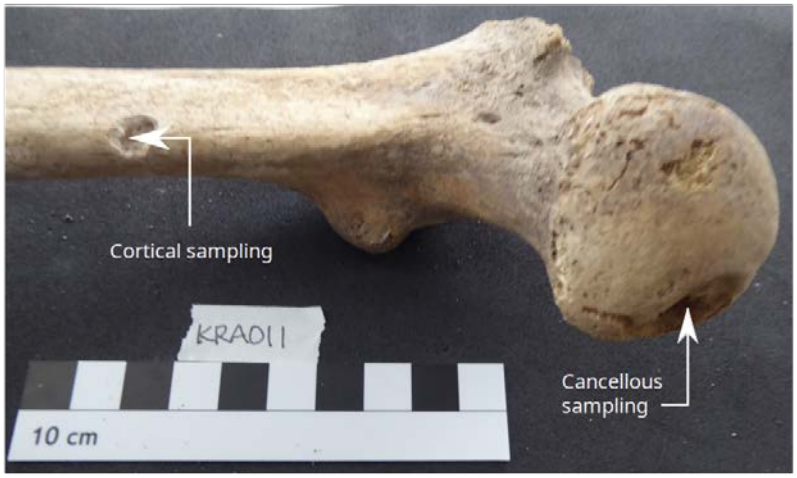

Figure S3: Femur (anterior view) showing drilling sites for the collection of both cortical and cancellous material.

1.2.1 Targeted sampling for pathogen DNA:

Teeth were cut at the cementoenamel junction (**Figure S4**) and between ~ 30 -70 mg powder was generated by removing the surface layer of the pulp chamber from the crown and, if not enough powder obtained, from the root with a dentist drill.

Figure S4: Example of crown and root being separated and sampled.

1.3 Supplementary analyses:

1.3.1 Deamination Patterns

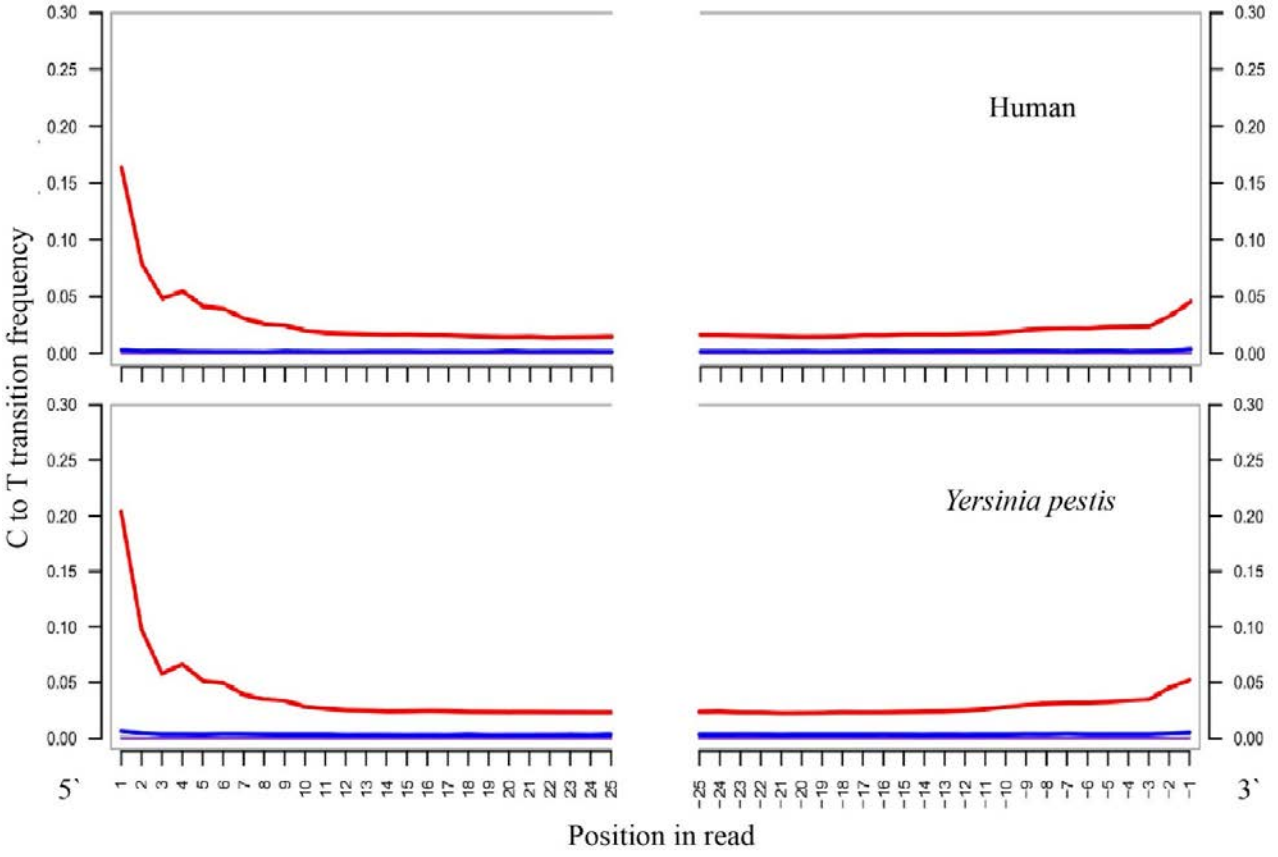

Figure S5. Representative comparison of deamination patterns in reads from the KRA004 dental pulp chamber libraries mapping to both the HG19 human reference and *Yersinia Pestis* CO92 reference genomes.

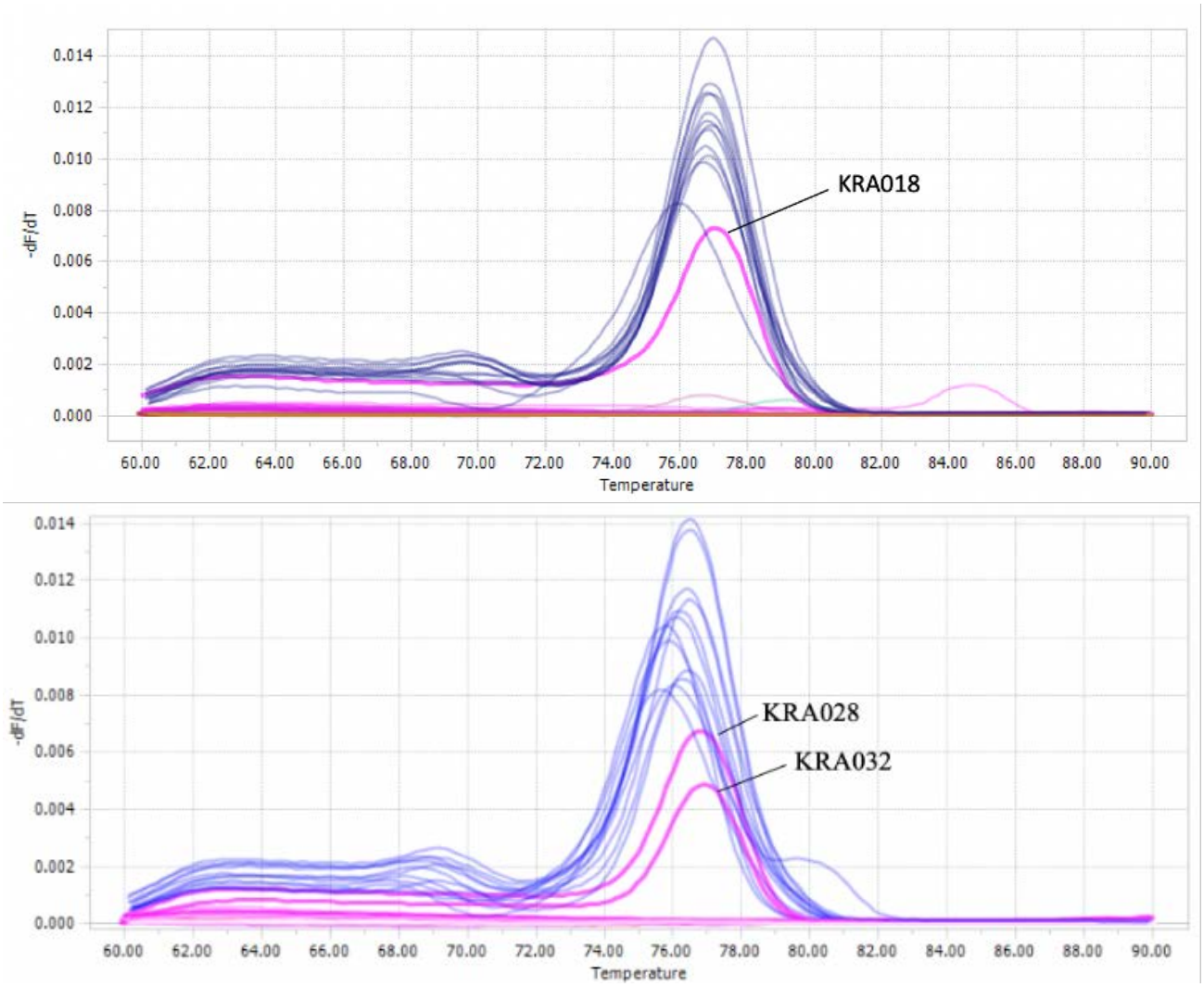

Figure S6. Melting curve of *pla* assay for KRA018 (left) and KRA028 and KRA032 (right) in pink, showing a peak at around 77°C. Standards ranging from $2.23x10^{-1}$ – $2.23x10^{4}$ are colored in purple.

1.3.2 Virulence factor presence/absence analyses

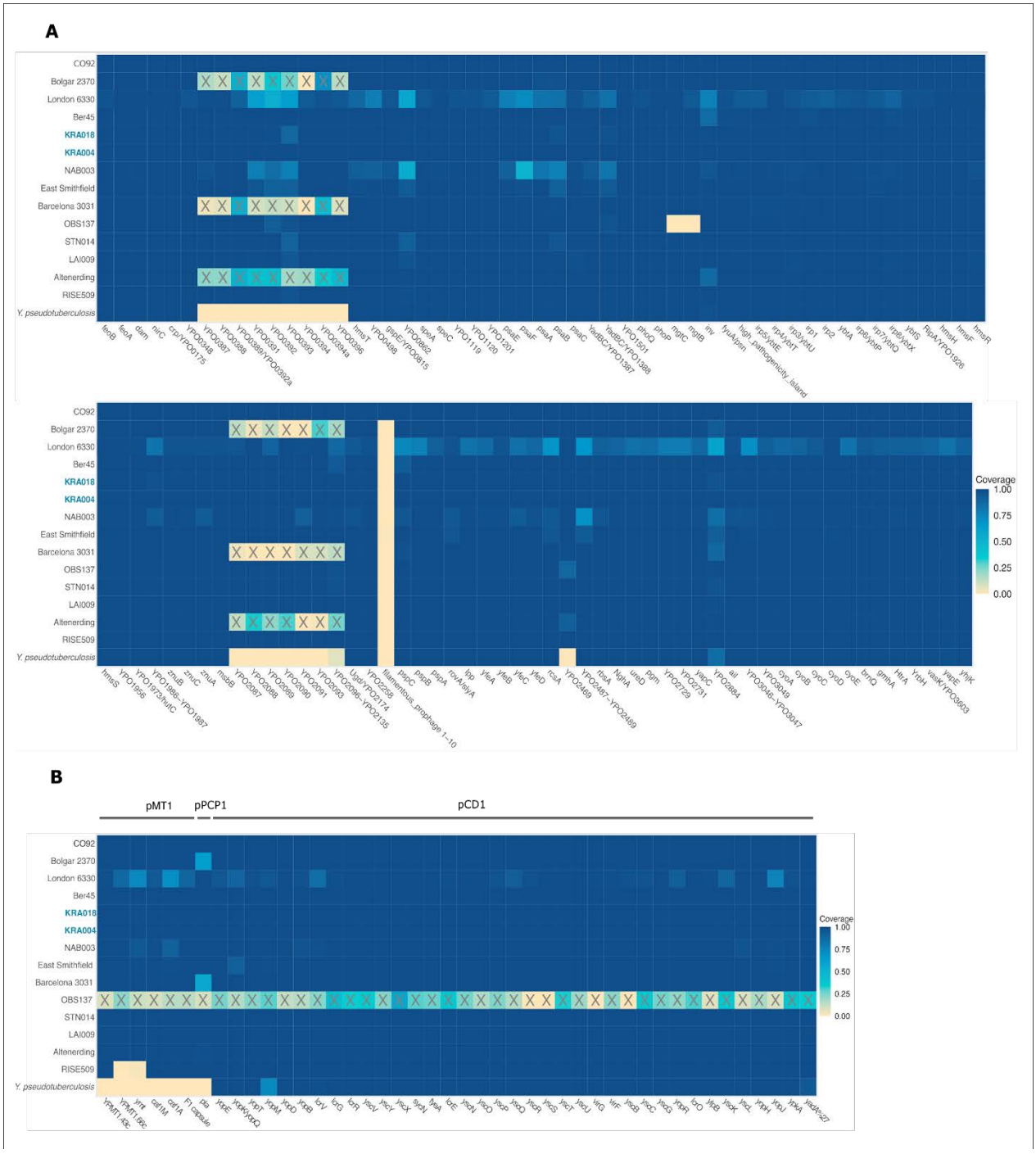

Figure S7a-b. Heatmaps showing genomic coverage of chromosomal (A) and plasmid-encoded (B) genes involved in virulence of *Y. pestis* for KRA004 and KRA018 (indicated in blue) and other ancient genomes as well as the CO92 reference genome and *Y. pseudotuberculosis* (IP32953). Coverage given in percent, "X" denotes cases where genes were not included in the probe set that was used for target enrichment for the respective genomes.

References:

1. Parker C, Rohrlach AB, Friederich S, Nagel S, Meyer M, Krause J, et al. A systematic investigation of human DNA preservation in medieval skeletons. Scientific Reports. 2020;10: 18225. doi:**10.1038/s41598-020-75163-w**
2. Dabney J, Meyer M. Extraction of Highly Degraded DNA from Ancient Bones and Teeth. In: Shapiro B, Barlow A, Heintzman PD, Hofreiter M, Paijmans JLA, Soares AER, editors. Ancient DNA: Methods and Protocols. New York, NY: Springer; 2019. pp. 25–29. doi:**10.1007/978-1-4939-9176-1_4**
3. Velsko I, Skourtanioti E, Brandt G. Ancient DNA Extraction from Skeletal Material. In: protocols.io [Internet]. 11 Dec 2020 [cited 28 Oct 2021]. Available: **https://www.protocols.io/view/ancient-dna-extraction-from-skeletal-material-baksicwe**

Additional File 2

Format: Excel spreadsheet (*.xlsx)

Title: Supplementary File 1

Description: Complete data table showing full descriptions of screening and capture data recovered from all samples analyzed in this study.

5. Manuscript 4

"Development of laboratory methods to isolate high molecular weight microbial DNA from dental calculus"

Cody Parker, Kurt Alt, Wolfgang Haak, Kirsten I Bos, Johannes Krause

In preparation

We present a proof-of-concept experiment designed to develop and evaluate a potential method for the isolation of high molecular weight oral microbiome DNA from modern dental calculus. We find that with some modification that current, highly available high molecular weight DNA extraction kits can be used to isolate DNA of sufficient length (>10kbp) for use in conjunction with sequencing technologies such as the Oxford Nanopore and PacBio sequencing platforms. In addition, we were able to verify that, in similar proportions to those found when using techniques intended for short-read sequencing such as on the Illumina platform, the DNA extracted from this method stems from microbes known to be integral parts of the oral microbiome.

Author contributions

CP is the primary author (95%) and was responsible for the processing, method development and optimization, sampling from, DNA extraction from all samples, preparation of all DNA libraries sequenced (85%) and their subsequent analyses (70%). JFW assisted in the analyses of samples. FA aided in the design and implementation of laboratory protocols. KA provided all samples and their associated ethical permissions for study. KB acted as co-supervisor, provided funding, aided in the experimental design of this study, and contributed

to the writing and editing of this manuscript. WH acted as co-supervisor, provided funding, and contributed to the writing and editing manuscript. JK acted as co-supervisor and provided funding for the study.

Author	Conception	Data analyses	Experimentation	Writing	Sample procurement
C.P.	20%	70%	85%	95%	N/A
J.F.Y.	N/A	30%	N/A	N/A	N/A
F.A.	N/A	N/A	15%	N/A	N/A
K.A.	10%	N/A	N/A	N/A	70%
K.B.	20%	N/A	N/A	5%	N/A
W.H.	10%	N/A	N/A	N/A	N/A
J.K..	40%	N/A	N/A	N/A	30%

Expanding the oral microbiome reference dataset using long read sequencing of modern dental calculus

Cody Parker[1], James Fellows Yates[1,2], Franziska Aron[1], Wolfgang Haak[1,2], Kirsten I Bos[1,2], Johannes Krause[1,2]

Affiliations:
[1]Max Planck Institute for the Science of Human History, Jena, Germany
[2]Max Planck Institute for Evolutionary Anthropology, Deutscher Platz 6, 04103 Leipzig, Germany

Cody Parker: parker@shh.mpg.de
James Fellows Yates: fellowsyates@shh.mpg.de
Franziska Aron: aron@shh.mpg.de
Wolfgang Haak: haak@shh.mpg.de
Kirsten I. Bos: bos@shh.mpg.de
Johannes Krause: krause@shh.mpg.de

Abstract

Studies into the evolution of the human microbiome are in high demand. This is particularly true of the human oral microbiome, as dental calculus has been shown to be an excellent source of both modern and ancient DNA stemming from the microbial flora that make up the oral microbiome. However, analyses of ancient microbes can be challenging, as investigations typically rely on mapping short, highly degraded ancient DNA fragments to modern reference databases. Of the 771 microbial species currently recognized as part of the human oral microbiome, full reference genomes are available for only 62% (475), and 30% remain known only as uncultivated phylotypes. The production of high-quality reference genomes from uncultivable species in a metagenomic context is typically done via the *de novo* assembly of shotgun sequencing results and is generally most successful when using a combination of short-read (e.g., Illumina) and long-read (e.g., Oxford Nanopore or PacBio) sequencing. The efficacy of long-read extraction techniques in the extraction of metagenomic microbial DNA from dental calculus, however, has not yet been tested. Here we present a proof-of concept experiment showing the successful extraction of microbial DNA fragments >12kbp from modern dental calculus and the subsequent successful mapping of said fragments to already described members of the human oral microbiome.

Introduction

The introduction of next-generation sequencing (NGS) techniques has drastically changed the field of ancient DNA (aDNA) analyses[1–3]. Using these high-throughput techniques, researchers are now able to use aDNA extracted from archaeological remains to study not just the evolution of the host species[4–8], but also associated pathogens[9–13] and the communities of microbial flora living within the host (i.e., the associated microbiomes)[14–17]. As a result, studies into the evolution of these microbiomes are in high demand[15,18–20]. This is particularly true of projects seeking to investigate the make-up of the ancient oral microbiome, as ancient dental calculus is not only readily available, but has also been shown to exhibit excellent preservation of ancient microbial DNA[20–23].

Within the oral cavity, several members of the oral microbiome are known to produce layers of biofilms which adhere to the exterior of teeth[24,25]. Dental calculus is formed via flash calcification of these biofilms. As new layers are deposited and calcified, the microbes, free DNA, and/or food particles to these biofilms is subsequently trapped and preserved[26–30]. In terms of DNA preservation, sequencing of DNA libraries derived from ancient dental calculus has been shown to yield exceptionally high-quality microbial DNA[22,23,31,32]. As such, ancient dental calculus has already been used to great effect in terms of elucidating changes in the human oral microbiome through time[15,19,20].

Investigations of the ancient oral microbiomes typically rely on reference mapping-based techniques to identify and analyses potential constituents of the host microbiome, as the highly degraded nature of aDNA can make the already daunting task of assembling *de novo* genomes from metagenomic samples even more challenging[33]. The reference mapping approach, however, is inherently limited to the investigation of only of those microbial species

that have been previously described, sequenced, and assembled into high-quality reference genomes. This is of particular concern for the investigation of the ancient oral microbiome, as of the 771 species currently thought to make up this microbial community, reference genomes are only available for 475 taxa (62%)[34]. Of the remaining 296 taxa, 231 are known only as uncultivated phylotypes, making the *de novo* assembly of metagenomic datasets the only possible method for the generation of high-quality reference genomes. It has been shown that the quality of assembled genomes can be greatly increased by utilizing a combination of datasets incorporating both short-read (e.g., that produced from the Illumina™ platform) and long-read (e.g., produced from the Oxford Nanopore™ and PacBio™ platforms, or inferred from techniques such as Hi-C library preparation) sequencing[35,36].

While the production of short-read metagenomic datasets from dental calculus is well described[37–39], long-read sequencing libraries, or their Hi-C equivalent, require high-molecular weight (HMW) input DNA. To date, it has not yet been confirmed that sufficiently long DNA fragments can be recovered from the microbial component of dental calculus using standard HMW DNA extraction techniques. As such, it is of value to not only test the efficacy of these methods in modern dental calculus, but also to verify that at least some portion of the resulting HMW DNA does indeed originate from known members of the oral microbiome before attempting widespread production of long-read libraries from dental calculus for the purpose of oral microbiome reference construction. Here we present one such test utilizing a dental calculus optimized protocol for the MagAttract High Molecular Weight DNA extraction kit™ (Qiagen), yielding metagenomic DNA >12kbp in length and reliably mapping back to known constituents of the human oral microbiome.

Methods

Sampling

Calculus samples were obtained from patients at the Danube Private University School of Dentistry. All donors were asked to fill out a basic health survey indicating their tobacco usage (present or past), alcohol consumption, dietary preference (e.g., vegetarian, vegan, or omnivore), as well as any pre-existing medical conditions (Table 1). All samples were removed directly from the donor, placed in a microcentrifuge tube, weighed, and immediately frozen for later analyses.

High molecular-weight DNA extraction

All samples were decalcified by incubation at room temperature (with rotation) for 48 hours in 900µl of solution consisting of 0.5M EDTA and 0.5% SDS. Proteinase K (100µl) was then added to digest freed proteins and incubation resumed for another 24 hours. Samples were then centrifuged for 2 minutes at 14000rmp to separate particulate matter and the resulting supernatant split into two equal volumes of 500µl. High-molecular weight DNA was then extracted from each reaction using the MagAttract HMW DNA extraction kit following the supplied protocols for fresh/frozen tissue scaled by 2.5x (total volume 1685µl per reaction) and each was eluted in 50µl of supplied buffer AE each for a total of 100µl of HMW DNA solution.

Quantification

All sample concentrations were first quantified using standard Qubit™ quantification. Fragment size was verified using standard protocols for genomic DNA on the Agilent TapeStation 4000.

Illumina sequencing

After the successful generation of HMW extract, 200ng of DNA from each extraction was diluted in 50µl of water and prepared for Illumina sequencing by first shearing the DNA to an average fragment length of ca. 400bp by sonication using a Covaris M220 focused ultrasonic sonicator. Double stranded sequencing libraries were then prepared using standard NEB T4 Polymerase protocols for blunt end repair[40,41] and Bst Polymerase protocols for adapter ligation (see Supplementary Materials). The unindexed libraries were then quantified via qPCR before double indexes (unique indexing on both the 5' and 3' ends of each fragment) were added using the suggested protocols for downstream Illumina sequencing (see Supplemental Materials). All samples were then sequenced to a target depth of ca. 5,000,000 reads (150bp paired end) on the Illumina HiSeq 4000 platform.

Confirmation of oral microbiome flora

Metagenomic sequencing data for all samples were first aligned to the hg19 human reference genome (accession number: GCF_000001405.13) to remove all mapping reads. The filtered, non-human, reads were then processed through the MALT[16] and MetaPhlAn[42] pipelines to screen for the presence of DNA mapping to known members of the human oral microbiome.

Results

As to the suitability of our dental calculus extraction protocols in yielding high-molecular weight DNA, we find that all screened samples yielded an average fragment size of 8.0237 ± 0.889 kbp with three individuals > 10 kbp (Figure 1). Additionally, we observe our samples to yield an average concentration of 9.805 ± 1.714 ng/µl per extraction (Figure 1). We find this yield more than sufficient for use on all long-read sequencing platforms.

In the Illumina short-read (150bp paired end) screening datasets, we find that, overall, 88.26% of reads map to bacterial species, 11.71% to Eukaryota, and of remaining 0.04% of reads mapping to viral species (Figure 2). Within those reads mapping to bacterial species, we find high quality mappings to multiple taxa known to be endemic to the human-oral microbiome in all individuals (Figure 3, Table 1). At the species and sub-species level, 36 of the top 40 represented taxa are known members of the oral microbiome (Table 1) or oral pathogens. Of the remaining four, *Clostridiodes difficle,*(160.59 reads assigned, normalized across samples) is a known human pathogen, commonly found as a false positive due to sequence identity issues between closely related taxon; *Neisseria gonorrhoeae* is a similarly pathogenic and has been known to infect the throat of infected individuals (In addition, *N. gonorhoea* (781.40 reads assigned, normalized across samples) shares much of the same core genome with the many other *Neisseria* species, some of which can colonize the oral cavity, making false positives and cross mapping highly probable); and *Kinella kingae's* (116.51 reads assigned, normalized across samples) habitat is currently unassigned, though several other members of the genus are known members of the oral microbiome; with another 354.59 (normalized across samples) reads assigned to uncultured bacteria, highlighting the need for further efforts to expand the oral microbiome reference database through metagenomic assembly.

Discussion

Although long-read sequencing and metagenomic assembly has not been attempted with these samples as of yet, we find the protocol discussed here of sufficient promise to warrant further testing. Expanding the existing human oral microbiome reference database is an ongoing project. As a proof of concept, the protocol presented here represent. one possible step to continue this process. The use of this protocol for the production of both long read short read,

next generation DNA sequencing libraries will, in conjunction with new metagenomic assembly techniques, help to not only increase the quality of existing reference genomes, but also help identify new and previously unassigned bacterial constituents of the human oral microbiome.

Author contributions:

CP designed, optimized, and performed all laboratory protocols in addition to conducting all analyses and writing of the manuscript. JFW assisted in the analyses of samples. FA aided in the design and implementation of laboratory protocols. WH, KB, and JK were involved in the study design as well as being the primary source of funding and supervision for the work contained within this manuscript.

Acknowledgements

The authors would like to thank the laboratory staff of the Max Planck Institute for the Science of Human History, Jena, Germany. In particular, the help of Antje Wissigot was instrumental to the success of this project. This study was funded by the Max Planck Society, the European Research Council (ERC) under the European Union's Horizon 2020 research and innovation program under grant agreements No 771234 – PALEoRIDER (WH, ABR) and Starting Grant No. 805268 CoDisEASe (to KIB).

Code Availability

All analyses programs used within this Manuscript are freely available from GitHub.

Malt: https://github.com/husonlab/malt

Eager: https://github.com/apeltzer/EAGER-GUI

MetaPhlAn: https://github.com/biobakery/MetaPhlAn2

Conflicts of Interests

The authors have no conflicts of interests to report.

Figures

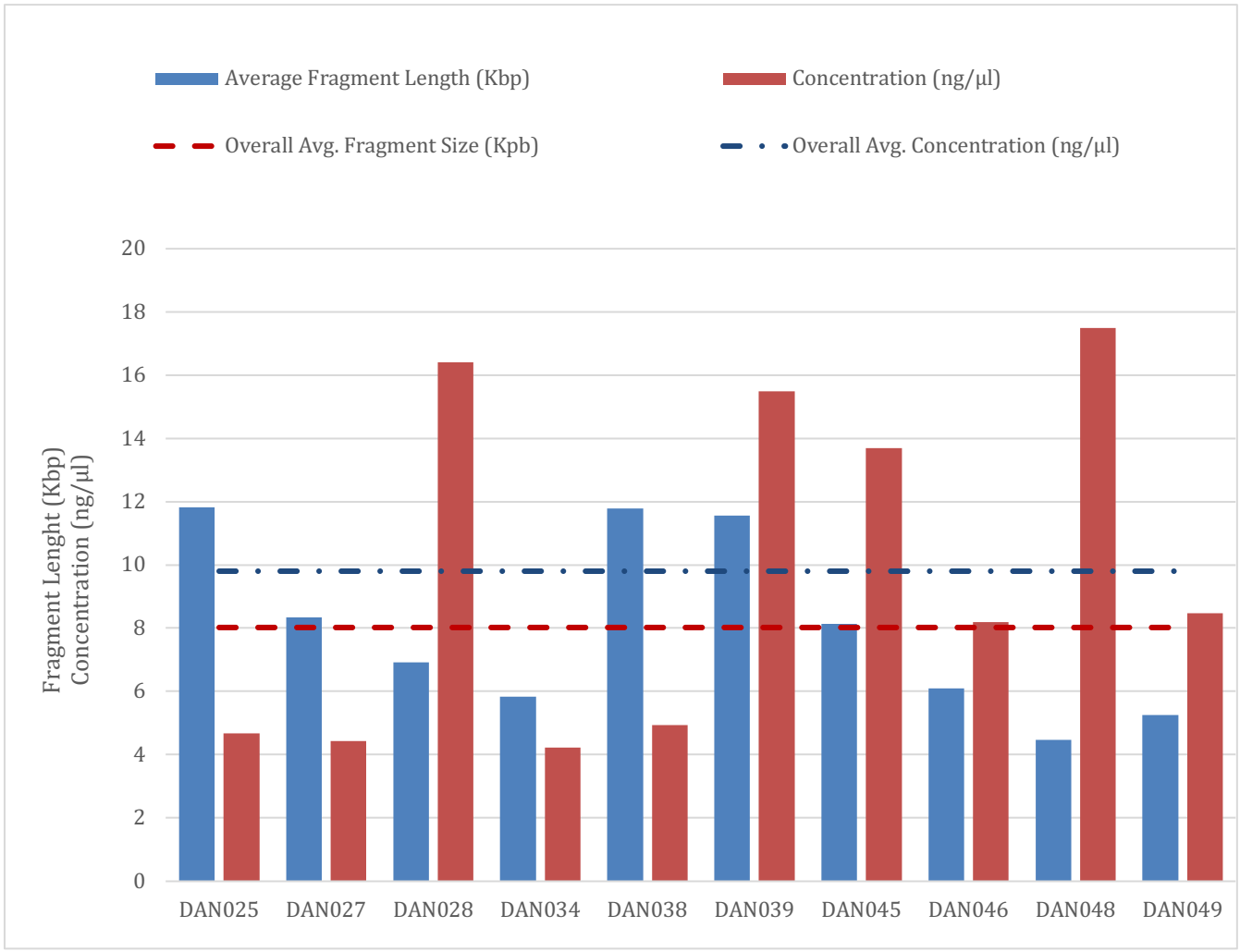

Figure 1. Concentration (Blue; ng/µl) and average fragment length (red; Kbp) of high molecular weight DNA extracts from each modern dental calculus sample as measured by TapeStation 4200. The dashed blue line represents the overall average concentration of 9.805 ± 1.714 ng/µl. The red the overall average fragment length of 8.0237 ± 0.889 Kbp. All error is measured as standard error of the mean.

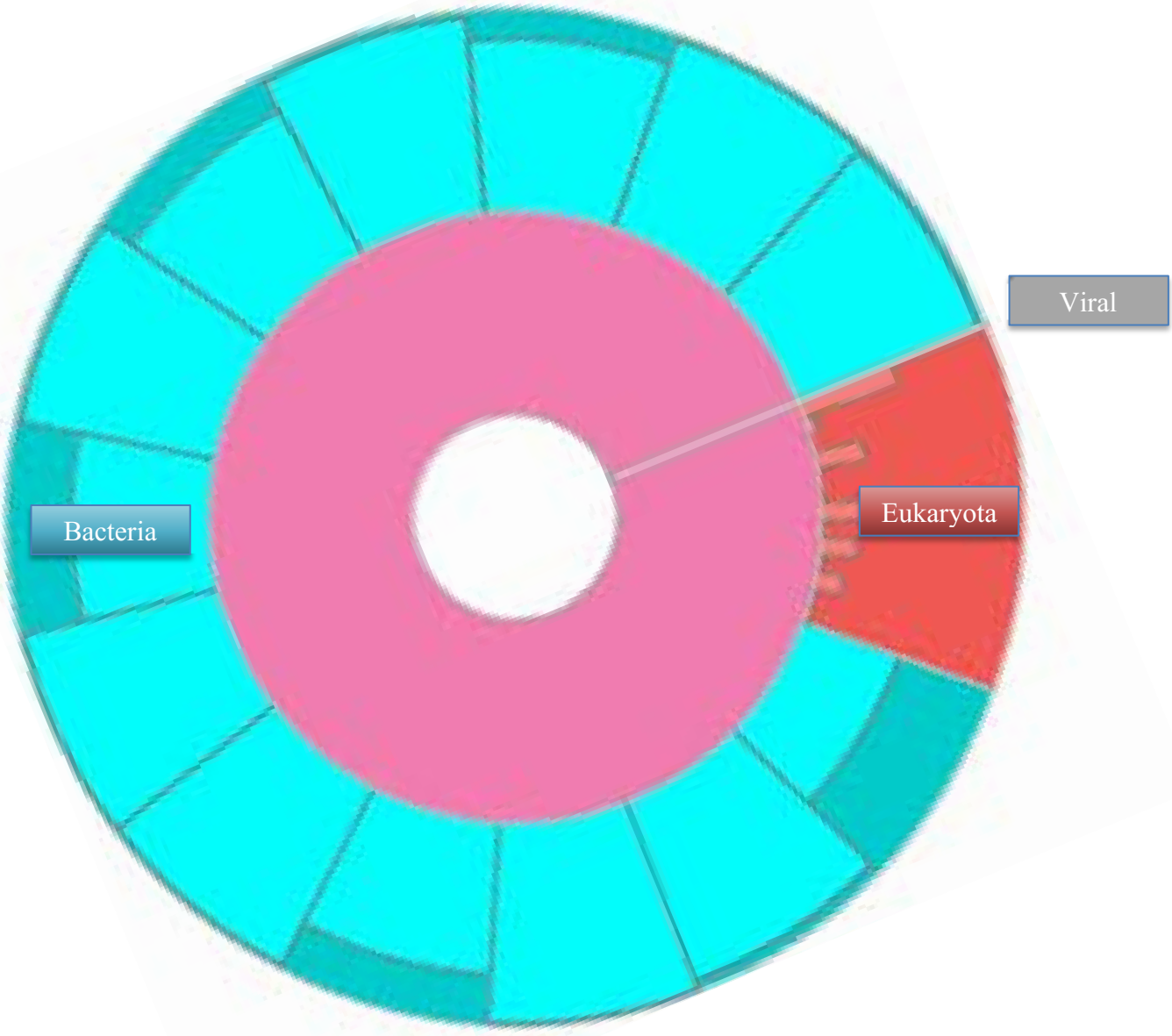

Figure 2. Relative proportion of reads mapping to bacteria (blue), Eukaryota (red),and viral (grey) species across all samples. Individual proportions are shown as lighter coloured bars within their respective categories.

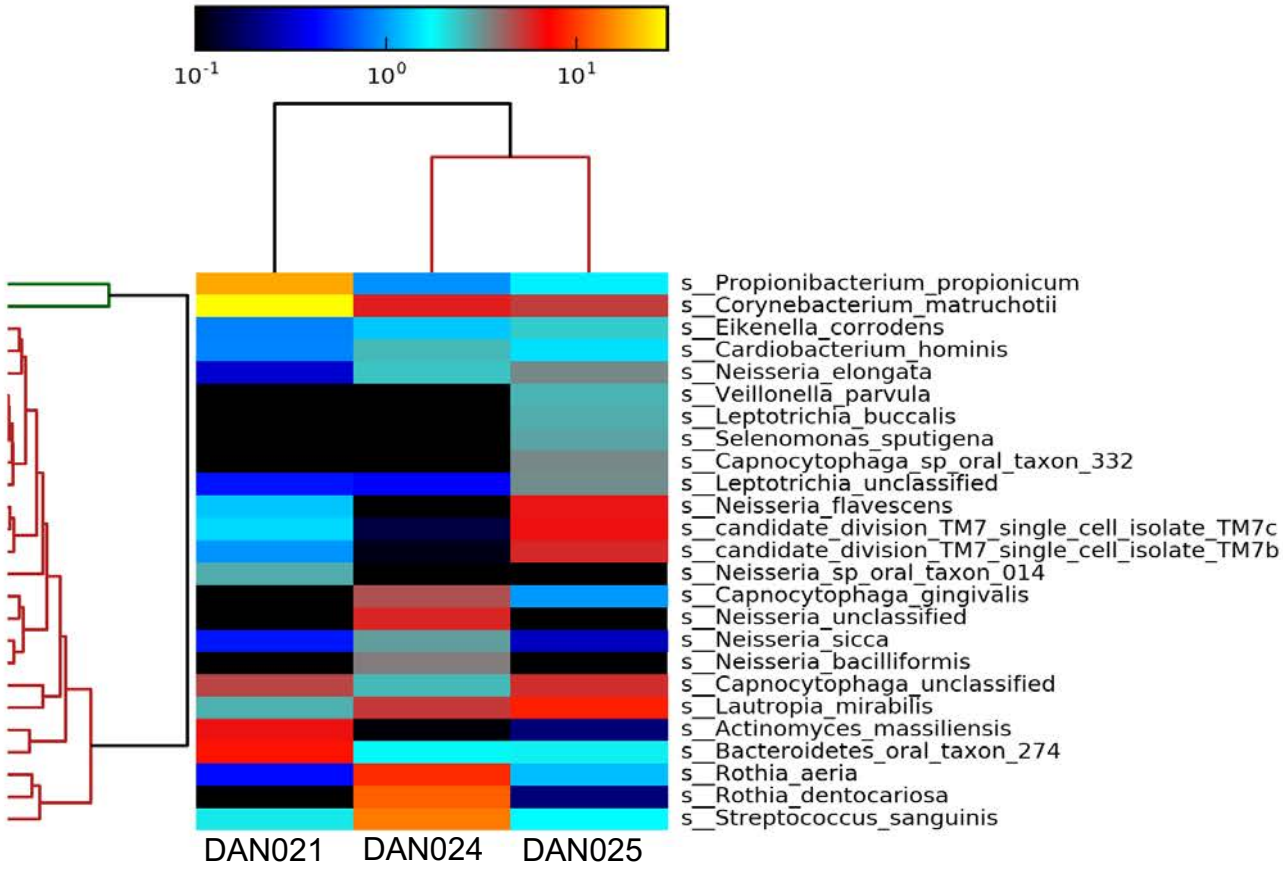

Figure 3. Heatmap showing the relative numbers of normalized reads assigned to oral microbiome taxa across three representative modern calculus samples.

Tables:

Table 1. Species level taxonomic chart showing the 40 most prevalent taxons, their habitat, and number of total reads assigned (normalized across samples) for all high molecular weight DNA modern dental calculus libraries analysed.

Taxon	Habitat	Normalized reads assigned
Ottowia sp. Oral taxon 894	Oral	7997.00
Actinomyces oris	Oral	6000.97
Actinomyces sp. Oral taxon 414	Oral	3652.33
Aggregatibacter aphrophilus	Oral	3525.93
Neisseria meningitidis	Oral	3115.34
Tannerella forsythia	Oral	2129.39
Porphyromonas gingivalis	Oral	1497.22
Streptococcus gordonii	Oral	978.38
Leptotrichia sp. Oral taxon 212	Oral	972.81
Streptococcus sp. VT 162	Oral	956.77
Olsenella sp. Oral taxon 807	*Oral*	*922.67*
Capnocytophaga sp. Oral taxon 323	Oral	905.01
Neisseria gonorrhoeae	Unassigned	781.40
Fretibacterium fastidiosum	Oral	638.10
Actinomyces radicidentis	Oral	403.36
Treponema sp. OMZ 838	Oral	376.83
Campylobacter gracilis	Oral	356.12
uncultured bacterium	N/A	354.59
Streptococcus sanguinis	Oral	249.42
Prevotella intermedia	Oral	245.50
Candidatus Saccharibacteria oral taxon TM7x	Oral	230.66
Schaalia meyeri	Oral	227.05
Streptococcus pneumoniae	Oral	186.71

Clostridioides difficile	Fecal	160.59
Streptococcus mitis	Oral	137.71
Rothia mucilaginosa	Oral	136.71
Aggregatibacter actinomycetemcomitans	Oral	123.02
Kingella kingae	Unassigned	116.51
Capnocytophaga haemolytica	Oral	114.05
Fusobacterium hwasookii	Oral	107.86
Haemophilus influenzae	Oral	91.44
Fusobacterium nucleatum	Oral	84.08
Selenomonas sp. Oral taxon 136	Oral	83.50
Streptococcus intermedius	Oral	83.13
Selenomonas sp. Oral taxon 478	Oral	81.94
Treponema putidum	Oral	73.41
Parvimonas micra	Oral	71.57
Streptococcus sp. Oral taxon 431	Oral	71.05
Streptococcus sp. A12	Oral	58.99
Campylobacter concisus	Oral	58.37

References:

1. Mardis, E. R. Next-generation DNA sequencing methods. Annu. Rev. Genomics Hum. Genet. **9**, 387–402 (2008).

2. Schuster, S. C. Next-generation sequencing transforms today's biology. Nat. Methods **5**, 16–18 (2008).

3. Knapp, M. & Hofreiter, M. Next Generation Sequencing of Ancient DNA: Requirements, Strategies and Perspectives. Genes **1**, 227–243 (2010).

4. Meyer, M. et al. A High-Coverage Genome Sequence from an Archaic Denisovan Individual. Science **338**, 222–226 (2012).

5. Burrell, A. S., Disotell, T. R. & Bergey, C. M. The use of museum specimens with high-throughput DNA sequencers. J. Hum. Evol. **79**, 35–44 (2015).

6. Broushaki, F. et al. Early Neolithic genomes from the eastern Fertile Crescent. Science **353**, 499 (2016).

7. Slatkin, M. & Racimo, F. Ancient DNA and human history. Proc. Natl. Acad. Sci. **113**, 6380–6387 (2016).

8. Marciniak, S. & Perry, G. H. Harnessing ancient genomes to study the history of human adaptation. Nat. Rev. Genet. **18**, 659–674 (2017).

9. Bos, K. I. et al. A draft genome of Yersinia pestis from victims of the Black Death. Nature **478**, 506–510 (2011).

10. Guedes, L. et al. First Paleogenetic Evidence of Probable Syphilis and Treponematoses Cases in the Brazilian Colonial Period. BioMed Res. Int. **2018**, (2018).

11. Schuenemann, V. J. et al. Genome-Wide Comparison of Medieval and Modern Mycobacterium leprae. Science **341**, 179–183 (2013).

12. Margaryan, A. et al. Ancient pathogen DNA in human teeth and petrous bones. Ecol. Evol. **8**, 3534–3542 (2018).

13. Maixner, F. et al. The 5300-year-old Helicobacter pylori genome of the Iceman. Science **351**, 162–165 (2016).

14. Warinner, C., Speller, C., Collins, M. J. & Lewis, C. M. Ancient human microbiomes. J. Hum. Evol. **79**, 125–136 (2015).

15. Adler, C. J. et al. Sequencing ancient calcified dental plaque shows changes in oral microbiota with dietary shifts of the Neolithic and Industrial revolutions. Nat. Genet. **45**, 450–455 (2013).

16. Herbig, A. et al. MALT: Fast alignment and analysis of metagenomic DNA sequence data applied to the Tyrolean Iceman. (2016) doi:10.1101/050559.

17. Lugli, G. A. et al. Ancient bacteria of the Ötzi's microbiome: a genomic tale from the Copper Age. Microbiome **5**, 5 (2017).

18. Groussin, M. et al. Unraveling the processes shaping mammalian gut microbiomes over evolutionary time. Nat. Commun. **8**, 14319 (2017).

19. Schnorr, S. L., Sankaranarayanan, K., Lewis, C. M. & Warinner, C. Insights into human evolution from ancient and contemporary microbiome studies. Curr. Opin. Genet. Dev. **41**, 14–26 (2016).

20. Warinner, C. Dental calculus and the evolution of the human oral microbiome. J. Calif. Dent. Assoc. **44**, (2016).

21. Mann, A. E. et al. Differential preservation of endogenous human and microbial DNA in dental calculus and dentin. Sci. Rep. **8**, 9822 (2018).

22. Preus, H. R., Marvik, O. J., Selvig, K. A. & Bennike, P. Ancient bacterial DNA (aDNA) in dental calculus from archaeological human remains. J. Archaeol. Sci. **38**, 1827–1831 (2011).

23. Warinner, C., Speller, C. & Collins, M. J. A new era in palaeomicrobiology: prospects for ancient dental calculus as a long-term record of the human oral microbiome. Philos. Trans. R. Soc. B Biol. Sci. **370**, 20130376 (2015).

24. Verma, D., Garg, P. K. & Dubey, A. K. Insights into the human oral microbiome. Arch. Microbiol. **200**, 525–540 (2018).

25. Wade, W. G. The oral microbiome in health and disease. Pharmacol. Res. **69**, 137–143 (2013).

26. Linossier, A., Gajardo, M. & Olavarria, J. Paleomicrobiological study in dental calculus: Streptococcus mutans. Scanning Microsc. **10**, 1005–13; discussion 1014 (1996).

27. Charlier, P. et al. The microscopic (optical and SEM) examination of dental calculus deposits (DCD). Potential interest in forensic anthropology of a bio-archaeological method. Leg. Med. **12**, 163–171 (2010).

28. Radini, A., Nikita, E., Buckley, S., Copeland, L. & Hardy, K. Beyond food: The multiple pathways for inclusion of materials into ancient dental calculus. Am. J. Phys. Anthropol. **162**, 71–83 (2017).

29. Henry, A. G., Brooks, A. S. & Piperno, D. R. Microfossils in calculus demonstrate consumption of plants and cooked foods in Neanderthal diets (Shanidar III, Iraq; Spy I and II, Belgium). Proc. Natl. Acad. Sci. **108**, 486–491 (2011).

30. Mickleburgh, H. L. & Pagán-Jiménez, J. R. New insights into the consumption of maize and other food plants in the pre-Columbian Caribbean from starch grains trapped in human dental calculus. J. Archaeol. Sci. **39**, 2468–2478 (2012).

31. Weyrich, L. S., Dobney, K. & Cooper, A. Ancient DNA analysis of dental calculus. J. Hum. Evol. **79**, 119–124 (2015).

32. Weyrich, L. S. et al. Neanderthal behaviour, diet, and disease inferred from ancient DNA in dental calculus. Nature **544**, 357–361 (2017).

33. Seitz, A. & Nieselt, K. Improving ancient DNA genome assembly. PeerJ **5**, e3126 (2017).

34. Escapa, I. F. et al. New Insights into Human Nostril Microbiome from the Expanded Human Oral Microbiome Database (eHOMD): a Resource for the Microbiome of the Human Aerodigestive Tract. mSystems **3**, (2018).

35. Frank, J. A. et al. Improved metagenome assemblies and taxonomic binning using long-read circular consensus sequence data. Sci. Rep. **6**, 25373 (2016).

36. Sanders, J. G. et al. Optimizing sequencing protocols for leaderboard metagenomics by combining long and short reads. Genome Biol. **20**, 226 (2019).

37. Cockburn, A. F. et al. High throughput DNA sequencing to detect differences in the subgingival plaque microbiome in elderly subjects with and without dementia. Investig. Genet. **3**, 19 (2012).

38. Parras-Moltó, M. & López-Bueno, A. Methods for Enrichment and Sequencing of Oral Viral Assemblages: Saliva, Oral Mucosa, and Dental Plaque Viromes. In The Human Virome: Methods and Protocols (eds. Moya, A. & Pérez Brocal, V.) 143–161 (Springer, 2018). Doi:10.1007/978-1-4939-8682-8_11.

39. Fagernäs, Z. et al. A unified protocol for simultaneous extraction of DNA and proteins from archaeological dental calculus. J. Archaeol. Sci. **118**, 105135 (2020).

40. Tabor, S., Struhl, K., Scharf, S. J. & Gelfand, D. H. DNA-dependent DNA polymerases. Curr. Protoc. Mol. Biol. **Chapter 3**, Unit3.5 (2001).

41. Green, M. R., Sambrook, J. & Sambrook, J. Molecular cloning: a laboratory manual. (Cold Spring Harbor Laboratory Press, 2012).

42. Segata, N. et al. Metagenomic microbial community profiling using unique clade-specific marker genes. Nat. Methods **9**, 811–814 (2012).

Additional Files

Additional File 1

Format: Word Document (*.docx)

Title: Supplementary Material

Description: Supplemental methods for the generation of high-molecular weight DNA datasets from modern dental calculus

Supplementary Material

High-molecular weight calculus DNA extraction protocol

Decalcification:

- Add 2-10mg of each sample to a 2µl LoBind along with tube with 700µl 0.5M EDTA
- Incubate at room temperature with constant rotation for ~48 hours
- Add 200µl 0.5M EDTA and 100µl 10mg/ml proteinase K for a total volume of 1000µl and incubate another 24 hours at room temperature with rotation

Extraction:

- Perform extraction using Qiagen High Molecular Weight MagAttract kits – scaled up from 200µl reaction to 2x 500µl reaction (extractions split into two tubes).
- Centrifuge samples 1400rpm for 2 minutes
- Add 500µl of supernatant to a new LoBind tube (2x per sample)
- Add 10µl of Rnase A
    - vortex and incubate at room temperature for 2 minutes
- Add 375ul buffer AL added
    - mix by pipetting
- Add 700µl buffer MB
- Add 100µl of well vortexed mag attract
- Incubate at 25°C and 1400rpm for 3 minutes
- Place in magnetic rack and allow 10 minutes to fully separate beads
- Remove supernatant
- Add 1750µl buffer MW1 and incubate at room temperature for 2 mins at 1400rpm
- Place in magnetic rack, allow 5 minutes for separation and remove supernatant

- Repeat wash
- Add 1750µl of buffer PE incubate, separate and remove supernatant as above (2x)
- While beads still bound to magnet: rinse with 1750µl H_2O, incubate for 1 minute, and remove supernatant
- Repeat water wash
- Remove from magnetic rack, add 50µl buffer AE (elution buffer) and incubate at room temperature for 3 minutes at 1400rpm
- Place in magnetic rack for 10 minutes
- Remove supernatant (extracted DNA) to new LoBind tube
- Repeat elution and combine eluates in single tube

Supplementary Table 1. Concentration (ng/µl) and total DNA (ng) recovered from each high-molecular weight DNA extraction

Sample:	Concentration (ng/µl)	Total DNA (ng) recovered
DAN045	40	4000
DAN028	36.4	3640
DAN044	26.2	2620
DAN048	20.8	2080
DAN046	19.9	1990
DAN049	15.6	1560
DAN024	13.8	1380
DAN039	10.6	1060
DAN038	9.12	912
DAN023	4.46	892
DAN025	10	1000
DAN034	8.02	802
DAN027	7.7	770
DAN035	6.56	656
DAN032	5.16	516
DAN031	4.42	442
DAN022	2.01	402
DAN037	3.72	372
DAN029	3.38	338
DAN033	3.3	330
DAN043	2.94	294
DAN047	2.94	294
DAN036	1.58	158
DAN026	0.758	75.8

Double-stranded Illumina library preparation:

Prepare blunt end repair assay [50 µl/rxn]

	stock concentration	*Final*	*Unit*	*1x Volume (µl)*
NEB Buffer 2	*10*	*1*	*x*	*5.00*
ATP	*10*	*1*	*mM*	*5.00*
BSA	*20*	*0.8*	*mg/ml*	*2.00*
dNTPs	*25*	*0.2*	*mM*	*0.40*
T4 PNK	*10*	*0.4*	*U*	*2.00*
T4 Polymerase	*3*	*0.024*	*U*	*0.40*
DNA or H2O				*20.00*
UV-Water				*15.20*
Assay total				*50.00*

• *Add 40µl mastermix and 10µl sample to each tube.*

• *Incubate at 15°C for 15 min, then at 25°C for 15 min.*

• *Purify with MinElute kit.*

• *Pre-heat EB containing 0,05% Tween to 50°C.*

• *Add 650 µl PB buffer to a new 1,5 ml LoBind tube and transfer the Blunt End Repair assay to the PB Puffer, vortex briefly.*

• *Load each reaction onto MinElute column and incubate for 1-2 minutes.*

• *Spin 30 sec at 13000 rpm and discard supernatant.*

• *Add 700 µl PE buffer.*

• *Spin 30 sec at 13000 rpm and discard supernatant.*

• *Dry spin for 1 min at 13000 rpm.*

• *Flip columns 180° and spin again for 1 min at 13000 rpm.*

• *Put column in new 1.5 ml LoBind tube.*

• *Elute in 20 µl EB containing 0.05% Tween, let stand for 1 min, then spin 1 min at 13000 rpm.*

Prepare adapter ligation assay [40 µl/rxn]:

	stock concentration	final	unit	1x Volume (µl)
Quick Ligase Buffer	2	1	x	20.00
Adapter Mix	10	0.25	µM	1.00
DNA or H2O				18.00
Assay total				39.00

• *Add 21 µl of mastermix and the complete eluate from the last step (~18 µl) to each tube.*

• *Add 1 µl of Quick ligase (5 U stock, 0.125 U final) to each library (mix by pipetting).*

• *Incubate at 22°C for 20 min.*

• *Purfiy with MinElute kit.*

• *Pre-heat EB containing 0.05% Tween to 50°C*

• *Add 650 µl PB buffer to a new 1.5 ml LoBind tube and transfer the Blunt End Repair assay to the PB Puffer, vortex briefly.*

• *Load each reaction onto MinElute column and incubate for 1-2 minutes.*

• *Spin 30 sec at 13000 rpm and discard supernatant.*

• *Add 700 µl PE buffer.*

• *Spin 30 sec at 13000 rpm and discard supernatant.*

• *Dry spin for 1 min at 13000 rpm.*

• *Flip columns 180° and spin again for 1 min at 13000 rpm.*

• *Put column in new 1.5 ml LoBind tube.*

• *Elute in 22 µl EB containing 0.05% Tween, let stand for 1 min, then spin 1 min at 13000 rpm.*

Prepare adapter fill in assay [40 µl/rxn]:

	stock concentration	final	unit	1x Volume (µl)
Thermopol Buffer	10	1	x	4.00
dNTPs	25	0.25	mM	0.40
Bst Polymerase	8	0.4	U	2.00
DNA or H2O				20.00
UV-Water				13.60
Assay total				40.00

• *Add 20 µl of mastermix and to the complete eluate from the last step.*

• *Incubate at 37°C for 30 min then 80°C for 10 min.*

• *Freeze at -20°C without purification.*

Library indexing protocol:

Prepare indexing assay [100 µl/rxn]:

	stock concentration	final	unit	1x Volume (µl)
Pfu Turbo Buffer	10	1	N/A	10.00
BSA	20	0.3	mg/ml	1.50
dNTPs	25	5	mM	3
DMSO		3	v/v%	3
Pfu Turbo Polymerase	2.5	0.05	U	2.00
P5 index	10	0.2	µM	2.00
P7 index	10	0.2	µM	2.00
DNA or H_2O	*(Calculate to 1.5x10^8 molecules input from qPCR of unindexed library)*			
UV treated H_2O				to 100µl
Assay total				100µl

Run assay in thermocycler with the following program:

Initial denaturing: 2 minutes at 95ºC

10x

1 minute at 98ºC

30 seconds at 58ºC

90 seconds at 72ºC

followed by: 10 minutes at 72ºC

Clean-up reaction using Ampure beads for left-right size selection (0.45 ratio followed by 0.75 ratio)

Dilute to 10nM for sequencing.

7. Discussion

The generation of aDNA datasets requires the destructive sampling of irreplaceable anthropological remains. Simultaneously, advances in next generation sequencing technology along with the introduction of targeted amplification of whole genomic DNA have greatly advanced the field of archaeogenetics in terms of both popularity and the demand for the destructive sampling. As these remains are often of considerable historical, archaeological, and cultural importance, the need to balance research into ancient genetics with the preservation of the anthropological record has, consequently, become a serious concern. To alleviate these concerns, it is increasingly imperative that researchers strive to develop more efficient, optimized, methodologies for both the generation and use of ancient genetic data obtained through destructive sampling.

6.1 The first systematic analyses of DNA preservation across historical skeletal elements

In Manuscript 1, we conduct the first, large-scale, systematic investigation of human DNA preservation across ancient (medieval) skeletal elements. By examining not only a wide range of potential sampling locations, but also several diagnostic metrics important for the successful downstream use of DNA isolated from destructive sampling across each sampling location we are able to confidently put forward seven aDNA sampling locations across four skeletal elements as potential alternatives to the destructive sampling of the petrous portion. While the petrous portion has been repeatedly shown, through both comparative studies and more generally through the numerous archaeogenetic studies which have utilized this sampling strategy, to be an excellent source of ancient DNA, we posit that under standard laboratory conditions (e.g., not sequencing to exhaustion for purposes such as whole genome assembly) sampling from the cementum, dentin, and dental pulp chamber of *in situ* teeth, as well as sampling from cortical bone stemming from the,superior vertebral arch, vertebral body, talus,

and distal phalanx is very likely to yield more than adequate human DNA for reliable use in the vast majority of population genetics analyses. Additionally, we find the teeth and vertebrae particularly well suited for analyses as they offer not only multiple high-yielding sampling locations per single instance of each element, but also have been shown to potentially harbour pathogen DNA (Schuenemann et al. 2011; 2011; Bos et al. 2011; 2014; Taylor et al. 1999), providing a more complete anthropological picture of a given site.

6.1.1 Challenges in assessing DNA preservation across skeletal elements

There are numerous factors influencing the analyses of host DNA retention in archaeological skeletal elements. First and foremost are the effects of different environmental effects of gross DNA preservation including the thermal age of a sample, soil condition, handling practices associated with burial (Collins et al. 2002; Smith et al. 2003), and potential contamination during recovery or processing of samples (Skoglund et al. 2014). Additionally, aside from a handful of well-studied sampling locations (e.g., the petrous pyramid, femora, and dentin), there are very few optimized DNA sampling protocols in publication for the majority of ancient human skeletal elements. This makes the exploration of potential differences in DNA preservation across skeletal elements more challenging, as ensuring that different studies are using comparable methods is not always possible. In Manuscript 1 we seek to mitigate any potential sources of variation in DNA preservation not associated with variance between sampling locations by restricting our sampling to skeletal elements gathered from contemporary individuals excavated from a single site and all exhibiting similar levels of morphological preservation. In addition, in Manuscript 2 we provide the fully detailed and optimized bone-powder generation methods for all the top performing sampling locations in Manuscript 1 in both written and video formats. The separate publication of these methods, in video format,

make protocols widely accessible and easily replicated throughout the aDNA and forensic communities.

6.1.2 DNA preservation in the petrous in comparison to other sampling locations

Very few systematic explorations of DNA retention across skeletal elements have been performed to date. The first such study to highlight the use of the petrous pyramid in ancient DNA research, Gamba *et al* 2014, was not, in fact a targeted study of DNA preservation across skeletal elements, but rather a population genetics study. As such, they examined just seven potential sampling locations across four skeletal elements (one metacarpal, one metatarsal, dentin from the roots and crowns of three molars, two rib fragments, seven petrous pyramids, and one portion of the surrounding temporal bone) across seven individuals, with the petrous pyramid being found to outperform all other sampling locations in terms of proportion of endogenous DNA recovered. While still a ground-breaking study which helped to elucidate the vast variation in DNA retention between skeletal elements, the low sample sizes for each selected sampling location make any meaningful statistical analyses challenging at best. Conversely, the first targeted study to show the utility of the petrous pyramid in comparison to other skeletal elements, Hansen *et al* 2017, examined the cementum of teeth (n=27), parietal bones (n=9), and cochlear region of the petrous pyramid (n=27) across twenty-seven individuals from the Bronze Age (n=6), Viking (n=11), and Historical (n=10) periods. The findings of this study indicate that, while the petrous pyramid has a higher overall proportion of human DNA recovered across all samples, when the petrous and teeth are both well preserved the cementum and dense cochlear region of the petrous pyramid perform equally well. The fact that both sampling locations are observed to have high utility indicates that a more thorough study including more sampling locations would be highly beneficial to our understanding of differential DNA preservation. Similarly, the more recent Sirak et al. 2020 study examined the

cochlear portion and ossicles recovered from ten individuals found no significant differences in human DNA proportions or library complexity between the two sampling locations, again indicating that the cochlear portion of the petrous pyramid is not unique in exhibiting potentially excellent DNA preservation in archaeological remains.

In Manuscript 1 we examine DNA recovery across a total of 23 sampling sites stemming from ten skeletal elements recovered from eleven contemporary individuals for a total of 247 sampling effort, making this the largest, most systematic investigation of DNA retention in archaeological remains to date. We report best performance in the dense cochlear portion of the petrous pyramid in comparison to 22 other sampling locations in terms of DNA recovery. However, when we further analyse these results in terms of standard practices (e.g., standard sequencing depths, capture-enrichment, and Y-haplogrouping) we find no difference in utility between the petrous pyramid; cortical bone from the distal phalanx; cementum, dentin, and material from the pulp chamber of the molar; cortical bone from the body and superior vertebral arch of the thoracic vertebrae; or dense material collected from the exterior of the talus.

6.1.3 Ethical issues surrounding the use of the petrous pyramid

The dense cochlear region of the petrous pyramid has been shown on numerous occasions to be an excellent source of endogenous human DNA from archaeological remains. As such, researchers have systematically targeted this sampling area for use in ancient population genetics studies. The increased demand for sampling of the petrous pyramid for use in ancient DNA analyses coupled with the particularly destructive nature of DNA sampling from this element and the petrous pyramid's widespread use in morphological and radio isotope studies has led to increasingly intense ethical debates over the utility its use (Prendergast and Sawchuk 2018; Booth 2019; Lewis-Kraus 2019; K. A. Sirak and Sedig 2019; Charlton, Booth,

and Barnes 2020). As such, it is imperative that alternative sampling locations be evaluated for their potential uses in the field.

Of the previously mentioned comparative studies, both Hansen *et al* 2014 and Sirak *et al* 2020 put forth potential alternative sampling sites based on a limited comparison of the petrous pyramid to a single, alternate, source (cementum and ossicles respectively). Additionally, the rarity of ossicle recovery in conjunction with their morphological importance makes the viability of ossicle sampling questionable in the case of Sirak et al. 2020. The fact that equally useful, alternative sampling locations can be found during the process of such limited study clearly indicates the need for broader, more in-depth comparative studies to aid ancient DNA researchers in the development of ethical sampling strategies tailored to each site of interest. Our findings in Manuscript 1 further this goal by not only further reinforcing the utility of cementum as an alternative to petrous sampling, but also elucidating 6 more potential sampling locations: dentin; material from the pulp chamber; and dense cortical bone from the exterior of the distal phalanx, talus, vertebral body, and superior vertebral arch.

6.1.4 Future directions

As previously mentioned, the myriad of variables influencing DNA preservation in archaeological remains as well as the numerous possible sampling locations to potentially be examined, means that no single study of differential DNA preservation across skeletal elements can reasonably be expected to be representative in the context of suggested sampling strategies for the aDNA analyses of all sites across all time periods. Instead, multiple studies across archaeological sites representative of different periods and climates, each encompassing as many skeletal elements and potential sampling locations as possible, are necessary to generate comprehensive sampling strategies for the ethical analyses of aDNA across a wide range of conditions. In addition, it is imperative that the methods used in these studies be

made widely accessible to not only ensure the comparability of results, but also make aDNA analyses a more feasible prospect in as many laboratories as possible. In Manuscripts A and B we seek to further this aim by providing a baseline of suggested sampling strategies and methods for the eight best performing sampling locations (out of 23 examined) from our investigation of differential DNA preservation in a representative temperate, medieval site.

6.2 Making the most out of destructive sampling during analyses

6.2.1 The utility of combined analyses in palaeopopulation genetics and pathogen screening

The majority of palaeopathogenomics and ancient microbiome studies do not generally report on the population genetics of a site. This is particularly true of pathogen screening, where it is common practice to target potential ancient pathogen DNA via sampling of the teeth (particularly of the dental pulp chamber) (Margaryan et al. 2018) or skeletal elements where pathology may be evident (Bos et al. 2014; Schuenemann et al. 2013) stemming from sites where historical or contextual evidence of infectious disease are clearly present (Wagner et al. 2014; Bos et al. 2016). Often, the skeletal elements used in these studies are seen to be of generally lesser value in terms of endogenous host DNA recovery, and as such if the host DNA is analysed it all, it is often done so through the sampling of "more optimal" sampling locations such as the dense cochlear region of the petrous pyramid should it be deemed of particular interest (e.g., Klunk 2019). Similarly, as the petrous pyramid has been shown to be a particularly poor source of ancient pathogen or microbiome DNA (Margaryan et al. 2018), population genetic investigations utilizing the petrous pyramid as the primary source of ancient DNA at sites without *a priori* evidence of infectious disease are often uninformative in terms of endogenous microbial content. As such, successful pathogen screening of these sites may require

further destructive sampling of archaeological remains if the ancient microbial community is to be examined. As a result, not only does aDNA sampling using sources either known to be poor in microbial content or solely screening sites for pathogens alone provide only a small part of the overall genetic story offered by the aDNA analyses of ancient remains but also contributes to the ethical dilemmas surrounding destructive sampling of aDNA analyses by not utilizing the full potential of the remains available.

These practices remain common, despite examples such as the famously successful discovery of ancient *Y. pestis* from Bronze and Iron Age samples from sites with no *a priori* evidence of plague (Rasmussen et al. 2015; Andrades Valtueña et al. 2017; Spyrou et al. 2018). In Manuscript 3 we report yet another example of the utility of combined analyses by presenting another example of plague detection in remains lacking pathological or contextual evidence of epidemic. We do so by detailing a novel post-Black Death, Second Pandemic *Y. pestis* genome discovered via the routine screening of the samples examined for the purposes of evaluating differential host DNA preservation across ancient skeletal elements in Manuscripts A and B. Furthermore, in conjunction with Manuscript 1's findings that the dental pulp chamber and two separate sampling locations on the vertebrae (cortical bone stemming from exterior the vertebral body and from the superior vertebral arch) can reliably provide levels of endogenous host DNA recovery adequate for most population genetic studies, we argue that combined analyses using genomic datasets generated from a wider variety of skeletal elements is an ethically sound strategy for providing a more complete genetic picture of a historical site.

6.2.2 Expanding the oral microbiome reference dataset.

In conjunction with the advances to ancient genetic studies brought about through the introduction of next generation sequencing, subsequent advances in metagenomic analyses of have made investigations into the evolution of the human microbiome more feasible (Herbig et al. 2016; Key et al. 2017; Seitz and Nieselt 2017). This is especially true of the oral and gut microbiomes, where the flora of each has been shown to be excellently preserved in mummified remains (Herbig et al. 2016; Maixner et al. 2016), coprolites (Iñiguez et al. 2003, Tito et al. 2012, Appelt et al. 2014), teeth, and ancient dental calculus (C. Warinner 2016). One challenge in the reconstruction of ancient microbiomes, however, is the significant gaps in reference material available for comparison.

This dearth of reference data stems from the inherent challenges associated with metagenomic genome assembly. Typically, high quality microbial reference genomes are assembled from isolated cultures of a single microbial source. However, a third of the human oral microbiome remains unculturable (Escapa et al. 2018), making assembly from isolated sources impossible. Studies of metagenomic assembly have suggested that using a mixture of long-read (e.g., Oxford nanopore, Hi-C, PacBio, etc) and short-read (e.g., Illumina) sequencing can greatly increase the quality and quantity of genomes assembled in this context (Seitz and Nieselt 2017; Sanders et al. 2019). Long-read sequencing can be challenging, as it requires high molecular weight DNA (often lost or explicitly excluded in most protocols geared towards the more popular short-read platforms) for input. While short-read sequencing of dental calculus has been used in both modern and ancient contexts extensively, no published study has, to date, attempted to evaluate the possibility of extracting high molecular weight, metagenomic DNA from this valuable substrate. As dental calculus (as previously discussed) has been observed to be an excellent source of oral microbiome flora DNA and contain only a

limited amount of host DNA (Mann et al. 2018), it is therefore of great value develop appropriate protocols for the extraction of metagenomic high molecular weight DNA to aid in the generation of new reference genomes.

In Manuscript 4 we develop and test a method for the extraction of high molecular weight DNA from modern dental calculus using an optimized Qiagen MagAttract™ High Molecular Weight Kit protocol. We find that this protocol provides for the recovery of high concentrations of DNA >12kbp from dental calculus. Furthermore, we successfully mapped this DNA to known members of the human oral microbiome community after sequencing,

6.2.3 Future directions

Despite the success of this experimental procedure, it remains untested in terms of its use in in long-read, metagenomic sequencing. As such, this should be addressed in future work before this protocol can be used in the generation of more robust metagenomic assemblies generated from the oral microflora within dental calculus.

6.3 Conclusions

Each time we sample from the archaeological record for the purposes of aDNA analyses we damage a small portion of it. As such, it is imperative that we make the best possible use of these remains to not only increase the chances of successful investigation, but also to minimize the waste of finite, culturally important, resources. Throughout the work presented in this thesis we take steps to mitigate the impact of destructive DNA sampling on the archaeological record by: A.) Systematically examining a broad range of anatomical sampling locations to build a framework by which researchers can employ less destructive and more efficient sampling strategies; B). Make the detailed methods necessary to sample from the most efficient anatomical sampling locations more widely available more and presented in a clear,

easy to follow format; C). Demonstrate the utility of combined analyses methods in producing a wider range of subjects available using destructive sampling; and D). Proving novel methods of DNA extraction to expand the reference datasets available to researchers. Finally, we propose that before researchers begin projects involving destructive sampling, they first ask the following questions:

1). *Of the elements available for sampling at a given site, which ones best suit the scale and scope of my project?* For example, if attempting to fully reconstruct high-coverage host genomes of a small cohort of individuals, sampling from the dense cochlear region of the petrous portion may be the best strategy, despite the inherent lack of supporting microbial DNA. However, if generating robust population genetics statistics for a larger sub-set of a population is the goal, sampling from alternative skeletal elements such as teeth can not only provide the necessary host SNP coverage necessary, but also allow for insights into the general health of the targeted population.

2). *How can I best use the data generated to fully explore the dynamics within the targeted site?* More inclusive screening techniques including combined analyses of population genetics and pathogen screening across a broader range of skeletal elements may increase the ability of a research project to more fully describe the dynamics within a site.

And 3). *Is the reference database necessary for this investigation robust enough to make the destruction of archaeological remains worthwhile?* If significant gaps are present, it may be more feasible to first attempt to fill those gaps using less valuable samples before proceeding.

7. References

Aberth, J. (2005). Introduction: The Black Death in History. In J. Aberth (Ed.), *The Black Death: The Great Mortality of 1348–1350: A Brief History with Documents* (pp. 1–7). Palgrave Macmillan US. https://doi.org/10.1007/978-1-137-10349-9_1

Adler, C. J., Haak, W., Donlon, D., & Cooper, A. (2011). Survival and recovery of DNA from ancient teeth and bones. *Journal of Archaeological Science*, *38*(5), 956–964. https://doi.org/10.1016/j.jas.2010.11.010

Alberti, F., Gonzalez, J., Paijmans, J. L. A., Basler, N., Preick, M., Henneberger, K., Trinks, A., Rabeder, G., Conard, N. J., Münzel, S. C., Joger, U., Fritsch, G., Hildebrandt, T., Hofreiter, M., & Barlow, A. (2018). Optimized DNA sampling of ancient bones using Computed Tomography scans. *Molecular Ecology Resources*, *18*(6), 1196–1208. https://doi.org/10.1111/1755-0998.12911

Andrades Valtueña, A., Mittnik, A., Key, F. M., Haak, W., Allmäe, R., Belinskij, A., Daubaras, M., Feldman, M., Jankauskas, R., Janković, I., Massy, K., Novak, M., Pfrengle, S., Reinhold, S., Šlaus, M., Spyrou, M. A., Szécsényi-Nagy, A., Tõrv, M., Hansen, S., … Krause, J. (2017, May 17). *The Stone Age Plague: 1000 years of Persistence in Eurasia* [Doc-type:workingPaper]. https://doi.org/10.1101/094243

Barker, H. (2021). Laying the Corpses to Rest: Grain, Embargoes, and *Yersinia pestis* in the Black Sea, 1346–48. *Speculum*, *96*(1), 97–126. https://doi.org/10.1086/711596

Bar-Oz, G., & Dayan, T. (2007). FOCUS: On the use of the petrous bone for estimating cranial abundance in fossil assemblages. *Journal of Archaeological Science*, *34*(9), 1356–1360. https://doi.org/10.1016/j.jas.2006.10.021

Basler, N., Xenikoudakis, G., Westbury, M. V., Song, L., Sheng, G., & Barlow, A. (2017). Reduction of the contaminant fraction of DNA obtained from an ancient giant panda bone. *BMC Research Notes*, *10*, 754. https://doi.org/10.1186/s13104-017-3061-3

Bellemain, E., Davey, M. L., Kauserud, H., Epp, L. S., Boessenkool, S., Coissac, E., Geml, J., Edwards, M., Willerslev, E., Gussarova, G., Taberlet, P., & Brochmann, C. (2013). Fungal palaeodiversity revealed using high-throughput metabarcoding of ancient DNA from arctic permafrost. *Environmental Microbiology*, *15*(4), 1176–1189. https://doi.org/10.1111/1462-2920.12020

Beniash, E., Stifler, C. A., Sun, C.-Y., Jung, G. S., Qin, Z., Buehler, M. J., & Gilbert, P. U. P. A. (2019). The hidden structure of human enamel. *Nature Communications*, *10*(1), 4383. https://doi.org/10.1038/s41467-019-12185-7

Boessenkool, S., Hanghøj, K., Nistelberger, H. M., Sarkissian, C. D., Gondek, A. T., Orlando, L., Barrett, J. H., & Star, B. (2017). Combining bleach and mild predigestion improves ancient DNA recovery from bones. *Molecular Ecology Resources*, *17*(4), 742–751. https://doi.org/10.1111/1755-0998.12623

Booth, T. J. (2019). A stranger in a strange land: A perspective on archaeological responses to the palaeogenetic revolution from an archaeologist working amongst palaeogeneticists. *World Archaeology*, *0*(0), 1–16. https://doi.org/10.1080/00438243.2019.1627240

Bos, K. I., Harkins, K. M., Herbig, A., Coscolla, M., Weber, N., Comas, I., Forrest, S. A., Bryant, J. M., Harris, S. R., Schuenemann, V. J., Campbell, T. J., Majander, K., Wilbur, A. K., Guichon, R. A., Wolfe Steadman, D. L., Cook, D. C., Niemann, S., Behr, M. A., Zumarraga, M., … Krause, J. (2014). Pre-Columbian mycobacterial genomes reveal seals as a source of New World human tuberculosis. *Nature*, *514*(7523), 494–497. https://doi.org/10.1038/nature13591

Bos, K. I., Herbig, A., Sahl, J., Waglechner, N., Fourment, M., Forrest, S. A., Klunk, J., Schuenemann, V. J., Poinar, D., Kuch, M., Golding, G. B., Dutour, O., Keim, P., Wagner, D. M., Holmes, E. C., Krause, J., & Poinar, H. N. (2016). Eighteenth century Yersinia pestis genomes reveal the long-term persistence of an historical plague focus. *ELife*, *5*, e12994. https://doi.org/10.7554/eLife.12994

Bos, K. I., Schuenemann, V. J., Golding, G. B., Burbano, H. A., Waglechner, N., Coombes, B. K., McPhee, J. B., DeWitte, S. N., Meyer, M., Schmedes, S., Wood, J., Earn, D. J. D., Herring, D. A., Bauer, P., Poinar, H. N., & Krause, J. (2011). A draft genome of Yersinia pestis from victims of the Black Death. *Nature*, *478*(7370), 506–510. https://doi.org/10.1038/nature10549

Bos, K. I., Stevens, P., Nieselt, K., Poinar, H. N., DeWitte, S. N., & Krause, J. (2012). Yersinia pestis: New Evidence for an Old Infection. *PLOS ONE*, *7*(11), e49803. https://doi.org/10.1371/journal.pone.0049803

Boskey, A. L. (1992). Mineral-matrix interactions in bone and cartilage. *Clinical Orthopaedics and Related Research*, *281*, 244–274.

Bramanti, B., Dean, K. R., Walløe, L., & Chr. Stenseth, N. (2019). The Third Plague Pandemic in Europe. *Proceedings of the Royal Society B: Biological Sciences*, *286*(1901). https://doi.org/10.1098/rspb.2018.2429

Brandt, G., Haak, W., Adler, C. J., Roth, C., Szécsényi-Nagy, A., Karimnia, S., Möller-Rieker, S., Meller, H., Ganslmeier, R., Friederich, S., Dresely, V., Nicklisch, N., Pickrell, J. K., Sirocko, F., Reich, D., Cooper, A., Alt, K. W., & Consortium, T. G. (2013). Ancient DNA Reveals Key Stages in the Formation of Central European Mitochondrial Genetic Diversity. *Science*, *342*(6155), 257–261. https://doi.org/10.1126/science.1241844

Briggs, A. W., Good, J. M., Green, R. E., Krause, J., Maricic, T., Stenzel, U., Lalueza-Fox, C., Rudan, P., Brajkovic, D., Kucan, Z., Gusic, I., Schmitz, R., Doronichev, V. B., Golovanova, L. V., de la Rasilla, M., Fortea, J., Rosas, A., & Pääbo, S. (2009). Targeted retrieval and analysis of five Neandertal mtDNA genomes. *Science (New York, N.Y.)*, *325*(5938), 318–321. https://doi.org/10.1126/science.1174462

Briggs, A. W., Stenzel, U., Johnson, P. L. F., Green, R. E., Kelso, J., Prüfer, K., Meyer, M., Krause, J., Ronan, M. T., Lachmann, M., & Pääbo, S. (2007). Patterns of damage in genomic DNA sequences from a Neandertal. *Proceedings of the National Academy of Sciences*, *104*(37), 14616–14621. https://doi.org/10.1073/pnas.0704665104

Briggs, A. W., Stenzel, U., Meyer, M., Krause, J., Kircher, M., & Pääbo, S. (2010). Removal of deaminated cytosines and detection of in vivo methylation in ancient DNA. *Nucleic Acids Research*, *38*(6), e87. https://doi.org/10.1093/nar/gkp1163

Brooks, M. E., Kristensen, K., Benthem, K. J. van, Magnusson, A., Berg, C. W., Nielsen, A., Skaug, H. J., Mächler, M., & Bolker, B. M. (2017). GlmmTMB Balances Speed and Flexibility Among Packages for Zero-inflated Generalized Linear Mixed Modeling. *The R Journal*, *9*(2), 378–400.

Brosset, M.-F. (2018). *Histoire de la Géorgie Depuis l'Antiquité Jusqu'au Xixe Siècle, Vol. 1: Histoire Ancienne, Jusqu'en 1469 de J.-C*. Forgotten Books.

Brotherton, P., Endicott, P., Sanchez, J. J., Beaumont, M., Barnett, R., Austin, J., & Cooper, A. (2007). Novel high-resolution characterization of ancient DNA reveals C > U-type base modification events as the sole cause of post mortem miscoding lesions. *Nucleic Acids Research*, *35*(17), 5717–5728. https://doi.org/10.1093/nar/gkm588

Broushaki, F., Thomas, M. G., Link, V., López, S., van Dorp, L., Kirsanow, K., Hofmanová, Z., Diekmann, Y., Cassidy, L. M., Díez-del-Molino, D., Kousathanas, A., Sell, C., Robson, H. K., Martiniano, R., Blöcher, J., Scheu, A., Kreutzer, S., Bollongino, R., Bobo, D., … Burger, J. (2016). Early Neolithic genomes from the eastern Fertile Crescent. *Science*, *353*(6298), 499. https://doi.org/10.1126/science.aaf7943

Bruns, F., & Weczerka, H. (n.d.). *Hansische Handelsstrassen. Textband. Weimar: Böhlau Verlag; 1967*.

Burrell, A. S., Disotell, T. R., & Bergey, C. M. (2015). The use of museum specimens with high-throughput DNA sequencers. *Journal of Human Evolution*, *79*, 35–44. https://doi.org/10.1016/j.jhevol.2014.10.015

Cafiero, C., Re, A., Stigliano, E., Bassotti, E., Moroni, R., & Grippaudo, C. (2019). Optimization of DNA extraction from dental remains. *ELECTROPHORESIS*, *40*(14), 1820–1823. https://doi.org/10.1002/elps.201900142

Campos, P. F., Craig, O. E., Turner-Walker, G., Peacock, E., Willerslev, E., & Gilbert, M. T. P. (2012). DNA in ancient bone – Where is it located and how should we extract it? *Annals of Anatomy - Anatomischer Anzeiger*, *194*(1), 7–16. https://doi.org/10.1016/j.aanat.2011.07.003

Carmichael, A. (2015). Plague persistence in western Europe: A hypothesis. In *Pandemic Disease in the Medieval World: Rethinking the Black Death* (pp. 157–191). Arc Humanities Press.

Cesana, D., Benedictow, O. J., & Bianucci, R. (2017). The origin and early spread of the Black Death in Italy: First evidence of plague victims from 14th-century Liguria (northern Italy). *Anthropological Science*, *125*(1), 15–24. https://doi.org/10.1537/ase.161011

Charlier, P., Huynh-Charlier, I., Munoz, O., Billard, M., Brun, L., & Grandmaison, G. L. de la. (2010). The microscopic (optical and SEM) examination of dental calculus deposits (DCD). Potential interest in forensic anthropology of a bio-archaeological method. *Legal Medicine*, *12*(4), 163–171. https://doi.org/10.1016/j.legalmed.2010.03.003

Charlton, S., Booth, T., & Barnes, I. (2020). The problem with petrous? A consideration of the potential biases in the utilization of pars petrosa for ancient DNA analysis. *World Archaeology*, *0*(0), 1–12. https://doi.org/10.1080/00438243.2019.1694062

Cingolani, P., Platts, A., Wang, L. L., Coon, M., Nguyen, T., Wang, L., Land, S. J., Lu, X., & Ruden, D. M. (2012). A program for annotating and predicting the effects of single nucleotide polymorphisms, SnpEff. *Fly*, *6*(2), 80–92. https://doi.org/10.4161/fly.19695

Clementz, M. T. (2012). New insight from old bones: Stable isotope analysis of fossil mammals. *Journal of Mammalogy*, *93*(2), 368–380. https://doi.org/10.1644/11-MAMM-S-179.1

Clouse, M. (2002). The Black Death Transformed: Disease and Culture in Early Renaissance Europe.Samuel K Cohn Jr. London and New York: Arnold and Oxford University Press, 2002, pp. 318, US$65.00 (HB) ISBN: 0-340-70646-5. *International Journal of Epidemiology*, *31*(6), 1280–1281. https://doi.org/10.1093/ije/31.6.1280

Cockburn, A. F., Dehlin, J. M., Ngan, T., Crout, R., Boskovic, G., Denvir, J., Primerano, D., Plassman, B. L., Wu, B., & Cuff, C. F. (2012). High throughput DNA sequencing to detect differences in the subgingival plaque microbiome in elderly subjects with and without dementia. *Investigative Genetics*, *3*(1), 19. https://doi.org/10.1186/2041-2223-3-19

Collins, M. J., Nielsen–Marsh, C. M., Hiller, J., Smith, C. I., Roberts, J. P., Prigodich, R. V., Wess, T. J., Csapò, J., Millard, A. R., & Turner–Walker, G. (2002). The survival of organic matter in bone: A review. *Archaeometry*, *44*(3), 383–394. https://doi.org/10.1111/1475-4754.t01-1-00071

Cooper, A., & Poinar, H. N. (2000). Ancient DNA: Do It Right or Not at All. *Science*, *289*(5482), 1139–
1139. https://doi.org/10.1126/science.289.5482.1139b

Coulson-Thomas, Y. M., Norton, A. L., Coulson-Thomas, V. J., Florencio-Silva, R., Ali, N., Elmrghni, S., Gil, C. D., Sasso, G. R. S., Dixon, R. A., & Nader, H. B. (2015). DNA and bone structure preservation in medieval human skeletons. *Forensic Science International*, *251*, 186–194. https://doi.org/10.1016/j.forsciint.2015.04.005

Cruz-Dávalos, D. I., Llamas, B., Gaunitz, C., Fages, A., Gamba, C., Soubrier, J., Librado, P., Seguin-Orlando, A., Pruvost, M., Alfarhan, A. H., Alquraishi, S. A., Al-Rasheid, K. A. S., Scheu, A., Beneke, N., Ludwig, A., Cooper, A., Willerslev, E., & Orlando, L. (2017). Experimental conditions improving in-solution target enrichment for ancient DNA. *Molecular Ecology Resources*, *17*(3), 508–522. https://doi.org/10.1111/1755-0998.12595

Curtis, D. R., & Roosen, J. (2017). The sex-selective impact of the Black Death and recurring plagues in the Southern Netherlands, 1349–1450. *American Journal of Physical Anthropology*, *164*(2), 246–259. https://doi.org/10.1002/ajpa.23266

Dabney, J., & Meyer, M. (2019). Extraction of Highly Degraded DNA from Ancient Bones and Teeth. In B. Shapiro, A. Barlow, P. D. Heintzman, M. Hofreiter, J. L. A. Paijmans, & A. E. R. Soares (Eds.), *Ancient DNA: Methods and Protocols* (pp. 25–29). Springer. https://doi.org/10.1007/978-1-4939-9176-1_4

Dabney, J., Meyer, M., & Pääbo, S. (2013). Ancient DNA Damage. *Cold Spring Harbor Perspectives in Biology*, *5*(7). https://doi.org/10.1101/cshperspect.a012567

Dadoyan, S. B. (n.d.). Samuēl Anetsʻi ew sharunakoghner—Zhamanakagrutʻiwn Adamitsʻ minchʻew 1776. In *Christian-Muslim Relations 1500—1900*. Brill. Retrieved September 20, 2021, from https://referenceworks.brillonline.com/entries/christian-muslim-relations-ii/samuel-anetsi-ew-sharunakoghner-zhamanakagrutiwn-adamits-minchew-1776-COM_31368

Damgaard, P. B., Margaryan, A., Schroeder, H., Orlando, L., Willerslev, E., & Allentoft, M. E. (2015). Improving access to endogenous DNA in ancient bones and teeth. *Scientific Reports*, *5*(1), 1–12. https://doi.org/10.1038/srep11184

Dehasque, M., Ávila-Arcos, M. C., Díez-del-Molino, D., Fumagalli, M., Guschanski, K., Lorenzen, E. D., Malaspinas, A.-S., Marques-Bonet, T., Martin, M. D., Murray, G. G. R., Papadopulos, A. S. T., Therkildsen, N. O., Wegmann, D., Dalén, L., & Foote, A. D. (2020). Inference of natural selection from ancient DNA. *Evolution Letters*, *4*(2), 94–108. https://doi.org/10.1002/evl3.165

Der Sarkissian, C., Allentoft, M. E., Ávila-Arcos, M. C., Barnett, R., Campos, P. F., Cappellini, E., Ermini, L., Fernández, R., da Fonseca, R., Ginolhac, A., Hansen, A. J., Jónsson, H., Korneliussen, T., Margaryan, A., Martin, M. D., Moreno-Mayar, J. V., Raghavan, M., Rasmussen, M., Velasco, M. S., … Orlando, L. (2015). Ancient genomics. *Philosophical Transactions of the Royal Society B: Biological Sciences*, *370*(1660), 20130387. https://doi.org/10.1098/rstb.2013.0387

DeWitte, S. N. (2014). Mortality Risk and Survival in the Aftermath of the Medieval Black Death. *PLoS ONE*, *9*(5). https://doi.org/10.1371/journal.pone.0096513

Donoghue, H. D., Spigelman, M., O'Grady, J., Szikossy, I., Pap, I., Lee, O. Y.-C., Wu, H. H. T., Besra, G. S., & Minnikin, D. E. (2015). Ancient DNA analysis – An established technique in charting the evolution of tuberculosis and leprosy. *Tuberculosis*, *95*, S140–S144. https://doi.org/10.1016/j.tube.2015.02.020

Drancourt, M., Aboudharam, G., Signoli, M., Dutour, O., & Raoult, D. (1998). Detection of 400-year-old Yersinia pestis DNA in human dental pulp: An approach to the diagnosis of ancient septicemia. *Proceedings of the National Academy of Sciences*, *95*(21), 12637–12640. https://doi.org/10.1073/pnas.95.21.12637

Eppinger, M., Worsham, P. L., Nikolich, M. P., Riley, D. R., Sebastian, Y., Mou, S., Achtman, M., Lindler, L. E., & Ravel, J. (2010). Genome Sequence of the Deep-Rooted Yersinia pestis Strain Angola Reveals New Insights into the Evolution and Pangenome of the Plague Bacterium. *Journal of Bacteriology*, *192*(6), 1685–1699. https://doi.org/10.1128/JB.01518-09

Ermini, L., Der Sarkissian, C., Willerslev, E., & Orlando, L. (2015). Major transitions in human evolution revisited: A tribute to ancient DNA. *Journal of Human Evolution*, *79*, 4–20. https://doi.org/10.1016/j.jhevol.2014.06.015

Escapa, I. F., Chen, T., Huang, Y., Gajare, P., Dewhirst, F. E., & Lemon, K. P. (2018). New Insights into Human Nostril Microbiome from the Expanded Human Oral Microbiome Database (eHOMD): A Resource for the Microbiome of the Human Aerodigestive Tract. *MSystems*, *3*(6). https://doi.org/10.1128/mSystems.00187-18

Fagernäs, Z., García-Collado, M. I., Hendy, J., Hofman, C. A., Speller, C., Velsko, I., & Warinner, C. (2020). A unified protocol for simultaneous extraction of DNA and proteins from archaeological dental calculus. *Journal of Archaeological Science*, *118*, 105135. https://doi.org/10.1016/j.jas.2020.105135

Fages, A., Hanghøj, K., Khan, N., Gaunitz, C., Seguin-Orlando, A., Leonardi, M., McCrory Constantz, C., Gamba, C., Al-Rasheid, K. A. S., Albizuri, S., Alfarhan, A. H., Allentoft, M., Alquraishi, S., Anthony, D., Baimukhanov, N., Barrett, J. H., Bayarsaikhan, J., Benecke, N., Bernáldez-Sánchez, E., … Orlando, L. (2019). Tracking Five Millennia of Horse Management with Extensive Ancient Genome Time Series. *Cell*, *177*(6), 1419-1435.e31. https://doi.org/10.1016/j.cell.2019.03.049

Falin, L. I. (1961). Histological and histochemical studies of human teeth of the Bronze and Stone Ages. *Archives of Oral Biology*, *5*(1), 5–13. https://doi.org/10.1016/0003-9969(61)90109-1

Feldman, M., Harbeck, M., Keller, M., Spyrou, M. A., Rott, A., Trautmann, B., Scholz, H. C., Päffgen, B., Peters, J., McCormick, M., Bos, K., Herbig, A., & Krause, J. (2016). A High-Coverage Yersinia pestis Genome from a Sixth-Century Justinianic Plague Victim. *Molecular Biology and Evolution*, *33*(11), 2911–2923. https://doi.org/10.1093/molbev/msw170

Feldman, M., Master, D. M., Bianco, R. A., Burri, M., Stockhammer, P. W., Mittnik, A., Aja, A. J., Jeong, C., & Krause, J. (2019). Ancient DNA sheds light on the genetic origins of early Iron Age Philistines. *Science Advances*, *5*(7), eaax0061. https://doi.org/10.1126/sciadv.aax0061

Frank, J. A., Pan, Y., Tooming-Klunderud, A., Eijsink, V. G. H., McHardy, A. C., Nederbragt, A. J., & Pope, P. B. (2016). Improved metagenome assemblies and taxonomic binning using long-read circular consensus sequence data. *Scientific Reports*, *6*(1), 25373. https://doi.org/10.1038/srep25373

Furtwängler, A., Reiter, E., Neumann, G. U., Siebke, I., Steuri, N., Hafner, A., Lösch, S., Anthes, N., Schuenemann, V. J., & Krause, J. (2018). Ratio of mitochondrial to nuclear DNA affects contamination estimates in ancient DNA analysis. *Scientific Reports*, *8*(1), 1–8. https://doi.org/10.1038/s41598-018-32083-0

Gamba, C., Fernández, E., Tirado, M., Deguilloux, M. F., Pemonge, M. H., Utrilla, P., Edo, M., Molist, M., Rasteiro, R., Chikhi, L., & Arroyo-Pardo, E. (2012). Ancient DNA from an Early Neolithic Iberian population supports a pioneer colonization by first farmers. *Molecular Ecology*, *21*(1), 45–56. https://doi.org/10.1111/j.1365-294X.2011.05361.x
Gansauge, M.-T., Gerber, T., Glocke, I., Korlević, P., Lippik, L., Nagel, S., Riehl, L. M., Schmidt, A., & Meyer, M. (2017). Single-stranded DNA library preparation from highly degraded DNA using T4 DNA ligase. *Nucleic Acids Research*, *45*(10), e79. https://doi.org/10.1093/nar/gkx033

Gansauge, M.-T., & Meyer, M. (2013). Single-stranded DNA library preparation for the sequencing of ancient or damaged DNA. *Nature Protocols*, *8*(4), 737–748. https://doi.org/10.1038/nprot.2013.038

Gansauge, M.-T., & Meyer, M. (2019). A Method for Single-Stranded Ancient DNA Library

Preparation. In B. Shapiro, A. Barlow, P. D. Heintzman, M. Hofreiter, J. L. A. Paijmans, & A. E. R. Soares (Eds.), *Ancient DNA: Methods and Protocols* (pp. 75–83). Springer. https://doi.org/10.1007/978-1-4939-9176-1_9

García-Garcerà, M., Gigli, E., Sanchez-Quinto, F., Ramirez, O., Calafell, F., Civit, S., & Lalueza-Fox, C. (2011). Fragmentation of Contaminant and Endogenous DNA in Ancient Samples Determined by Shotgun Sequencing; Prospects for Human Palaeogenomics. *PLoS ONE*, *6*(8). https://doi.org/10.1371/journal.pone.0024161

Gaudio, D., Fernandes, D. M., Schmidt, R., Cheronet, O., Mazzarelli, D., Mattia, M., O'Keeffe, T., Feeney, R. N. M., Cattaneo, C., & Pinhasi, R. (2019). Genome-Wide DNA from Degraded Petrous Bones and the Assessment of Sex and Probable Geographic Origins of Forensic Cases. *Scientific Reports*, *9*(1), 1–11. https://doi.org/10.1038/s41598-019-44638-w

Gilbert, M. T. P., Bandelt, H.-J., Hofreiter, M., & Barnes, I. (2005). Assessing ancient DNA studies. *Trends in Ecology & Evolution*, *20*(10), 541–544. https://doi.org/10.1016/j.tree.2005.07.005

Gilbert, M. T. P., Hansen, A. J., Willerslev, E., Turner-Walker, G., & Collins, M. (2006). Insights into
the processes behind the contamination of degraded human teeth and bone samples with exogenous sources of DNA. *International Journal of Osteoarchaeology*, *16*(2), 156–164. https://doi.org/10.1002/oa.832

Ginolhac, A., Rasmussen, M., Gilbert, M. T. P., Willerslev, E., & Orlando, L. (2011). mapDamage: Testing for damage patterns in ancient DNA sequences. *Bioinformatics*, *27*(15), 2153–2155. https://doi.org/10.1093/bioinformatics/btr347

Gottfried, R. S. (2010). *Black Death*. Simon and Schuster.

Green, M. H. (2014). *Pandemic disease in the medieval world: Rethinking the Black Death*.

Green, M. H. (2018). Putting Africa on the Black Death map: Narratives from genetics and history. *Afriques. Débats, Méthodes et Terrains d'histoire*, *09*, Article 09. https://doi.org/10.4000/afriques.2125

Green, M. R., Sambrook, J., & Sambrook, J. (2012). *Molecular cloning: A laboratory manual* (4th ed). Cold Spring Harbor Laboratory Press.
Groussin, M., Mazel, F., Sanders, J. G., Smillie, C. S., Lavergne, S., Thuiller, W., & Alm, E. J. (2017). Unraveling the processes shaping mammalian gut microbiomes over evolutionary time. *Nature Communications*, *8*(1), 14319. https://doi.org/10.1038/ncomms14319

Guedes, L., Dias, O., Neto, J., Ribeiro da Silva, L. da P., Mendonça de Souza, S. M. F., & Iñiguez, A. M. (2018). First Paleogenetic Evidence of Probable Syphilis and Treponematoses Cases in the Brazilian Colonial Period. *BioMed Research International*, *2018*. https://doi.org/10.1155/2018/8304129

Guellil, M., Kersten, O., Namouchi, A., Luciani, S., Marota, I., Arcini, C. A., Iregren, E., Lindemann, R. A., Warfvinge, G., Bakanidze, L., Bitadze, L., Rubini, M., Zaio, P., Zaio, M., Neri, D., Stenseth, N. C., & Bramanti, B. (2020). A genomic and historical synthesis of plague in 18th century

Eurasia. *Proceedings of the National Academy of Sciences*, *117*(45), 28328–28335. https://doi.org/10.1073/pnas.2009677117

Günther, T., & Nettelblad, C. (2019). The presence and impact of reference bias on population genomic studies of prehistoric human populations. *PLOS Genetics*, *15*(7), e1008302. https://doi.org/10.1371/journal.pgen.1008302

Haak, W., Balanovsky, O., Sanchez, J. J., Koshel, S., Zaporozhchenko, V., Adler, C. J., Sarkissian, C. S. I.
D., Brandt, G., Schwarz, C., Nicklisch, N., Dresely, V., Fritsch, B., Balanovska, E., Villems, R., Meller, H., Alt, K. W., Cooper, A., & Consortium, the G. (2010). Ancient DNA from European Early Neolithic Farmers Reveals Their Near Eastern Affinities. *PLOS Biology*, *8*(11), e1000536. https://doi.org/10.1371/journal.pbio.1000536

Haak, W., Forster, P., Bramanti, B., Matsumura, S., Brandt, G., Tänzer, M., Villems, R., Renfrew, C., Gronenborn, D., Alt, K. W., & Burger, J. (2005). Ancient DNA from the First European Farmers in 7500-Year-Old Neolithic Sites. *Science*, *310*(5750), 1016–1018. https://doi.org/10.1126/science.1118725

Haensch, S., Bianucci, R., Signoli, M., Rajerison, M., Schultz, M., Kacki, S., Vermunt, M., Weston, D. A., Hurst, D., Achtman, M., Carniel, E., & Bramanti, B. (2010). Distinct Clones of Yersinia pestis Caused the Black Death. *PLoS Pathogens*, *6*(10). https://doi.org/10.1371/journal.ppat.1001134

Hagelberg, E., Bell, L. S., Allen, T., Boyde, A., Jones, S. J., Clegg, J. B., Hummel, S., Brown, T. A., & Ambler, R. P. (1991). Analysis of Ancient Bone DNA: Techniques and Applications [and Dicussion]. *Philosophical Transactions: Biological Sciences*, *333*(1268), 399–407. JSTOR.

Handt, O., Höss, M., Krings, M., & Pääbo, S. (1994). Ancient DNA: Methodological challenges. *Experientia*, *50*(6), 524–529. https://doi.org/10.1007/BF01921720

Hansen, A. J., Willerslev, E., Wiuf, C., Mourier, T., & Arctander, P. (2001). Statistical Evidence for Miscoding Lesions in Ancient DNA Templates. *Molecular Biology and Evolution*, *18*(2), 262–265. https://doi.org/10.1093/oxfordjournals.molbev.a003800

Hansen, H. B., Damgaard, P. B., Margaryan, A., Stenderup, J., Lynnerup, N., Willerslev, E., & Allentoft, M. E. (2017). Comparing Ancient DNA Preservation in Petrous Bone and Tooth Cementum. *PLOS ONE*, *12*(1), e0170940. https://doi.org/10.1371/journal.pone.0170940

Harakalova, M., Mokry, M., Hrdlickova, B., Renkens, I., Duran, K., van Roekel, H., Lansu, N., van Roosmalen, M., de Bruijn, E., Nijman, I. J., Kloosterman, W. P., & Cuppen, E. (2011). Multiplexed array-based and in-solution genomic enrichment for flexible and cost-effective targeted next-generation sequencing. *Nature Protocols*, *6*(12), 1870–1886. https://doi.org/10.1038/nprot.2011.396

Harkins, K. M., & Stone, A. C. (2015). Ancient pathogen genomics: Insights into timing and adaptation. *Journal of Human Evolution*, *79*, 137–149. https://doi.org/10.1016/j.jhevol.2014.11.002

Harney, É., Cheronet, O., Fernandes, D. M., Sirak, K., Mah, M., Bernardos, R., Adamski, N., Broomandkhoshbacht, N., Callan, K., Lawson, A. M., Oppenheimer, J., Stewardson, K., Zalzala, F., Anders, A., Candilio, F., Constantinescu, M., Coppa, A., Ciobanu, I., Dani, J., … Pinhasi, R. (2021). A minimally destructive protocol for DNA extraction from ancient teeth. *Genome Research*, *31*(3), 472–483. https://doi.org/10.1101/gr.267534.120

Hegel, K. (1869). *Die Chroniken der niedersächsischen städte*. S. Hirzel.
Henry, A. G., Brooks, A. S., & Piperno, D. R. (2011). Microfossils in calculus demonstrate consumption of plants and cooked foods in Neanderthal diets (Shanidar III, Iraq; Spy I and II, Belgium). *Proceedings of the National Academy of Sciences*, *108*(2), 486–491. https://doi.org/10.1073/pnas.1016868108

Herbig, A., Maixner, F., Bos, K. I., Zink, A., Krause, J., & Huson, D. H. (2016). *MALT: Fast alignment and analysis of metagenomic DNA sequence data applied to the Tyrolean Iceman*. https://doi.org/10.1101/050559

Hermmann, V. (2018). Die ehemalige Marktkirsche St. Marien in Halle (Saale). Bau- und Grabbefunde der Ausgrabungen von 2004 bis 2006. In *Der Markt der Staft Halle im Mittelalter. Ausgrabungen zu Marktkirche, Kirchhof und erzbischOflichem Kaufhaus.* (pp. 15–140). Harald Meller.

Higgins, D., & Austin, J. J. (2013). Teeth as a source of DNA for forensic identification of human remains: A review. *Science & Justice: Journal of the Forensic Science Society*, *53*(4), 433–441. https://doi.org/10.1016/j.scijus.2013.06.001

Higgins, D., Rohrlach, A. B., Kaidonis, J., Townsend, G., & Austin, J. J. (2015). Differential Nuclear and Mitochondrial DNA Preservation in Post-Mortem Teeth with Implications for Forensic and Ancient DNA Studies. *PLOS ONE*, *10*(5), e0126935. https://doi.org/10.1371/journal.pone.0126935

Higuchi, R., Bowman, B., Freiberger, M., Ryder, O. A., & Wilson, A. C. (1984). DNA sequences from the quagga, an extinct member of the horse family. *Nature*, *312*(5991), 282–284. https://doi.org/10.1038/312282a0
Hofreiter, M., Jaenicke, V., Serre, D., von Haeseler, A., & Pääbo, S. (2001). DNA sequences from multiple amplifications reveal artifacts induced by cytosine deamination in ancient DNA. *Nucleic Acids Research*, *29*(23), 4793–4799. https://doi.org/10.1093/nar/29.23.4793

Höss, M., Jaruga, P., Zastawny, T. H., Dizdaroglu, M., & Paabo, S. (1996). DNA Damage and DNA Sequence Retrieval from Ancient Tissues. *Nucleic Acids Research*, *24*(7), 1304–1307. https://doi.org/10.1093/nar/24.7.1304

Hübler, R., Key, F. M., Warinner, C., Bos, K. I., Krause, J., & Herbig, A. (2019). HOPS: Automated detection and authentication of pathogen DNA in archaeological remains. *Genome Biology*, *20*(1), 280. https://doi.org/10.1186/s13059-019-1903-0

Hunter, P. (2014). Pulling teeth from history. *EMBO Reports*, *15*(9), 923–925. https://doi.org/10.15252/embr.201439353

Itan, Y., Powell, A., Beaumont, M. A., Burger, J., & Thomas, M. G. (2009). The Origins of Lactase Persistence in Europe. *PLOS Computational Biology*, *5*(8), e1000491. https://doi.org/10.1371/journal.pcbi.1000491

Jaenicke-Després, V., Buckler, E. S., Smith, B. D., Gilbert, M. T. P., Cooper, A., Doebley, J., & Pääbo, S. (2003). Early Allelic Selection in Maize as Revealed by Ancient DNA. *Science*, *302*(5648), 1206–1208. https://doi.org/10.1126/science.1089056

Kaestle, F. A., & Horsburgh, K. A. (2002). Ancient DNA in anthropology: Methods, applications, and ethics. *American Journal of Physical Anthropology*, *119*(S35), 92–130. https://doi.org/10.1002/ajpa.10179
Kawasaki, T., Takahashi, S., & Ikeda, K. (1985). Hydroxyapatite high-performance liquid chromatography: Column performance for proteins. *European Journal of Biochemistry*, *152*(2), 361–371. https://doi.org/10.1111/j.1432-1033.1985.tb09206.x

Keller, M., Spyrou, M. A., McCormick, M., Bos, K. I., Herbig, A., & Krause, J. (2019). Ancient Yersinia pestis genomes provide no evidence for the origins or spread of the Justinianic Plague. *BioRxiv*, 819698. https://doi.org/10.1101/819698

Kemp, B. M., & Smith, D. G. (2005). Use of bleach to eliminate contaminating DNA from the surface of bones and teeth. *Forensic Science International*, *154*(1), 53–61. https://doi.org/10.1016/j.forsciint.2004.11.017

Key, F. M., Posth, C., Krause, J., Herbig, A., & Bos, K. I. (2017). Mining Metagenomic Data Sets for Ancient DNA: Recommended Protocols for Authentication. *Trends in Genetics*, *33*(8), 508–520. https://doi.org/10.1016/j.tig.2017.05.005
Keyser, Erich. (1941). *Deutsches Städtebuch, Band II - Mitteldeutschland. Stuttgart:* W. Kohlhammer.

Kimura, B., Marshall, F. B., Chen, S., Rosenbom, S., Moehlman, P. D., Tuross, N., Sabin, R. C., Peters, J., Barich, B., Yohannes, H., Kebede, F., Teclai, R., Beja-Pereira, A., & Mulligan, C. J. (2011). Ancient DNA from Nubian and Somali wild ass provides insights into donkey ancestry and domestication. *Proceedings of the Royal Society B: Biological Sciences*, *278*(1702), 50–57. https://doi.org/10.1098/rspb.2010.0708

Klunk, J., Duggan, A. T., Redfern, R., Gamble, J., Boldsen, J. L., Golding, G. B., Walter, B. S., Eaton, K., Stangroom, J., Rouillard, J.-M., Devault, A., DeWitte, S. N., & Poinar, H. N. (2019). Genetic resiliency and the Black Death: No apparent loss of mitogenomic diversity due to the Black Death in medieval London and Denmark. *American Journal of Physical Anthropology*, *169*(2), 240–252. https://doi.org/10.1002/ajpa.23820

Knapp, M., & Hofreiter, M. (2010). Next Generation Sequencing of Ancient DNA: Requirements, Strategies and Perspectives. *Genes*, *1*(2), 227–243. https://doi.org/10.3390/genes1020227

Kocher, A., Papac, L., Barquera, R., Key, F. M., Spyrou, M. A., Hübler, R., Rohrlach, A. B., Aron, F., Stahl, R., Wissgott, A., van Bömmel, F., Pfefferkorn, M., Mittnik, A., Villalba-Mouco, V., Neumann, G. U., Rivollat, M., van de Loosdrecht, M. S., Majander, K., Tukhbatova, R. I., … Kühnert, D. (2021). Ten millennia of hepatitis B virus evolution. *Science (New York, N.Y.)*, *374*(6564), 182–188. https://doi.org/10.1126/science.abi5658

Kolman, C. J., & Tuross, N. (2000). Ancient DNA analysis of human populations. *American Journal of Physical Anthropology*, *111*(1), 5–23. https://doi.org/10.1002/(SICI)1096-8644(200001)111:1<5::AID-AJPA2>3.0.CO;2-3

Korlević, P., Gerber, T., Gansauge, M.-T., Hajdinjak, M., Nagel, S., Aximu-Petri, A., & Meyer, M. (2015). Reducing microbial and human contamination in DNA extractions from ancient bones and teeth. *BioTechniques*, *59*(2), 87–93. https://doi.org/10.2144/000114320

Korneliussen, T. S., Albrechtsen, A., & Nielsen, R. (2014). ANGSD: Analysis of Next Generation Sequencing Data. *BMC Bioinformatics*, *15*(1), 356. https://doi.org/10.1186/s12859-014-0356-4

Krause, J., Fu, Q., Good, J. M., Viola, B., Shunkov, M. V., Derevianko, A. P., & Pääbo, S. (2010). The complete mitochondrial DNA genome of an unknown hominin from southern Siberia. *Nature*, *464*(7290), 894–897. https://doi.org/10.1038/nature08976

Larson, G., Albarella, U., Dobney, K., Rowley-Conwy, P., Schibler, J., Tresset, A., Vigne, J.-D., Edwards, C. J., Schlumbaum, A., Dinu, A., Bălăçsescu, A., Dolman, G., Tagliacozzo, A., Manaseryan, N., Miracle, P., Wijngaarden-Bakker, L. V., Masseti, M., Bradley, D. G., & Cooper, A. (2007). Ancient DNA, pig domestication, and the spread of the Neolithic into Europe. *Proceedings of the National Academy of Sciences*, *104*(39), 15276–15281. https://doi.org/10.1073/pnas.0703411104

Lassen, C., Hummel, S., & Herrmann, B. (1994). Comparison of DNA extraction and amplification from ancient human bone and mummified soft tissue. *International Journal of Legal Medicine*, *107*(3), 152–155. https://doi.org/10.1007/BF01225603

Latham, K. E., & Miller, J. J. (2019). DNA recovery and analysis from skeletal material in modern forensic contexts. *Forensic Sciences Research*, *4*(1), 51–59. https://doi.org/10.1080/20961790.2018.1515594

Lazaridis, I., Mittnik, A., Patterson, N., Mallick, S., Rohland, N., Pfrengle, S., Furtwängler, A., Peltzer, A., Posth, C., Vasilakis, A., McGeorge, P. J. P., Konsolaki-Yannopoulou, E., Korres, G., Martlew, H., Michalodimitrakis, M., Özsait, M., Özsait, N., Papathanasiou, A., Richards, M., … Stamatoyannopoulos, G. (2017). Genetic origins of the Minoans and Mycenaeans. *Nature*, *548*(7666), 214–218. https://doi.org/10.1038/nature23310

Leney, M. D. (2006). Sampling Skeletal Remains for Ancient DNA (aDNA): A Measure of Success. *Historical Archaeology*, *40*(3), 31–49. JSTOR.

Lenth, R., Singmann, H., Love, J., Buerkner, P., & Herve, M. (2019). *emmeans: Estimated Marginal Means, aka Least-Squares Means* (1.4.2) [Computer software]. https://CRAN.R-project.org/package=emmeans

León, M. S. P. de, Koesbardiati, T., Weissmann, J. D., Milella, M., Reyna-Blanco, C. S., Suwa, G., Kondo, O., Malaspinas, A.-S., White, T. D., & Zollikofer, C. P. E. (2018). Human bony labyrinth is an indicator of population history and dispersal from Africa. *Proceedings of the National Academy of Sciences*, *115*(16), 4128–4133. https://doi.org/10.1073/pnas.1717873115

Lewis, K., Epstein, S., Godoy, V. G., & Hong, S.-H. (2008). Intact DNA in ancient permafrost. *Trends in Microbiology*, *16*(3), 92–94. https://doi.org/10.1016/j.tim.2008.01.002

Lewis-Kraus, G. (2019, January 17). Is Ancient DNA Research Revealing New Truths—Or Falling Into Old Traps? *The New York Times*. https://www.nytimes.com/2019/01/17/magazine/ancient-dna-paleogenomics.html

Li, H., & Durbin, R. (2009). Fast and accurate short read alignment with Burrows-Wheeler transform. *Bioinformatics (Oxford, England)*, *25*(14), 1754–1760. https://doi.org/10.1093/bioinformatics/btp324

Lindahl, T. (1993). Recovery of antediluvian DNA. *Nature*, *365*(6448), 700. https://doi.org/10.1038/365700a0

Linné Kausrud, K., Viljugrein, H., Frigessi, A., Begon, M., Davis, S., Leirs, H., Dubyanskiy, V., & Stenseth, N. C. (2007). Climatically driven synchrony of gerbil populations allows large-scale plague outbreaks. *Proceedings of the Royal Society B: Biological Sciences*, *274*(1621), 1963–1969. https://doi.org/10.1098/rspb.2007.0568

Linossier, A., Gajardo, M., & Olavarria, J. (1996). Paleomicrobiological study in dental calculus: Streptococcus mutans. *Scanning Microscopy*, *10*(4), 1005–1013; discussion 1014.

Llamas, B., Valverde, G., Fehren-Schmitz, L., Weyrich, L. S., Cooper, A., & Haak, W. (2017). From the field to the laboratory: Controlling DNA contamination in human ancient DNA research in the high-throughput sequencing era. *STAR: Science & Technology of Archaeological Research*, *3*(1), 1–14. https://doi.org/10.1080/20548923.2016.1258824

Llorente, M. G., Jones, E. R., Eriksson, A., Siska, V., Arthur, K. W., Arthur, J. W., Curtis, M. C., Stock, J. T., Coltorti, M., Pieruccini, P., Stretton, S., Brock, F., Higham, T., Park, Y., Hofreiter, M., Bradley, D. G., Bhak, J., Pinhasi, R., & Manica, A. (2015). Ancient Ethiopian genome reveals extensive Eurasian admixture in Eastern Africa. *Science*, *350*(6262), 820–822. https://doi.org/10.1126/science.aad2879

Loreille, O., Koshinsky, H., Fofanov, V. Y., & Irwin, J. A. (2011). Application of next generation sequencing technologies to the identification of highly degraded unknown soldiers' remains. *Forensic Science International: Genetics Supplement Series*, *3*(1), e540–e541. https://doi.org/10.1016/j.fsigss.2011.10.013

Lugli, G. A., Milani, C., Mancabelli, L., Turroni, F., Ferrario, C., Duranti, S., van Sinderen, D., & Ventura, M. (2017). Ancient bacteria of the Ötzi's microbiome: A genomic tale from the Copper Age. *Microbiome*, *5*(1), 5. https://doi.org/10.1186/s40168-016-0221-y

MacArthur, W. P. (1949). The Identification of Some Pestilences Recorded in the Irish Annals. *Irish Historical Studies*, *6*(23), 169–188. JSTOR.

MacHugh, D. E., Larson, G., & Orlando, L. (2017). Taming the Past: Ancient DNA and the Study of Animal Domestication. *Annual Review of Animal Biosciences*, *5*(1), 329–351. https://doi.org/10.1146/annurev-animal-022516-022747

Maixner, F., Krause-Kyora, B., Turaev, D., Herbig, A., Hoopmann, M. R., Hallows, J. L., Kusebauch, U., Vigl, E. E., Malfertheiner, P., Megraud, F., O'Sullivan, N., Cipollini, G., Coia, V., Samadelli, M., Engstrand, L., Linz, B., Moritz, R. L., Grimm, R., Krause, J., … Zink, A. (2016). The 5300-year-old Helicobacter pylori genome of the Iceman. *Science*, *351*(6269), 162–165. https://doi.org/10.1126/science.aad2545

Malainey, M. E. (2011). Ancient DNA and the Polymerase Chain Reaction. In M. E. Malainey (Ed.), *A Consumer's Guide to Archaeological Science: Analytical Techniques* (pp. 237–253). Springer. https://doi.org/10.1007/978-1-4419-5704-7_16

Malmström, H., Gilbert, M. T. P., Thomas, M. G., Brandström, M., Storå, J., Molnar, P., Andersen, P. K., Bendixen, C., Holmlund, G., Götherström, A., & Willerslev, E. (2009). Ancient DNA Reveals Lack of Continuity between Neolithic Hunter-Gatherers and Contemporary Scandinavians. *Current Biology*, *19*(20), 1758–1762. https://doi.org/10.1016/j.cub.2009.09.017

Malmström, H., Svensson, E. M., Gilbert, M. T. P., Willerslev, E., Götherström, A., & Holmlund, G. (2007). More on contamination: The use of asymmetric molecular behavior to identify authentic ancient human DNA. *Molecular Biology and Evolution*, *24*(4), 998–1004. https://doi.org/10.1093/molbev/msm015

Mann, A. E., Sabin, S., Ziesemer, K., Vågene, Å. J., Schroeder, H., Ozga, A. T., Sankaranarayanan, K., Hofman, C. A., Fellows Yates, J. A., Salazar-García, D. C., Frohlich, B., Aldenderfer, M., Hoogland, M., Read, C., Milner, G. R., Stone, A. C., Lewis, C. M., Krause, J., Hofman, C., … Warinner, C. (2018). Differential preservation of endogenous human and microbial DNA in dental calculus and dentin. *Scientific Reports*, *8*(1), 9822. https://doi.org/10.1038/s41598-018-28091-9

Marciniak, S., & Perry, G. H. (2017). Harnessing ancient genomes to study the history of human adaptation. *Nature Reviews. Genetics*, *18*(11), 659–674. https://doi.org/10.1038/nrg.2017.65

Mardis, E. R. (2008). Next-Generation DNA Sequencing Methods. *Annual Review of Genomics and Human Genetics*, *9*(1), 387–402. https://doi.org/10.1146/annurev.genom.9.081307.164359

Margaryan, A., Hansen, H. B., Rasmussen, S., Sikora, M., Moiseyev, V., Khoklov, A., Epimakhov, A., Yepiskoposyan, L., Kriiska, A., Varul, L., Saag, L., Lynnerup, N., Willerslev, E., & Allentoft, M. E. (2018). Ancient pathogen DNA in human teeth and petrous bones. *Ecology and Evolution*, *8*(6), 3534–3542. https://doi.org/10.1002/ece3.3924

Matero, P., Pasanen, T., Laukkanen, R., Tissari, P., Tarkka, E., Vaara, M., & Skurnik, M. (2009). Real-time multiplex PCR assay for detection of Yersinia pestis and Yersinia pseudotuberculosis. *APMIS*, *117*(1), 34–44. https://doi.org/10.1111/j.1600-0463.2008.00013.x

Mathieson, I., Lazaridis, I., Rohland, N., Mallick, S., Patterson, N., Roodenberg, S. A., Harney, E., Stewardson, K., Fernandes, D., Novak, M., Sirak, K., Gamba, C., Jones, E. R., Llamas, B., Dryomov, S., Pickrell, J., Arsuaga, J. L., de Castro, J. M. B., Carbonell, E., … Reich, D. (2015). Genome-wide patterns of selection in 230 ancient Eurasians. *Nature*, *528*(7583), 499–503. https://doi.org/10.1038/nature16152

McCormick, M. (2003). Rats, Communications, and Plague: Toward an Ecological History. *The Journal of Interdisciplinary History*, *34*(1), 1–25. https://doi.org/10.1162/002219503322645439

Meyer, M., Fu, Q., Aximu-Petri, A., Glocke, I., Nickel, B., Arsuaga, J.-L., Martínez, I., Gracia, A., de Castro, J. M. B., Carbonell, E., & Pääbo, S. (2014). A mitochondrial genome sequence of a hominin from Sima de los Huesos. *Nature*, *505*(7483), 403–406. https://doi.org/10.1038/nature12788

Meyer, M., & Kircher, M. (2010). Illumina Sequencing Library Preparation for Highly Multiplexed Target Capture and Sequencing. *Cold Spring Harbor Protocols*, *2010*(6), pdb.prot5448. https://doi.org/10.1101/pdb.prot5448

Meyer, M., Kircher, M., Gansauge, M.-T., Li, H., Racimo, F., Mallick, S., Schraiber, J. G., Jay, F., Prüfer, K., Filippo, C. de, Sudmant, P. H., Alkan, C., Fu, Q., Do, R., Rohland, N., Tandon, A., Siebauer, M., Green, R. E., Bryc, K., … Pääbo, S. (2012). A High-Coverage Genome Sequence from an Archaic Denisovan Individual. *Science*, *338*(6104), 222–226. https://doi.org/10.1126/science.1224344

Mickleburgh, H. L., & Pagán-Jiménez, J. R. (2012). New insights into the consumption of maize and other food plants in the pre-Columbian Caribbean from starch grains trapped in human dental calculus. *Journal of Archaeological Science*, *39*(7), 2468–2478. https://doi.org/10.1016/j.jas.2012.02.020

Morozova, I., Kasianov, A., Bruskin, S., Neukamm, J., Molak, M., Batieva, E., Pudło, A., Rühli, F. J., & Schuenemann, V. J. (2020). New ancient Eastern European Yersinia pestis genomes illuminate the dispersal of plague in Europe. *Philosophical Transactions of the Royal Society B: Biological Sciences*, *375*(1812), 20190569. https://doi.org/10.1098/rstb.2019.0569

Mullis, KB. (1990). Target amplification for DNA analysis by the polymerase chain reaction. *Annales de Biologie Clinique*, *48*(8), 579–582.

Mundorff, A. Z., Bartelink, E. J., & Mar-Cash, E. (2009). DNA Preservation in Skeletal Elements from the World Trade Center Disaster: Recommendations for Mass Fatality Management*,†. *Journal of Forensic Sciences*, *54*(4), 739–745. https://doi.org/10.1111/j.1556-4029.2009.01045.x

Nagaoka, T., & Kawakubo, Y. (2015). Using the petrous part of the temporal bone to estimate fetal age at death. *Forensic Science International*, *248*, 188.e1-7. https://doi.org/10.1016/j.forsciint.2015.01.009

Namouchi, A., Guellil, M., Kersten, O., Hänsch, S., Ottoni, C., Schmid, B. V., Pacciani, E., Quaglia, L., Vermunt, M., Bauer, E. L., Derrick, M., Jensen, A. Ø., Kacki, S., Cohn, S. K., Stenseth, N. C., & Bramanti, B. (2018). Integrative approach using *Yersinia pestis* genomes to revisit the historical landscape of plague during the Medieval Period. *Proceedings of the National Academy of Sciences*, *115*(50), E11790–E11797. https://doi.org/10.1073/pnas.1812865115

Nanci, A. (2017). *Ten Cate's Oral Histology—9th Edition* (9th ed.). Elsevier. https://www.elsevier.com/books/ten-cates-oral histology/nanci/978-0-323-48518-0

Nerlich, A. G., Haas, C. J., Zink, A., Szeimies, U., & Hagedorn, H. G. (1997). Molecular evidence for tuberculosis in an ancient Egyptian mummy. *The Lancet*, *350*(9088), 1404. https://doi.org/10.1016/S0140-6736(05)65185-9

Neumann, G. U. (2020). *Tooth Sampling from the inner pulp chamber for ancient DNA Extraction*. https://doi.org/10.17504/protocols.io.bqebmtan

Norén, A., Lynnerup, N., Czarnetzki, A., & Graw, M. (2005). Lateral angle: A method for sexing using the petrous bone. *American Journal of Physical Anthropology*, *128*(2), 318–323. https://doi.org/10.1002/ajpa.20245

Ole J. Benedictow. (2006). *The Black Death 1346-1353: The Complete History* (1 edition). Boydell Press.

Orfanou, E., Himmel, M., Aron, F., & Haak, W. (2020, December 11). *Minimally-invasive sampling of pars petrosa (os temporale) for ancient DNA extraction*. Protocols.Io. https://www.protocols.io/view/minimally-invasive-sampling-of-pars-petrosa-os-tem-bqd8ms9w

Orlando, L., Bonjean, D., Bocherens, H., Thenot, A., Argant, A., Otte, M., & Hänni, C. (2002). Ancient DNA and the Population Genetics of Cave Bears (Ursus spelaeus) Through Space and Time. *Molecular Biology and Evolution*, *19*(11), 1920–1933. https://doi.org/10.1093/oxfordjournals.molbev.a004016

Overballe-Petersen, S., Orlando, L., & Willerslev, E. (2012). Next-generation sequencing offers new insights into DNA degradation. *Trends in Biotechnology*, *30*(7), 364–368. https://doi.org/10.1016/j.tibtech.2012.03.007
Pääbo, S. (1985). Molecular cloning of Ancient Egyptian mummy DNA. *Nature*, *314*(6012), 644–645. https://doi.org/10.1038/314644a0

Pääbo, S., Gifford, J. A., & Wilson, A. C. (1988). Mitochondrial DNA sequences from a 7000-year old brain. *Nucleic Acids Research*, *16*(20), 9775–9787. https://doi.org/10.1093/nar/16.20.9775

Pääbo, S., Poinar, H., Serre, D., Jaenicke-Després, V., Hebler, J., Rohland, N., Kuch, M., Krause, J., Vigilant, L., & Hofreiter, M. (2004). Genetic Analyses from Ancient DNA. *Annual Review of Genetics*, *38*(1), 645–679. https://doi.org/10.1146/annurev.genet.37.110801.143214

Palsdottir, A. H., Bläuer, A., Rannamäe, E., Boessenkool, S., & Hallsson, J. (2019). *Not a limitless resource: Ethics and guidelines for destructive sampling of archaeofaunal remains*. https://doi.org/10.1098/rsos.191059

Parker, C., Rohrlach, A. B., Friederich, S., Nagel, S., Meyer, M., Krause, J., Bos, K. I., & Haak, W. (2020). A systematic investigation of human DNA preservation in medieval skeletons. *Scientific Reports*, *10*(1), 18225. https://doi.org/10.1038/s41598-020-75163-w

Parkhill, J., Wren, B. W., Thomson, N. R., Titball, R. W., Holden, M. T., Prentice, M. B., Sebaihia, M., James, K. D., Churcher, C., Mungall, K. L., Baker, S., Basham, D., Bentley, S. D., Brooks, K.,

Cerdeño-Tárraga, A. M., Chillingworth, T., Cronin, A., Davies, R. M., Davis, P., … Barrell, B. G. (2001). Genome sequence of Yersinia pestis, the causative agent of plague. *Nature*, *413*(6855), 523–527. https://doi.org/10.1038/35097083

Parras-Moltó, M., & López-Bueno, A. (2018). Methods for Enrichment and Sequencing of Oral Viral Assemblages: Saliva, Oral Mucosa, and Dental Plaque Viromes. In A. Moya & V. Pérez Brocal (Eds.), *The Human Virome: Methods and Protocols* (pp. 143–161). Springer. https://doi.org/10.1007/978-1-4939-8682-8_11

Pellegrini, M., Pouncett, J., Jay, M., Pearson, M. P., & Richards, M. P. (2016). Tooth enamel oxygen "isoscapes" show a high degree of human mobility in prehistoric Britain. *Scientific Reports*, *6*(1), 34986. https://doi.org/10.1038/srep34986

Peltzer, A., Jäger, G., Herbig, A., Seitz, A., Kniep, C., Krause, J., & Nieselt, K. (2016). EAGER: Efficient ancient genome reconstruction. *Genome Biology*, *17*(1), 60. https://doi.org/10.1186/s13059-016-0918-z

Perry, R. D., & Fetherston, J. D. (1997). Yersinia pestis—Etiologic agent of plague. *Clinical Microbiology Reviews*, *10*(1), 35–66.

Pickrell, J. K., & Reich, D. (2014). Toward a new history and geography of human genes informed by ancient DNA. *Trends in Genetics: TIG*, *30*(9), 377–389. https://doi.org/10.1016/j.tig.2014.07.007

Pilli, E., Vai, S., Caruso, M. G., D'Errico, G., Berti, A., & Caramelli, D. (2018). Neither femur nor tooth: Petrous bone for identifying archaeological bone samples via forensic approach. *Forensic Science International*, *283*, 144–149. https://doi.org/10.1016/j.forsciint.2017.12.023
Pinhasi, R., Fernandes, D. M., Sirak, K., & Cheronet, O. (2019). Isolating the human cochlea to generate bone powder for ancient DNA analysis. *Nature Protocols*, *14*(4), 1194–1205. https://doi.org/10.1038/s41596-019-0137-7

Pinhasi, R., Fernandes, D., Sirak, K., Novak, M., Connell, S., Alpaslan-Roodenberg, S., Gerritsen, F., Moiseyev, V., Gromov, A., Raczky, P., Anders, A., Pietrusewsky, M., Rollefson, G., Jovanovic, M., Trinhhoang, H., Bar-Oz, G., Oxenham, M., Matsumura, H., & Hofreiter, M. (2015). Optimal Ancient DNA Yields from the Inner Ear Part of the Human Petrous Bone. *PLOS ONE*, *10*(6), e0129102. https://doi.org/10.1371/journal.pone.0129102

Pinhasi, R., & Mays, S. (2008). *Advances in Human Palaeopathology*. John Wiley & Sons.
Posth, C., Nägele, K., Colleran, H., Valentin, F., Bedford, S., Kami, K. W., Shing, R., Buckley, H., Kinaston, R., Walworth, M., Clark, G. R., Reepmeyer, C., Flexner, J., Maric, T., Moser, J., Gresky, J., Kiko, L., Robson, K. J., Auckland, K., … Powell, A. (2018). Language continuity despite population replacement in Remote Oceania. *Nature Ecology & Evolution*, *2*(4), 731–740. https://doi.org/10.1038/s41559-018-0498-2

Prendergast, M. E., Lipson, M., Sawchuk, E. A., Olalde, I., Ogola, C. A., Rohland, N., Sirak, K. A., Adamski, N., Bernardos, R., Broomandkhoshbacht, N., Callan, K., Culleton, B. J., Eccles, L., Harper, T. K., Lawson, A. M., Mah, M., Oppenheimer, J., Stewardson, K., Zalzala, F., … Reich, D. (2019). Ancient DNA reveals a multistep spread of the first herders into sub-Saharan Africa. *Science*, *365*(6448). https://doi.org/10.1126/science.aaw6275

Prendergast, M. E., & Sawchuk, E. (2018). Boots on the ground in Africa's ancient DNA 'revolution': Archaeological perspectives on ethics and best practices. *Antiquity*, *92*(363), 803–815. https://doi.org/10.15184/aqy.2018.70

Preus, H. R., Marvik, O. J., Selvig, K. A., & Bennike, P. (2011). Ancient bacterial DNA (aDNA) in dental calculus from archaeological human remains. *Journal of Archaeological Science*, *38*(8), 1827–1831. https://doi.org/10.1016/j.jas.2011.03.020

Prüfer, K., Stenzel, U., Hofreiter, M., Pääbo, S., Kelso, J., & Green, R. E. (2010). Computational challenges in the analysis of ancient DNA. *Genome Biology*, *11*(5), R47. https://doi.org/10.1186/gb-2010-11-5-r47

Quinlan, A. R., & Hall, I. M. (2010). BEDTools: A flexible suite of utilities for comparing genomic features. *Bioinformatics*, *26*(6), 841–842. https://doi.org/10.1093/bioinformatics/btq033
R Core Team. (2016). *R: A language and environment for statistical computing*. R Foundation For Statistical Computing. https://www.R-projects.org/

RACINE, J. S. (2012). RSTUDIO: A PLATFORM-INDEPENDENT IDE FOR R AND SWEAVE. *Journal of Applied Econometrics*, *27*(1), 167–172.

Radini, A., Nikita, E., Buckley, S., Copeland, L., & Hardy, K. (2017). Beyond food: The multiple pathways for inclusion of materials into ancient dental calculus. *American Journal of Physical Anthropology*, *162*(S63), 71–83. https://doi.org/10.1002/ajpa.23147
Raoult, D., Aboudharam, G., Crubézy, E., Larrouy, G., Ludes, B., & Drancourt, M. (2000). Molecular identification by "suicide PCR" of Yersinia pestis as the agent of Medieval Black Death. *Proceedings of the National Academy of Sciences*, *97*(23), 12800–12803. https://doi.org/10.1073/pnas.220225197

Rascovan, N., Sjögren, K.-G., Kristiansen, K., Nielsen, R., Willerslev, E., Desnues, C., & Rasmussen, S. (2019). Emergence and Spread of Basal Lineages of Yersinia pestis during the Neolithic Decline. *Cell*, *176*(1), 295-305.e10. https://doi.org/10.1016/j.cell.2018.11.005

Rasmussen, S., Allentoft, M. E., Nielsen, K., Orlando, L., Sikora, M., Sjögren, K.-G., Pedersen, A. G., Schubert, M., Van Dam, A., Kapel, C. M. O., Nielsen, H. B., Brunak, S., Avetisyan, P., Epimakhov, A., Khalyapin, M. V., Gnuni, A., Kriiska, A., Lasak, I., Metspalu, M., … Willerslev, E. (2015). Early Divergent Strains of Yersinia pestis in Eurasia 5,000 Years Ago. *Cell*, *163*(3), 571–582. https://doi.org/10.1016/j.cell.2015.10.009

Renaud, G., Hanghøj, K., Willerslev, E., & Orlando, L. (2017). gargammel: A sequence simulator for ancient DNA. *Bioinformatics*, *33*(4), 577–579. https://doi.org/10.1093/bioinformatics/btw670

Renaud, G., Schubert, M., Sawyer, S., & Orlando, L. (2019). Authentication and Assessment of Contamination in Ancient DNA. In B. Shapiro, A. Barlow, P. D. Heintzman, M. Hofreiter, J. L. A. Paijmans, & A. E. R. Soares (Eds.), *Ancient DNA: Methods and Protocols* (pp. 163–194). Springer. https://doi.org/10.1007/978-1-4939-9176-1_17

Renaud, G., Slon, V., Duggan, A. T., & Kelso, J. (2015). Schmutzi: Estimation of contamination and endogenous mitochondrial consensus calling for ancient DNA. *Genome Biology*, *16*(1), 224. https://doi.org/10.1186/s13059-015-0776-0

Rivollat, M., Mendisco, F., Pemonge, M.-H., Safi, A., Saint-Marc, D., Brémond, A., Couture-Veschambre, C., Rottier, S., & Deguilloux, M.-F. (2015). When the Waves of European Neolithization Met: First Paleogenetic Evidence from Early Farmers in the Southern Paris Basin. *PLOS ONE*, *10*(4), e0125521. https://doi.org/10.1371/journal.pone.0125521

Rizzi, E., Lari, M., Gigli, E., De Bellis, G., & Caramelli, D. (2012). Ancient DNA studies: New perspectives on old samples. *Genetics Selection Evolution*, *44*(1), 21. https://doi.org/10.1186/1297-9686-44-21

Rohland, N., Glocke, I., Aximu-Petri, A., & Meyer, M. (2018). Extraction of highly degraded DNA from ancient bones, teeth and sediments for high-throughput sequencing. *Nature Protocols*, *13*(11), 2447–2461. https://doi.org/10.1038/s41596-018-0050-5

Rohland, N., & Hofreiter, M. (2007). Ancient DNA extraction from bones and teeth. *Nature Protocols*, *2*(7), 1756–1762. https://doi.org/10.1038/nprot.2007.247
Rollo, F., Amici, A., Salvi, R., & Garbuglia, A. (1988). Short but faithful pieces of ancient DNA. *Nature*, *335*(6193), 774. https://doi.org/10.1038/335774a0

Samia, N. I., Kausrud, K. L., Heesterbeek, H., Ageyev, V., Begon, M., Chan, K.-S., & Stenseth, N. C. (2011). Dynamics of the plague–wildlife–human system in Central Asia are controlled by two epidemiological thresholds. *Proceedings of the National Academy of Sciences*, *108*(35), 14527–14532. https://doi.org/10.1073/pnas.1015946108

Sanders, J. G., Nurk, S., Salido, R. A., Minich, J., Xu, Z. Z., Zhu, Q., Martino, C., Fedarko, M., Arthur, T. D., Chen, F., Boland, B. S., Humphrey, G. C., Brennan, C., Sanders, K., Gaffney, J., Jepsen, K., Khosroheidari, M., Green, C., Liyanage, M., … Knight, R. (2019). Optimizing sequencing protocols for leaderboard metagenomics by combining long and short reads. *Genome Biology*, *20*(1), 226. https://doi.org/10.1186/s13059-019-1834-9

Sankararaman, S., Mallick, S., Dannemann, M., Prüfer, K., Kelso, J., Pääbo, S., Patterson, N., & Reich, D. (2014). The landscape of Neandertal ancestry in present-day humans. *Nature*, *507*(7492), 354–357. https://doi.org/10.1038/nature12961

Sawyer, S., Krause, J., Guschanski, K., Savolainen, V., & Pääbo, S. (2012). Temporal Patterns of Nucleotide Misincorporations and DNA Fragmentation in Ancient DNA. *PLoS ONE*, *7*(3). https://doi.org/10.1371/journal.pone.0034131

Scheu, A., Hartz, S., Schmölcke, U., Tresset, A., Burger, J., & Bollongino, R. (2008). Ancient DNA provides no evidence for independent domestication of cattle in Mesolithic Rosenhof, Northern Germany. *Journal of Archaeological Science*, *35*(5), 1257–1264. https://doi.org/10.1016/j.jas.2007.08.012

Schmid, B. V., Büntgen, U., Easterday, W. R., Ginzler, C., Walløe, L., Bramanti, B., & Stenseth, N. C. (2015). Climate-driven introduction of the Black Death and successive plague reintroductions

into Europe. *Proceedings of the National Academy of Sciences*, *112*(10), 3020–3025. https://doi.org/10.1073/pnas.1412887112

Schnorr, S. L., Sankaranarayanan, K., Lewis, C. M., & Warinner, C. (2016). Insights into human evolution from ancient and contemporary microbiome studies. *Current Opinion in Genetics & Development*, *41*, 14–26. https://doi.org/10.1016/j.gde.2016.07.003

Schubert, M., Ginolhac, A., Lindgreen, S., Thompson, J. F., AL-Rasheid, K. A., Willerslev, E., Krogh, A., & Orlando, L. (2012). Improving ancient DNA read mapping against modern reference genomes. *BMC Genomics*, *13*(1), 178. https://doi.org/10.1186/1471-2164-13-178

Schuenemann, V. J., Bos, K., DeWitte, S., Schmedes, S., Jamieson, J., Mittnik, A., Forrest, S., Coombes, B. K., Wood, J. W., Earn, D. J. D., White, W., Krause, J., & Poinar, H. N. (2011). Targeted enrichment of ancient pathogens yielding the pPCP1 plasmid of Yersinia pestis from victims of the Black Death. *Proceedings of the National Academy of Sciences*, *108*(38), E746–E752. https://doi.org/10.1073/pnas.1105107108

Schuenemann, V. J., Singh, P., Mendum, T. A., Krause-Kyora, B., Jäger, G., Bos, K. I., Herbig, A., Economou, C., Benjak, A., Busso, P., Nebel, A., Boldsen, J. L., Kjellström, A., Wu, H., Stewart, G. R., Taylor, G. M., Bauer, P., Lee, O. Y.-C., Wu, H. H. T., … Krause, J. (2013). Genome-Wide Comparison of Medieval and Modern Mycobacterium leprae. *Science*, *341*(6142), 179–183. https://doi.org/10.1126/science.1238286

Schuster, S. C. (2008). Next-generation sequencing transforms today's biology. *Nature Methods*, *5*(1), 16–18. https://doi.org/10.1038/nmeth1156

Segata, N., Waldron, L., Ballarini, A., Narasimhan, V., Jousson, O., & Huttenhower, C. (2012). Metagenomic microbial community profiling using unique clade-specific marker genes. *Nature Methods*, *9*(8), 811–814. https://doi.org/10.1038/nmeth.2066

Seifert, L., Wiechmann, I., Harbeck, M., Thomas, A., Grupe, G., Projahn, M., Scholz, H. C., & Riehm, J. M. (2016). Genotyping Yersinia pestis in Historical Plague: Evidence for Long-Term Persistence of Y. pestis in Europe from the 14th to the 17th Century. *PLOS ONE*, *11*(1), e0145194. https://doi.org/10.1371/journal.pone.0145194

Seitz, A., & Nieselt, K. (2017). Improving ancient DNA genome assembly. *PeerJ*, *5*, e3126. https://doi.org/10.7717/peerj.3126

Sholts, S. B., Bell, J. A., & Rick, T. C. (2016). Ecce Homo: Science and Society Need Anthropological Collections. *Trends in Ecology & Evolution*, *31*(8), 580–583. https://doi.org/10.1016/j.tree.2016.05.002

Sirak, K. A., Fernandes, D. M., Cheronet, O., Novak, M., Gamarra, B., Balassa, T., Bernert, Z., Cséki, A., Dani, J., Gallina, J. Z., Kocsis-Buruzs, G., Kővári, I., László, O., Pap, I., Patay, R., Petkes, Z., Szenthe, G., Szeniczey, T., Hajdu, T., & Pinhasi, R. (2017). A minimally-invasive method for sampling human petrous bones from the cranial base for ancient DNA analysis. *BioTechniques*, *62*(6), 283–289. https://doi.org/10.2144/000114558

Sirak, K. A., & Sedig, J. W. (2019). Balancing analytical goals and anthropological stewardship in the midst of the paleogenomics revolution. *World Archaeology*, *0*(0), 1–14. https://doi.org/10.1080/00438243.2019.1617190

Sirak, K., Fernandes, D., Cheronet, O., Harney, E., Mah, M., Mallick, S., Rohland, N., Adamski, N., Broomandkhoshbacht, N., Callan, K., Candilio, F., Lawson, A. M., Mandl, K., Oppenheimer, J., Stewardson, K., Zalzala, F., Anders, A., Bartík, J., Coppa, A., … Pinhasi, R. (2020). Human auditory ossicles as an alternative optimal source of ancient DNA. *Genome Research*. https://doi.org/10.1101/gr.260141.119

Skoglund, P., & Mathieson, I. (2018). Ancient Genomics of Modern Humans: The First Decade. *Annual Review of Genomics and Human Genetics*, *19*, 381–404. https://doi.org/10.1146/annurev-genom-083117-021749

Skoglund, P., Northoff, B. H., Shunkov, M. V., Derevianko, A. P., Pääbo, S., Krause, J., & Jakobsson, M. (2014). Separating endogenous ancient DNA from modern day contamination in a Siberian Neandertal. *Proceedings of the National Academy of Sciences*, *111*(6), 2229–2234. https://doi.org/10.1073/pnas.1318934111

Slatkin, M., & Racimo, F. (2016). Ancient DNA and human history. *Proceedings of the National Academy of Sciences*, *113*(23), 6380–6387. https://doi.org/10.1073/pnas.1524306113
Slavin, P. (2021). Out of the West: Formation of a Permanent Plague Reservoir in South-Central Germany (1349–1356) and its Implications∗. *Past & Present*, *252*(1), 3–51. https://doi.org/10.1093/pastj/gtaa028

Slon, V., Hopfe, C., Weiß, C. L., Mafessoni, F., Rasilla, M. de la, Lalueza-Fox, C., Rosas, A., Soressi, M., Knul, M. V., Miller, R., Stewart, J. R., Derevianko, A. P., Jacobs, Z., Li, B., Roberts, R. G., Shunkov, M. V., Lumley, H. de, Perrenoud, C., Gušić, I., … Meyer, M. (2017). Neandertal and Denisovan DNA from Pleistocene sediments. *Science*, *356*(6338), 605–608. https://doi.org/10.1126/science.aam9695

Smith, C. I., Chamberlain, A. T., Riley, M. S., Stringer, C., & Collins, M. J. (2003). The thermal history of human fossils and the likelihood of successful DNA amplification. *Journal of Human Evolution*, *45*(3), 203–217. https://doi.org/10.1016/S0047-2484(03)00106-4

Smith, T. M., Olejniczak, A. J., Zermeno, J. P., Tafforeau, P., Skinner, M. M., Hoffmann, A., Radovčić, J., Toussaint, M., Kruszynski, R., Menter, C., Moggi-Cecchi, J., Glasmacher, U. A., Kullmer, O., Schrenk, F., Stringer, C., & Hublin, J.-J. (2012). Variation in enamel thickness within the genus Homo. *Journal of Human Evolution*, *62*(3), 395–411. https://doi.org/10.1016/j.jhevol.2011.12.004

Soubrier, J., Gower, G., Chen, K., Richards, S. M., Llamas, B., Mitchell, K. J., Ho, S. Y. W., Kosintsev, P., Lee, M. S. Y., Baryshnikov, G., Bollongino, R., Bover, P., Burger, J., Chivall, D., Crégut-Bonnoure, E., Decker, J. E., Doronichev, V. B., Douka, K., Fordham, D. A., … Cooper, A. (2016). Early cave art and ancient DNA record the origin of European bison. *Nature Communications*, *7*(1), 1–7. https://doi.org/10.1038/ncomms13158

Spyrou, M. A., Tukhbatova, R. I., Feldman, M., Drath, J., Kacki, S., Beltrán de Heredia, J., Arnold, S., Sitdikov, A. G., Castex, D., Wahl, J., Gazimzyanov, I. R., Nurgaliev, D. K., Herbig, A., Bos, K. I., &

Krause, J. (2016). Historical Y. pestis Genomes Reveal the European Black Death as the Source of Ancient and Modern Plague Pandemics. *Cell Host & Microbe*, *19*(6), 874–881. https://doi.org/10.1016/j.chom.2016.05.012

Spyrou, M. A., Tukhbatova, R. I., Wang, C.-C., Valtueña, A. A., Lankapalli, A. K., Kondrashin, V. V., Tsybin, V. A., Khokhlov, A., Kühnert, D., Herbig, A., Bos, K. I., & Krause, J. (2018). Analysis of 3800-year-old Yersinia pestis genomes suggests Bronze Age origin for bubonic plague. *Nature Communications*, *9*(1), 1–10. https://doi.org/10.1038/s41467-018-04550-9

Stamatakis, A. (2006). RAxML-VI-HPC: maximum likelihood-based phylogenetic analyses with thousands of taxa and mixed models. *Bioinformatics (Oxford, England)*, *22*(21), 3. https://doi.org/10.1093/bioinformatics/btl446

Stenseth, N. C., Samia, N. I., Viljugrein, H., Kausrud, K. L., Begon, M., Davis, S., Leirs, H., Dubyanskiy, V. M., Esper, J., Ageyev, V. S., Klassovskiy, N. L., Pole, S. B., & Chan, K.-S. (2006). Plague dynamics are driven by climate variation. *Proceedings of the National Academy of Sciences*, *103*(35), 13110–13115. https://doi.org/10.1073/pnas.0602447103

Sun, Y.-C., Jarrett, C. O., Bosio, C. F., & Hinnebusch, B. J. (2014). Retracing the Evolutionary Path that Led to Flea-Borne Transmission of Yersinia pestis. *Cell Host & Microbe*, *15*(5), 578–586. https://doi.org/10.1016/j.chom.2014.04.003

Tabor, S., Struhl, K., Scharf, S. J., & Gelfand, D. H. (2001). DNA-dependent DNA polymerases. *Current Protocols in Molecular Biology*, *Chapter 3*, Unit3.5. https://doi.org/10.1002/0471142727.mb0305s37

Taylor, G. M., Goyal, M., Legge, A. J., Shaw, R. J., & Young, D. (1999). Genotypic analysis of Mycobacterium tuberculosis from medieval human remains. *Microbiology*, *145*(4), 899–904. https://doi.org/10.1099/13500872-145-4-899

Thorvaldsdóttir, H., Robinson, J. T., & Mesirov, J. P. (2013). Integrative Genomics Viewer (IGV): High-performance genomics data visualization and exploration. *Briefings in Bioinformatics*, *14*(2), 178–192. https://doi.org/10.1093/bib/bbs017

Titball, R. W., & Williamson, E. D. (2001). Vaccination against bubonic and pneumonic plague. *Vaccine*, *19*(30), 4175–4184. https://doi.org/10.1016/S0264-410X(01)00163-3

Trinkaus, E. (2018). The labyrinth of human variation. *Proceedings of the National Academy of Sciences*, *115*(16), 3992–3994. https://doi.org/10.1073/pnas.1804794115

Ubelaker, D. H. (2010). Issues in Forensic Anthropology. In *A Companion to Biological Anthropology* (pp. 412–426). John Wiley & Sons, Ltd. https://doi.org/10.1002/9781444320039.ch23

Ulshöfer, K. (1983). Der hällische Salzhandelund in Hall und das Salz. In *Beiträge zur hällischen Stadt- und Salinengeschichte ed. By Kuno Ulshöfer and Herta Beutter* (pp. 95–112). Jan Thorbecke.

Vadyvaloo, V., Jarrett, C., Sturdevant, D. E., Sebbane, F., & Hinnebusch, B. J. (2010). Transit through the Flea Vector Induces a Pretransmission Innate Immunity Resistance Phenotype in Yersinia pestis. *PLOS Pathogens*, *6*(2), e1000783. https://doi.org/10.1371/journal.ppat.1000783

Velsko, I., Skourtanioti, E., & Brandt, G. (2020, December 11). *Ancient DNA Extraction from Skeletal Material*. Protocols.Io. https://www.protocols.io/view/ancient-dna-extraction-from-skeletal-material-baksicwe

Venables, W. N., & Ripley, B. D. (2002). *Modern Applied Statistics with S* (4th ed.). Springer-Verlag. https://doi.org/10.1007/978-0-387-21706-2

Verma, D., Garg, P. K., & Dubey, A. K. (2018). Insights into the human oral microbiome. *Archives of Microbiology*, *200*(4), 525–540. https://doi.org/10.1007/s00203-018-1505-3

Wade, W. G. (2013). The oral microbiome in health and disease. *Pharmacological Research*, *69*(1), 137–143. https://doi.org/10.1016/j.phrs.2012.11.006

Wagner, D. M., Klunk, J., Harbeck, M., Devault, A., Waglechner, N., Sahl, J. W., Enk, J., Birdsell, D. N., Kuch, M., Lumibao, C., Poinar, D., Pearson, T., Fourment, M., Golding, B., Riehm, J. M., Earn, D. J. D., DeWitte, S., Rouillard, J.-M., Grupe, G., … Poinar, H. (2014). Yersinia pestis and the Plague of Justinian 541–543 AD: A genomic analysis. *The Lancet Infectious Diseases*, *14*(4), 319–326. https://doi.org/10.1016/S1473-3099(13)70323-2

Warinner, C. (2016). Dental calculus and the evolution of the human oral microbiome. *Journal of the California Dental Association*, *44*(7). https://par.nsf.gov/biblio/10025833-dental-calculus-evolution-human-oral microbiome

Warinner, C., Speller, C., & Collins, M. J. (2015). A new era in palaeomicrobiology: Prospects for ancient dental calculus as a long-term record of the human oral microbiome. *Philosophical Transactions of the Royal Society B: Biological Sciences*, *370*(1660), 20130376. https://doi.org/10.1098/rstb.2013.0376

Warinner, C., Speller, C., Collins, M. J., & Lewis, C. M. (2015). Ancient human microbiomes. *Journal of Human Evolution*, *79*, 125–136. https://doi.org/10.1016/j.jhevol.2014.10.016

Weissensteiner, H., Pacher, D., Kloss-Brandstätter, A., Forer, L., Specht, G., Bandelt, H.-J., Kronenberg, F., Salas, A., & Schönherr, S. (2016). HaploGrep 2: Mitochondrial haplogroup classification in the era of high-throughput sequencing. *Nucleic Acids Research*, *44*(W1), W58-63. https://doi.org/10.1093/nar/gkw233

Weyrich, L. S., Dobney, K., & Cooper, A. (2015). Ancient DNA analysis of dental calculus. *Journal of Human Evolution*, *79*, 119–124. https://doi.org/10.1016/j.jhevol.2014.06.018

Weyrich, L. S., Duchene, S., Soubrier, J., Arriola, L., Llamas, B., Breen, J., Morris, A. G., Alt, K. W., Caramelli, D., Dresely, V., Farrell, M., Farrer, A. G., Francken, M., Gully, N., Haak, W., Hardy, K., Harvati, K., Held, P., Holmes, E. C., … Cooper, A. (2017). Neanderthal behaviour, diet, and disease inferred from ancient DNA in dental calculus. *Nature*, *544*(7650), 357–361. https://doi.org/10.1038/nature21674

Wickham, H. (2016). *ggplot2: Elegant Graphics for Data Analysis* (2nd ed.). Springer International Publishing. https://doi.org/10.1007/978-3-319-24277-4

Willerslev, E., & Cooper, A. (2005). Ancient DNA. *Proceedings. Biological Sciences*, *272*(1558), 3–16. https://doi.org/10.1098/rspb.2004.2813

Wood, J. W., Ferrell, R. J., & Dewitte-Aviña, S. N. (2003). The temporal dynamics of the fourteenth-century Black Death: New evidence from English ecclesiastical records. *Human Biology*, *75*(4), 427–448. https://doi.org/10.1353/hub.2003.0067

Yates, J. A. F., Lamnidis, T. C., Borry, M., Valtueña, A. A., Fagernäs, Z., Clayton, S., Garcia, M. U., Neukamm, J., & Peltzer, A. (2021). Reproducible, portable, and efficient ancient genome reconstruction with nf-core/eager. *PeerJ*, *9*, e10947. https://doi.org/10.7717/peerj.10947

Yue, R. P. H., Lee, H. F., & Wu, C. Y. H. (2017). Trade routes and plague transmission in pre-industrial Europe. *Scientific Reports*, *7*. https://doi.org/10.1038/s41598-017-13481-2
Zhou, H., Yu, Z., Hu, Y., Tu, J., Zou, W., Peng, Y., Zhu, J., Li, Y., Zhang, A., Yu, Z., Ye, Z., Chen, H., & Jin, M. (2009). The Special Neuraminidase Stalk-Motif Responsible for Increased Virulence and Pathogenesis of H5N1 Influenza A Virus. *PLOS ONE*, *4*(7), e6277. https://doi.org/10.1371/journal.pone.0006277

8. Summary

Ancient DNA analyses are a crucial part of modern archaeological assessment which help to elucidate previously hidden historical dynamics. However, to utilize this tool, it is u necessary to cause irrevocable damage to the archaeological record through the destructive sampling of archaeological remains. As such, it is imperative that there be balance between data production and the stewardship of the anthropological record. This dissertation focuses on developing and optimizing laboratory methods aimed at maximizing the usable data generated from destructive sampling while minimizing the damage to the archaeological record. Across the four manuscripts presented here I explore ancient DNA recovery across multiple skeletal elements; make those methods publicly available; demonstrate the utility of expanded screening techniques in uncovering unexpected historical events; and optimize a method for extracting high-molecular weight DNA from dental calculus with the intent to expand the oral microbiome reference database through metagenomic assemblies.

Manuscript 1 presents the analyses of DNA yield and quality from 23 sampling locations across 10 skeletal elements recovered from each of 11 medieval individuals. We find that while destructive sampling of the dense cochlear region of the petrous pyramid does provide the highest yields of endogenous human DNA, the cementum, dentin, and pulp chamber of molars; cortical bone of the vertebral body and superior vertebral arch; cortical bone from the distal phalanx; and cortical bone from the exterior of the talus all exhibit excellent DNA preservation with yields consistently high enough (in both quantity and quality) for the vast majority of population genetic assessments. Despite the popularity of ancient DNA studies, this is the first large scale, systematic, investigation of DNA preservation across a host of skeletal elements and associated sampling locations and, as such, will serve as an important baseline for the formation of ethical sampling strategies using archaeological remains.

One of the challenges presented in Manuscript 1 was in the lack of appropriate sampling protocols for many of the sampling locations analysed. This lack of published protocols results in considerable wastage, in both the time and money spent on aDNA research using non-standard remains as well as the irreplaceable archaeological remains themselves. Manuscript 2 presents the complete sampling protocols used in Manuscript 1 published in both text and video format. The resulting, real-time, tutorial makes the utilization of these anatomical sampling locations easily accessible to a wide audience.

Manuscript 3 presents a case study in the utility of the rigorous and routine screening of aDNA datasets for potential findings outside of the original scope of a project. Here I present two high-coverage *Y. pestis* genomes recovered from the remains used in Manuscripts A and B. These genomes were recovered from remains where there were no archaeological evidence of infection and were discovered only through the expanded screening of the datasets. Here we find not only a new example of *Pestis secunda*, a post-Black Death, Second Pandemic strain genetically linked to the ongoing Third Pandemic, but also the genome of a new, earlier example of the same strain which appears to be the direct link between the Black Death and all other described examples of *Pestis secunda*. Additionally, we find the first verifiable traces of *Y. pestis* infection in post-cranial remains, further reinforcing the importance of broad screening techniques.

Manuscript 4 presents an optimized method for the extraction of high molecular weight DNA from modern dental calculus. Reference genomes are available for ca 60% of those species thought to make up the human oral microbiome. As this is a metagenomic substrate, assembly of new reference genomes using only short-read sequencing is challenging at best. The introduction of methods to bolster the efficacy of metagenomic assembly of the oral microbiome by the addition of long read sequencing will help to fill these gaps and make the subsequent investigations of the ancient oral microbiome more informative.

There is a single common thread throughout this dissertation: The only way to ethically use ancient DNA analyses from archaeological remains is to maximize the utility of each instance of destructive sampling to generate a clearer, more complete picture of the genetic landscape of a given individual and site.

8. Zusammenfassung

Prä-/Historische DNA-Analysen sind ein wichtiger Bestandteil moderner archäologischer Untersuchungen, die dazu beitragen, bisher verborgene historische Kausalitäten zu erläutern. Um dieses Instrument zu nutzen, ist es jedoch unumgänglich, durch die destruktive Entnahme von Proben aus archäologischen Überresten unwiderrufliche Schäden an den archäologischen Fundstücken zu verursachen. In diesem Zusammenhang ist ein Gleichgewicht zwischen der Datenproduktion und dem Schutz der anthropologischen Überreste unabdingbar. Diese Dissertation konzentriert sich auf die Entwicklung und Optimierung von Labormethoden, die darauf abzielen, die verwertbaren Daten, die durch destruktive Probenahmen gewonnen werden, zu maximieren und gleichzeitig die Schäden an den archäologischen Funden zu minimieren. In den vier hier vorgestellten Manuskripten untersuche ich die Gewinnung historischer DNA aus verschiedenen Skelettelementen, stelle diese Methoden öffentlich zur Verfügung, demonstriere den Nutzen erweiterter Screening-Techniken bei der Aufdeckung unerwarteter historischer Ereignisse und optimiere eine Methode zur Extraktion hochmolekularer DNA aus Zahnstein mit dem Ziel, die Referenzdatenbank des oralen Mikrobioms durch metagenomische Zusammenstellungen zu erweitern.

In Manuskript 1 werden die Analysen der DNA-Ausbeute und -Qualität von 23 Probenahmestellen an 10 verschiedenen Skelettelementen vorgestellt, die von 11 mittelalterlichen Individuen entnommen wurden. Wir stellen fest, dass die destruktive Entnahme von Proben aus der dichten Cochlea-Region des Pars Petrosa zwar die höchste Ausbeute an endogener menschlicher DNA liefert, dass aber auch das Cementum, das Dentin und die Pulpakammer der molaren Zähne, der kortikale Knochen des Wirbelkörpers und des oberen Wirbelbogens, der kortikale Knochen des distalen Phalanx und der kortikale Knochen von der

Außenseite des Talus alle einen ausgezeichneten DNA-Erhalt aufweisen und die Ausbeute durchweg hoch genug ist (sowohl in Bezug auf die Quantität als auch die Qualität) für die große Mehrheit der populationsgenetischen Analysen. Trotz der Beliebtheit prä-/historischer DNA-Studien ist dies die erste groß angelegte, systematische Untersuchung der DNA-Erhaltung bei einer Vielzahl von Skelettelementen und den dazugehörigen Entnahmestellen und wird als solche eine wichtige Grundlage für die Entwicklung ethischer Probenahmestrategien bei archäologischen Überresten darstellen.

Eine der Herausforderungen in Manuskript 1 war das Fehlen geeigneter Probenahmeprotokolle für viele der untersuchten Entnahmestellen. Dieser Mangel an veröffentlichten Protokollen führt zu einer beträchtlichen Verschwendung von Zeit und Geld, die für die prä-/historische DNA-Forschung unter Verwendung von nicht-standardisierbaren Überresten aufgewendet werden, sowie der unersetzlichen archäologischen Überreste selbst. Manuskript 2 enthält die vollständigen Probenahmeprotokolle, die in Manuskript 1 verwendet wurden, sowohl im Text- als auch im Videoformat. Das daraus resultierende Echtzeit-Tutorial macht die Verwendung dieser anatomischen Probenahmestellen einem breiten Publikum leicht zugänglich.

Manuskript 3 ist eine Fallstudie über die Zweckdienlichkeit des rigorosen und routinemäßigen Screenings von prä-/historischen DNA-Datensätzen auf potenzielle Ergebnisse außerhalb des ursprünglichen Projektumfangs. Hier stelle ich zwei Y.-pestis-Genome mit hoher Coverage vor, welche aus den in den Manuskripten 1 und 2 verwendeten Überresten gewonnen wurden. An den Individuuen wurden vorab keinerlei archäologische Hinweise auf eine Infektion festgestellt. Diese Pathogene wurden erst durch das erweiterte Screening der Datensätze entdeckt. Hierbei handelt es sich nicht nur um ein neues Beispiel für Pestis

secunda, einen Stamm der Zweiten Pandemie nach dem schwarzen Tod, der genetisch mit der laufenden Dritten Pandemie verbunden ist, sondern auch das Genom eines bisher unentdeckten, früheren Vertreters von Pestis secunda, welcher die direkte genetische Verbidnung zwischen dem Schwarzen Tod und allen bereits bekannten Arten von Pestis secunda zu sein scheint. Darüber hinaus finden wir die ersten nachweisbaren Spuren von Y. pestis-Infektionen in postkranialen Überresten, welches die Bedeutung breit angelegter Screening-Techniken weiter unterstreicht.

In Manuskript 4 wird eine optimierte Methode zur Extraktion von hochmolekularer DNA aus modernem Zahnstein vorgestellt. Referenzgenome sind für etwa 60 % der Arten verfügbar, von denen man annimmt, dass sie das menschliche orale Mikrobiom bilden. Da es sich um ein metagenomisches Substrat handelt, ist die Erstellung neuer Referenzgenome nur mit Hilfe von Short-Read-Sequenzierung bestenfalls eine Herausforderung. Die Einführung von Methoden, die die Effizienz der metagenomischen Assemblierung des oralen Mikrobioms durch die Ergänzung von Long-Read-Sequenzierung verbessern, wird dazu beitragen, diese Lücken zu schließen und die nachfolgenden Untersuchungen des prä-/historischen oralen Mikrobioms noch aufschlussreicher zu machen.

Eine Grundidee lässt sich in der gesamten Dissertation erkennen; Die einzige Möglichkeit, prä-/historische DNA-Analysen aus archäologischen Überresten auf ethische Weise zu nutzen, besteht darin, den Nutzen jeder einzelnen destruktiven Probenahme zu maximieren, um ein klareres, vollständigeres Bild der genetischen Landschaft einer bestimmten Stätte und des Individuums zu erhalten.

9. Appendix 1: Author's contributions to figures representing experimental data

Manuscript 1: Parker et al. (2020), Scientific Reports

Figure(s)	**Contribution (%)**	**Notes**
2-6	40%	Evaluated data and formatting, coded formatting (R statistical language)
S11-S17	30%	Evaluated data and formatting, coded formatting (R statistical language)

Manuscript 2: Parker et al. 2021, JoVE

Figure(s)	**Contribution (%)**	**Notes**
N/A	N/A	No original figures representing experimental data

Manuscript 3: Parker et al. (In preparation)

Figure(s)	**Contribution (%)**	**Notes**
2	5%	Evaluated data
S5	100%	N/A
S6-S7	0%	N/A

Manuscript 4: Parker et al. (in preparation)

Figure(s)	**Contribution (%)**	**Notes**
1-2	100%	N/A
3	10%	formatting

10. Eigenständigkeitserklaerung

Entsprechend §5 Abs. 4 der Promotionsordnung der Biologisch-Pharmazeutischen Fakultät der Friedrich-Schiller-Universität Jena, erkläre ich, dass mir die geltende Promotionsordnung der Fakultät bekannt ist. Ich bezeuge, dass ich die vorliegende Dissertation selbst angefertigt habe und keine Textabschnitte eines Dritten oder eigener Prüfungsarbeiten ohne Kennzeichnung übernommen und alle von mir benutzten Hilfsmittel, persönliche Mitteilungen sowie Quellen in meiner vorliegenden Arbeit angegeben habe. Zudem habe ich alle Personen, die mir bei der Auswahl und Auswertung sowie bei der Erstellung der Manuskripte unterstützt haben, in der Auflistung der Manuskripte und den entsprechenden Danksagungen namentlich erwähnt. Zudem versichere ich, dass ich die Hilfe eines Promotionsberaters nicht in Anspruch genommen haben und auch Dritten von mir keine unmittelbaren sowie mittelbaren geldwerte Leistungen für Arbeiten, die im Zusammenhang mit dieser Dissertation stehen, erhalten haben. Die vorliegende Promotion wurde zuvor weder für eine staatliche oder andere wissenschaftliche Prüfung eingereicht, also auch einer anderen Hochschule als Dissertation vorgelegt.

Jena, den 12/12/2021

Cody Parker

11. Acknowledgements

I would first like to thank my supervisors Dr. Wolfgang Haak, Dr. Kirsten I. Bos and Prof. Johannes Krause for inviting me to join the Department of Archaeogenetics at the Max Planck Institute for the Science of Human History and allowing me the opportunity use my passion for laboratory science to aid the field of archaeogenetics.

I would also like to thank of the other PI's, postdocs, PhD candidates, and laboratory technicians at the institute for their time, patience, and support. Specifically, I would like to thank Thiseas Lamnidis, James Fellows Yates, Aida Andrades Valtueña, Aditya Lankapalli, Karen Giffin, and Rodrigo Barquera for their friendship and support throughout my time here. I would also like to thank the members of the IT and HR departments of the MPI-SHH for their continuous efforts to ensure that whatever things I may had broken got appropriately fixed.

On a personal note, I'd like to thank Elizabeth Nelson, Franziska Aron, Karen Giffin, and Marieke van de Loosdrect, all of whom offered their unconditional support, took late night phone calls and texts, and were just generally always there for anything I could possibly need.

To Dr. Adam Ben Rohrlach: thank you for your unofficial supervision, and of course the beer.

Finally, I would like to thank my partner, Elizabeth Parker. None of this would have been possible without you having my back every second of every day throughout this trying ordeal.
To my children Rose, Hazel, and Samuel Parker: Thank you for being my inspiration, you really make me believe anything is possible.